Targeting the mechanism of 5-FU chemoresistance in colorectal cancer by metabolic reprogramming of tumor associated macrophages

Khaldoun Gharzeddine

THÈSE

Pour obtenir le grade de

DOCTEUR DE L'UNIVERSITÉ GRENOBLE ALPES

École doctorale : CSV- Chimie et Sciences du Vivant
Spécialité : Virologie - Microbiologie - Immunologie
Unité de recherche : IAB : Epigenetics, Environment, Cell Plasticity, Cancer (UGA / Inserm U1209 / CNRS UMR 5309)

Ciblage du mécanisme de chimiorésistance au 5-FU dans le cancer colorectal par reprogrammation métabolique des macrophages associés à la tumeur

Targeting the mechanism of 5-FU chemoresistance in colorectal cancer by metabolic reprogramming of tumor associated macrophages

Présentée par :

Khaldoun GHARZEDDINE

Direction de thèse :

Thomas DECAENS UGA et CHU de Grenoble	Directeur de thèse
Arnaud MILLET Inserm	Co-encadrant de thèse

Rapporteurs :

Eva HAMADE
PROFESSEUR, Université Libanaise
Philippe SAAS
PROFESSEUR DES UNIVERSITES, Université de Franche-Comté

Thèse soutenue publiquement le **20 octobre 2022**, devant le jury composé de :

Eva HAMADE PROFESSEUR, Université Libanaise	Rapporteure
Philippe SAAS PROFESSEUR DES UNIVERSITES, Université de Franche-Comté	Rapporteur
Walid RACHIDI PROFESSEUR DES UNIVERSITES, Université Grenoble Alpes	Président
Philippe FRACHET MAITRE DE CONFERENCES HDR, Université Grenoble Alpes	Examinateur
Carlos ROSSA JUNIOR PROFESSEUR ASSOCIE, Universidade de Araraquara	Examinateur

Invités :

Thomas Decaens
PROFESSEUR DES UNIVERSITES - PRATICIEN HOSPITALIER, Faculté de Médecine - Université Grenoble Alpes
Arnaud Millet

CHARGE DE RECHERCHE, INSERM

This project has received funding from the European Union's Horizon 2020 research and Innovation programme under the H2020-MSCA-ITN-2018 Grant Agreement n. 812772.

Funded by the European Union

All Figures used in this manuscript were created with BioRender.com

The wind follows the path of our sailing ship

for we are the wind,

we are the sea,

we are the ship…

Acknowledgments

First, I would like to thank the honorable jury members for reading and reviewing my thesis Prof. Philippe SAAS, Prof. Eva HAMADE, Prof. Walid RACHIDI and Prof. Philippe FRACHET.

During these three years, I experienced a lot of good and tough moments. I would like to express my gratitude and love to the people who stood by my side and supported me.

I was lucky to be a member in Team Mechanobiology, Immunity and Cancer at the Institute for Advanced Biosciences. I would like to thank Prof. Thomas Decaens for granting me this opportunity. My PhD would not be the same without the head of the team and my mentor Dr. Arnaud MILLET. Not only he is a great scientific researcher and a notable supervisor whom I learned a lot from scientifically, he is a great supporter as well. When I encountered a critical health issue during the beginning of the third year of my thesis, I got to know the other side of Dr. Arnaud, the medical doctor and the caring father. He followed my medical situation and supported me. Because of him, I was not afraid that I would lose my thesis. Because of him I felt that it'll be fine. Arnaud, thank you a million.

Also, I would like to thank Marie Malier who helped me when needed and showed extreme care and support. To her I say in FRENCH: *Merci mille fois*. Thankfully, our former Master II students: Walaa Jradi, Bailassan Haidar, Clara Hennot and Benedicte Demoustier were so kind and always showed up whenever I needed their help or assistance. Additionally, I would like to thank the rest of the team: Dr. Gael Roth and Dr. Marie-Hélène Laverriere and our former technician, Magali Court. And I would like to thank team Patrice Marche with whom we shared the offices, the lab as well as scientific discussions.

I was an early sage researcher in Phys2BioMed ITN Network funded by European Union's Horizon 2020 research and innovation program under the Marie Skłodowska-Curie grant agreement No 812772. I would like to thank Antonia Samore for her care and support. Also, I would like to thank Prof. Jean-Luc Pellequer, Prof. Felix Rico and Prof. Malgorzata Lekka for our network's collaborations. Finally, a warm-hearted thank you for the early stage researchers Harinderbir Kaur, Kajangi Gnanachandran, Mar Eroles Navarro and Shruti Kalkarni who shared with me their cultures and great memories during the network's events.

My friends made Grenoble feels like home. Dr. Mariam Mroweh thank you for being my companion in the lab, in each and every medical visit and for holding my back. Anna-Maria Alazzi thank you for your warm heart and for bracing mine through thick and thin. Mohamed Graiess, 'Le Khoya', thank you for being an older brother to me and a person to rely on. Amani Shreim, thank you for being around through my ups and downs and for loving Elissa, right? Hasan Safwan-Zaiter, thank you for being my music companion, best friend and a great supporter. Nour El Husseini, Sara El Badawi, Jihad Omar, Amal Al Kadi and Zeina Wehbe thank you for being part of the best memories that I have at the IAB. Amale El Khatib, Malak Faraj and Lama Shamseddine thank you for sharing with me the greatest memories of Grenoble. Jinan Al Sayegh, Lara Noureddine, Halima Makarem, Hadi Sarieddine, Nagham Aramouni and Nadia Al Awar thank you for proving that distance cannot break a friendship's bond.

My family, Gharzeddine and Abi Farrage, gave me ultimate love and support. I would like to thank my Grandma, aunts, uncles and their families; The tragedy of the departure of my beloved aunt, Rouwaida, at 23rd of January 2022 is a forever-lasting scar in my heart. I would like to thank her for the great memories that she has left me with; I would like to thank my beloved uncle Ramzi, who left us in May 14 2022, for being a role model to me since my childhood.

Alaa El Masry, I always feel happy and proud when people think that we are twins. Thank you for being my childhood friend and brother; Marwa Abi Farraj, thank you for being the most courageous, righteous and soulful person I've ever known; Mirna Gharzeddine, thank you for being an older loving and caring sister; Sara El Masry, thank you for your wisdom, love and believing in my ''pdf''', great minds think alike, right? A big thank you for the affectionate ladies Rim, Mayssam, Mirna, Tania, Reina, Zeina, Ola and Hala and for the reliable bros Fayssal, Mazen and Saiid.

My education was the most important thing to my dad, Refaat. He worked hard so that this day would come. Thanks Dad. I hope that this would make up for the great things that you did for me; Everything that I have reached or will reach in the future is owed to my great mother, Amal, to her sacrifices, hard work, tears and smiles. *Mama*, Thank you for your patience, love and care; Dalia, my precious sister, is the person who I always look up to in order to get rid of my fears and pain. Thank you for taking good care of me during Aya's sickness and mine; My youngest sister, the brave and the beautiful Aya, taught me courage, persistence and endurance throughout her journey in fighting cancer. She backed me up when she knew about my sickness whilst she was the one who needed that support. Thank you for being full of joy and for making me strong and proud.

Finally, I would like to thank HIM for all of the great blessings that he has given me.

This thesis is dedicated to

The sacrifices of **Refaat Gharzeddine** and **Amal Abi Farrage Gharzeddine**

The love of **Dalia Gharzeddine** and **Aya Gharzeddine**

The precious memory of **Rouwaida Gharzeddine El Masry**

Résumé

Le microenvironnement tumoral (TME) consiste en un réseau très complexe des cellules stromales et tumorales ainsi que de facteurs environnementaux comme l'hypoxie qui définissent collectivement l'état de la tumeur. L'un des acteurs clés au sein du TME sont les macrophages, appelés macrophages associés aux tumeurs (TAM). Les TAM interfèrent avec le développement et la progression des tumeurs soit en les inhibant, soit en les favorisant par la médiation de fonctions immunosuppressives et en favorisant la chimiorésistance. Ainsi, nous avons pu démontré que l'hypoxie module la biologie des macrophages et augmente l'expression protéique de la DPD (*dihydropyrimidine dehydrogenase*) qui est une enzyme qui catabolise le 5-fluorouracile (5-FU), une chimiothérapie de première ligne dans les cancers digestifs. Ce mécanisme confère une chimiorésistance au 5-FU dans les cancers colorectaux humains (CRC). De plus, nous avons montré que ce mécanisme est contrôlé au niveau traductionnel *via* la stabilisation de HIF-2α. Enfin, nous avons prouvé que seuls les macrophages humains présentent une expression significative de la DPD dans les tumeurs du CRC, les cellules cancéreuses de cancer colorectaux en exprimant peu ainsi que les macrophages de rongeurs. Pour surmonter cette chimiorésistance contrôlée par la déprivation en oxygène, nous avons développé, dans ce travail de thèse, une stratégie de reprogrammation métabolique des macrophages en ciblant l'expression de DPD. Pour ce faire, nous avons utilisé des antagonistes contre le récepteur du facteur de stimulation des colonies de macrophages (M-CSF R). En effet, il a été rapporté que le facteur de transcription SP1 est activé par le M-CSF et contrôle l'expression de DPD. Dans notre étude, nous rapportons que bien que tous les antagonistes ciblent la voie M-CSF R *via* l'inhibition de ses domaines kinases, un seul antagoniste, Edicotinib, cible spécifiquement l'expression de DPD dans les macrophages humains, rendant les cellules cancéreuses du côlon sensibles au 5-FU. Cependant, nous avons démontré que cet effet est médié indépendamment de SP1 et p-ERK, mais lié à la capacité d'Edicotinib à déstabiliser HIF2α en hypoxie. En outre, nous avons constaté que l'edicotinib reprogramme de manière significative les macrophages métaboliquement. Cette reprogrammation métabolique est aussi associée à une régulation négative des gènes associés à une polarisation de type M2. Ces résultats ouvrent la voie au développement de nouvelles stratégies pour surmonter la chimiorésistance dans le CRC et moduler le rôle des TAMs dans le microenvironnement tumoral.

Abstract

The tumor microenvironment (TME) consists of a highly complex network of stromal and tumoral cells along with other tumor specific factors such as hypoxia, which collectively define the state of the tumor. One of the key players of immune cells within TME are macrophages, hereby called tumor associated macrophages (TAMs). TAMs interfere in the development and progression of tumors either by suppressing it or promoting it through mediating immunosuppressive functions and advocating chemoresistance against chemotherapeutic treatments. In this context, we demonstrated that hypoxia modulates the biology of macrophages and upregulates the expression of dihydropyrimidine dehydrogenase (DPD), which is an enzyme that catabolizes the chemotherapeutic agent 5-fluorouracil (5-FU). This mechanism confers a chemoresistance in human colorectal cancer (CRC). Nevertheless, we showed that this mechanism is controlled at the translational level via the stabilization of HIF-2α. Finally, we proved that only human macrophages display upregulated expression and activity of DPD in CRC tumors where neither colon cancerous cells nor rodents' macrophages showed any significant DPD levels. Secondarily, to overcome this oxygen-controlled chemoresistance we aimed to develop a strategy to reprogram macrophages metabolically by targeting DPD expression. To do so we used antagonists against the Macrophage Colony Stimulatory Factor Receptor (M-CSF R). Indeed, it was reported that the transcription factor SP1 is activated by M-CSF and possibly control DPD expression. In our study, we report that although all antagonists target M-CSF R pathway via the inhibition its kinases domains, only one antagonist, Edicotinib, specifically targets DPD expression in human macrophages rendering colon cancer cells sensitive to 5-FU. However, we have demonstrated that this effect is mediated independently from SP1 and p-ERK, but related to the ability of Edicotinib to destabilize HIF2α in hypoxia. Nonetheless, we found that Edicotinib significantly reprograms macrophages metabolically. This metabolic reprogramming is notably associated with a downregulation of M2 genes. Taken altogether, these interesting and paramount findings insist on the crucial roles that macrophages and hypoxia display within the TME of CRC and pave the way to develop new strategies to overcome chemoresistance in CRC and ameliorate the efficacy of the treatment.

Table of Contents

List of Figures

List of Tables

List of Abbreviations

5-FU: 5-Fluorouracil

5-FUH2: 5-Dihydrodluorouracil

AFM: Atomic Force Microscopy

ALOX15: Arachidonate 15-lipooxygenase

ARG: Arginase

Bcl-X: B-cell lymphoma-extra

C1P: ceramide-1 phosphate

Casp: caspase

CCL: CC Chemokine Ligand

CD: Cluster of Differentiation

CH2THF: 5,10-methylenetetrahydrofolate

CRC: Colorectal Cancer

CSF-1 R: Colony Stimulatory Factor Receptor

CSF-1: Colony Stimulatory Factor

CXCL: CXC Chemokine Ligand

DPD: dihydropyrimidine dehydrogenase

DPYD : Dihydropyrimidine Dehydrogenase Gene

DPYS: dihydropyrimidinase

dTDP: deoxythymidine diphosphate

dTMP: deoxythymidine monophosphate

dTTP: deoxythymidine triphosphate

dUDP: deoxyuridine diphosphate

dUMP: deoxyuridine monophosphate

DUSP1: dual specificity phosphatase – 1

dUTP: deoxyuridine triphosphate

dUTPase: deoxyuridine triphosphatase

eIF4E2: Eukaryotic Translation Initiation Factor 4E Family Member 2

EMT: Epithelial-to-Mesenchymal Transition

ERK: Extracellular Signal Regulated Kinase

FASN : Fatty Acid Synthase

FBAL: α-fluoro-β-alanine

FdUDP: fluorodeoxyuridine diphosphate

FdUMP: fluorodeoxyuridine monophosphate

FdUR: fluorodeoxyuridine

FdUTP: fluorodeoxyuridine triphosphate

FIH: Factor Inhibiting HIF

FIMP: Fms interacting protein

FUDP: fluorouridine diphosphate

FUMP: fluorouridine monophosphate

FUPA: α-fluoro-β-ureido propionic acid

FUR: fluorouridine

FUTP: fluorouridine triphosphate

G6PD: Glucose-6-Phosphate Dehydrogenase

GAPDH: Glyceraldehyde 3-Phosphate Dehydrogenase

GLUL : Glutamate Ammonia Ligase

GS: Glutamine Synthase

HIF: Hypoxia Inducible Factor

HL: Hodgkin Lymphoma

HRE: Hypoxia responsive element

HSC: Hematopoietic Stem Cell

IDO: Indoleamine 2,3-dioxygenase

IFN: Interferon

IL : Interleukin

JMD: Juxtamembrane Domain

LDHA: Lactate Dehydrogenase A

LPS : Lipopolysaccharide

MCM : Macrophage Conditioned Media

M-CSF R: Macrophage Colony Stimulatory Factor Receptor

M-CSF: Macrophage Colony Stimulatory Factor

MDSC: Myeloid Derived Suppressor Cells

MEK/MAPKK: Mitogen Activated Protein Kinase Kinase

MMP: Matrix Metalloprotease

MP: Monocyte Progenitor

mTORC: Mechanistic Target of Rapamycin Complex

NADPH: Nicotinamide Adenine Dinucleotide Phosphate

NO: Nitric Oxide

NOS: Nitric Oxide Synthase

NPM: nucleophosmin

NSCLC: Non-Small Cell Lung Cancer

PDGF : Platelet Derived Growth Factor

PDH: Pyruvate Dehydrogenase

PDK: Pyruvate Dehydrogenase Kinase

PHD: Prolyl Hydroxylase

PI3K: Phosphatidylinositol-3-Kinase

PIP2: phosphatidylinositol 4,5-bisphosphate

PKC: protein-kinase C

PMA : Phorbol 12-myristate 13-acetate

PSTPIP2: proline serine threonine phosphatase interacting protein 2

PTPN12: PEST-family tyrosine phosphatases 12

pVHL: Von Hippel Lindau protein

PYK2: protein tyrosine kinase 2-beta; β-cat: β-catenin

RA: Rheumatoid Arthritis

RNR: ribonucleotide reductase

ROS: Reactive Oxygen Species

RTK: Receptor Tyrosine Kinase

SDH: Succinate Dehydrogenase

SFK: Src family kinase

SIRPα : Signal Regulatory Protein α

SP1: Signal Protein 1

STAT: Signal Transducer and Activator of Transcription

SYK: spleen associated tyrosine kinase

TAMs: Tumor Associated Macrophages

TDPK: thymidine diphosphate kinase

TEMs: Tumor Educated Macrophages

TGCT: Tensynovial Giant Cell Tumor

TGF: Tumor Growth Factor

TGM2: Transglutaminase 2

Th : T helper

TK: thymidine kinase

TLR: Toll Like Receptor

TME: Tumor Microenvironment

TMPK: thymidine monophosphate kinase

TNF : Tumor Necrosis Factor

TP: thymidine phosphorylase

TS: thymidylate synthase

U: Uracil

UDG: uracil DNA glycosylase

UDPK: uridine diphosphate kinase

UH2: Dihydrouracil

UMPK: uridine monophosphate kinase

UP: uridine phosphorylase

UPB1: β-ureidopropionate

VEGF : Vascular and Endothelial Growth Factor

Chapter I

General Introduction to Macrophages, Key Players in the Tumor Microenvironment

I. The Tumor Microenvironment

A solid tumor does not only consist of isolated masses of malignant cells but a variety of other non-malignant resident or infiltrating cells, surrounding blood vessels, lymphatic vessel, fibroblasts, as well as signaling molecules and secreting factors (Hui & Chen, 2015). These peculiar components build a complex network known as the tumor microenvironment (TME) Figure 1 (F. R. Balkwill et al., 2012). In addition, there are other physical and environmental parameters, such as tissue oxygenation and the extracellular matrix (ECM), which are major parameters influencing the TME (P. Lu et al., 2012; Petrova et al., 2018).

One of the main feature of the components of TME is reciprocity as the interaction between these elements shapes the tumor, interferes in its development and progression and defines its clinical outcome (Joyce & Pollard, 2009).

Within TME, macrophages, herby called tumor associated macrophages (TAMs), are the most well characterized type of tumor related immune cells (Mantovani et al., 2017). Depending on the area of the tumoral tissue and on the patients, TAMs can constitute a large part of the immune compartment forming a major and driving component in the TME as they play a prominent active role from the early stages of carcinogenesis to the progression of the tumor (Qian & Pollard, 2010; Van Overmeire et al., 2014). The majority of evidence support the pro-tumoral role that TAMs exert (Qian & Pollard, 2010; Q. Zhang et al., 2012), however other studies have demonstrated the role of TAMs as anti-tumoral (Bernsmeier et al., 2020; Bruns et al., 2015). This could be in part explained by the degree of plasticity that macrophages generally show in response to external stimuli which elucidates the diverse roles that TAMs play within TME (Boutilier & Elsawa, 2021).

In this chapter, I will introduce macrophages and their general characteristics. I will then focus on the importance of these cells in the context on cancer as one of the major mediators in the TME.

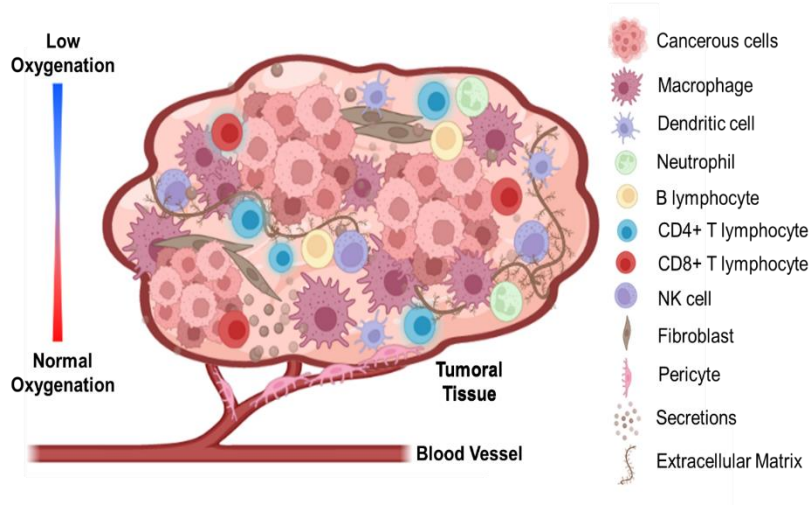

Figure 1 Components of the Tumor Microenvironment (TME)

The TME consists of cancerous cells as well as stromal cells including various immune cells, fibroblasts and pericytes. Other important parameters make up the TME such as tissue oxygenation and the extracellular matrix as well as secreted substances such as chemokines and cytokines.

II. Macrophages

II-1. Historical Glance

In mid 1800s, Rudolf Virchow, known as the father of modern pathology, discovered that there is an accumulation of large white cells within tumors (F. Balkwill & Mantovani, 2001). This shed lights on the implication of immune cells as important regulators during the development and progression of a tumor. Since that time, detailed understanding on the roles of immune cells in the tumor has been carried out and results showed that a variety of cells of lymphoid and myeloid origin are present within the invasion margin of a solid tumor (Hanahan & Weinberg, 2011). Intriguingly, macrophages were highlighted as important key players in healthy and malignant tissues and have become the subject of interest in the research field of immunology and cancer biology (Ngambenjawong et al., 2017).

In 1882, macrophages were first discovered by Elie Metchinkoff, who was honored as the father of Innate Immunity (S. Gordon, 2016). By microscopic observation, he discovered that certain mobile cells responded to the thorns which he had introduced to the starfish larvae and engulfed them. He called these cells as phagocytes. In 1908, Metchinkoff won the Nobel prize for his discovery that built a fundamental part of the immune response.

II-2. Macrophages by Definition

Back in history to Metchinkoff's discovery, phagocytes were classified based on their size as macrophages, big cells, and microphages which are the smaller phagocytes and are now known as neutrophils (S. Gordon, 2016). Dissecting the word ''macrophage'' into two parts, we get the meaning of it: ''macro'' in Greek (makros) means large and ''phage'' in Greek (phagein) means to eat. Thus, macrophages are one of the important phagocytic cells in our body along with dendritic cells and neutrophils.

Macrophages are a population of innate immune cells (N. Wang et al., 2014). Tissue macrophages are versatile cells that are present in all body tissues and they are appraised as the tissue gate keepers (Wynn et al., 2013). In quiescent conditions, they constitute up to 15% of total cell number (Italiani & Boraschi, 2014). This number is dependent on the state of the tissues where they can be highly present depending on the tissue stimuli.

Macrophages are heterogeneous and exhibit anatomical and functional diversity (Gautier et al., 2012). They are called differently depending on their tissue in which they reside. For instance, osteoclast are bone macrophages, alveolar macrophages are found in the lungs and Kupffer cells are the resident macrophages present in the liver. Macrophages are the first sensors and responders to any change or external stimuli and play crucial and diverse roles in the body.

II-3. Ontogeny of Macrophages

In 1960s, Van Furth proposed that all tissue macrophages were originated from the circulatory adult blood monocytes that migrate into tissues under a variety of stimuli. This observation prevailed for years before the emerging of new evidence that showed that tissue macrophages could be also independent from blood monocytes (van Furth & Cohn, 1968; Volkman et al., 1983). In the last few years, accumulating results have drastically revised the understanding of macrophages in regards to their origin. Two discoveries have weakened the notion that macrophages are only derived from only blood monocytes. First, macrophages were found to be originated from embryonic progenitors that seed developing tissues before birth and give rise to fetal tissue macrophages (Ginhoux et al., 2010; Schulz et al., 2012). And second, tissue resident macrophages have the self-renewal and self-maintenance capabilities through local proliferation (Gentek et al., 2014).

During embryogenesis, there are two phases of hematopoiesis: primitive and definitive hematopoiesis. The former takes place in the yolk sac and give rise to macrophages independently from monocytic progenitors where at this stage, red blood cells and only macrophages from the white blood cells are produced due to the restriction of progenitors in the yolk sac,

Figure **2** (Samokhvalov et al., 2007). And the latter takes place in the fetal liver, which acts as the major hematopoietic organ, by hematopoietic stem cells (HSCs). The fetal liver becomes the source of circulating monocytes. However, HSCs from the bone marrow become the primary site of hematopoiesis only in the perinatal period and thus give rise to other immune lineages (Orkin & Zon, 2008). Thus, macrophages in the fetal and adult tissues are originated from the yolk sac, fetal liver and bone marrow, Figure 2.

During embryogenesis and adulthood, macrophage precursors seed the tissues in different dynamic waves varying between organs, age and macrophage subsets giving rise to resident macrophages (S. Gordon & Taylor, 2005; Varol et al., 2015). In some organs such as the brain, lung and liver, resident macrophages named microglia, alveolar macrophages and Kupffer cells, respectively, originate during embryogenesis and are maintained in the adulthood by self-renewal. However, in other organs such as the colon, skin and heart, most macrophages are replaced by the differentiation of monocyte precursors during hematopoiesis giving rise to monocyte-derived resident macrophages.

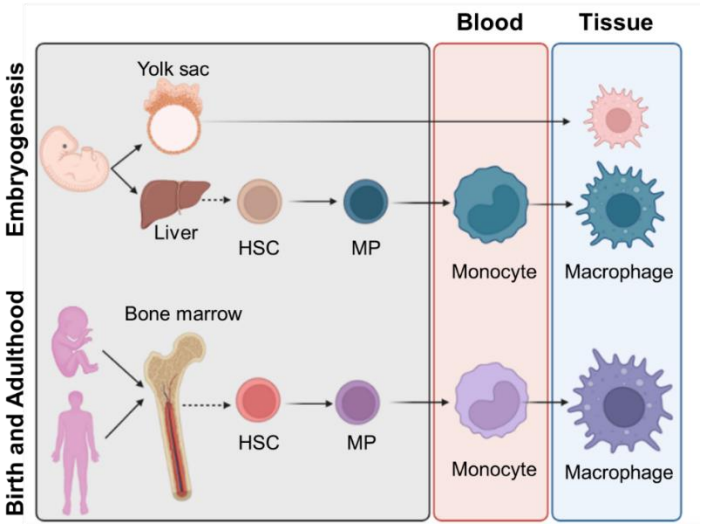

Figure 2 Ontogeny of Macrophages

Tissue macrophages are originated from the yolk sac or fetal liver during embryogenesis or from the bone marrow after birth and adulthood. Hematopoiesis occurs in the fetal liver and bone marrow and is a process that generates tissue circulatory monocytes from hematopoietic stemm cells (HSCs) after which monocytes infiltrate the tissues and differentiate to macrophages. However, macrophages which are derived from the yolk sac are differentiated into the tissues independently from circulatory monocytes. HSC: Hematopoeitic stem cell. MP: monocyte progenitor.

II-4. Functions of Macrophages

In addition to the unique functions that they possess which is specific to the tissue in which they are residing, macrophage operate several important functions in almost every biological aspect starting from development, homeostasis, antigen presentation and driving immune response to active control of inflammation resolution and wound healing. Since they are present in all tissues, macrophages act as a homeostatic ‘’organ’’ (Okabe & Medzhitov, 2016). In normal physiological state as well as after tissue damage, they regulate tissue homeostasis by acting as sentinels and responding to any challenging stimulus. They are one of the main antigen-presenting cells (APCs) which aid in the activation of the adaptive immunity compartment (Allavena et al., 2008; N. Fujiwara & Kobayashi, 2005).

In regards to inflammation, its resolution is crucial not only for the termination of the inflammatory response but also for the maintenance of the tissue integrity. Macrophages play a role in resolving inflammation by functioning in the clearance of apoptotic cells. It is known that a bunch of cells undergo apoptosis in our body, these cells should be cleared away to maintain the physiological state of a tissue. This process is known as efferocytosis, where macrophages are its key player, and serves as a waste disposal as well as a resolving and termination of inflammation mechanism (Goren et al., 2009). It was shown that macrophages engulf neutrophils and erythrocytes in spleen and liver resolving problems of neutropenia, splenomegaly and reduced body weight (Gordy et al., 2011).

Moreover, macrophages coordinate processes that are implicated in tissue formation of the extracellular matrix and new blood vessels through angiogenesis (Wynn et al., 2013). Not only they instruct angiogenesis in normal vessel formation, wound healing and development, but macrophages also regulate angiogenesis in cancers and inflammatory conditions (De Palma & Lewis, 2013).

It has been clear for years now that macrophages are key mediators in the context of solid tumor. Their functions within the TME will be described and reviewed in details in the next part of the introduction.

II-5. Plasticity of Macrophages

Differentiation of Tissue Macrophages

Macrophages exhibit diverse and tissue-specific phenotypes and functions. During the process of tissue macrophage differentiation, a macrophage progenitor receives a tissue-identity signal promoting its local differentiation into a tissue-resident and specific macrophage (Okabe & Medzhitov, 2016). Subsequently, this tissue-resident macrophage receives signals reporting local functional aspects. This confers a specific polarization or activation phenotype to the macrophage Figure 3. Once the functional demand is met, the signal which induced it as well as the activation phenotype that this macrophage acquired will subside allowing the macrophage to return to its initial state so that it is ready to respond to other stimuli and demands.

Results from transplanting peritoneal macrophages to the alveolar cavity resulted in modifications of some gene expression from peritoneal-macrophage signature towards an alveolar-macrophage signature where some gene expression of peritoneal macrophages were retained (Lavin et al., 2014). This illustrates the presence of irreversible and reversible programs that a macrophage encounters for its differentiation and polarization, respectively.

Figure 3 The Phenotype of Macrophages: a Product of Differentiation and Polarization

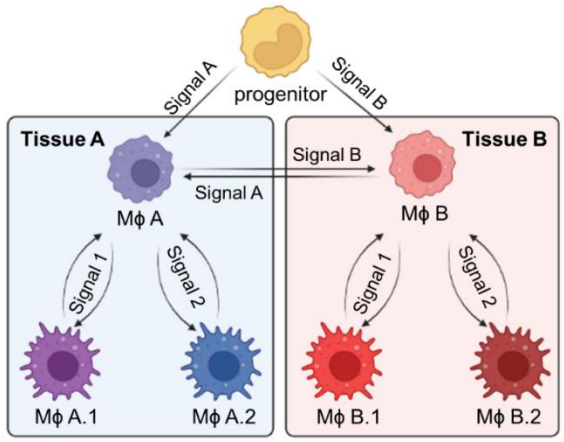

A macrophage progenitor infiltrates a tissue and differentiate into a macrophage as a consequence of the tissue-specific signal that it encounters. This tissue macrophage can be polarized into different states depending on the different signal that is stimulated. Mϕ: macrophage.

Polarization of Macrophages

Macrophages exhibit a plastic phenotype which is a product of its differentiation and polarization. Accordingly, differentiated macrophages can then be activated and characterized into different phenotypes based on different stimuli that they encounter (Okabe & Medzhitov, 2016). From this concept, the M1/M2 dichotomy of macrophages emerged (Murray, 2017).

Indeed, a macrophage polarization refers to the activation state of these cells at a single time point (Cassetta et al., 2011). But due to their plasticity, the activation state that macrophages have acquired is not fixed and can be altered and changed to a different one based on the integration of multiple signals from the microenvironment. Thus, a M2 macrophage can be reprogrammed to a M1 macrophage and vice versa. This is dependent on environmental changes that a macrophages sense such as cytokines and growth factors secretions, inflammation and injury as well as hypoxia and the physical environment.

Classically activated macrophages, known as M1 macrophages, are typically induced by Th1 cytokines including lipopolysaccharide (LPS), Interferon gamma (IFN-γ) and tumor necrosis factor alpha (TNF-α) (Bashir et al., 2016; Locati et al., 2013). These macrophages are said to be pro-inflammatory as they secrete high levels of proinflammatory cytokines including IL-6, IL-12, IL-23 and TNF-α (Verreck et al., 2004). They also aid in activating type-1 T cell (Th1) response. At the metabolic level point of view, M1 macrophages favor glycolytic metabolism as well as NADPH, lipids and nucleotides synthesis. Accordingly, during infections, they play a role in eliminating the pathogen through the activation of nicotinamide adenine dinucleotide phosphate (NADPH), production of nitric oxide (NO) which acts as an inflammatory mediator as well as the generation of reactive oxygen species (ROS). Moreover, not only M1 macrophages have a robust anti-microbial activity but in the context of cancer, they also exert an anti-tumoral activity. Additionally, as a result of these functions, M1 macrophages mediate ROS-induced tissue damage and impair tissue regeneration and wound healing. In humans, these macrophages are identified by their expression of CD86 and CD64 at their surface (Stöger et al., 2012). This inflammatory response as well as the tissue damage are usually protected and reverted by their opposing subset: M2 macrophages.

M2 macrophages which are also known as alternatively activated macrophages are anti-inflammatory macrophages which are polarized by Th2 cytokines including IL-4, IL-13 and IL-10. While IL-4 and IL-13 govern M2 polarization via activating STAT6 pathway through IL-4 receptor, IL-10 drives this polarization by the activation of STAT3 pathway via IL-10 receptor (Porta et al., 2015). Contrary to M1 macrophages, M2 macrophages are characterized by the low production of IL-12 and high production of IL-10 and TGF-β, both which exert immunosuppressive functions. Regarding their functions, M2 macrophages play a role in Th2 immunity and clearance as they phagocytose debris and apoptotic cells dampening the inflammatory response. They aid in tissue remodeling and repair as well as wound healing as they

possess pro-angiogenic and pro-fibrotic functions. In the context of cancer, Conversely to metabolic signature of M1 macrophages, M2 macrophages are associated with oxidative phosphorylation. Concerning cancer, M2 macrophages are known to be pro-tumoral as they secrete immunosuppressive cytokines that suppresses the anti-tumoral functions of CD8+ T cells and NK cells, orchestrate angiogenesis through secretion of VEGF and promote metastasis (Jetten et al., 2014). M2 macrophages are identified by an increase expression of CD206, CD163 and TGM2 (Jaguin et al., 2013). The M1/M2 dichotomy of macrophages is summarized in Table 1.

The distinct phenotypic subsets of macrophages are not simply reflected by M1/M2 phenotypes but rather by the activation stimulus being exerted on these cells. Thus, M2 macrophages are further subdivided into four different subsets as such: M2a, M2b, M2c and M2d (Mantovani et al., 2004). IL-4 and IL-13 induce the M2a subset which in turn produces high levels of CD206, decoy receptor IL-1 receptor II (IL-1RII) and IL-1 receptor antagonist (IL1Ra). On the other hand, M2b subset produces both pro-inflammatory and anti-inflammatory cytokines including IL-1β, IL-6, TNF-α and IL-10, respectively. This subset is activated by the stimulation with immune complexes (ICs) as well as Toll-like receptor (TLR) agonists or IL-1 receptor ligands. M2c subset is activated by IL-10 and glucocorticoids exhibiting anti-inflammatory functions against apoptotic cells through the secretion of immunosuppressive cytokines IL-10 and TGF-β. Last, M2d macrophages are induced by TLR agonists and adenosine and suppress the production of pro-inflammatory cytokines and favors the secretion of anti-inflammatory cytokines as well as VEGF supporting angiogenesis.

Table 1 Macrophage Polarization States

Macrophage Polarization State	**Classically Activated** **M1 Macrophage**	**Alternatively Activated** **M2 Macrophage**
Stimuli driving the polarization	LPS, IFN- γ and TNF- α	IL-4, IL-13 and IL-10
Secretions	IL-6, IL-12, IL-23 and TNF- α	IL-10 and TGF-β VEGF
Surface Markers	CD86, CD64	CD206, CD163, TGM2
Functions	• Pro-inflammatory • Anti-tumoral • Anti-microbial • Tissue damage • Impairement of tissue regeneration and wound healing • Glycolysis	• Anti-inflammatory and immunosuppressive • Pro-tumoral • Phagocytosis and efferocytosis • Angiogenesis and metastasis • Tissue remodeling and repair • Oxidative phosphorylation

III. Tumor Associated Macrophages (TAMs)

III-1. Ontogeny of TAMs

The characterization of macrophages based on their ontogeny in a physiological state, had raised the question of the origin of macrophages at the tumoral sites. TAMs were first considered to be originated exclusively from blood monocytes through tissue infiltration by chemotaxis. However, their origin was reconsidered in several tumor types (Bowman et al., 2016; Loyher et al., 2018; Zhu et al., 2017).

Circulating blood monocytes are recruited to the tumor by multiple factors secreted by stromal and tumoral cells in TME including chemokines such as CCL2 and cytokines such as colony stimulatory factor – 1 (CSF-1) as well as members of the VEGF family (Franklin et al., 2014). Some results seem to show that in most tumor models in mice, blocking the CCL2/CCR2 axis, which is a main axis that fuels monocyte trafficking, decreased the infiltration and the abundance of TAMs (Mondini et al., 2019). These studies favored the idea that TAMs originate mainly from bone-marrow derived monocytes expressing CCR2.

Additionally, myeloid-derived suppressor cells (MDSCs), which are a type of myeloid leukocytes related to immunosuppression, were known as another main circulating precursor of TAMs (Bronte et al., 2016).

Based on the tumoral tissue localization, the roles of TAMs, either monocyte-derived or embryonic-derived, remain to be fully understood.

III-2. TAMs in a Hypoxic TME

Hypoxia, a major feature in the TME

During the development and progression of a tumor, both cancerous cells and stromal cells have restricted access to nutrients and oxygen (Pouysségur et al., 2006). This is mainly due to the fact that the majority of solid tumors are subjected to hypoxia due to the redundant cellular expansion, aberrant vascularization resulting in a poor blood supply. Some years ago, hypoxia became more appreciated as a critical environmental feature within the TME. (Mazure et al., 1996; Shweiki et al., 1992).

When hypoxia is present, cells within the TME should respond in order to restore the availability of oxygen. This is reflected by various responses such as the induction of angiogenesis and metabolic reprogramming of cells, recruitment other cells as well as proliferation and autophagy. These mechanisms that counteract the shortage of oxygen contribute to a hostile tumor microenvironment and fosters tumor progression.

Hypoxia-driving mechanisms

A tumor becomes hypoxic as a consequence of the oxygen supply and consumption in which the pressure of oxygen drops to a median of 0 – 20 mmHg which is approximately 1 – 2 % or below. In normal tissues, the oxygen tension is around 5 % in liver and 13 % in blood (Vaupel et al., 1989).

Tumor hypoxia could be mediated by several mechanisms within TME. First is the perfusion-restricted hypoxia which is an acute transient and cyclic form of hypoxia that is mediated by the insufficient oxygen delivery (Vaupel & Harrison, 2004). This is resulted by fluctuations of oxygen supply due to aberrant blood vessels undergoing opening and closing. Diffusion-restricted hypoxia is another mechanism present in tumors. It is also known as chronic or permanent hypoxia that is characterized by sustained restriction in oxygen diffusion. It usually occurs due to the inadequate delivery of oxygen when a tumor expands beyond the nutritive blood vessels. Hypoxic tumors can also develop following a reduction in oxygen transport capacity by the blood, a mechanism known as anemic hypoxia.

Hypoxia Inducible Factors

During low oxygen levels, several cellular responses, which will be briefly stated and described in this chapter, are modulated. These events are influenced by the oxygen availability and genes encoding Hypoxia-inducible factor (HIF) and von Hippel Lindau protein (pVHL) (Forsythe et al., 1996; G. L. Wang et al., 1995). The HIFs are a family of heterodimeric transcription factors HIF1, HIF2 and HIF3 which consist of labile oxygen sensitive alpha subunit (HIFα) known as HIF-1α, HIF-2α and HIF-3α, respectively, and a constitutively expressed β subunit (Kaelin & Ratcliffe, 2008; Semenza, 2010).

In normal oxygen levels, normoxia, the heterodimer between the two subunits is usually dissociated (Dabral et al., 2019). This dissociation is in part dictated by an pVHL-dependent degradation mechanism where hydroxylation of two proline residues, 402 and 562, in the HIF-1α subunit is mediated by the prolyl hydroxylase (PHD) triggering the recognition of HIF-1α by E3 ubiquitin ligase, pVHL, ensuring its proteosomal degradation as illustrated in Figure 4 (Jaakkola et al., 2001; Majmundar et al., 2010).

Moreover, studies have shown that mutations in VHL, gene encoding the protein pVHL, mediated the bypassing of ubiquitination degradation of HIF-1α conferring its stabilization in normoxia (Maxwell et al., 1999). Additionally, HIF-1α is also regulated independently from pVHL, by the induction of factor inhibiting HIF (FIH) which leads to the hydroxylation of an aspargine residue preventing the localization of HIF-1α with the co-activators p300 and CBP and thus disabling the resulting transcriptional activation (Masoud & Li, 2015).

In contrast, under hypoxic conditions, PHDs fail to hydroxylate the proline residues of HIF-1α and pVHL is unable to mediate its degradation (Foster et al., 2014). This leads to the stabilization of HIF-1α. Not only hypoxia stabilizes HIF-1α, but HIF-2α as well (Franovic et al., 2009). Once stabilized, HIF-1α translocates to the nucleus where it dimerizes with HIF-1β forming the active HIF-1 that in turn binds to the hypoxia-responsive elements (HREs) regulating the expression of various target genes (Zimna & Kurpisz, 2015).

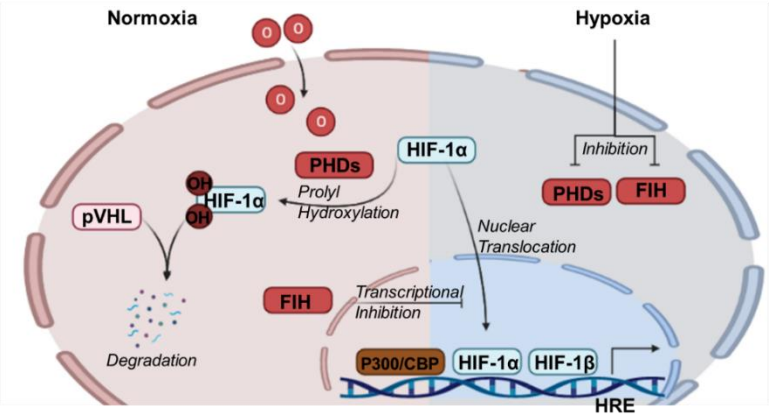

Figure 4 Modulation of Hypoxia Inducible Factor 1 α at Normal or Hypoxic Conditions

Under normal oxygen levels, Prolyl hydroxylation of HIF-1α is conferred by PHDs. This will allow the recognition of hydroxylated HIF-1α by pVHL which displays the ubiquitination activity mediating its degradation. Moreover, under normal oxygen levels, FIH is activated and it inhibits the translocation of HIF-1α and its coupling to p300/CBP and HIF-1β thus inhibiting the transcription of HIF targets. On the other hand, when levels of oxygen decrease, HIF-1α is stabilized due to the inhibition of PHDs and FIH. This permits the translocation of HIF-1α, its coupling to P300/CBP as well as its dimerization with HIF-1β mediating the transcription of its targets. HIF-1: Hypoxia Inducible Factor – 1 , PHDs: Prolyl Hydroxylase, pVHL: Von Hippel Lindau protein, FIH: Factor Inhibiting HIF, HRE: Hypoxia responsive element.

Outcomes of Hypoxia on the Tumor-Associated Macrophages

Immune cells are a major population of cells apart from the cancerous cells in the TME. Hypoxia has the tendency to modulate various immune cells facilitating immunosuppression and thus promoting the aggressiveness of a tumor.

Several results revealed that macrophages infiltrate hypoxic regions within TME. This is mainly mediated by their recruitment through several hypoxia-induced chemoattractants such as semaphorin 3A (Sema3A), endothelial-monocyte-activating polypeptide II (EMAPII), stromal cell derived factor 1α (SDF1α), CCL2, CCL5 and M-CSF which are secreted by the hypoxic tumoral or stromal cells (Casazza et al., 2013; Murdoch et al., 2004; Tripathi et al., 2014). Once

macrophages infiltrate and become associated with the tumoral region, their mobility is reduced. This is a consequence of hypoxia-dependent mechanisms which are explained by the decrease in expression of CCR2 and CCR5 in macrophages resulting in the disruption of their signaling pathway trapping TAMs in the hypoxic tumoral areas (Bosco et al., 2004).

Hypoxia was evidenced to confer the immunosuppressive and pro-tumoral functions of TAMs. Hypoxic TAMs can promote angiogenesis by directly upregulating the expression of VEGFs and its receptor or upregulating the angiogenic modulators such as matrix metalloprotease 7 (MMP7) which in turn enables the migration and invasion of tumoral cells (Burke et al., 2003; Casazza et al., 2013) . Moreover, tumoral cells expressing high levels of endothelin 1 and 2 assist the release of MMP2 and MMP9 from macrophages promoting the TAM-dependent migratory response (Grimshaw et al., 2004).

Besides, hypoxia plays a fundamental role in immunosuppression and evasion indirectly through their effect on TAMs which in turn affects other immune cells. For instance, the increase secretion of IL-10 and prostaglandin E2 by tumoral cells halts the immune response by promoting the immunosuppressive role of TAMs (Alleva et al., 1993) Additionally, TAMs cultured with hypoxic tumoral cells were shown to increase the expression of indoleamine 2,3-dioxygenase (IDO) which results in the inhibition of the proliferation of T cells (L.-Y. Ye et al., 2016).

Indeed, it was demonstrated in our lab that hypoxia modulates the biology of macrophages (Court et al., 2017). Aiming to explore the molecular signature of macrophages of different activation states in normoxic incubators (18.6% oxygen) versus hypoxic incubator (3% oxygen), proteomic results revealed the presence of polarization-specific and oxygen-sensor proteins in macrophages. For instance, arachidonate 15-lipooxygenase (ALOX15), which is a M(IL4, IL13) polarization – specific protein was upregulated under hypoxic conditions and associated with increased apoptotic cells phagocytosis . These results are crucial to better understand the biological behaviors of macrophages in real healthy and tumoral tissues.

III-3. TAMs and Metabolism in TME

TAMs and TME – A Bidirectional Metabolic Relationship

As noted earlier, macrophages exert distinct functions and are characterized by their plasticity. On that account, their metabolic profile is dynamic and important within TME. The metabolic influence of cancerous cells on TAMs is not unidirectional but rather there exists a bidirectional metabolic relationship. This bidirectional relationship is illustrated in Figure **5**.

CSF1 is one of the major cytokines that recruits monocyte-derived macrophages to the tumoral site and favors their polarization toward an M2-like phenotype (DeNardo et al., 2011). This was shown to be coupled to the upregulation of fatty acid oxidation (Park et al., 2015) and the secretion

of a variety of immunosuppressive and pro-tumoral factors such as EGF (Wyckoff et al., 2004) and IL-10. The secretion of CSF1 and VEGFA is dependent on the environmental cues such as pH and hypoxia.

Hypoxia, is usually associated to increased lactate availability. Cancerous cells undergo glycolysis metabolizing glucose into lactate which is believed to be elevated in hypoxic TME. Lactate metabolism is crucial for the reeducation of TAMs by hypoxic TME toward a pro-tumoral M2-like phenotype that display poorly glycolytic profile and upregulation of fatty acid oxidation (Colegio et al., 2014; N. Liu et al., 2019).

On top of that, increased lactate availability aids in the catabolism of arginine by arginase 1 (ARG1) and ARG2 in TAMs leading to the synthesis and polyamines which are tumor-supporting factors (Carmona-Fontaine et al., 2017). On the contrary, these TAMs have decreased expression of nitric oxide synthase (NOS2), that acts oppositely to arginases, which produces anticancer mediators such as nitric oxide and citrulline.

Subsequently, TAMs exposed to hypoxia, conferred by lactate availability, secrete various cytokines possessing metabolic functions such as IL-6, TNF, CCL5 and CCL18. IL-6 advocates glycolysis by facilitating the phosphorylation of phosphoglycerate kinase (PGK) by 3-phosphoinositide-dependent protein kinase (PDPK1). TNF, CCL5 and CCL18 enhance the synthesis of multiple factors that promote glycolysis including HCK2, PGK1, lactate dehydrogenase A (LDHA), pyruvate kinase, pyruvate dehydrogenase kinase 1 (PDK1), pyruvate dehydrogenase (PDH), glucose-6-phosphate dehydrogenase (G6PD) as well as SLC2A1 (Jeong et al., 2019; S. Lin et al., 2017; H. Ye et al., 2018).

Figure 5 Metabolic Crosstalk between Tumor Associated Macrophages and the Tumor Microenvironment

Tumoral cells rely on glycolysis and nutrients biosynthesis for their proliferation. Performing glycolysis, they release elevated levels of lactate to the TME which is also mediated by Hypoxia. Moreover, CSF1 is also released and plays a role in attracting TAMs towards TME. Both CSF1 and lactate promote the reprogramming of M1-TAMs into M2-TAMs. This provides a tumor promoting environment since M1-TAMs mediate glycolysis releasing increased amounts of ROS and NOS2 which have a tumoricidal effect. Contrary to that, M2-TAMs are associated to increased OXPHOS, FAO and ARG1/2 expression. Collectively, their metabolic profile lead to increased lactate production as well as EGF, TNF, IL-6, CCL5 and CCL18 which facilitate the advocates tumor glycolysis. Moreover, M2 TAMs favors a hypoxic TME which in turn facilitates the progression of the tumor.

Metabolism of Glucose

TAMs depend on glycolysis to infiltrate tumoral regions and their production of ATP sustains their motility (Kes et al., 2020; Zheng et al., 2020). TAMs underwrite tumor progression by increasing the nutrients that the TME needs and mediating robust immunosuppressive functions. Hypoxia was shown in *in vivo* mouse tumor model to upregulate the expression of DNA damage inducible

transcript 4 (DDT4) which is an inhibitor of mechanistic target of rapamycin complex 1 (mTORC1) (Wenes et al., 2016). This results in an increased oxidative phosphorylation coupled to a decrease in glucose intake leading to increased glucose availability in the TME which in turn facilitates neo-angiogenesis. Additionally, human TAMs display lower glyceraldehyde 3-phosphate dehydrogenase (GAPDH) and succinate dehydrogenase (SDH) activity (Miller et al., 2017).

Metabolism of Amino Acids

Alongside their inadequate glycolytic profile, M2-like TAMs display increased consumption of glutamine which is explained by high levels of glutamine transporters and metabolic enzymes (Choi et al., 2015). The glutamine/glutamate pathway is essential for TAMs for energetic requirements. For instance, glutamate-ammonia ligase (GLUL), also known as glutamine synthetase (GS), catalyzes the conversion of glutamate into glutamine and its inhibition favors the repolarization of TAMs towards a M1-like phenotype followed by increase in glycolytic flux and succinate availability (Palmieri et al., 2017).

Lactate derived from the tumors induces the expression of ARG1 in TAMs via ERK1/2/STAT3 and HIF-1α stabilization (Mu et al., 2018; L. Zhang & Li, 2020). ARG1 enhances the production of ornithine and polyamines stimulating M2 genes and mediating the pro-tumoral role of TAMs (Rabold et al., 2017).

Moreover, TAMs express IDO which allows the deprivation of tryptophan and thus contribute to an immunosuppressive microenvironment by acting on suppressing the T-cell response (Zhao et al., 2012). Additionally, upon reducing tryptophan, IDO catalyzed the transformation of tryptophan to kynurenine that exerts a negative influence on the proliferation of T cells (Mezrich et al., 2010).

Metabolism of Fatty Acids

Tumor tissues are characterized by aberrant activation of de novo lipogenesis reflected by elevated expression of fatty acid synthase (FASN), acetyl-CoA carboxylase (ACC) and ATP citrate lyase which collectively promote the tumor progression (Baenke et al., 2013). The metabolism of fatty acids shape TAMs whereby M2-like TAMs exhibit elevated consumption of fatty acids. This is due to IL-4 – driven activation of signal transducer and activator of transcription 6 (STAT6) accompanied by increased fatty acid oxidation (Vats et al., 2006). Furthermore, results from *in vivo* murine models showed that inhibition of fatty acid oxidation switched the polarization of TAMs towards M1-like phenotype (Hossain et al., 2015).

Moreover, in renal carcinoma, results have revealed that TAMs produce high levels of eicosanoids through the activation of 15-lipoxygenase-2 (15-LOX-2) which acts as a regulator of lipid

homeostasis as well as to the mediation of increased expression of CCL2 and IL-10 in TAMs conferring immune tolerance (Daurkin et al., 2011; Snodgrass & Brüne, 2019).

III-4. Targeting TAMs in TME

Evidence have shown that the abundance of TAMs in the TME is usually correlated with poor prognosis as well as resistance to treatments and therapies (S. R. Gordon et al., 2017). Proceeding with that, targeting TAMs is considered as a promising immunotherapeutic strategy which can be achieved by various ways which are briefly mentioned below.

One way to decrease the accumulation of TAMs in the TME is to limit the infiltration of monocyte-derived macrophages in the tumoral region. As mentioned earlier, macrophages are recruited to tumor areas via chemokines such as CCL2, CCL5, CXCL12 and CSF-1 (Franklin et al., 2014), thus inhibiting these signals by antagonizing either the ligands or their receptors on macrophages have gained interest in today's research fields and have shown a potential therapeutic value in several tumors (Ngambenjawong et al., 2017). For instance, inhibition of CCL2 resulted in a reduction in the tumor burden as well as metastasis in different tumor models including breast, prostate, mung and liver cancers (M. Li et al., 2013).

As a result of the studies that showed that high levels of CCL2 was in serum and tumoral sites were associated with poor prognosis in solid tumors such as breast cancer (Lebrecht et al., 2004), two main drugs, carlumab (CNTO 888) which is a CCL2-neutralizing antibody and PF-04136309 which is a small molecule inhibitor targeting CCR2, are being tested in clinical trials. Carlumab reduced the recruitment of CD68+ macrophages and tumor growth in a prostate cancer mouse model (Loberg et al., 2007). A phase I clinical trial was carried out in 44 patients to study the tolerance to various carlumab doses by which results concluded that carlumab is well tolerated accompanied by a 1000 fold increase of free CCL2 compared to baseline (Sandhu et al., 2013, p.). Following, a phase II clinical trial was carried out in patients with castrasian-resistant metastatic prostate cancer and results did not report any therapeutic efficacy of carlumab as a single anti-tumor agent as it did not block the CCRL2/CCR2 axis. On the other hand, PF-04136309, in combination with FOLFIRINOX chemotherapy, was assessed in a phase Ib clinical trial in patients suffering from pancreatic cancer to establish the safety, tolerability and the recommended phase 2 oral dose (Nywening et al., 2016). 47 patients were recruited for the study by which 39 of them received the combination therapy whereas 8 patients had only FOLFIRINOX. Results showed that the combination treatment is safe and well tolerated where an objective tumor response was observed in 49% of patients compared to no objective response in those who only received FOLFIRINOX.

Second approach to target TAMs is to selectively deplete TAMs. This is achieved by engaging the apoptosis of these cells using clodronate liposomes, zoledronic acid and trabectedin (Zheng et al., 2017). These bisphosphonates were reported to inhibit the proliferation and migration of macrophages leading to their programmed death (Rogers & Holen, 2011). Moreover, targeting the

CSF1R signaling became an attractive target to deplete TAMs due to the important functions that this signaling play in macrophages. This will be shed lights on and explained further in chapter III.

Further to this, macrophages reprogramming was shown to be efficient in therapies. Repolarizing macrophages towards a M1 like phenotype renders the immune system activated and deliberate the anti-tumoral effect. This is usually mediated by several inhibitors such as PI3K inhibitors, RON inhibitor and ANG-2 receptor inhibitor (Kaczanowska et al., 2013; Kaneda et al., 2016; Nowak et al., 2015; Peterson et al., 2016; Sharda et al., 2011).

In addition, using agonists for CD40, which is a member of TNF receptor family, was shown to exert tumor inhibitory effects in several tumor mice models and using these agonists in combination with anti-CSF1R antibodies resulted in reprogramming of TAMs creating a pro-inflammatory environment (Hoves et al., 2018). As a result, CP-870,893, an agonist to CD40 antibodies is being tested in clinical trials. Treating patients with solid tumors with CP-870,893 was well tolerated and lead to an objective response and anti-tumor activity (Vonderheide et al., 2007).

Furthermore, emerging from the fact that activation of Toll-like receptors (TLRs) polarizes macrophages towards a pro-inflammatory phenotype, several TLR synthetic ligands have been tested in several cancer models (Kaczanowska et al., 2013). Results have revealed that agonists of TLR7 and TLR8 (3M-052) in melanoma induced the repolarization of macrophages which was accompanied by a better tumoricidal activity (Singh et al., 2014). Regarding clinical trials, two TLR7 ligands, 852A and imiquimod, as well as one TLR9 ligand, IMO-2055, are being tested. A phase I clinical trial of 852A on patients with advanced tumors was well tolerated and showed reversible side effects (Dudek et al., 2007). Also, in a prospective clinical trial of a skin metastasis breast cancer, Imiquimod was tested and resulted in a an increased lymphoid immune infiltration along with tumor regression (Adams et al., 2012). Last but not least, IMO-2055 in combination with erlotinib and bevacizumab was tested in clinical trials on patients suffering from advanced metastatic non-small cell lung cancer (NSCLC) where results showed good tolerability with a potential antitumor activity (Smith et al., 2014).

Adding to this, several other treatments were shown to reprogram M2 macrophages to M1 macrophages favoring the anti-tumoral effect. These mediate the inhibition of IL10, TGF-β and IDO which were shown to overcome the resistance to immunotherapy (Sharma et al., 2017). Other tyrosine kinases such as sorafenib was reported to reprogram macrophages to M1 followed by the downregulation of IL-10 secretion.

Nevertheless, CD47, is expressed on cancerous cells and this moderates the ’DON’T EAT ME’’ signal which blocks the phagocytic ability of macrophages by interacting with SIRP-α expressed on macrophages (Matlung et al., 2017). Blocking the CD47-SIRPα signaling axis pilots the phagocytosis of cancerous cells by TAMs and enhances the CD8+ T cell response (X. Zhang et al., 2018).

Chapter II

Hypoxic TAMs and Chemoresistance in Colorectal Cancer

Chapter Two – Part One

Introduction

I. Colorectal Cancer

Colorectal cancer (CRC) is reckoned as one of the main diagnosed cancers in the world and it accounts for a large percentage of cancer-related deaths worldwide (Bray et al., 2018). In women, it is considered as the second frequently diagnosed cancer while it is the third most common in men. Several factors are associated with the incidence of CRC (Dekker et al., 2019). These include hereditary factors as well other environmental factors such as smoking, food diet, body fat and obesity as well as diseases such as type – 2 diabetes and inflammatory bowel syndrome.

Depending on the stage of CRC tumors, several treatment strategies are followed. In addition to the surgical treatment which are considered as cornerstone of curative intent treatment, several classes of drugs inhibitors have been studied and evaluated as single or multiple treatment regimens (Veenstra & Krauss, 2018). These involve chemotherapeutic agents such as fluorouracil or capecitabine and oxaliplatin, biologics such as bevacizumab which is an anti-VEGF monoclonal antibody as well as immunotherapies and kinase inhibitors. In this context, 5-fluorouracil represents one of most effective and commonly used chemotherapeutic agent in treating CRC (Blondy et al., 2020). However, several patients develop chemoresistance against 5-FU and this is due to several parameters employed in the TME.

In this chapter, I will focus on 5-FU and its metabolism in the body which reflects its activity and response. Moreover, the aftermost focal point of this chapter will be on dihydropyrimidine dehydrogenase (DPD) which is an enzyme that catabolizes fluorouracils and plays a role in chemoresistance against 5-FU.

II. 5-Fluorouracil (5-FU)

II-1. 5-FU Treatments in Tumors

In 1954 Rutman, Cantarow and Paschkis demonstrated that uracil is swiftly incorporated into rat hepatomas compared to non-malignant tissues (Rutman et al., 1954). Owing to the finding that uracil is preferentially taken up by the tumor, and due to the fact that carbon-F is stable, 5-fluorouracil (5-FU) was first synthesized by Heidelberger and his colleagues (Heidelberger et al., 1957). 5-FU is a fluorinated analogue of uracil where a hydrogen atom is substituted by fluorine at the fifth carbon in the 5-FU molecule (Vértessy & Tóth, 2009).

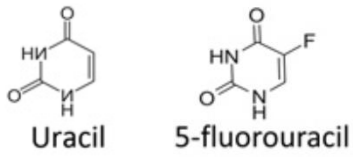

Figure 6 Chemical Structure of Uracil and 5-fluorouracil

5-FU is a chemotherapeutic drug that is commonly applied to various malignant tumors such as breast, esophageal, stomach, pancreatic as well as head and neck tumors (Vodenkova et al., 2020). Moreover, 5-FU is the centerpiece of CRC treatment either administered orally or intra-venously where it is intracellularly converted into its active metabolites (Sargent et al., 2009).

Despite being one of the safest drugs, some side effects and toxicities result in a proportion of CRC patients (Vodenkova et al., 2020). This is demonstrated by fatigue, fever, nausea, vomiting, diarrhea, mucositis and stomatitis. Other toxic effects encompass anemia, leukopenia, thrombocytopenia, neutropenia as well as neuropathy. Recently, treatment with 5-FU alone has been ceased and it was modulated biologically to improve the therapeutic effectiveness as well as the cytotoxicity (Chionh et al., 2017). In that concern, Leucovorin (LV, Folinic acid) was used in combination with 5-FU to protect from the cytotoxic effects caused by 5-FU. Additionally, to increase the efficacy of the treatments, 5-FU/LV is combined with oxaliplatin and/or irinotecan as FOLFOX and FOLFIRI, respectively (Gustavsson et al., 2015; Tournigand et al., 2004). Oxaliplatin is a diaminocyclohexane platinum complex that forms DNA adducts. Irinotecan plays a role in inhibiting the topoisomerase I during replication which leads to double strand breaks and thus cell death. These combination therapies have become noticed as the most efficacious cytotoxic treatment strategies in metastatic CRC that resulted in better response and survival.

II-2. Mechanism of Action of 5-FU – Anabolism

5-FU was one of the first drugs discovered to exhibit an anti-tumoral effect (Heidelberger et al., 1957). This is mainly conciliated by its action on inhibiting thymidylate synthase (TS) resulting in a disruption in the deoxynucleotide pools which are essential for DNA replication (Daher et al., 1990; Horowitz & Chargaff, 1959).

5-FU by itself does not display any cytotoxic effect (Vodenkova et al., 2020). However, its conversion into active metabolites such as 5-fluorouridine-5'-triphosphate (FUTP), 5-fluoro-2'-deoxyuridine-5'-triphosphate (FdUTP) and 5-fluoro-2'-deoxyuridine-5'-monophosphate (FdUMP) evinces this cytotoxic effect. These are known as anabolic reactions of 5-FU, which only comprose 1-3 % of its metabolism, which are illustrated in details in Figure 7.

Following its entrance into cancer cells, 5-FU is converted to fluorodeoxyuridine (FdUR) by thymidine phosphorylase (TP). FdUR is secondarily phosphorylated by thymidine kinase (TK) into fluorodeoxyuridine monophosphate (FdUMP) which is then phosphorylated to the active metabolite fluorodeoxyuridine triphosphate (FdUTP) through two-phosphorylation steps catalyzed by uridine monophosphate kinase (UMPK) and uridine diphosphate kinase (UDPK). The active metabolite FdUTP is incorporated into DNA instead of 2'-deoxythymidine-5'-triphosphate (dTTP) resulting in DNA damage (Longley et al., 2003).

Alternatively, 5-FU is converted into 5-fluorouridine monophosphate (FUMP). This involves two enzymes: uridine phosphorylase (UP) that converts 5-FU to fluorouridine (FUR) and uridine kinase (UK) that converts the latter to FUMP. Subsequently, UMPK phosphorylates FUMP to fluorouridine diphosphate (FUDP). FUDP has two different fates, it can either be phosphorylated by UDPK to the active metabolite fluorouridine triphosphate (FUTP) which is incorporated into RNA instead of uridine-5'-triphosphate (UTTP) leading to RNA damage or converted to fluorodeoxyuridine diphosphate (FdUDP) by ribonucleotide reductase (RNR). FdUDP is then phosphorylated to the active metabolite fluorodeoxyuridine triphosphate (FdUTP) by UDPK where it facilitates DNA damage as explained in the previous paragraph.

Figure 7 Anabolic Reaction of 5-FU in cancerous cells

5-FU undergoes anabolic reactions in the cancerous cells to facilitate its cytotoxic function. As soon as it enters cancer cells, 5-FU is either converted to FdUR by TP or FUR by UP. FdUR is then phosphorylated by TK to FdUMP which inhibits TS. Moreover, FdUMP can be also phosphorylatedby UMPK to FdUDP which is then phosphorylated to FdUTP by UDPK. FdUTP is an active molecule which leads to damage of DNA. On the other hand, FUR is phosphorylated by UK to FUMP. Subsequently, FUMP is phosphorylated by UMPK to FUDP that can be converted to FdUP by RNR or further phosphorylated to FUTP by UDPK. The active molecule FUTP leads to the damage of RNA. Abbreviations: 5-FU: 5-fluouracil; TP: thymidine phosphorylase; FdUR: fluorodeoxyuridine; TK: thymidine kinase; TS: thymidylate synthase; FdUMP: fluorodeoxyuridine monophosphate; FdUDP: fluorodeoxyuridine diphosphate; FdUTP: fluorodeoxyuridine triphosphate; UP: uridine phosphorylase; FUR: fluorouridine; FUMP: fluorouridine monophosphate; FUDP: fluorouridine diphosphate; FUTP: fluorouridine triphosphate; UMPK: uridine monophosphate kinase; UDPK: uridine diphosphate kinase; RNR: ribonucleotide reductase.

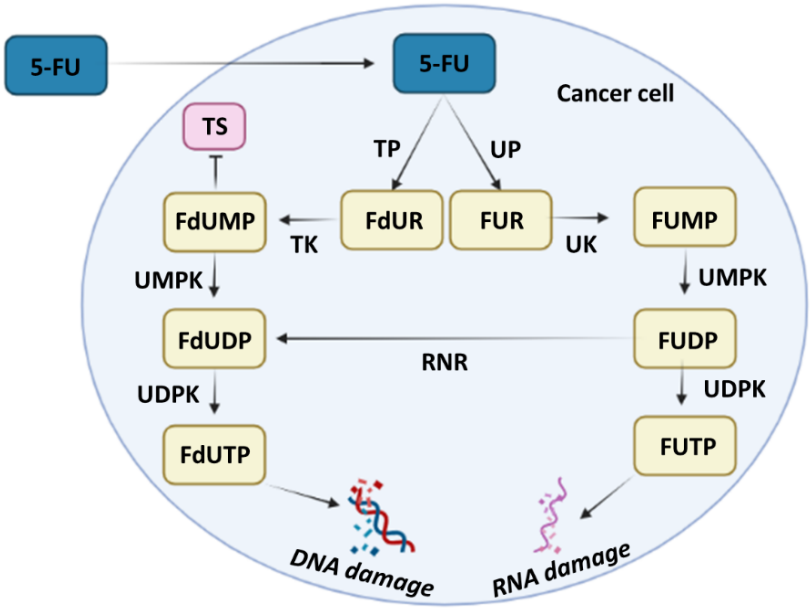

The headmost function that 5-FU plays in cytotoxicity is that it inhibits the activity of TS (Vodenkova et al., 2020), detailed in Figure 8. Normally, TS is an enzyme that catalyzes the conversion of deoxyuridine monophosphate (dUMP) to deoxythymidine monophosphate (dTMP) with the aid of 5,10-methylenetetrahydrofolate (CH2THF) that serves as methyl group donor. dTMP is then phosphorylated consequently to deoxythymidine diphosphate (dTDP) and deoxythymidine triphosphate (dTTP) emulating DNA synthesis and repair.

On the contrary and due to the conversion of 5-FU to its active metabolite FdUMP, the activity of TS is blocked (Miura et al., 2010). FdUMP competes with dUMP by binding to the nucleotide binding site of TS forming a stable ternary complex with it and CH2THF. Eventually, the ternary complex blocks the access of dUMP and thus inhibits the synthesis of dTMP. Correspondingly, imbalance of dNTPs is resulted and dUMP is accumulated which is then phosphorylated to dUTP (Mitrovski et al., 1994). dNTPs imbalance as well as increased dUTPs result in DNA damage (Yoshioka et al., 1987). Hereafter, DNA synthesis is disrupted and thus tumor cell death is induced. Finally, it is worthy to mention that the extent of DNA damage also depends on the levels of deoxyuridine triphosphatase (dUTPase) which hydrolyzes dUTP to dUMP (Tóth et al., 2007) as well as uracil DNA glycosylase (UDG) (Mauro et al., 1993) which can both overcome the increased levels of dUTP decreasing DNA damage. Additionally, dTMP can be salvaged by thymidine kinase (TK) that phosphorylated thymidine into dTMP.

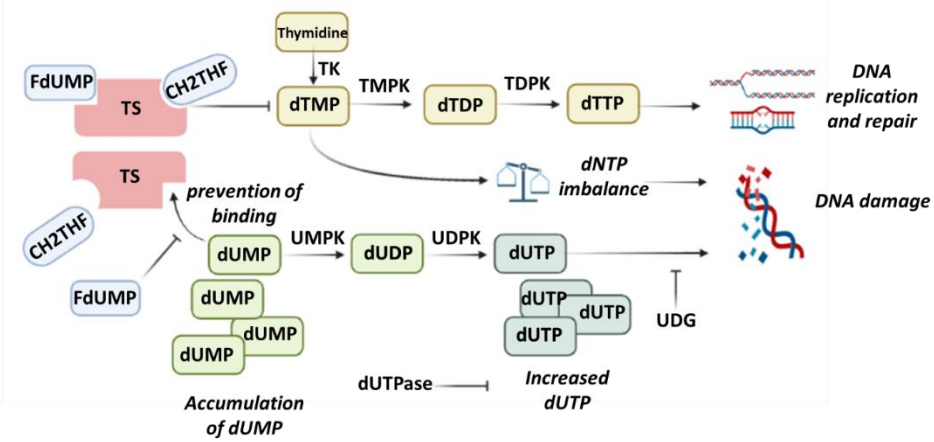

Figure 8 Mechanism of inhibiting thymine synthase by 5-FU

FdUMP competes with dUMP in binding to the binding site of TS and thus forms a stable ternary complex with TS and CH2THF. Upon forming the ternary complex, FdUMP inhibits DNA replication and repair by inhibiting the synthesis of dTMP thus decreasing the availability of dTTPs. Moreover, dNTP imbalance is resulted which leads to DNA damage. Unbinding of dUMP leads to its accumulation. Consequently, dUMP is phosphorylated by UMPK to dUDP which is then phosphorylated to dUTP by UDPK. This leads to elevated levels of dUTP and as a result the DNA is damaged. On the contrary, presence of dUTPase and UDG can protect from DNA damage. Also, dTMP can be salvaged from thymidine by TK and thus, DNA replication and repair are facilitated. Abbrevations: FdUMP: fluorodeoxyuridine monophosphate; CH2THF: 5,10-methylenetetrahydrofolate; dTMP:deoxythymidine monophosphate; dTDP: deoxythymidine diphosphate; dTTP: deoxythymidine triphosphate; TMPK: thymidine monophosphate kinase; TDPK: thymidine diphosphate kinase; dUMP: deoxyuridine monophosphate; dUDP: deoxyuridine diphosphate; dUTP: deoxyuridine triphosphate; UMPK: uridine monophosphate kinase; UDPK: uridine diphosphate kinase; UDG: uracil DNA glycosylase; TK: thymidine kinase; dUTPase: deoxyuridine triphosphatase.

II-3. Catabolism of 5-FU

A huge population of patients develop chemoresistance against 5-FU. This is in part explained by the poor bioavailability of 5-FU which is resulted from its catabolic degradation (Miura et al., 2010), represented in Figure 9. 5-FU is degraded by dihydropyrimidine dehydrogenase (DPD) into dihydrofluorouracil (5-FUH2) which is an inactive molecule (Milano & McLeod, 2000). 5-FUH2 is further degraded and converted into α-fluoro-β-ureido propionic acid (FUPA) then into α-fluoro-β-alanine (FBAL) and urea by dihydropyrimidinase (DPYS) then β-ureidopropionate (UPB1), respectively.

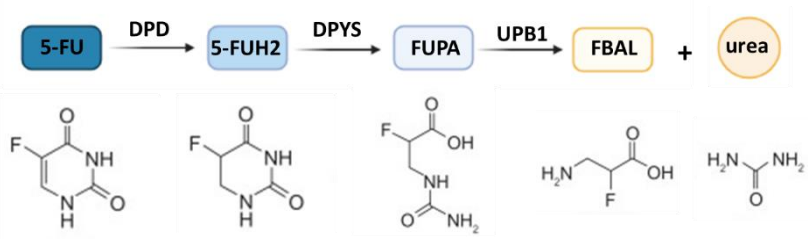

Figure 9 Catabolic Pathway of 5-FU in hepatocytes

DPD catalyzes the catabolism of 5-FU by converting it to 5-FUH2. The latter is subsequently converted to FUPA under the action of DPYS. UPB1 catalyzes the conversion of FUPA into FBAL and urea which are eliminated subsequently through excretion. Abbreviations: 5-FU: 5-fluorouracil; DPD: dihydropyrimidine dehydrogenase; 5-FUH2: 5-dihydrofluorouracil; DPYS: dihydropyrimidinase; FUPA: α-fluoro-β-ureido propionic acid; UPB1: β-ureidopropionate; FBAL: α-fluoro-β-alanine.

II-4. Resistance to 5-FU in CRC – Implications of TAMs

One of the major barriers in efficient cancer treatment is chemoresistance which is developed in patients (Schiavoni et al., 2013). Chemoresistance to drugs can be either innate and genetically present in tumoral cells or acquired during the treatment course (Hammond et al., 2016; Longley & Johnston, 2005). It is also manifested either against a single chemotherapeutic agent or against a class of agents sharing the same mechanism of action which explains the reason lying behind the treatment failure in most patients suffering from metastatic diseases (Veenstra & Krauss, 2018).

In CRC, it has been demonstrated that 40% of patients who encountered resection followed by receiving 5-FU-based adjuvant chemotherapy experience recurrence or die within 8 years of follow-up (Sargent et al., 2009). In addition, an approximation of 50% or patients suffering from metastatic CRC develop resistance to 5-FU with a five-year survival rate up to 12% (Giacchetti et al., 2000).

Several factors, extrinsic and intrinsic, confer the chemoresistance against an agent (Gerlinger et al., 2012). For instance, genetic, epigenetic, transcriptomic and proteomic signature of cancerous cells define the intrinsic factors (Mansoori et al., 2017). Importantly, extrinsic factors comprise the

constituents of the TME including pH, hypoxia as well as the signaling between stromal, infiltrating cells and the tumoral ones (Gatenby et al., 2010; Junttila & de Sauvage, 2013).

In CRC as well as other solid tumors, immune cells generally and macrophages specifically have been noticed as key components in chemoresistance (Rutkowski et al., 2012). Indeed, there is evidence emphasizing on the negative correlation between the infiltration of TAMs and CRC progression (J. Zhang et al., 2016). Results have reported that clearing TAMs potentiates the efficiency of 5-FU in mediating its cytotoxicity on tumoral cells. For instance, conditioned media from TAMs (TAM-CM) counteract 5-FU induced cytotoxicity and it was shown that the TAM-CM are rich in putrescine which decreases cleaved caspase-3 and JNK pathway activation playing a role in abolishing the cytotoxic effects of 5-FU (Hedbrant et al., 2015).. Further to this, TAMs were shown to induce chemoresistance against 5-FU in CRC through releasing putrescine (X. Zhang et al., 2016). It has been demonstrated that the increase in the infiltration of macrophages that is observed in CRC tissues is directly associated with an increase in chemoresistance against 5-FU (Yin et al., 2017, p.). A proposed mechanism is IL-6 release from TAMs activating the IL6R/STAT3/miR-204-5p pathway in cancer cells leading to resistance to 5-FU (Yin et al, 2017).

III. Dihydropyrimidine Dehydrogenase (DPD)

III-1. Expression of DPD

Dihydropyrimidine dehydrogenase (DPD), is a rate limiting enzyme in the catabolism of pyrimidine bases, including 5-FU (Milano & McLeod, 2000; Miura et al., 2010). It is encoded by the *DPYD* gene which is mapped on the chromosome 1p22 (Johnson et al., 1997). It is a single copy gene containing 4400 nucleotides that encompasses 23 exons and known to be highly polymorphic (Hasegawa et al., 2005; van Kuilenburg, 2004). The expression of this enzyme is reported in cancer cells to be controlled at the transcriptional and translational levels by SP1, SP3 transcription factors, hypermethylation of *DPYD* promoter as well as microRNAs (miRs) such as miR-27a and miR-27b (Ezzeldin et al., 2005; Meulendijks et al., 2015; X. Zhang et al., 2006).

DPD is a cytoplasmic protein (Van Kuilenburg et al., 1997). It is found to be expressed in a variety of tissues, yet the liver is known to be the master organ for the expression of DPD (Naguib et al., 1985). Moreover, peripheral blood mononuclear cells as well as macrophages are known to express DPD in addition to various cancerous cells. It has been reported that DPD expressed in the liver is responsible for metabolizing the majority of 5-FU (Longley et al., 2003).

III-2. Polymorphism of DPYD

Stemming back to section II.3 in this chapter, DPD reduces the availability of 5-FU and it was reported that in the expression of DPD in tumors facilitates resistance (Matsuyama et al., 2006). However, absence of this enzyme or any genetic alteration in it result in deficiency in its enzymatic activity (Omura, 2003). DPD has a broad range of enzymatic deficiencies ranging from partial loss

of its activity to complete loss. These deficiencies which are observed is several patients can consequently lead to 5-FU induced toxicity (Ciccolini et al., 2006; Milano et al., 1999). To elaborate more, the activity of DPD is highly variable between individuals where there is at least 3 – 5 % of people exhibiting a deficiency in the activity of DPD (Diasio et al., 1988; Etienne et al., 1994). Moreover, patients treated with 5-FU bearing some single nucleotide polymorphism in *DPYD* have been associated with grade 3 and 4 of toxicities.

There are several putative causes that explain the variations in the activity of DPD observed between patients. These include the drug-drug interactions, circadian patterns that DPD exhibits as well as differences in genders and ethnicities (Diasio, 1998; Etienne et al., 1994; Milano et al., 1992). More than 50 different mutations have been discovered in *DPYD* gene. Polymorphism of *DPYD* has been reported as an autosomal recessive disease. The most common mutation which accounts for half of the known mutations, is DPYD*2A, known as IVS14p 1 G>A, site mutation (Sulzyc-Bielicka et al., 2008; van Kuilenburg, 2004). This mutation is associated with life-threatening 5-FU toxicity since it leads to exon skipping resulting in a deletion of 165 base pairs in the mRNA. Several other major single nucleotide polymorphisms have been documented including 106 G>A, 131 C>A, 474 C>T and 832 G>A as well as deletions such as delTCAT295-298, delTG1039-1042, delC1897 among others (Sharma et al., 2017) .

III-3. DPD and 5-FU Pharmacokinetics

5-FU displays a narrow therapeutic index which is associated to the variability in the pharmacokinetics of 5-FU in patients (Meyerhardt & Mayer, 2005). These variabilities limit the efficacy of the treatment as extreme toxicities could be resulted which consequently affect the administration of optimal therapeutic courses in patients. In most cancers, where the treatment relies on 5-FU or other fluoropyrimidines, the pharmacokinetics profile is inconstant.

As far as 5-FU is administered orally, a maximum percentage of 1-3% of the administered dose mediates its cytotoxic effects on malignant as well as non-malignant cells following its anabolism (Sharma et al., 2017; Vodenkova et al., 2020). However, a vast majority of 5-FU are either excreted directly in the urine (5-20 %) or undergo catabolism where 5-FU is inactivated and then eliminated afterwards by excretion (80-85%).

Investigating the kinetics of 5-FU in cancer patients using radiolabeled 5-FU, it has been shown that 60 – 90% of the administered 5-FU is excreted out as in the urine or during exhalation within a duration of 24 hours prior of administration (Takiuchi & Ajani, 1998). Furthermore, it has been reported that the half-life of 5-FU in blood *in vivo* lies only in the range between 10 to 20 minutes following administration implying that its pharmacokinetics is characterized by an extremely short half-life (Tanaka et al., 2000).

In the light of the pivotal role that DPD exerts on the disposition of 5-FU, it is known that any modification in the expression and activity of DPD dramatically alters the pharmacokinetic profile of 5-FU (Diasio, 1998; van Kuilenburg, 2004). In other words, if the *DPYD* gene is impaired, its

protein expression is downregulated or its activity is impacted, a sharp increase in the half-life of 5-FU is observed explained by the decrease of its clearance. Studies have clearly demonstrated that patients displaying deficiency in DPD, present an increased half-life up to 5 hours (Bocci et al., 2006). Moreover, the levels of 5-FU in plasma were reported to be immensely higher in patients with 5-FU deficiency highlighting the great impact that DPD has on the disposition and the pharmacokinetic profile of 5-FU (Ciccolini et al., 2006).

III-4. DPD and 5-FU Treatment Efficacy

DPD conveys a circadian pattern (Naguib et al., 1985). Various studies have demonstrated that the expression of DPD is variable during the tumor progression and between different tumor types. This justifies the difference outcomes and the variance regarding the responses of the tumors to 5-FU treatment . Furthermore, tumoral cells were noted to express levels of DPD which vary depending on the type of the tumor and the patient. These results clearly demonstrate that there exists a positive correlation between the level of expression of DPD in tumors and the resistance to anti-cancer chemotherapeutic agents (Ciaparrone et al., 2006; Jensen et al., 2007).

In many cancers, DPD has become a potential predictive marker of 5-FU response as it is acknowledged that the activity of DPD is negatively correlated to the responsiveness and efficacy of 5-FU. In particular, high expression of DPD and its activity play a role in the development of 5-FU resistance (Panczyk, 2014). On the other hand, low DPD expression and activity results in reduction of 5-FU catabolism and consequently effective accumulation of 5-FU inside tumoral cells (Kunicka et al., 2016).

In-vitro overexpression of DPD by malignant cells were reported to enhance the resistance to 5-FU. Similarly, in CRC cells, elevated mRNA expression of *DPYD* has been associated directly with chemoresistance against 5-FU (Salonga et al., 2000). Additionally, patients suffering from advanced CRC showed a correlation between the low levels of *DPYD* and better response to 5-FU based therapy and a lower response rate were observed with higher mRNA expression in tumor tissues (Vallböhmer et al., 2006).

Contrary to better 5-FU response, recent studies have demonstrated that a total DPD deficiency, and in some cases partial deficiencies, result in a fatal outcome upon 5-FU treatment (Johnson et al., 1999). This is due to the toxicity that is developed due to the accumulation of 5-FU. The most frequent side effects arising from 5-FU treatments in DPD-deficient patients are digestive and heamatological toxicities (Bocci et al., 2006; Lyss et al., 1993).

Chapter Two - Part Two
Aim and Hypothesis

Within the TME of various solid tumors, TAMs have been associated with poor prognosis. In CRC, the role of TAMs remains controversial. Although TAMs have been recognized recently to establish a poor prognosis in CRC as well as to play a role in mediating chemoresistance against 5-FU, the mechanism behind this particular role is still poorly understood. Moreover, although it has been demonstrated that hypoxia interferes in chemoresistance in various tumors and they are implicated in modulating the biology of macrophages within the TME, hypoxia is still not appreciated in such studies. Thus, we aimed to study and explore the role of macrophages in a hypoxic environment on the resistance to 5-FU treatment in CRC.

We hypothesized that hypoxia interferes in the biology of macrophages and directly modify these cells affecting their role in mediating 5-FU chemoresistance.

Chapter Two - Part Three

Results

Research

ARTICLE

1

Published OnlineFirst October 13, 2021; DOI: 10.1158/0008-5472.CAN-21-1572

Hypoxia Drives Dihydropyrimidine Dehydrogenase Expression in Macrophages and Confers Chemoresistance in Colorectal Cancer

Marie Malier[1,2,3], Khaldoun Gharzeddine[1,2,4], Marie-Hélène Laverriere[1,2,5], Sabrina Marsili[6,7], Fabienne Thomas[6,7], Thomas Decaens[2,3,8], Gael Roth[1,2,3], and Arnaud Millet[1,2,3]

ABSTRACT

Colorectal adenocarcinoma is a leading cause of death worldwide, and immune infiltration in colorectal tumors has been recognized recently as an important pathophysiologic event. In this context, tumor-associated macrophages (TAM) have been related to chemoresistance to 5-fluorouracil (5-FU), the first-line chemotherapeutic agent used in treating colorectal cancers. Nevertheless, the details of this chemoresistance mechanism are still poorly elucidated. In the current study, we report that macrophages specifically overexpress dihydropyrimidine dehydrogenase (DPD) in hypoxia, leading to macrophage-induced chemoresistance to 5-FU via inactivation of the drug. Hypoxia-induced macrophage DPD expression was controlled by HIF2α. TAMs constituted the main contributors to DPD activity in human colorectal primary or secondary tumors, while cancer cells did not express significant levels of DPD. In addition, contrary to humans, macrophages in mice do not express DPD. Together, these findings shed light on the role of TAMs in promoting chemoresistance in colorectal cancers and identify potential new therapeutic targets.

Significance: Hypoxia induces HIF2α-mediated overexpression of dihydropyrimidine dehydrogenase in TAMs, leading to chemoresistance to 5-FU in colon cancers.

Introduction

Colorectal cancers are a leading cause of death worldwide and constitute the third cancer-related cause of death in the United States (1). Chemotherapy is one of the tools used to treat these tumors; however, some patients do not respond well to treatment, resulting in poor prognosis. This chemoresistance is caused by various mechanisms such as drug inactivation, drug efflux from targeted cells, and modifications of target cells (2, 3). Interestingly, the importance of tumor microenvironment in chemoresistance has recently garnered attention. The tumor immune microenvironment, notably through its innate immune part that is mainly composed of tumor-associated macrophages (TAM), deserves particular attention (4, 5). TAMs have been associated with bad prognosis in the case of various solid tumors (6) and have been shown to orchestrate a defective immune response to tumors (7). It has been suggested that TAMs are reprogrammed by cancerous cells to secondarily become supporting elements of tumor growth (8). The involvement of macrophages in colorectal cancer has been controversial, and only recently has the association between $CD163^+$ TAMs and a poorer prognosis been recognized (9, 10). Their implication in chemoresistance, particularly against 5-fluorouracil (5-FU), a first-line chemotherapy in colorectal cancer, has been reported previously (11, 12). This suggests that targeting macrophages could be an effective way to increase treatment efficiency. However, the precise mechanisms by which TAMs participate in creating chemoresistance in human colorectal tumors are still poorly understood. The underappreciated impact of hypoxia on macrophage biology (13) and the increasingly recognized role of hypoxia in resistance to anticancer treatments and cancer relapse (14), lead us to reassess the role of hypoxic macrophages in chemoresistance. On the basis of the abundance of macrophages in colorectal cancer, we hypothesized that hypoxia could directly modulate macrophage involvement in 5-FU resistance.

Materials and Methods

Cell culture

RAW264.7, CT-26, RKO, and HT-29 were purchased from ATCC. RAW were maintained in high-glucose DMEM (Gibco) supplemented with 10% FBS (Gibco) at 37°C, CT-26 and RKO were maintained in RPMI (Gibco) supplemented with 10% FBS (Gibco) at 37°C, and HT-29 were maintained in McCoy's medium (Gibco) supplemented with 10% FBS (Gibco) at 37°C. All cells were routinely tested for *Mycoplasma* contamination using MycoAlert detection kit (Lonza). All cells have been used in the following year of their reception.

Human samples

Human blood samples from healthy deidentified donors were obtained from EFS (French national blood service) as part of an authorized protocol (CODECOH DC-2018–3114). Donors gave

[1]Team Mechanobiology, Immunity and Cancer, Institute for Advanced Biosciences Inserm 1209 – UMR CNRS 5309, Grenoble, France. [2]Grenoble Alpes University, Grenoble, France. [3]Department of Hepatogastroenterology, University Hospital Grenoble-Alpes, Grenoble, France. [4]Research Department, University Hospital Grenoble-Alpes, Grenoble, France. [5]Department of Pathological Anatomy and Cytology, University Hospital Grenoble-Alpes, Grenoble, France. [6]CRCT Inserm U037, Toulouse University 3, Toulouse, France. [7]Claudius Regaud Institute, IUCT-Oncopole, Toulouse, France. [8]Team Tumor Molecular Pathology and Biomarkers, Institute for Advanced Biosciences UMR Inserm 1209 – CNRS 5309, Grenoble, France.

Note: Supplementary data for this article are available at Cancer Research Online (http://cancerres.aacrjournals.org/).

Corresponding Author: Arnaud Millet, Institute for Advanced Biosciences, Grenoble 38000, France. Phone: 33-6-66-88-34-82; E-mail: arnaud.millet@inserm.fr

Cancer Res 2021;81:5963–76

doi: 10.1158/0008-5472.CAN-21-1572

Published OnlineFirst October 13, 2021; DOI: 10.1158/0008-5472.CAN-21-1572

signed consent for use of their blood in this study. Tumor samples were obtained from the department of pathology of the university hospital of Grenoble as part of a declared sample collection AC-2014-2949. Patient selection criteria were a diagnostic of colorectal adenocarcinoma and tissue samples availability for the primary tumor and liver metastasis. Clinical characteristics of the patients are reported in the table (Supplementary Table). All patients gave their signed consent for this study as part of an authorized protocol (INDS MR4916160120) and the study was conducted in accordance with the Declaration of Helsinki.

Animals

Eight-week-old Balb/c female mice were obtained from Charles River. Animals were housed and bred at Plateforme de Haute Technologie Animale (PHTA) UGA core facility (Grenoble, France), EU0197, agreement C38-51610006, under specific pathogen–free conditions, temperature-controlled environment with a 12-hour light/dark cycle and ad libitum access to water and diet. Animal housing and procedures were conducted in accordance with the recommendations from the Direction des Services Vétérinaires, Ministry of Agriculture of France, according to European Communities Council Directive 2010/63/EU and according to recommendations for health monitoring from the Federation of European Laboratory Animal Science Associations. Protocols involving animals were reviewed by the local ethic committee "Comité d'Ethique pour l'Expérimentation Animale no. #12, Cometh-Grenoble" and approved by the Ministry of Research under the authorization number (January 2020) APAFIS#22660-2019103110209599.

Human macrophage differentiation from monocytes

Monocytes were isolated from leukoreduction system chambers of healthy EFS donors using differential centrifugation (Histopaque 1077, Sigma) to obtain peripheral blood mononuclear cells. $CD14^+$ microbeads (Miltenyi Biotec) were used to select monocytes according to the manufacturer's instructions. Monocytes were plated in RPMI (Life Technologies) supplemented with 10% SAB (Sigma), 10 mmol/L HEPES (Life Technologies), MEM Non-essential amino acids (Life Technologies) and 25 ng/mL MCSF (Miltenyi Biotec). Differentiation was obtained after 6 days of culture. Hypoxic cultures were performed in a hypoxic chamber authorizing an oxygen partial pressure control (HypoxyLab).

Bone marrow–derived macrophage differentiation

Bone marrow was extracted from the femurs of Balb/c mice in RPMI and then filtered by a 70 μm cell strainer. Cells were washed in RPMI and cultured in RPMI (Gibco) supplemented with 10% of FBS (Gibco) and mouse MCSF at 25 ng/mL (Miltenyi Biotec) for 6 days. Medium was refreshed at day 3. Differentiation was assessed by flow cytometry through membrane expression analysis of F4/80.

Macrophage conditioned medium

Macrophages were cultured at 1×10^6 cells per well in 12-well plates with RPMI supplemented with 10% SAB with DMSO (vehicle), Gimeracil (Sigma-Aldrich) 1 μg/mL, 5-FU (ACCORD HEALTHCARE) 0.1 μg/mL, 5-FU 1 μg/mL, 5-FU 0.1 μg/mL + Gimeracil 1 μg/mL or 1 μg/mL + Gimeracil 1 μg/mL during 24 hours in normoxia and hypoxia. The produced macrophage conditioned medium (MCM) was added for 48 hours to HT-29 and RKO, which were plated previously at 3×10^5 cells per well during 24 hours. Then cancer cells were collected, counted and the mortality rate assessed by flow cytometry (Annexin V and 7-AAD).

RNAi

siRNAs (GE Dharmacon) were transfected at a final concentration of 50 nmol/L using Lipofectamine (RNAiMAx, Life Technologies).

Expression of human dihydropyrimidine dehydrogenase in mice macrophages

RAW264.7 were transduced using lentivirus particles with the open reading frame (ORF) of the human dihydropyrimidine dehydrogenase (DPD) gene (mGFP-tagged) inserted in a pLenti-C-mGFP-P2A-Puro plasmid (Origen Technologies). Control RAW were obtained using the lentivirus particles containing the plasmid without the DPD ORF sequence (pLenti-C-mGFP-P2A-Puro).

RNA isolation and qPCR analysis for gene expression

Cells were directly lyzed and RNA was extracted using the NucleoSpin RNA kit components (Macherey Nagel) according to the manufacturer's instructions. Reverse transcription was performed using the iScript Ready-to-use cDNA supermix components (Bio-Rad). qPCR was then performed with the iTaq universal SYBR green supermix components (Bio-Rad) on a CFX96 (Bio-Rad). Quantification was performed using the $\Delta\Delta C_t$ method.

Immunoblotting

Cells were lyzed in RIPA buffer supplemented with antiprotease inhibitors (AEBSF 4 mmol/L, Pepstatine A 1 mmol/L, and Leupeptine 0.4 mmol/L; Sigma-Aldrich) and HIF-hydroxylase inhibitor (DMOG 1 mmol/L, Sigma-Aldrich). Proteins were quantified by BCA assay (Thermo Fisher Scientific) and 15 μg of total protein were run on SDS-PAGE gels. Proteins were transferred from SDS-PAGE gels to polyvinylidene difluoride membrane (Bio-Rad), blocked with TBS-Tween supplemented with 5% milk, primary antibodies were incubated at 1 μg/mL overnight 4°C. After washing with TBS, the membrane was incubated with a horseradish peroxidase-conjugated secondary antibody (Jackson Immunoresearch). Signal was detected by chemoluminescence (Chemi-Doc Imaging System, Bio-Rad) after exposition to West Pico ECL (Thermo Fisher Scientific).

Proteomics

Cells are directly lyzed in Laemmli buffer and prepared and analyzed as described previously (13). Briefly, the protein equivalent of 300,000 cells for each sample was loaded on NuPAGE Bis-Tris 4%–12% acrylamide gels (Life Technologies). Electrophoretic migration was controlled to allow each protein sample to be split into six gel bands. Gels were stained with R-250 Coomassie blue (Bio-Rad) before excising protein bands. Gel slices were washed then dehydrated with 100% acetonitrile (Merck Millipore), incubated with 10 mmol/L DTT (dithiothreitol, Merck Millipore), followed by 55 mmol/L iodoacetamide (Merck Millipore) in the dark. Alkylation was stopped by adding 10 mmol/L DTT in 25 mmol/L ammonium bicarbonate. Proteins were digested overnight at 37°C with Trypsin/Lys-C Mix (Promega) according to manufacturer's instructions. After extraction, fractions were pooled, dried, and stored at −80°C until further analysis. The dried extracted peptides were resuspended and analyzed by online nano-LC (Ultimate 3000, Thermo Fisher Scientific) directly linked to an impact IITM Hybrid Quadrupole Time of-Flight (QTOF) instrument fitted with a CaptiveSpray ion source (Bruker Daltonics). All data were analyzed using MaxQuant software (version 1.5.2.8) and the Andromeda search engine. The FDR was set to 1% for both proteins and peptides, and a minimum length of seven amino acids was set. MaxQuant scores peptide identifications based on a search with an initial permissible mass deviation for the precursor ion

Published OnlineFirst October 13, 2021; DOI: 10.1158/0008-5472.CAN-21-1572

of up to 0.07 Da after time-dependent recalibration of the precursor masses. Fragment mass deviation was allowed up to 40 ppm. The Andromeda search engine was used to match MS-MS spectra against the Uniprot human database (https://www.uniprot.org/). Enzyme specificity was set as C terminal to Arg and Lys, cleavage at proline bonds and a maximum of two missed cleavages were allowed. Carbamidomethylation of cysteine was selected as a fixed modification, whereas N-terminal protein acetylation and methionine oxidation were selected as variable modifications. The "match between runs" feature of MaxQuant was used to transfer identification information to other LC/MS-MS runs based on ion masses and retention times (maximum deviation 0.7 minutes); this feature was also used in quantification experiments. Quantifications were performed using the label-free algorithms. A minimum peptide ratio counts of two and at least one "razor peptide" were required for quantification. The label-free quantification metric was used to perform relative quantification between proteins identified in different biological conditions, protein intensities were normalized on the basis of the MaxQuant "protein group.txt" output (reflecting a normalized protein quantity deduced from all peptide intensity values). Potential contaminants and reverse proteins were strictly excluded from further analysis. Three analytic replicates from three independent biological samples (donors) were analyzed for each normoxic and hypoxic conditions. Missing values were deduced from a normal distribution (width: 0.3; down shift: 1.8) using the Perseus (version 1.5.5.3) after data acquisition package contained in MaxQuant (www.maxquant.org). Data were further analyzed using JMP software (v.13.0.0, SAS Institute Inc.). Proteins were classed according to the paired Welch test difference (difference between the mean value for triplicate MS-MS analyses for the two compared conditions), and the median fold change between the two compared conditions.

Immunochemistry

A total of 3-μm-thick consecutive tissue sections were prepared from formalin-fixed and paraffin-embedded tissues. Deparaffinization, rehydration, antigen retrieval, and peroxidase blocking were performed on a fully automated system BENCHMARK ULTRA (Roche) according to manufacturer recommendations. The sections were incubated with the following primary antibodies: anti-CD68 clone Kp1 (Dako) and anti-DPD (Thermo Fisher Scientific). Revelation was performed using the Ultraview DAB revelation kit (Roche). Nuclei were counterstained with hematoxylin solution (Dako). Images were captured using an APERIO ATS scanner (Leica).

Immunofluorescence

Formalin-fixed and paraffin-embedded human tissue samples were sectioned at 3 μm thickness. Samples were deparaffinized by xylene and hydrated by baths of decreasing concentrations of ethanol. Antigen retrieval was achieved using IHC-TekTM Epitope Retrieval Steamer Set (IW-1102, IHCworld) in IHC-TekTM Epitope Retrieval (IW-1100, IHCworld) for 40 minutes. Nonspecific binding sites were blocked by 1% BSA in PBS. Samples were incubated with the primary antibodies: Monoclonal Mouse anti-Human CD68 clone PG-M1 at 0.4 μg/mL, Mouse anti-Human CD163 clone EDHu-1 at 10 μg/mL, anti-Human HIF2α at 4 μg/mL, and DPD polyclonal antibody at 3 μg/mL for 1 hour at room temperature followed by an incubation of secondary antibodies: Alexa Fluor 488 goat anti-mouse IgG (H+L) and Alexa Fluor 546 goat anti-rabbit IgG (H+L) both at 4 μg/mL for 30 minutes at room temperature. Nuclei were stained by Hoechst 33342 at 5 μg/mL for 5 minutes at room temperature. Images were captured under ×20 magnification using ApoTome microscope (Carl Zeiss) equipped with a camera AxioCam MRm, collected by AxioVision software and analyzed using ImageJ software.

Flow cytometry

Flow cytometry data were acquired on an Accuri C6 (BD) flow cytometer. The reagents used were: AnnexinV-FITC, mouse anti-F4/80-PE clone REA126 and mouse anti-human CD11b-FITC from Miltenyi Biotech and 7-AAD staining solution from BD Pharmingen. Doublet cells were gated out by comparing forward scatter signal height (FSC-H) and area (FSC-A). At least 10,000 events were collected in the analysis gate. Median fluorescence intensity was determined using Accuri C6 software (BD).

Cancer cell line mRNA *DPYD* expression

Cancer cell line gene expression data were collected from the Cancer Cell Line Encyclopedia (CCLE; https://portals.broadinstitute.org/ccle). Briefly, sequencing was performed on the Illumina HiSeq 2000 or HiSeq 2500 instruments, with sequence coverage of no less than 100 million paired 101 nucleotides-long reads per sample. RNA-sequencing (RNA-seq) reads were aligned to the B37 version of human genome using TopHat version 1.4. Gene and exon-level RPKM values were calculated using pipeline developed for the GTEx project (15, 16). The cell lines were classified on the basis of their tissue origin resulting in 24 different groups. The number of cell lines in each group is indicated. The histogram plot was generated using the JMP software (SAS).

Mice and human mRNA *DPYD* expression analysis

Genevestigator 7.5.0 (https://genevestigator.com/gv/) is a search engine that summarizes datasets in metaprofiles. GENEVESTIGATOR integrates manually curated and quality-controlled gene expression data from public repositories (17). In this study, the Condition Tools Search was used to obtain DPD mRNA levels obtained from human (*Homo sapiens*) and mice (*Mus musculus*) in various anatomic parts. Mean of logarithmic level of expression obtained from AFFIMETRIX expression microarrays was used to generate a cell plot from selected results related to macrophages and monocytes. The lowest and the highest expression results in both series (human and mice) were used to evaluate the expression level in the dataset. Cell plot was generated using the JMP software (SAS).

DPD activity measurements

Because DPD is involved in the hydrogenation of uracil (U) into dihydrouracil (UH2), DPD activity was indirectly evaluated in the cell culture supernatants by determining the concentration of U and its metabolite UH2 followed by the calculation of the UH2/U ratio. These analyses were performed in the Pharmacology Laboratory of Institut Claudius-Regaud (France) using an high performance liquid chromatography (HPLC) system composed of Alliance 2695 and diode array detector 2996 (Waters), according to a previously described method (18). Uracil (U), dihydrouracil (UH2), 5-FU, ammonium sulfate 99%, acetonitrile (ACN) gradient chromasolv for HPLC and 2-propanol were purchased from Sigma. Ethyl acetate Scharlau was of HPLC grade and purchased from ICS. Water from Milli-Q Advantage A10 and MultiScreen-HV 96-well plates were used (Merck Millipore). Calibration ranges were 3.125–200 ng/mL for U and 25–500 ng/mL for UH2 and 5-FU (5 μg/mL) was used as an internal standard. We have validated that gimeracil does not interfere with 5-FU measurements, using calibrated 5-FU samples with and without gimeracil. For the 5-FU kinetics experiments, no internal standard was added to the samples and the amount of 5-FU in the supernatant was quantified by the peak area corresponding to 5-FU.

Published OnlineFirst October 13, 2021; DOI: 10.1158/0008-5472.CAN-21-1572

Quantification and statistical analysis

Statistics were performed using Graph Pad Prism 7 (Graph Pad Software Inc). When two groups were compared, we used a two-tailed Student *t* test for a normal distribution and a Mann–Whitney nonparametric test otherwise. When more than two groups were compared, we used a one-way ANOVA analysis with a Tukey *post hoc* test. Tumor growth curves were analyzed using two-ways ANOVA using the open access TumorGrowth software (19). All error bars represent means with SEM. All group numbers and explanation of significant values are presented within the figure legends.

Data availabilty

All mass spectrometry proteomics data were deposited on the Proteome- Xchange Consortium website (http://proteomecentral.proteomexchange.org) via the PRIDE partner repository, dataset identifier: PXD006354.

See Supplementary Materials and Methods for further details.

Results

Macrophages confer a chemoresistance to 5-FU in a low-oxygen environment

To evaluate the effect that tumor-infiltrating macrophages have on chemotherapy, we analyzed the impact of the coculture with macrophages on cancer cells growth. We chose two human colorectal cancer cell lines, sensitive to 5-FU, differing from their genetic background to avoid any specific genetic cell line involvement: RKO (p53 and APC WT) and HT-29 (p53 and APC mutated) cells. To examine the role of oxygen, we performed these experiments in normoxia ($N = 18.6\%$ O_2) and in hypoxia ($H = 25$ mm Hg $\sim 3\%$ O_2). We observed that in hypoxia, monocyte-derived macrophages (MDM) confer a chemoresistance toward 5-FU that is not observed in normoxia (**Fig. 1A**). To determine whether MDM act directly on 5-FU, we used MCM containing 5-FU or none. It has been previously reported that macrophages are resistant to 5-FU (20). Nonconditioned 5-FU strongly inhibited HT-29 and RKO proliferation independently of oxygen concentration (**Fig. 1B** and **C**). MCM without 5-FU had little effect on the proliferation of HT-29 (**Fig. 1B**) and RKO (**Fig. 1C**) cells. Meanwhile, MCM with 5-FU at 1 μg/mL inhibited cell growth in normoxia but not in hypoxia, advocating for a protection against 5-FU inhibition mediated by hypoxic MDM (**Fig. 1B** and **C**). As RKO cells were found sensitive to a lower concentration of 5-FU (0.1 μg/mL), MDM were able to protect RKO against 5-FU at this concentration, not only in hypoxia but also in normoxia (**Fig. 1C**). This observation led us to consider an inactivation mechanism of 5-FU driven by macrophages with an increased efficiency in hypoxia. A previously proposed mechanism for macrophage-induced chemoresistance in colorectal cancer was related to their ability to secrete IL6, leading to an inhibition of cancer cell apoptosis (11). We first tried to verify whether we could confirm the presence of IL6 in our conditioned medium (CM) by human MDMs in normoxia and in hypoxia and found no spontaneous secretion (<10 pg/mL) of IL6 (Supplementary Fig. S1A). As the conditioning by MDM provided a complete protection, we then hypothesized that a direct action of macrophages on 5-FU was the likely mechanism. To obtain a molecular explanation of the differing effect under various oxygen concentrations, we performed a proteomic analysis of human macrophages in hypoxia compared with normoxia. Our quantitative proteomic approach revealed that DPD is strongly overexpressed in hypoxia (**Fig. 1D**). DPD (coded by the *DPYD* gene) is the rate-limiting enzyme of the pyrimidine degradation pathway. DPD adds two hydrogen atoms to uracil, with NADPH as an obligatory cofactor, leading to dihydrouracil, which is secondarily degraded to β-alanine under the control of DPYS and UPB1 (**Fig. 1E**). 5-FU is a fluorinated analog of uracil reduced by DPD to 5-fluorodihydrouracil, an inactive compound (**Fig. 1F**). We confirmed through immunoblotting the increased expression of DPD in hypoxia when compared with the basal expression in normoxia (Supplementary Fig. S1B). Because the putative action of DPD on 5-FU is related to its enzymatic activity, we also confirmed that DPD expression in hypoxic MDM was functional, leading to an increase of the dihydrouracil to uracil ratio in the extracellular medium (**Fig. 1G**). To precise the role of macrophages in the 5-FU chemoresistance, we analyzed DPD expression in RKO and HT-29 cancer cells. We found no significant level of expression of DPD at the protein level, neither in HT-29 nor in RKO cells, irrespective of the oxygen concentration (Supplementary Fig. S2A and S2B). Furthermore, we found a downregulation of the *DPYD* mRNA in HT-29 and in RKO, emphasizing a defective transcription of the *DPYD* gene (Supplementary Fig. S2C). It has been reported that the transcription factor PU.1 drives the expression of *DPYD* and that EZH2 is responsible for the histone H3K27 trimethylation at the *DPYD* promotor site, leading to its downregulation in colon cancer cells (21). We thus confirmed that the pharmacologic inhibition of the methyltransferase EZH2 by the specific inhibitor GSK126 led to a detectable level of *DPYD* mRNA in RKO cells (Supplementary Fig. S2D).

Chemoresistance to 5-FU is driven by increased DPD activity in hypoxic macrophages

To confirm the inactivation of 5-FU by macrophage's DPD and its potential clinical relevance, we analyzed the kinetics of 5-FU degradation in normoxia and hypoxia. As 5-FU is a small molecule, its diffusion in tissues is quite high. Indeed, following 4 days of oral ingestion of 5-FU, the plasmatic concentration was found to be approximately 1 μg/mL (22). The mean 5-FU concentration was 0.411 ± 0.381 (μg/g of tissue) in the tumor portions of the specimens and 0.180 ± 0.206 (μg/g of tissue) in the normal portions in colorectal cancers (23). As TAMs represent 2%–10% of cells in colorectal cancer tumors, especially localized in the invasion front (9) and because 1 g of tissue typically contains approximately 10^8 cells (24), a reasonable estimated ratio in colorectal cancer is approximately 10^6 macrophages/g of tissue. According to 5-FU reported concentration, an estimated relevant ratio in colorectal cancer is 1 μg of 5-FU/10^6 macrophages. We interestingly found that 2 μg of 5-FU could be eliminated by 10^6 MDM in hypoxia in less than 24 hours and that normoxic MDM were unable to completely eliminate this quantity in 48 hours (**Fig. 2A**). We validated that 5-FU degradation was due to DPD catalytic activity using gimeracil, a specific inhibitor of DPD (**Fig. 2B** and **C**). 5-FU induced death in HT-29 and RKO cells irrespective of the concentration of oxygen and the presence of gimeracil, demonstrating that no significant DPD activity is present in these cells (**Fig. 2D** and **F**; Supplementary Fig. S2A and S2B). Whereas MCM with 5-FU at 1 μg/mL induced cell death in HT-29 cells in normoxia, its cytotoxic effect dramatically decreased in hypoxia and this was reverted by gimeracil inhibition of DPD activity in MDM (**Fig. 2D**). Following these results, 5-FU chemoresistance appears to be based solely on DPD activity in macrophages promoted by hypoxia. We observed a similar result using a three-dimensional (3D) tumor model growth of HT-29 exposed to MCM (**Fig. 2E**; Supplementary Fig. S3A), and we confirmed the generality of this mechanism in RKO cells (**Fig. 2F**). To confirm that oxygen was the main factor controlling DPD expression in hypoxia, we verified that DPD was not induced or repressed by 5-FU itself (**Fig. 2G**). We also explored whether cancerous cells can modulate DPD expression in macrophages. Using a transwell coculture assay between

Published OnlineFirst October 13, 2021; DOI: 10.1158/0008-5472.CAN-21-1572

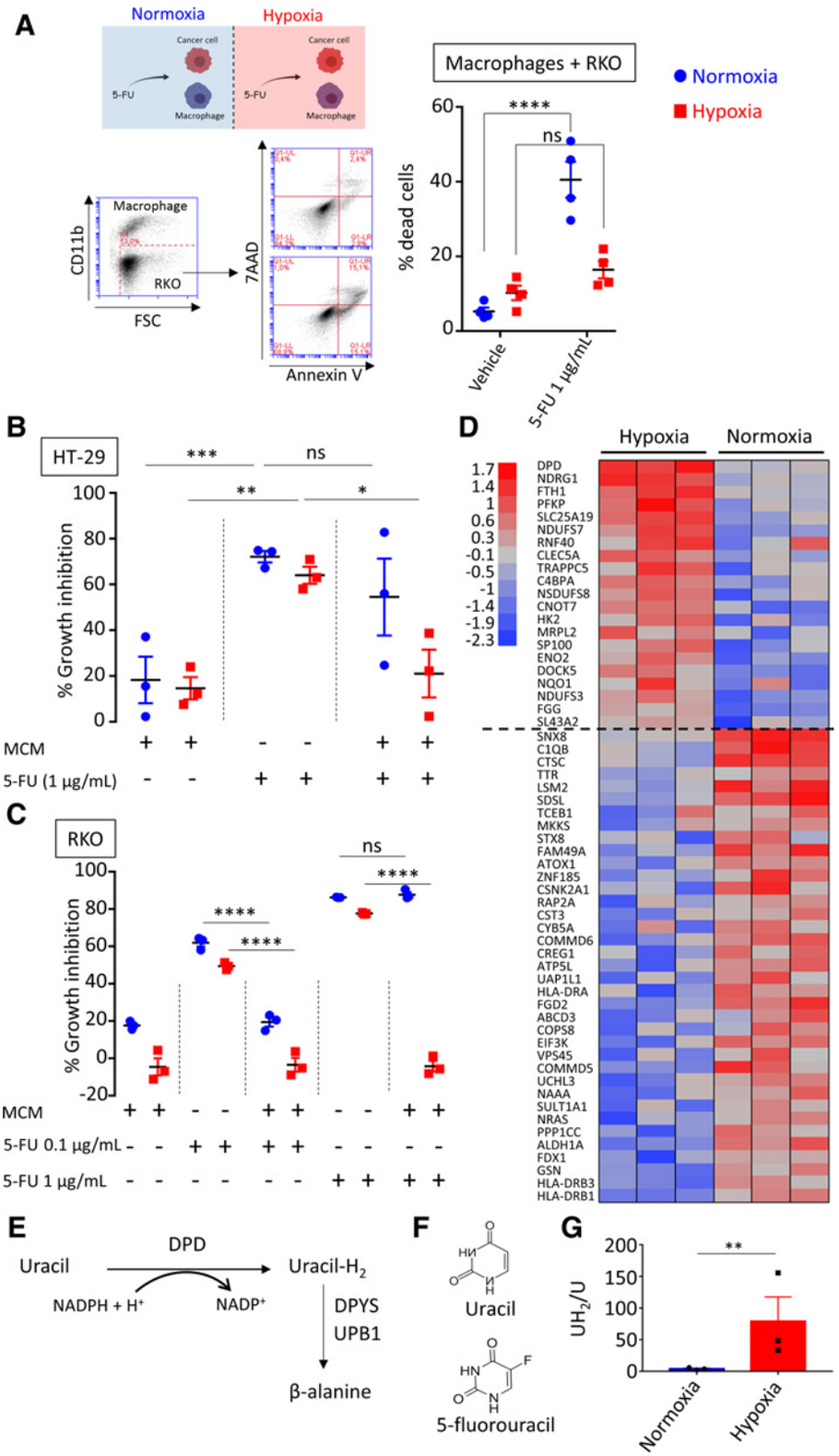

Figure 1.

Macrophages confer a chemoresistance to 5-FU in hypoxia. **A,** Top left, induction of death in RKO cells by 5-FU in a cocultured assay with macrophages in normoxia (blue) and hypoxia (red). 5-FU was used at 1 µg/mL. Dead cancer cells were defined as CD11b-AnnexinV+7-AAD± cells by flow cytometry. The gating strategy is represented on the bottom left. Dead cell quantification is represented on the right ($n = 4$). **B,** Growth inhibition of HT-29 cells by MCM(∅), 5-FU, and CM(5-FU) in normoxia (blue), and in hypoxia (red), 5-FU was used at 1 µg/mL ($n = 3$). **C,** Growth inhibition of RKO cells by MCM (∅), 5-FU, and MCM (5-FU) in normoxia (blue) and in hypoxia (red) 5-FU was used at 0.1 and 1 µg/mL ($n = 3$). **D,** Protein heatmap of macrophages in hypoxia and normoxia. Proteins were selected by a fold change > 2 and $P < 0.01$. Proteins were organized according to descending mean z-score of hypoxic proteins. **E,** Schematic presentation of the rate-limiting steps of the pyrimidine degradation pathway involving DPD. **F,** Chemical structures of uracil and 5-FU. **G,** Dihydrouracil/uracil ratio measured by HPLC in the macrophage supernatant from macrophages cultured in normoxia and hypoxia ($n = 3$). Statistical significance was determined using a one-way ANOVA analysis with Tukey *post hoc* test (**A–C**). Statistical significance was performed using a two-tailed paired *t* test (**G**). Error bars, mean ± SEM.*, $P < 0.05$; **, $P < 0.01$; ***, $P < 0.001$; ****, $P < 0.0001$; ns, nonsignificant.

Published OnlineFirst October 13, 2021; DOI: 10.1158/0008-5472.CAN-21-1572

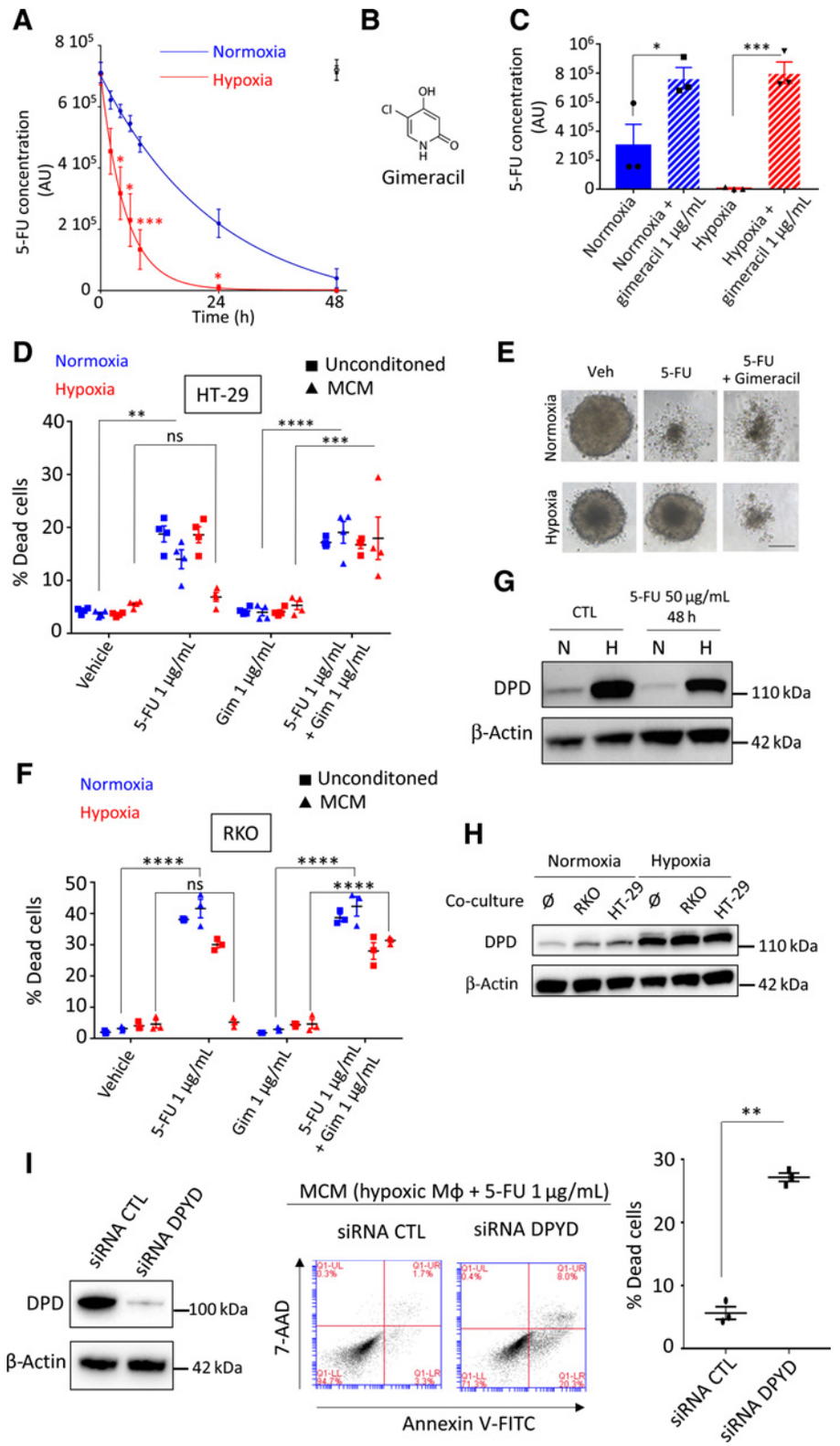

Figure 2.

Chemoresistance to 5-FU is driven by DPD activity in macrophages. **A,** Kinetics of 5-FU degradation by macrophages obtained by HPLC. 5-FU initial concentration was 1 µg/mL. Normoxia, blue; hypoxia, red. 5-FU without macrophages was stable during the 48 hours period of study in normoxia (full black circle) and in hypoxia (empty black circle; $n = 3$). **B,** Chemical structure of gimeracil, a specific inhibitor of DPD. **C,** 5-FU degradation due to DPD activity in macrophages inhibited by gimeracil at 48 hours. 5-FU initial concentration was 1 µg/mL. Normoxia, blue; hypoxia, red ($n = 3$). **D,** Induction of death in HT-29 in normoxia (blue) and in hypoxia (red) by nonconditioned medium (square) and conditioned medium (triangle). Dead cells were defined as AnnexinV+ cells in flow cytometry. 5-FU was used at 1 µg/mL and gimeracil at 1 µg/mL ($n = 4$). **E,** Inhibition of growth and death induction in 3D tumoroïd of HT-29 cells in normoxia and hypoxia. Tumoroïds were exposed to MCM (vehicle), MCM (5-FU 1 µg/mL), and MCM (5-FU 1 µg/mL + gimeracil 1 µg/mL). Pictures were obtained with a phase contrast microscope. Scale bar, 200 µm ($n = 8$). **F,** Induction of death in RKO in normoxia (blue) and in hypoxia (red) by nonconditioned medium (square) and conditioned medium (triangle). Dead cells were defined as AnnexinV+ cells in flow cytometry. 5-FU was used at 1 µg/mL and gimeracil at 1 µg/mL ($n = 3$). **G,** Immunoblot of DPD expression in macrophages exposed to 5-FU at 50 µg/mL during 48 hours ($n = 3$). **H,** Immunoblot of DPD expression in macrophages transwell cocultured with HT-29 or RKO in normoxia and hypoxia ($n = 3$). **I,** Immunoblot analysis of DPD expression in hypoxic macrophages transiently transfected with siRNA against DPD and nonsilencing control siRNA (left). MCM from macrophages treated with siRNA against DPD restore sensitivity to 5-FU in RKO cells (middle; representative of three independent experiments). Quantification of induced apoptosis was done with flow cytometry (right; $n = 3$). Statistical significance was determined using a one-way ANOVA analysis with Tukey *post hoc* test (**A**, **C**, **D**, and **F**) and by paired Student *t* test for (**I**). Error bars, mean ± SEM. *, $P < 0.05$; **, $P < 0.01$; ***, $P < 0.001$; ****, $P < 0.0001$; ns, nonsignificant.

Published OnlineFirst October 13, 2021; DOI: 10.1158/0008-5472.CAN-21-1572

cancerous cells and macrophages, we did not find any modulation in DPD expression in MDM (**Fig. 2H**). Similarly, we observed no induction of DPD expression in cancer cells when exposed to MCM (Supplementary Fig. S3B). In addition, we further confirmed that when applying medium conditioned from MDM with DPD loss of function through siRNA depletion, the cancer cell sensitivity to 5-FU was restored (**Fig. 2I**). To assess the efficiency of DPD degradation of 5-FU, we also performed a direct coculture assay between RKO cancerous cells and MDM. We found that MDM protected RKO cells from 5-FU in a DPD enzymatic activity dependent manner. Indeed, DPD inhibition by gimeracil restored RKO sensitivity to 5-FU (Supplementary Fig. S3C).

DPD expression in hypoxic macrophages is under the control of HIF2α

We discovered that a decreased oxygen concentration was able to increase the expression of DPD in human macrophages. To gain further insight into this, we carried out the transition of macrophages to various oxygen environments, to study the way DPD is controlled. We observed that DPD expression was inversely correlated to oxygen levels during the transitions (**Fig. 3A** and **B**). The evolution of DPD expression was then analyzed with the help of a first-order differential equation (**Fig. 3C**). This analysis revealed that the DPD half-life does not decrease during transition from hypoxia to normoxia, excluding DPD degradation as the only mechanism controlling DPD expression (**Fig. 3C**). We have confirmed this analysis using proteasome inhibitors (MG132 and bortezomib), which do not modify DPD decreased expression during a hypoxia to normoxia transition (Supplementary Fig S4A). These results suggested a synthesis control of DPD expression rather than a degradation control. We then noted that hypoxic transitions were associated with the production of a functional DPD resulting in an increased dihydrouracil/uracil ratio in the extracellular medium (Supplementary Fig. S4B). Besides, we observed that profound hypoxic conditions (7 mm Hg $\sim$ 1% O_2), similarly to moderate hypoxic conditions, induced DPD overexpression (Supplementary Fig. S4C). As hypoxic-induced factors HIF1α and HIF2α are known to be stabilized during hypoxic transitions, we checked whether their stabilization could be implicated in DPD overexpression. We found that HIF1α stabilization in hypoxic human macrophages was not involved in DPD increased expression, as siRNA-mediated depletion of HIF1α did not modify DPD protein synthesis in hypoxia (**Fig. 3D**). Using siRNA depletion, we demonstrated that DPD overexpression in hypoxia is under the control of a HIF2α-dependent mechanism (**Fig. 3E**). We next sought to determine whether the expression of DPD is transcriptionally controlled when macrophages are exposed to low-oxygen environments. To do so, we analyzed mRNA levels of oxygen-sensitive genes in macrophages (*VEGFA*, *NDRG1*, *P4HA1*, *SLC2A1*) in the transition from normoxia to hypoxia or from hypoxia to normoxia. We discovered that the *DPYD* mRNA level did not present any significant variation of its level of expression compared with oxygen responsive genes (**Fig. 3F**). We confirmed the absence of transcriptional control by inhibiting the synthesis of new mRNAs with actinomycin D and found no effect on DPD protein synthesis during a hypoxic transition (**Fig. 3G**). We further confirmed the translation-mediated control expression of DPD using translation inhibition by cycloheximide (Supplementary Fig. S4D). This absence of correlation between the mRNA level and the protein expression level suggested a HIF2a-related mechanism independent of its direct transcription factor activity. Recently, it has been demonstrated that the initial steps of protein synthesis such as the binding of the eukaryotic translational initiation factor E (eIF4E), part of the eIF4F initiation complex, to mRNA are repressed in hypoxia. Another complex, involving $eIF4E_2$ (an homolog of eIF4E normally involved in translation inhibition in normoxia), RBM4 (RNA binding protein 4), and HIF2α has been proposed to interact with mRNA mediating a selective cap-dependent protein synthesis in low oxygen environments (25, 26). Interestingly, the participation of HIF2α in this complex is independent of its transcription factor activity (26). Using these results, we depleted the expression of eIF4E and $eIF4E_2$ in macrophages using specific siRNAs and found that hypoxia-induced DPD synthesis is an $eIF4E_2$-dependent process (**Fig. 3H**). These results suggested that DPD expression in hypoxia is controlled by HIF2α independently of its transcription factor activity in an $eIF4E_2$-dependent mechanism.

TAMs in human colon cancer tissues harbor the principal component of DPD expression in tumors

We have demonstrated that DPD expression in macrophages confers a chemoresistance to 5-FU. To assess the clinical relevance of this result, we further determined the relative expression of DPD in various cellular populations found in colorectal tumors and colorectal liver metastasis. We first used RNA-seq analysis in various cancer cell lines from the CCLE and confirmed that the 59 cancer cell lines originating from colon cancer presented the lowest level of expression for *DPYD* when compared with other types of cancers (**Fig. 4A**). This result confirmed what we had observed for two colon cancer cell lines RKO and HT-29 (Supplementary Fig. S2C), and emphasized a preeminent role of macrophages in DPD-induced chemoresistance in tumors. We further analyzed tissue samples from patients suffering from colorectal cancer with liver metastasis and found that the strongest expression of DPD was found in areas with a predominance of $CD68^+$ macrophages (**Fig. 4B**). Tumor cells did not present a significant level of DPD expression in metastasis when compared with neighboring TAMs (**Fig. 4C**). Furthermore, in primary tumors, macrophages were also found to express the highest level of DPD, with no detectable expression found in cancer cells (**Fig. 4D**). We further confirmed that macrophages represent the main source of DPD expression, by showing that strongly DPD+ cells were also $CD68^+$ using an immunofluorescence coexpression analysis, both in liver metastasis (**Fig. 4E**) and primary tumors (**Fig. 4F**). Because CD68 has been found to be less specific than previously thought as a macrophage marker (27), we confirmed our results using the CD163 macrophage marker. We confirmed that DPD+ cells are $CD163^+$ TAMs in liver metastasis and primary tumors (Supplementary Fig. S5A and S5B). These results are consistent with previous IHC analysis of colorectal cancer tissues, demonstrating that cancer cells do not express DPD whereas normal cells that are morphologically similar to macrophages present a strong expression (28). We further confirmed that DPD expressing cells in primary tumors and liver metastasis also express HIF2α (Supplementary Fig. S5C and S5D). All these results indicate that DPD expression in colorectal cancers at the primary site and liver metastasis belongs to macrophages, under the control of oxygen.

Rodents' macrophages do not express significant levels of DPD

To assess the generality of the oxygen control of DPD expression in macrophages we checked whether this mechanism still holds in rodents. Surprisingly, we found that mice bone marrow–derived macrophages (BMDM) do not express a significant level of mouse DPD in normoxia or hypoxia despite the presence of the protein in the mouse liver (**Fig. 5A**). No detectable level of *dpyd* mRNA was found in BMDM from BALB/c mice (Supplementary Fig. S6A). We used open datasets from microarrays to compare the expression of *DPYD* mRNA levels in humans to those in mice. We found that *DPYD* presented the

Published OnlineFirst October 13, 2021; DOI: 10.1158/0008-5472.CAN-21-1572

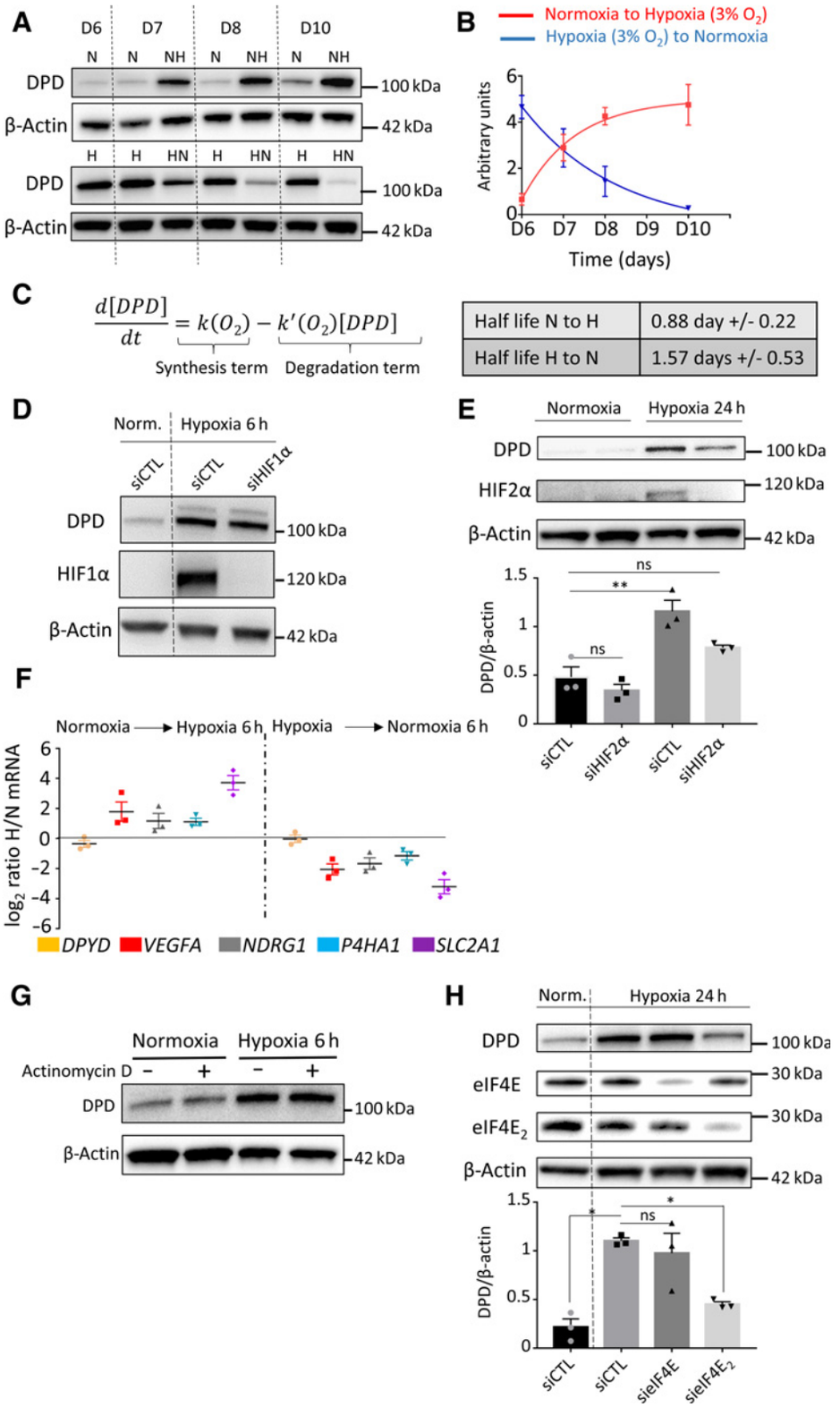

Figure 3.

DPD expression in hypoxic macrophages is under the control of HIF2α and eIF4E2. **A,** Immunoblot of DPD expression in normoxia (N) and hypoxia (H) and during transition from normoxia to hypoxia (NH) and hypoxia to normoxia (HN; $n = 4$). **B,** Quantification of the expression of DPD from immunoblots of **A** for normoxia-to-hypoxia and hypoxia-to-normoxia transitions ($n = 4$). **C,** Left, mathematical model fitting DPD expression curves from **B**. Right, DPD half-life extracted from the model. **D,** Immunoblot analysis of DPD and HIF1α in macrophages exposed to hypoxia (7 mm Hg) for 6 hours under siRNA silencing of HIF1α. β-Actin was used as loading control ($n = 3$). **E,** Immunoblot of DPD expression in normoxia and during normoxia-to-hypoxia transition (hypoxia $PO_2 = 7$ mm Hg) under siRNA silencing of HIF2α ($n = 3$). **F,** mRNA expression ratio NH/N and HN/H transitions (hypoxia $PO_2 = 25$ mm Hg) determined by qPCR for the following genes: *DPYD*, *VEGFA*, *NDRG1*, *P4HA1*, and *SLC2A1*. Macrophages were previously cultured in normoxia or hypoxia ($n = 3$). **G,** Immunoblot of DPD expression during normoxia-to-hypoxia (hypoxia $PO_2 = 7$ mm Hg) transition with macrophages previously exposed to actinomycin D at 1 μg/mL for 20 minutes ($n = 3$). **H,** Immunoblot of DPD expression during normoxia-to-hypoxia transition (hypoxia $PO_2 = 7$ mm Hg) under siRNA silencing of eIF4E2 and eIF4E ($n = 3$). Statistical significance was determined using a one-way ANOVA analysis with Tukey *post hoc* test (**E** and **H**). Error bars, mean ± SEM. *, $P < 0.05$; **, $P < 0.01$; ns, nonsignificant.

Published OnlineFirst October 13, 2021; DOI: 10.1158/0008-5472.CAN-21-1572

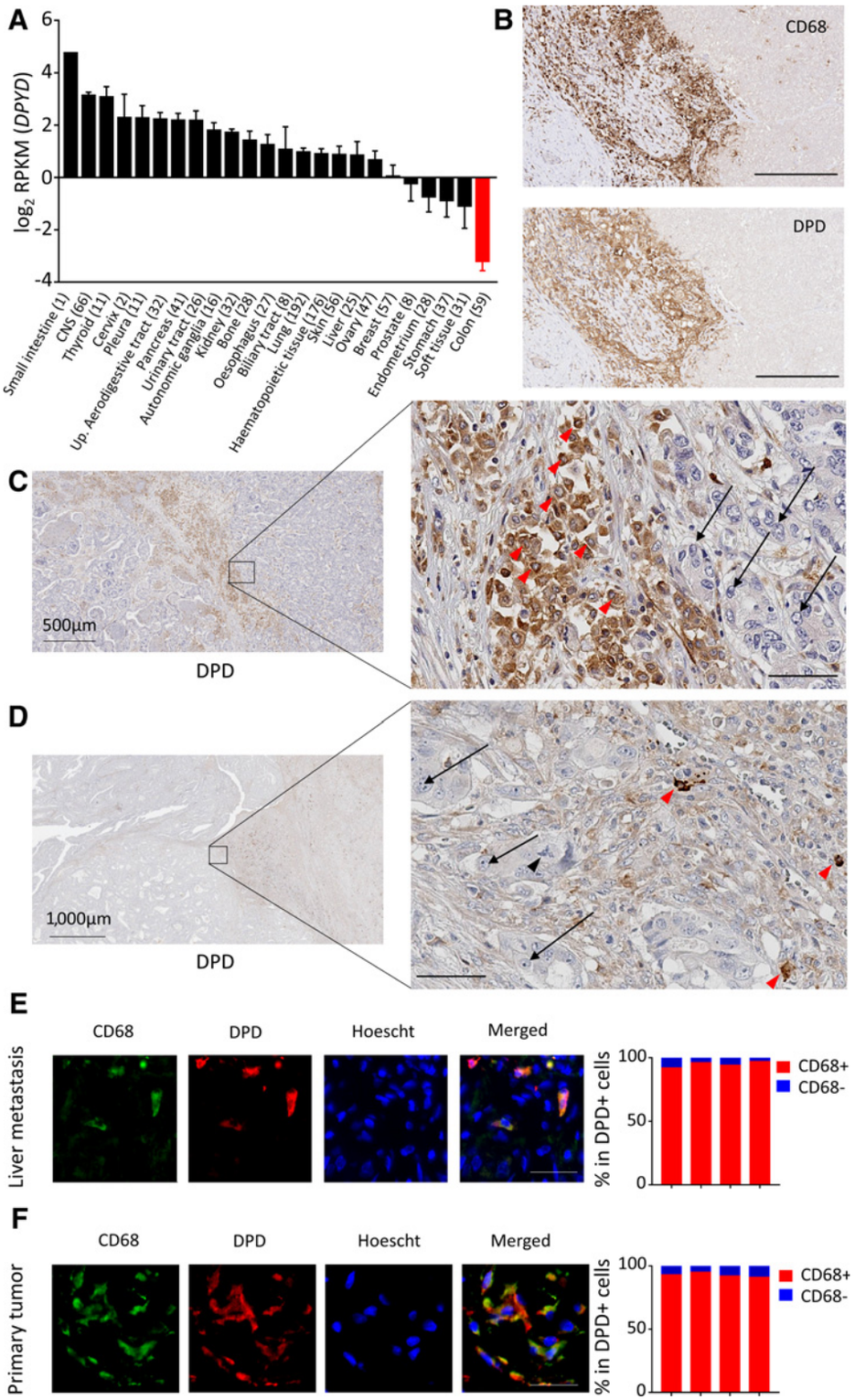

Figure 4.

Macrophages harbor the main DPD expression in colorectal cancer. **A,** RNA-seq analysis of *DPYD* expression in various cancer cell lines from the CCLE. Colon cancer cell lines are in red. **B,** Immunochemistry analysis of CD68 (top) and DPD (bottom) expression in liver metastasis of colorectal cancer ($n = 15$). Scale bar, 200 µm. **C,** Immunochemistry analysis of DPD expression in various cell populations in liver metastasis. Red arrowheads, macrophages; black arrows, metastatic cancerous cells ($n = 15$; zoomed image scale bar, 60 µm). **D,** Immunochemistry analysis of DPD expression in primary tumors. Red arrowheads, macrophages; black arrows, cancer cells; black arrowhead, tripolar mitosis of a cancer cell ($n = 15$; zoomed image scale bar, 60 µm). **E,** Left, immunofluorescence staining in liver metastatic tissues, with CD68 in green, DPD in red, and nuclei stained by Hoescht in blue ($n = 4$). Scale bar, 50 µm. Right, quantification of $CD68^+$ cells in the group of DPD-expressing cells ($n = 4$ patients). **F,** Immunofluorescence staining in primary tumors, with CD68 in green, DPD in red, nuclei stained by Hoescht in blue ($n = 4$). Scale bar, 50 µm. Right, quantification of $CD68^+$ cells in the group of DPD-expressing cells ($n = 4$ patients).

highest levels of expression in the monocyte/macrophages lineage in humans, contrary to what was found in mice where macrophages expressed few mRNA *dpyd* molecules compared with other cellular lineages (**Fig. 5B**). This observation suggested a repression of the mRNA synthesis in mice macrophages. We discovered that the RAW264.7 mice macrophage cell line presented the same pattern with no protein expression in normoxia or hypoxia, confirmed by the absence of DPD enzymatic acitivity (**Fig. 5C**). And this was correlated

Published OnlineFirst October 13, 2021; DOI: 10.1158/0008-5472.CAN-21-1572

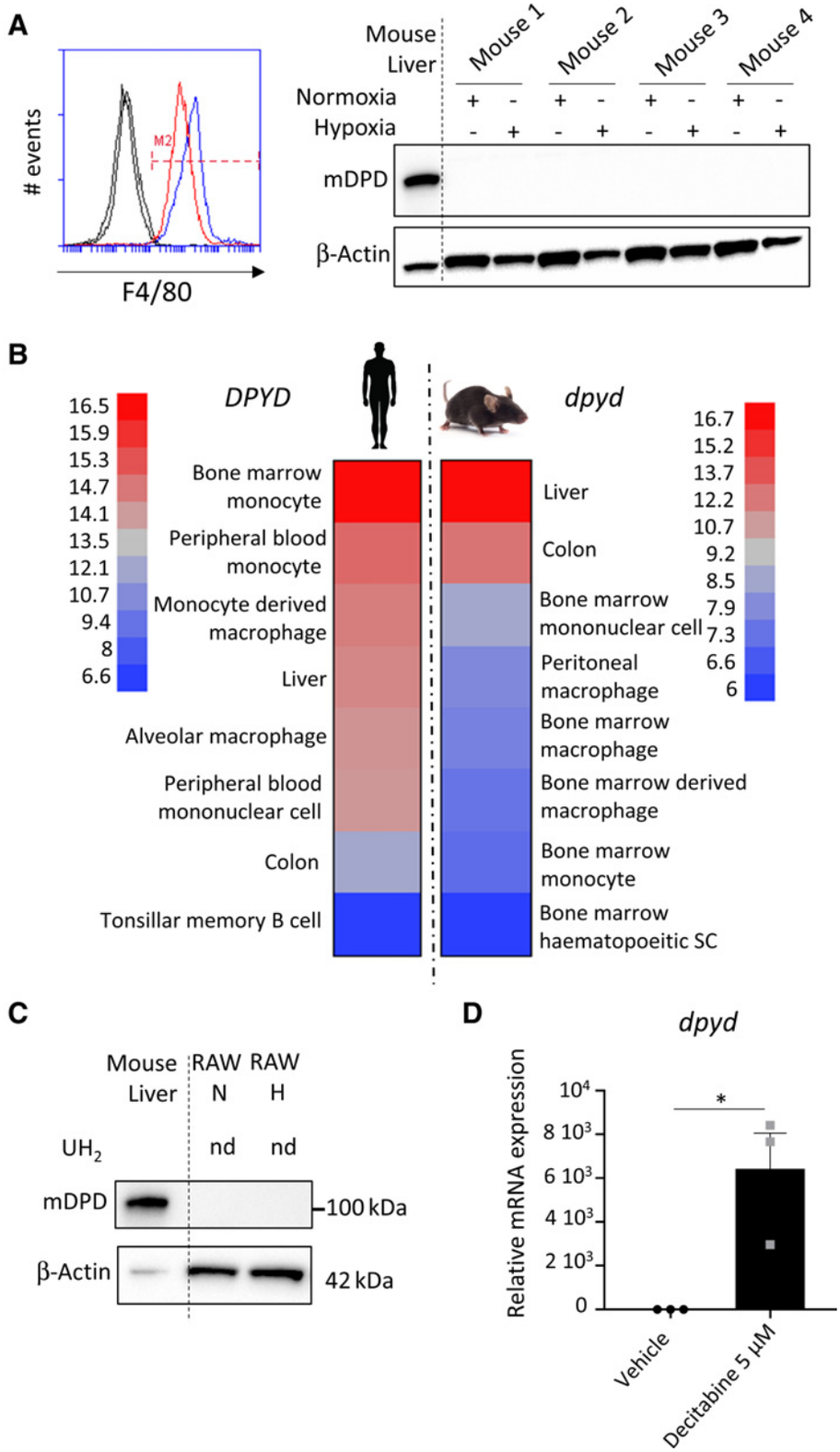

Figure 5.

Mice macrophages do not express DPD. **A,** BMDMs were differentiated in normoxia and hypoxia. F4/80 was studied by flow cytometry (left) and mouse DPD (mDPD) expression by immunoblot (right; $n = 4$). Mouse liver was used as a positive control for mDPD. **B,** Microarray analysis of *DPYD* mRNA expression in monocytes/macrophage populations in mice and humans. In each group, the highest and lowest level of expression was used to scale the heatmap. **C,** RAW264.7 macrophages were cultivated in normoxia and in hypoxia. mDPD expression was studied by immunoblot. No production of dihydrouracil was found in RAW supernatant using HPLC. nd, nondetected. **D,** *dpyd* mRNA level of expression in RAW macrophages exposed to decitabine at 5 μmol/L during 24 hours ($n = 3$).

Published OnlineFirst October 13, 2021; DOI: 10.1158/0008-5472.CAN-21-1572

with the absence of mRNA of *dpyd* in these cells (Supplementary Fig. S6B). We then confirmed the epigenetic control of gene expression using 5-aza-2′deoxycytidine (decitabine), a DNA hypomethylation agent. Indeed, decitabine led to a strong increase in *dpyd* mRNA level of expression in treated RAW macrophages compared with nontreated cells (**Fig. 5D**). This result suggested that DNA methylation in mice is, at least in part, responsible for *dpyd* repressed expression. To further confirm the generality of this finding we analyzed DPYD mRNA expression in TAMs from colorectal cancers and breast cancers in mice and confirm the low level of expression of DPYD in mice macrophages (Supplementary Fig. S7).

Transduced human DPD in mice macrophages leads to 5-FU chemoresistance *in vivo*

To obtain a mice model mimicking the human DPD expression in macrophages, we transduced the ORF of the human *DPYD* gene under the control of a cytomegalovirus promoter incorporated into a lentivirus to obtain "DPD-humanized" mice macrophages (**Fig. 6A**). CM of mice macrophages expressing DPD were able to confer chemoresistance to CT-26 (a mice colon cancer cell line that does not express DPD) demonstrating the functionality of the transduced DPD (**Fig. 6B**). We also observed that wild-type macrophages were associated with a weak decrease of 5-FU–induced growth inhibition compared with macrophages expressing DPD, demonstrating that the DPD-induced chemoresistance mechanism is probably the most efficient one (**Fig. 6B**). To confirm the relationship between DPD expression in macrophages and chemoresistance in colorectal cancers, a tumor assay in mice was performed. CT-26 and RAW macrophages expressing or not human DPD were implanted into flanks of BALB/c mice. Ten days after the implantation, 5-FU was injected intraperitoneally at 25 mg/kg during 5 days for 2 consecutive weeks (**Fig. 6C**). We confirmed that tumors harboring macrophages expressing DPD were more resistant to 5-FU than the control tumors with wild-type macrophages (**Fig. 6D–F**), indicating that DPD expression in TAMs promotes chemoresistance *in vivo*.

Discussion

In recent years, the immune system has become a key element in the understanding of the mechanisms involved in the tumor interaction with its surrounding healthy tissue as well as a provider of new therapeutic strategies. The tumor immune microenvironment is composed of various types of immune cells. Nevertheless, TAMs usually represent quantitatively the largest population found in solid cancers. TAMs are involved in tumor growth, immune evasion, neoangiogenesis, and treatment resistance. Using depletion methods, a large number of studies have reported an increased chemosensitivity when macrophages are removed from the tumor (5). Furthermore, coculture studies have revealed macrophage-mediated resistance mechanisms to various anti-cancer drugs such as paclitaxel, doxorubicin, etoposide, or gemcitabine (29, 30). Specifically, depletion of $MHCII^{lo}$ TAMs leads to an increased sensitivity to taxol-induced DNA damage and apoptosis (31). Another key point is that TAMs were mainly found in hypoxic areas where they can further favor hypoxia by secreting VEGFA, leading to the formation of an abnormal vasculature (32). Accordingly, mechanisms involving macrophages-induced chemoresistance rely usually on the secretions of factors by macrophages, such as pyrimidine nucleosides (deoxycytidine) inhibiting gemcitabine induction of apoptosis in pancreatic ductal adenocarcinoma (33). In colorectal cancer, the implication of macrophages in chemoresistance has also been suggested on the basis of *in vitro* and *in vivo* studies. The proposed mechanisms are diverse but also involve secreted factors. For example, it has been proposed that IL6 secreted by macrophages can stimulate STAT3 in cancer cells inducing the inhibition of the RAB22A/BCL2 pathway through miR-204-5p expression, thereby leading to chemoresistance to 5-FU (11). Similarly the secretion of putrescin, a member of the polyamine family, by macrophages was shown to suppress the JNK/Caspase 3 pathway in cancer cells, providing a protection against 5-FU (12).

To understand the involvement of TAMs in chemoresistance in colorectal cancer, we designed the current study to incorporate oxygen concentration as a key environmental parameter. We previously reported that the oxygen availability in macrophages' environment greatly influences their immune functions such as their ability to clear apoptotic cells (13). As colon tissues are naturally exposed to levels of oxygen that are usually lower than 5% O_2 (34) with values that could reach even lower values (<1% O_2) in tumors, oxygen appears as a fundamental parameter to understand macrophage involvement in chemoresistance. We found that hypoxic macrophages provide a chemoresistance to 5-FU when cocultured with cancer cells contrary to normoxic macrophages (**Fig. 1A**). We then verified whether a secreted factor by human macrophages could provide a chemoresistance and finally found a direct effect of hypoxic macrophages on 5-FU (**Fig. 1B** and **C**). Our molecular analysis revealed that the DPD, an enzyme of the pyrimidine catabolism pathway, is overexpressed in hypoxic human macrophages providing a direct chemoresistance mechanism relying on its enzymatic activity (**Fig. 2A**, **C**, **D**, **E**, **F**, and **I**; Supplementary Fig. S3). It is known for more than thirty years that DPD expression in the liver limits 5-FU biodisponibility (35) and its expression in peripheral mononuclear cells is the gold standard to detect defects in DPD activity due to mutations to prevent 5-FU intolerance in patients (36). Despite this knowledge, no systematic analysis of the control of DPD expression and functions in human macrophages in the tumor microenvironment was performed before this study. We have discovered that in hypoxia, DPD is under the control of HIF2α independently of its transcription factor activity (**Fig. 3E–G**). This control was also found to be under the control of $eIF4E_2$ (**Fig. 3H**). This protein has been proposed to be part of a translation initiation complex, comprising HIF2α, which is only active in hypoxia (25, 26). This complex is one of the mechanisms involved in the adaptive protein synthesis in hypoxia, mitigating the global shutdown of translation taking place in this context (37).

DPD expression in macrophages seemed to be particularly relevant in colorectal cancer where cancer cells present a low expression level of the protein in primary tumors as well as in liver metastasis (**Fig. 4**; Supplementary Fig. S5A and S5B). This general feature seems to rely on the epigenetic control of DPD expression in cancer cells. Indeed, many colon cancer cells lines have been noted to harbor a histone H3K27me3 mark that blocks the fixation of the transcription factor PU.1, leading to the inhibition of DPD mRNA transcription (21). We further found that macrophages in mice do not express DPD due to a repression of its transcriptional expression (**Fig. 5**). This finding forced us to reevaluate previous *in vivo* models that were used to assess the involvement of macrophages in colorectal cancer, as DPD expression in macrophages was lacking in these models. Indeed, we showed the importance of DPD activity in macrophages and found that it represents the main quantitative source of degradation of 5-FU in human colorectal tumors. To demonstrate the relevance of this mechanism to chemoresistance, we designed an *in vivo* model using mice macrophages expressing the transduced human DPD. This model offered us the possibility to validate the importance of DPD expression in TAMs leading to 5-FU

Published OnlineFirst October 13, 2021; DOI: 10.1158/0008-5472.CAN-21-1572

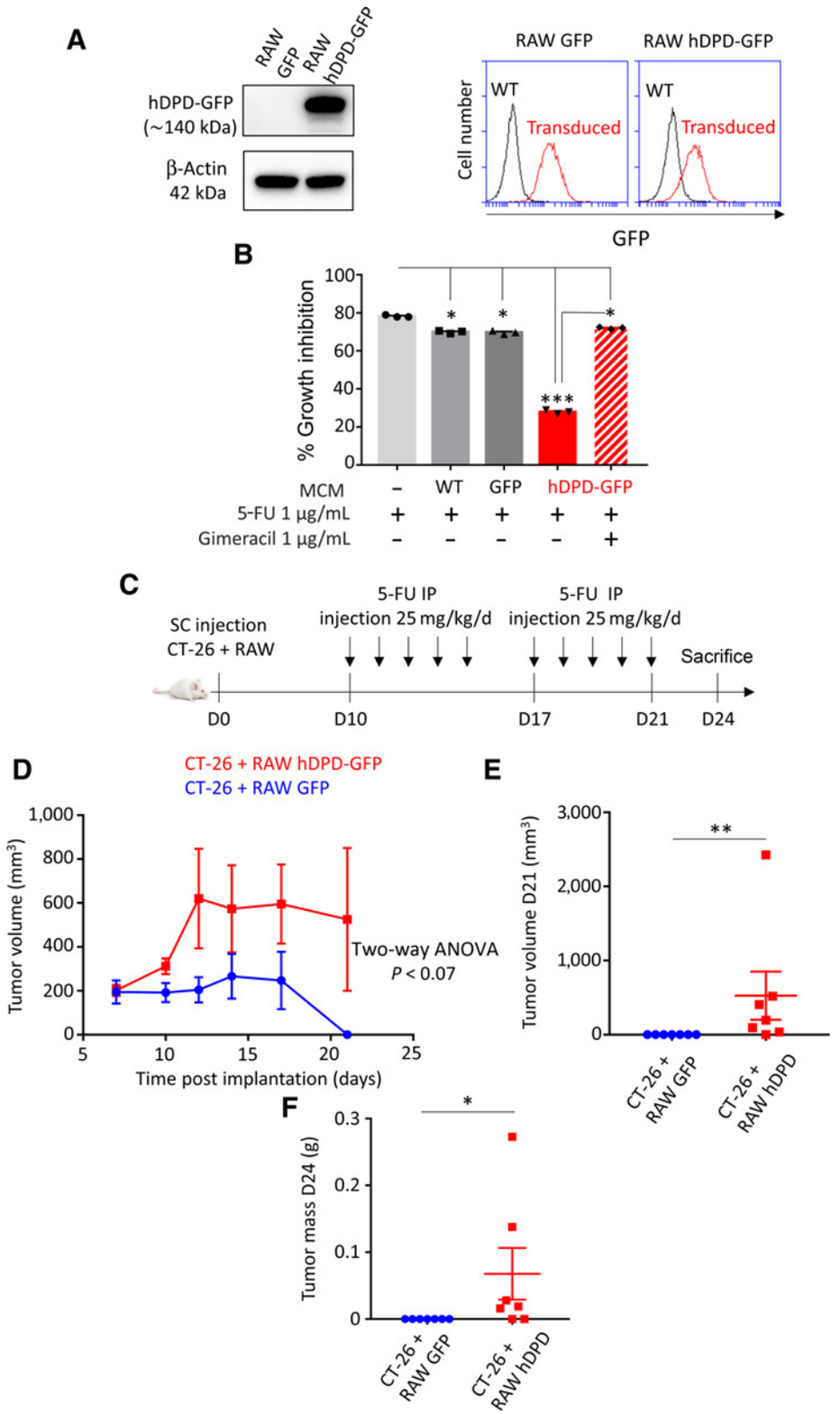

Figure 6.

Transduced human DPD in mice macrophages leads to 5-FU chemoresistance *in vivo*. **A,** Left, immunoblot of RAW macrophages transduced to express GFP and human DPD (hDPD)-GFP. Right, transduced GFP and hDPD-GFP proteins levels of expression analyzed by flow cytometry. **B,** Growth inhibition of CT-26, after 48 hours, under the presence of CM containing 5-FU (0.1 μg/mL) exposed to macrophages WT, expressing GFP or hDPD-GFP for 24 hours. Gimeracil was used to block hDPD activity at 1 μg/mL. **C,** Tumor assay was performed on female Balb/c mice of 7 weeks. A total of 10^6 CT-26 and 10^6 RAW were implanted subcutaneously. After 10 days, daily bolus of 5-FU 25 mg/kg was injected intraperitoneally according to the timeline represented. **D,** Tumor growth was followed during the protocol ($n = 7$ in each group). **E,** Tumor size was determined at day 21 (last day of 5-FU injection protocol). **F,** Tumor weight was determined at day 24 ($n = 7$ in each group). Statistical significance was determined using a one-way ANOVA analysis with Tukey *post hoc* test (**B**), a two-way ANOVA analysis for tumor growth curves (**D**), and a Mann–Withney test (**E** and **F**). Error bars, mean ± SEM. *, $P < 0.05$; **, $P < 0.01$; ***, $P < 0.001$.

Published OnlineFirst October 13, 2021; DOI: 10.1158/0008-5472.CAN-21-1572

chemoresistance. Supporting these results, previous clinical studies have suggested that DPD mRNA expression is a marker of chemoresistance in colorectal cancer. These studies usually assumed that DPD expression is mainly found in cancer cells, contrary to what we have observed. Nevertheless, the mRNA level in the bulk of the tumor is correlated with a low response to 5-FU confirming its relevance (38–41). The results obtained in our study suggest that the main predictive factor for 5-FU response is DPD expression in macrophages located in tumors and liver metastasis. That expression is probably important in the invasive front, where TAMs seem to concentrate (9). Furthermore, the invasion front is known to be a hypoxic area in colorectal cancers (42). Because the mechanism identified in this study relied on quantitative expression of DPD by macrophages, the assessment of the spatial heterogeneity of DPD expression will be necessary to stratify patients in various response groups for chemotherapy (43). Thus this study constitutes an important progress in the understanding of the role of the tumor immune environment in chemoresistance to 5-FU in colorectal cancer. Finally, further clinical studies are needed to confirm the clinical relevance of these findings and validate DPD expression in macrophages as a new predictive marker of response to 5-FU–based treatments.

Authors' Disclosures

A. Millet reports grants from Inserm ATIP Avenir grant, Fondation AGIR pour les maladies chroniques, Ligue nationale contre le cancer, European Union's Horizon 2020, and Fondation MSD-Avenir during the conduct of the study. No disclosures were reported by the other authors.

Authors' Contributions

M. Malier: Investigation, writing–review and editing. **K. Gharzeddine:** Investigation, writing–review and editing. **M.-H. Laverriere:** Investigation. **S. Marsili:** Investigation. **F. Thomas:** Investigation. **T. Decaens:** Supervision. **G.S. Roth:** Validation, investigation. **A. Millet:** Conceptualization, resources, data curation, formal analysis, supervision, funding acquisition, validation, investigation, visualization, methodology, writing–original draft, project administration, writing–review and editing.

Acknowledgments

A. Millet is supported by the ATIP/Avenir program (Inserm and La ligue nationale contre le cancer). M. Malier is supported by the APMC Fondation (Agir pour les Maladies Chroniques). K. Gharzeddine is supported by the ITN (International Training Network) Phys2Biomed project, which is funded from the European Union's Horizon 2020 research and innovation programme under the Marie Skøodowska-Curie grant agreement no. 812772. This work is supported by the ERiCAN program of Fondation MSD-Avenir (Reference DS-2018-0015). The authors gratefully acknowledge Florent Chuffart from the EpiMed core facility (http://epimed.univ-grenoble-alpes.fr) for his support and assistance in this work. The authors would like to thank Xavier Fonrose, Edwige Col, Magali Court, and Floriane Laurent for their technical assistance. The authors thank the zoo technicians of PHTA facility for animal housing and care. They thank Lemoigne, Federspiel, and Plasse from the University Hospital of Grenoble-Alpes for kindly providing clinical grade 5-FU.

The costs of publication of this article were defrayed in part by the payment of page charges. This article must therefore be hereby marked *advertisement* in accordance with 18 U.S.C. Section 1734 solely to indicate this fact.

Received May 19, 2021; revised August 17, 2021; accepted October 7, 2021; published first October 13, 2021.

References

1. Siegel RL, Miller KD, Jemal A. Cancer statistics, 2020. CA Cancer J Clin 2020;70:7–30.
2. Marin JJG, Sanchez de Medina F, Castaño B, Bujanda L, Romero MR, Martinez-Augustin O, et al. Chemoprevention, chemotherapy, and chemoresistance in colorectal cancer. Drug Metab Rev 2012;44:148–72.
3. Vasan N, Baselga J, Hyman DM. A view on drug resistance in cancer. Nature 2019;575:299–309.
4. Binnewies M, Roberts EW, Kersten K, Chan V, Fearon DF, Merad M, et al. Understanding the tumor immune microenvironment (TIME) for effective therapy. Nat Med 2018;24:541–50.
5. Ruffell B, Coussens LM. Macrophages and therapeutic resistance in cancer. Cancer Cell 2015;27:462–72.
6. Yang M, McKay D, Pollard JW, Lewis CE. Diverse functions of macrophages in different tumor microenvironments. Cancer Res 2018;78:5492–503.
7. DeNardo DG, Ruffell B. Macrophages as regulators of tumour immunity and immunotherapy. Nat Rev Immunol 2019;19:369–82.
8. Aras S, Zaidi MR. TAMeless traitors: macrophages in cancer progression and metastasis. Br J Cancer 2017;117:1583–91.
9. Pinto ML, Rios E, Durães C, Ribeiro R, Machado JC, Mantovani A, et al. The two faces of tumor-associated macrophages and their clinical significance in colorectal cancer. Front Immunol 2019;10:1875.
10. Ye L, Zhang T, Kang Z, Guo G, Sun Y, Lin K, et al. Tumor-infiltrating immune cells act as a marker for prognosis in colorectal cancer. Front Immunol 2019;10:2368.
11. Yin Y, Yao S, Hu Y, Feng Y, Li M, Bian Z, et al. The Immune-microenvironment confers chemoresistance of colorectal cancer through macrophage-derived IL6. Clin Cancer Res 2017;23:7375–87.
12. Zhang X, Chen Y, Hao L, Hou A, Chen X, Li Y, et al. Macrophages induce resistance to 5-fluorouracil chemotherapy in colorectal cancer through the release of putrescine. Cancer Lett 2016;381:305–13.
13. Court M, Petre G, Atifi ME, Millet A. Proteomic signature reveals modulation of human macrophage polarization and functions under differing environmental oxygen conditions. Mol Cell Proteomics 2017;16:2153–68.
14. Henze A-T, Mazzone M. The impact of hypoxia on tumor-associated macrophages. J Clin Invest 2016;126:3672–9.
15. Barretina J, Caponigro G, Stransky N, Venkatesan K, Margolin AA, Kim S, et al. The Cancer Cell Line Encyclopedia enables predictive modeling of anticancer drug sensitivity. Nature 2012;483:603–7.
16. Tsherniak A, Vazquez F, Montgomery PG, Weir BA, Kryukov G, Cowley GS, et al. Defining a cancer dependency map. Cell 2017;170:564–76.
17. Hruz T, Laule O, Szabo G, Wessendorp F, Bleuler S, Oertle L, et al. Genevestigator V3: a reference expression database for the meta-analysis of transcriptomes. Adv Bioinforma 2008;2008:420747.
18. Thomas F, Hennebelle I, Delmas C, Lochon I, Dhelens C, Tixidre CG, et al. Genotyping of a family with a novel deleterious DPYD mutation supports the pretherapeutic screening of DPD deficiency with dihydrouracil/uracil ratio. Clin Pharmacol Ther 2016;99:235–42.
19. Enot DP, Vacchelli E, Jacquelot N, Zitvogel L, Kroemer G. TumGrowth: an open-access web tool for the statistical analysis of tumor growth curves. OncoImmunology 2018;7:e1462431.
20. Ve?tvička V, Bilej M, Kincade PW. Resistance of macrophages to 5-fluorouracil treatment. Immunopharmacology 1990;19:131–8.
21. Wu R, Nie Q, Tapper EE, Jerde CR, Dunlap GS, Shrestha S, et al. Histone H3K27 trimethylation modulates 5-fluorouracil resistance by inhibiting PU.1 binding to the DPYD promoter. Cancer Res 2016;76:6362–73.
22. Zheng J-F, Wang H-D. 5-Fluorouracil concentration in blood, liver and tumor tissues and apoptosis of tumor cells after preoperative oral 5′-deoxy-5-fluorouridine in patients with hepatocellular carcinoma. World J Gastroenterol 2005;11:3944–7.
23. Tanaka-Nozaki M, Onda M, Tanaka N, Kato S. Variations in 5-fluorouracil concentrations of colorectal tissues as compared with Dihydropyrimidine Dehydrogenase (DPD) enzyme activities and DPD messenger RNA levels. Clin Cancer Res 2001;7:2783–7.
24. Wilson ZE, Rostami-Hodjegan A, Burn JL, Tooley A, Boyle J, Ellis SW, et al. Inter-individual variability in levels of human microsomal protein and hepatocellularity per gram of liver. Br J Clin Pharmacol 2003;56:433–40.
25. Ho JJD, Wang M, Audas TE, Kwon D, Carlsson SK, Timpano S, et al. Systemic reprogramming of translation efficiencies on oxygen stimulus. Cell Rep 2016;14:1293–300.

Published OnlineFirst October 13, 2021; DOI: 10.1158/0008-5472.CAN-21-1572

26. Uniacke J, Holterman CE, Lachance G, Franovic A, Jacob MD, Fabian MR, et al. An oxygen-regulated switch in the protein synthesis machinery. Nature 2012; 486:126–9.
27. Ruffell B, Au A, Rugo HS, Esserman LJ, Hwang ES, Coussens LM. Leukocyte composition of human breast cancer. Proc Natl Acad Sci U S A 2012;109:2796–801.
28. Kamoshida S, Shiogama K, Matsuoka H, Matsuyama A, Shimomura R, Inada K, et al. Immunohistochemical demonstration of dihydropyrimidine dehydrogenase in normal and cancerous tissues. Acta Histochem Cytochem 2003;36:471–9.
29. Mitchem JB, Brennan DJ, Knolhoff BL, Belt BA, Zhu Y, Sanford DE, et al. Targeting tumor-infiltrating macrophages decreases tumor-initiating cells, relieves immunosuppression, and improves chemotherapeutic responses. Cancer Res 2013;73:1128–41.
30. Shree T, Olson OC, Elie BT, Kester JC, Garfall AL, Simpson K, et al. Macrophages and cathepsin proteases blunt chemotherapeutic response in breast cancer. Genes Dev 2011;25:2465–79.
31. Olson OC, Kim H, Quail DF, Foley EA, Joyce JA. Tumor-associated macrophages suppress the cytotoxic activity of antimitotic agents. Cell Rep 2017;19: 101–13.
32. Murdoch C, Muthana M, Coffelt SB, Lewis CE. The role of myeloid cells in the promotion of tumour angiogenesis. Nat Rev Cancer 2008;8:618–31.
33. Halbrook CJ, Pontious C, Kovalenko I, Lapienyte L, Dreyer S, Lee H-J, et al. Macrophage-released pyrimidines inhibit gemcitabine therapy in pancreatic cancer. Cell Metab 2019;29:1390–9.
34. Keeley TP, Mann GE. Defining physiological normoxia for improved translation of cell physiology to animal models and humans. Physiol Rev 2018;99:161–234.
35. Diasio RB, Harris BE. Clinical pharmacology of 5-fluorouracil. Clin Pharmacokinet 1989;16:215–37.
36. Chazal M, Etienne MC, Renée N, Bourgeon A, Richelme H, Milano G. Link between dihydropyrimidine dehydrogenase activity in peripheral blood mononuclear cells and liver. Clin Cancer Res 1996;2:507–10.
37. Lee P, Chandel NS, Simon MC. Cellular adaptation to hypoxia through hypoxia inducible factors and beyond. Nat Rev Mol Cell Biol 2020;21:268–83.
38. Ichikawa W, Uetake H, Shirota Y, Yamada H, Nishi N, Nihei Z, et al. Combination of dihydropyrimidine dehydrogenase and thymidylate synthase gene expressions in primary tumors as predictive parameters for the efficacy of fluoropyrimidine-based chemotherapy for metastatic colorectal cancer. Clin Cancer Res 2003;9:786–91.
39. Salonga D, Danenberg KD, Johnson M, Metzger R, Groshen S, Tsao-Wei DD, et al. Colorectal tumors responding to 5-fluorouracil have low gene expression levels of dihydropyrimidine dehydrogenase, thymidylate synthase, and thymidine phosphorylase. Clin Cancer Res 2000;6:1322–7.
40. Shirota Y, Ichikawa W, Uetake H, Yamada H, Nihei Z, Sugihara K. Intratumoral dihydropyrimidine dehydrogenase messenger RNA level reflects tumor progression in human colorectal cancer. Ann Surg Oncol 2002;9:599–603.
41. Soong R, Shah N, Salto-Tellez M, Tai BC, Soo RA, Han HC, et al. Prognostic significance of thymidylate synthase, dihydropyrimidine dehydrogenase and thymidine phosphorylase protein expression in colorectal cancer patients treated with or without 5-fluorouracil-based chemotherapy. Ann Oncol 2008; 19:915–9.
42. Righi A, Sarotto I, Casorzo L, Cavalchini S, Frangipane E, Risio M. Tumour budding is associated with hypoxia at the advancing front of colorectal cancer. Histopathology 2015;66:982–90.
43. Marusyk A, Janiszewska M, Polyak K. Intratumor heterogeneity: the rosetta stone of therapy resistance. Cancer Cell 2020;37:471–84.

Cancer Research
The Journal of Cancer Research (1916–1930) | The American Journal of Cancer (1931–1940)

AACR American Association for Cancer Research

Hypoxia Drives Dihydropyrimidine Dehydrogenase Expression in Macrophages and Confers Chemoresistance in Colorectal Cancer

Marie Malier, Khaldoun Gharzeddine, Marie-Hélène Laverriere, et al.

Cancer Res 2021;81:5963-5976. Published OnlineFirst October 13, 2021.

Supplementary Figure S1

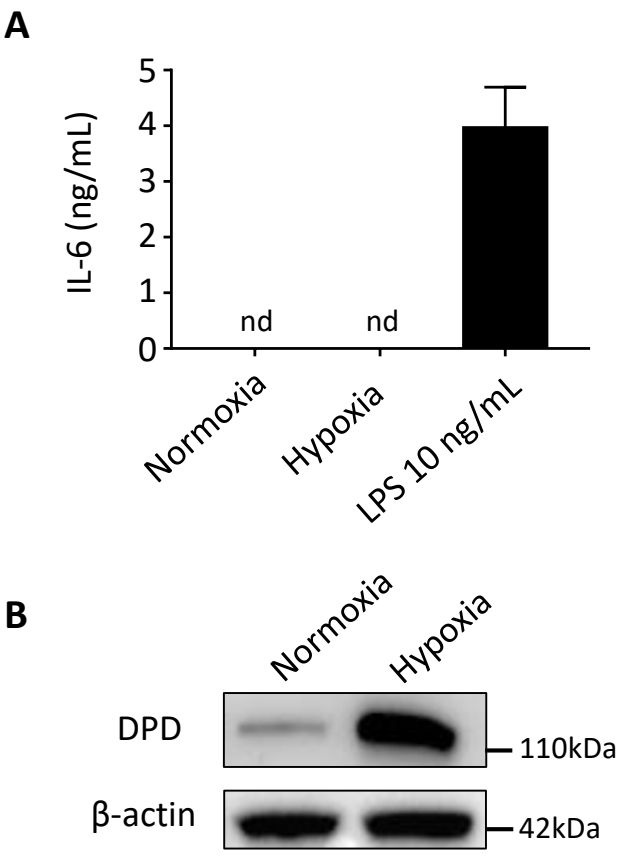

Supplementary Figure S2

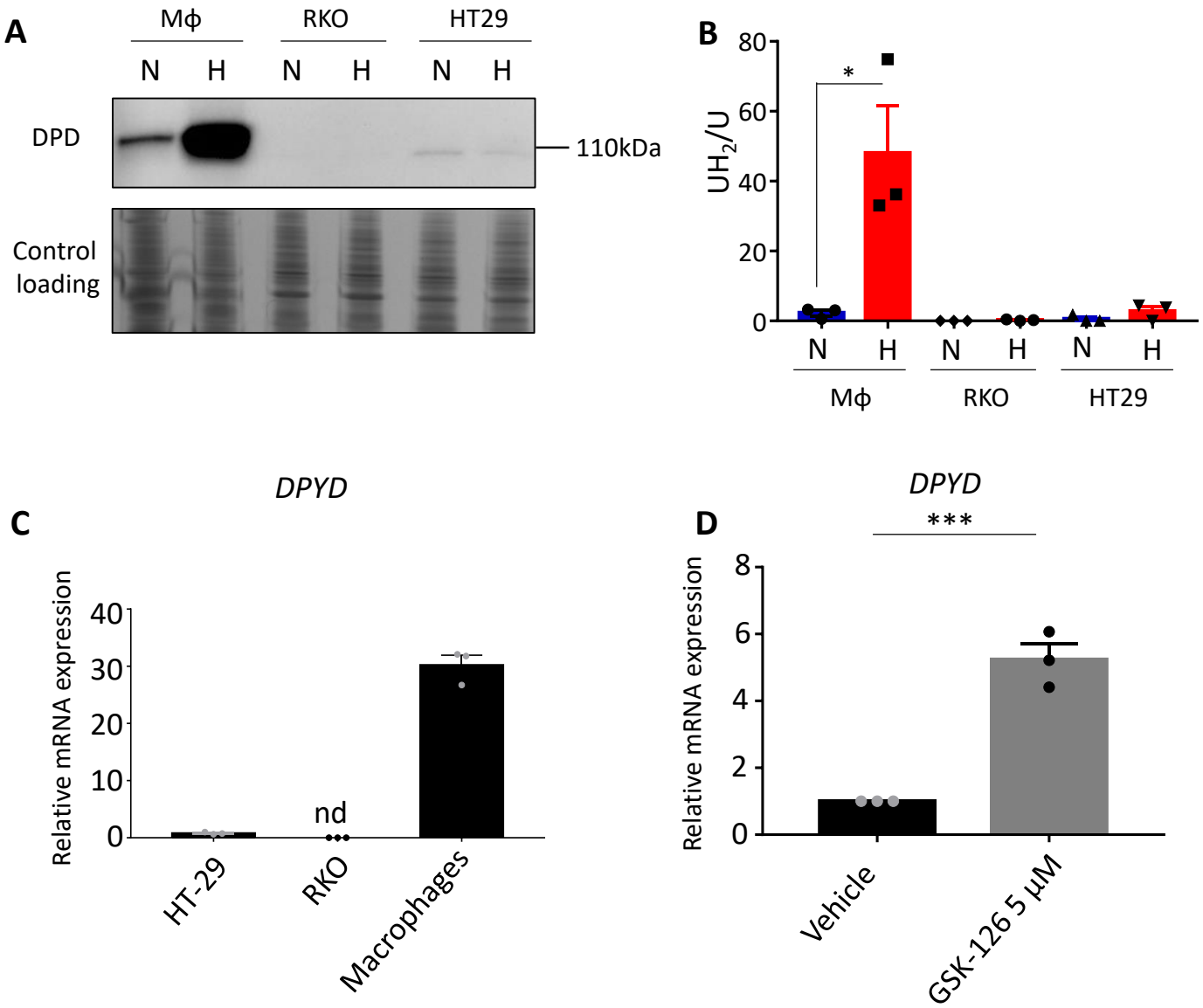

Supplementary Figure S3

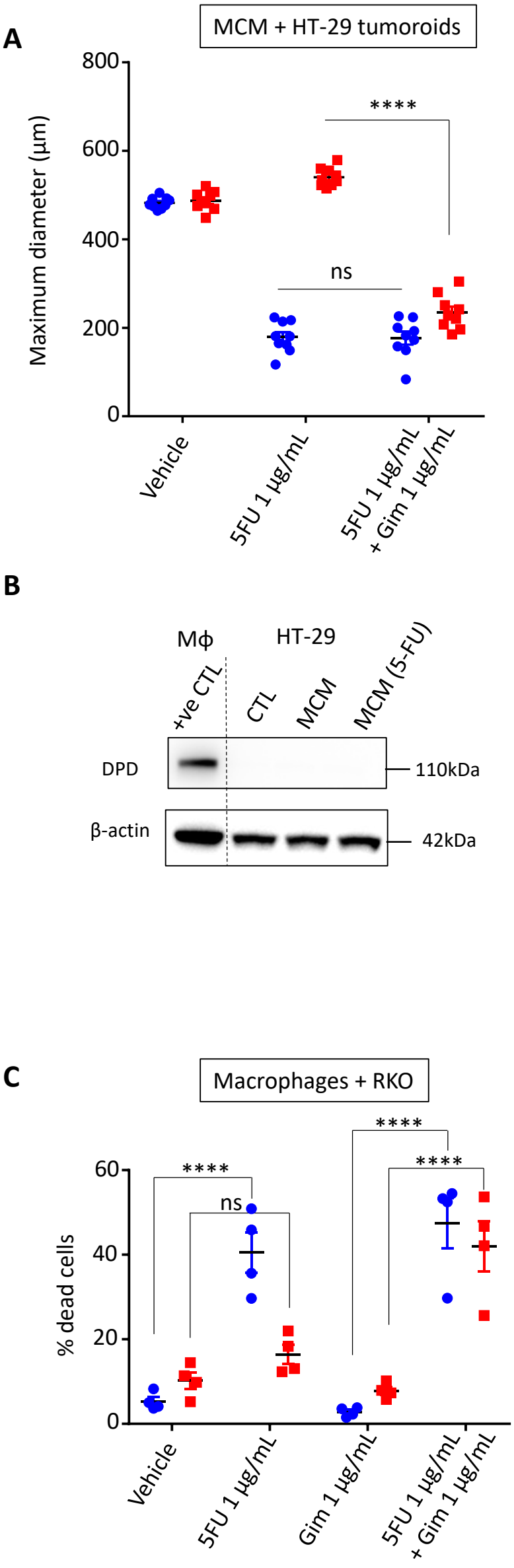

Supplementary Figure S4

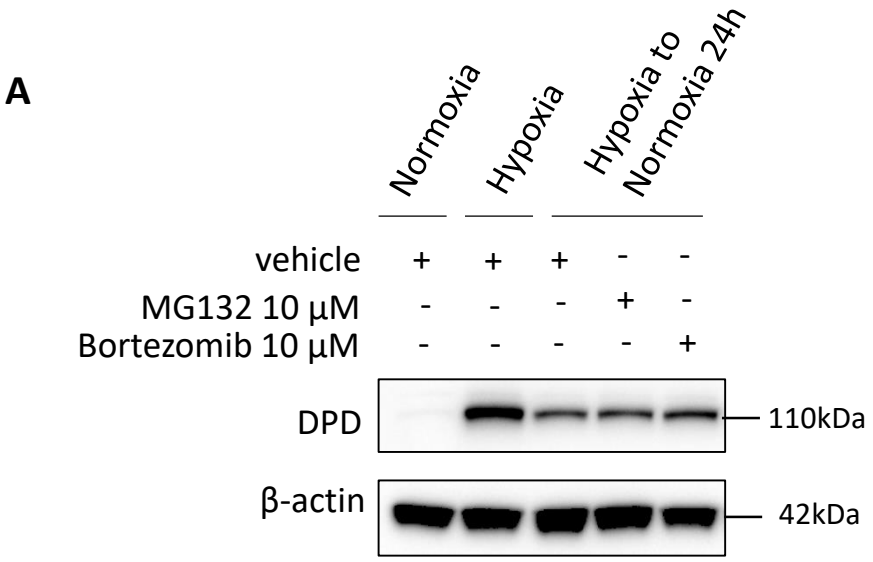

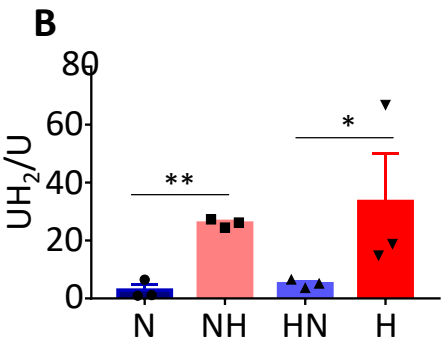

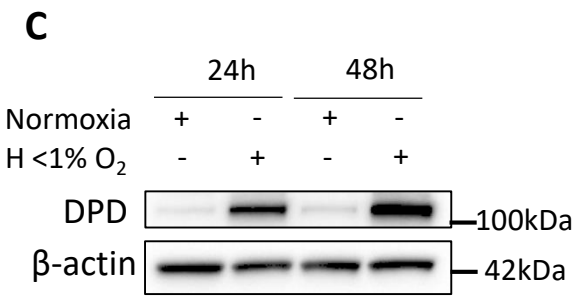

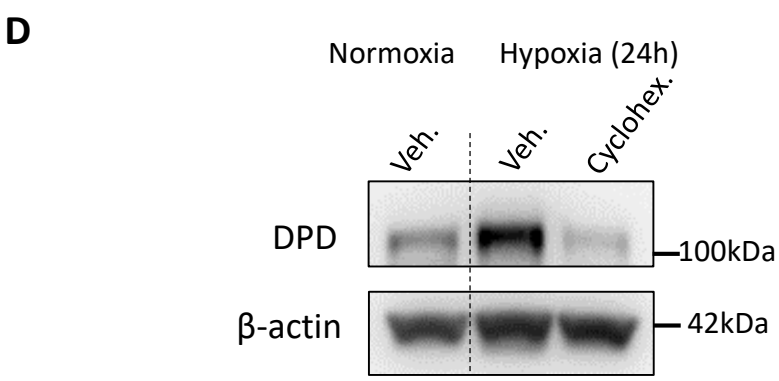

Supplementary Figure S5

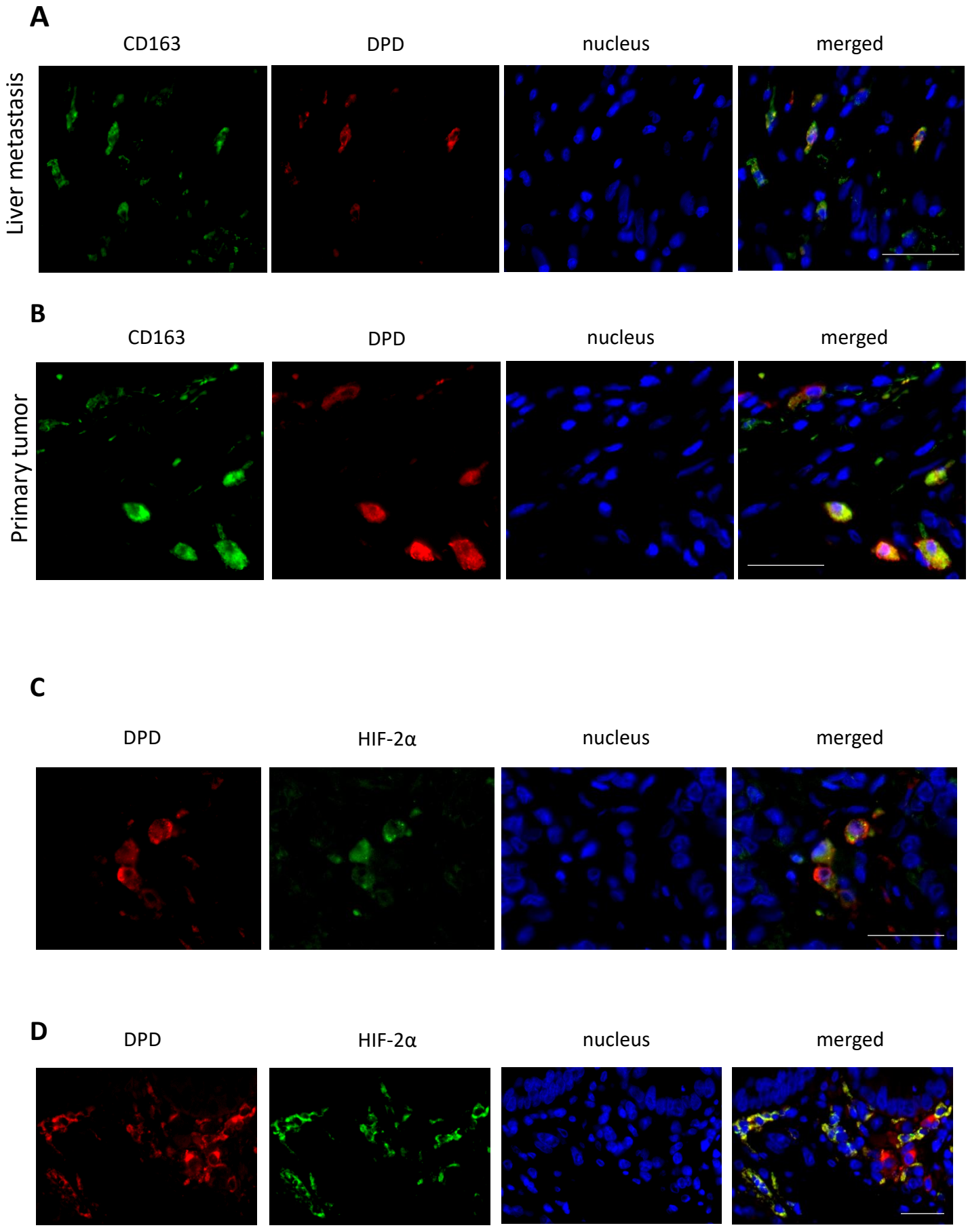

Supplementary Figure S6

A

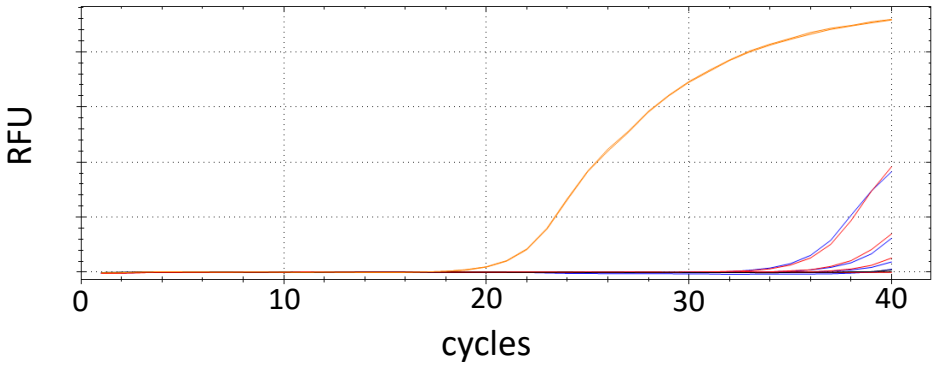

B

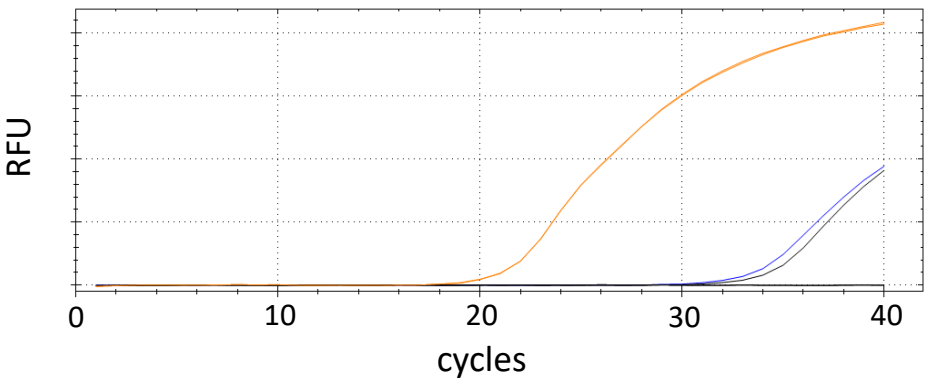

Supplementary Figure S7

A

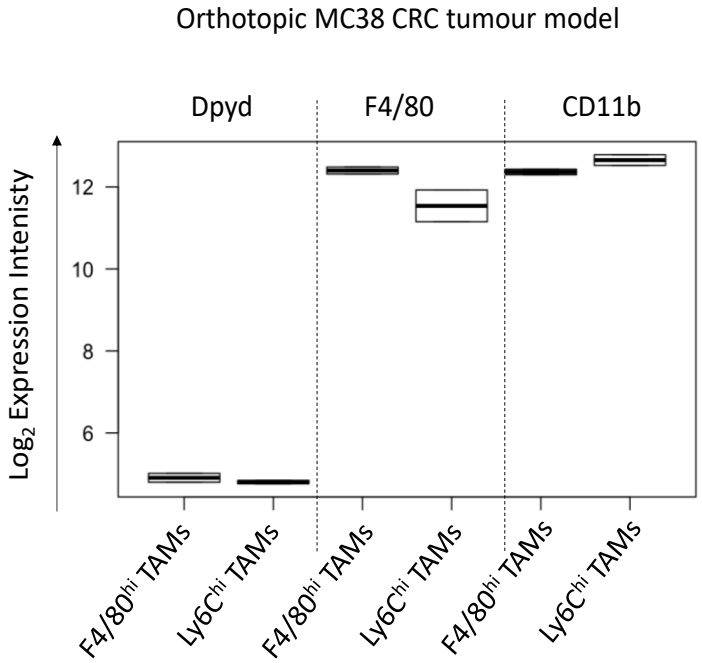

B

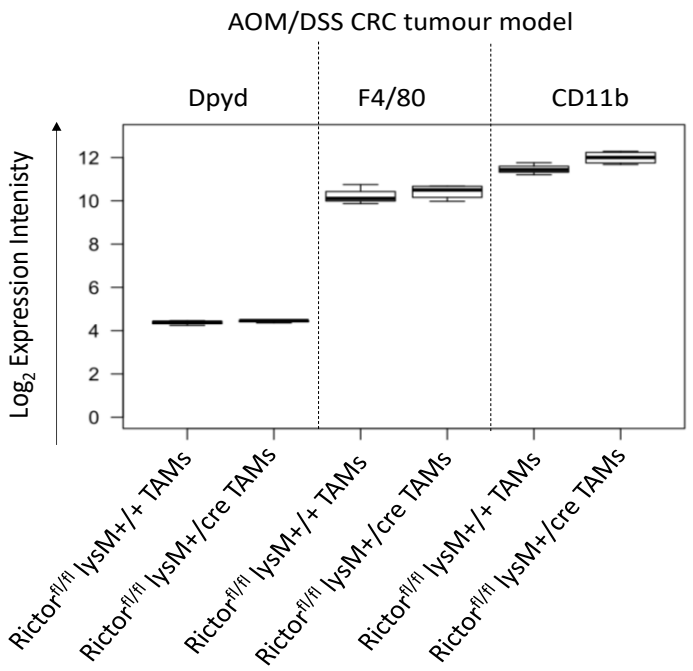

C

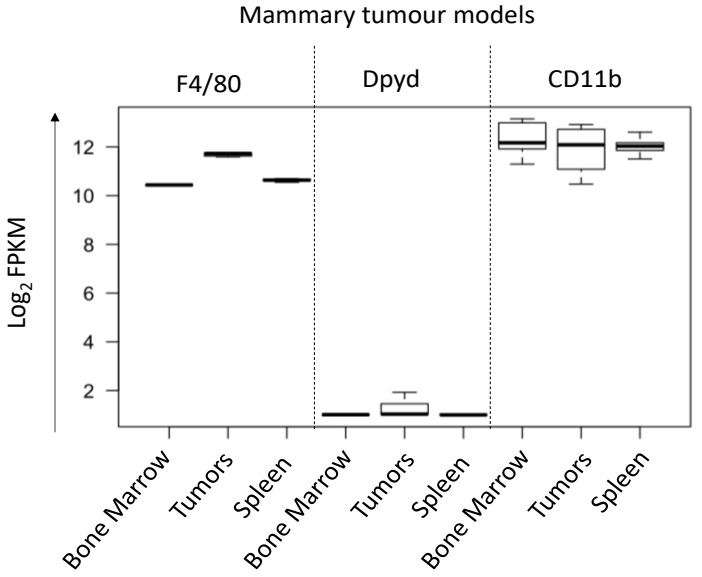

Malier et al

Hypoxia drives dihydropyrimidine dehydrogenase expression in macrophages and confers chemoresistance in colorectal cancer

Contents

Supplementary Figures Legends

Figure S1. Hypoxic macrophages overexpress DPD

A, IL-6 secretion of normoxic and hypoxic macrophages using LPS stimulation as a positive control determined by ELISA (n=3). No secreted IL-6 was detected (threshold at 10 pg/mL) in normoxic and hypoxic macrophages. nd=non detected. **B**, Immunoblot analysis of DPD expression in human macrophages differentiated in normoxia and hypoxia (n= 10).

Figure S2. DPD expression in colorectal cancer cells is repressed compared to macrophages

A, Immunoblot analysis of DPD expression in human macrophages, RKO and HT-29 cells in normoxia and hypoxia (n=3). **B**, Dihydrouracil to uracil ratio in the supernatant of human macrophages, RKO and HT-29 cells in normoxia and hypoxia measured by HPLC (n=3). **C**, qPCR analysis of *DPYD* mRNA in human macrophages, RKO and HT-29 cells (n=3). nd=non detected **D**, qPCR analysis of *DPYD* mRNA in RKO cells exposed to GSK-126 (an EZH2 inhibitor) at 5 µM during 96h (n=3).

Error bars represent mean $\pm$ sem, *p<0.05, *** p<0.001, nd=not detected

Figure S3. Loss of enzymatic function of DPD in macrophages restore the cancer cell sensitivity to 5-FU

A, Quantification of the largest diameter of HT-29 tumoroids from fig. 2E exposed to MCM from normoxic MDM (blue) and hypoxic MDM (red). (n=8). **B,** DPD expression in HT-29 exposed to hypoxic macrophage conditioned medium with and without 5-FU was analysed by immunoblot. Macrophage has been used as a positive control for DPD. Representative immunoblot from three independent experiments. **C**, Induction of death in RKO cells by 5-FU in a co-cultured assay with macrophages in normoxia (blue) and hypoxia (red). 5-FU was used at 1 µg/mL and gimeracil at 1 µg/mL. Dead cancer cells were defined as $CD11b^{-}AnnexinV^{+}$ cells by flow cytometry as in Figure 1A (n=4).
Statistical significance was determined using a one-way ANOVA analysis with Tukey post hoc test. Error bars represent mean $\pm$ sem , ****p<0.0001, ns=non significant

Figure S4. DPD activity follows its expression in hypoxia

A, DPD expression during transition from hypoxia to normoxia is not modulated by proteasome inhibitors (MG132 10µM, bortezomib 10 µM). Transition was performed from O_2 25 mmHg to 145 mmHg during 24h (representative of three independent experiments). **B**, DPD activity determined in the supernatant of macrophages cultured in normoxia and hypoxia for 24h. Macrophages were

previously differentiated in normoxia and hypoxia permitting to study the activity of DPD following transitions (n=3). **C**, Immunoblot of DPD expression in profound hypoxia for 24h and 48h (PO_2 =7mmHg; n=4). **D,** Immunoblot of DPD expression during a transition in hypoxia with translation inhibition mediated by cycloheximide at 1µg/mL during 24h (PO_2 =25mmHg; n=3). Veh. = vehicle, Cyclohex.= cycloheximide.

Figure S5. DPD expression is found in CD163+ TAM and HIF2a expressing macrophages

A, Immunofluorescence staining in liver metastatic tissues. CD163 is in green, DPD in red, nuclei are stained by Hoescht in blue (n=4; scale bar= 50 µm). **B**, Immunofluorescence staining in primary tumors. CD163 is in green, DPD in red, nuclei are stained by Hoescht in blue (n=4; scale bar= 50 µm). **C**, Immunofluorescence staining in liver metastasis. HIF2α is in green, DPD in red, nuclei are stained by Hoescht in blue (n=4; scale bar= 50 µm). **D**, Immunofluorescence staining in primary tumors. HIF2α is in green, DPD in red, nuclei are stained by Hoescht in blue (n=4; scale bar= 50 µm).

Figure S6. Mice macrophages do not express DPD

A, qPCR analysis of mouse DPYD expression in BMDM. Mice liver was used as a positive control (yellow line). Mouse DPYD expression was analysed in macrophages from 4 different mice in normoxia (blue line) and in hypoxia (red line) for 7 days. The No-RT condition was used as a negative control (black line). **B**, qPCR analysis of DPYD expression in RAW264.7. Mice liver was used as a positive control (yellow line). Mice DPYD expression was analysed (blue line, Representative of three independent experiments).The No-RT condition was used as a negative control (black line).

Figure S7. TAM do not express significant levels of *DPYD* in mice.

A, mRNA expression of Dpyd, F4/80 and CD11b in tumor associated macrophages sorted from colorectal tumors in an orthotopic MC38 model. TAMs were separated in two populations according to their expression of F4/80 and Ly6C. Data extracted from GSE 67953 (Afik R et al. J Exp Med. 2016 Oct 17;213(11):2315-2331. doi: 10.1084/jem.20151193). **B**, mRNA expression of Dpyd, F4/80 and CD11b in tumor associated macrophages sorted from colorectal tumors in an AOM/DSS models. TAMs were separated from CT (Rictor flox/flox LysM+/+) and Rictor deficient mice (Rictor flox/flox LysM+/cre). Data extracted from GSE 96525. (Katholnig K, et al. JCI Insight. 2019 Oct 17;4(20):e124164. doi: 10.1172/jci.insight.124164). C, mRNA expression of Dpyd, F4/80 and CD11b in tumor associated macrophages sorted from mammary tumors, spleen and bone marrow in two

mammary tumor models (KEP and MMTV-NeuT). Data extracted from GSE 126268. (Tuit S et al. Cell Rep. 2019 Oct 29;29(5):1221-1235.e5. doi: 10.1016/j.celrep.2019.09.067.

Supplementary Materials and Methods

Further information and requests for resources and reagents should be directed to and will be fulfilled by the corresponding author Arnaud Millet (arnaud.millet@inserm.fr).

Resource table

REAGENT or RESOURCE	SOURCE	IDENTIFIER
Antibodies		
Human CD11b-APC	Miltenyi Biotec	Cat#:130-110-554, RRID:AB_2654667
Mouse F4/80-PE clone REA126	Miltenyi Biotec	Cat#:130-116-499, RRID:AB_2727574
Mouse monoclonal anti-human and mice DPYD (immunoblots)	Clinisciences	Cat#:sc-271308, RRID:AB_10610363
Rabbit polyclonal anti-human DPYD (immunochemistry and immunofluorescence)	Life Technologies	Cat#:PA522302, RRID:AB_11152973
Anti-βactin (immunoblots)	Sigma Aldrich	Cat#:A2228, RRID:AB_476697
Anti-HIF1α (immunoblots)	BD Bioscience	Cat#:610958, RRID:AB_398271
Anti-HIF2α (immunoblots)	Clinisciences	Cat#:sc-46691, RRID:AB_627523
Anti-eIF4E (immunoblots)	Clinisciences	Cat#:sc-9976, RRID:AB_627502
Anti-eIF4E2 (immunoblots)	Clinisciences	Cat#:GTX82524, RRID:AB_11179164
Anti-CD68 (immunochemistry)	Dako	Cat#:M0876, RRID:AB_2074844
Ant-CD163 (immunochemistry)	AbD Serotec	Cat#:MCA1853, RRID:AB_2074540
Anti mouse IgG HRP	Life technologies	Cat#:G21040, RRID:AB_2536527
Anti Rabbit IgG HRP	Life technologies	Cat#:G21234, RRID:AB_1500696
Anti mouse IgG alexa Fluor 488	Invitrogen	Cat#:A11029, RRID:AB_138404
Anti rabbit IgG alexa Fluor 546	Invitrogen	Cat#:A11010, RRID:AB_2534077
Biological Samples		
Human leukoreduction system chambers	EFS	
Chemicals		
5-Fluorouracil (5-FU)	ACCORD HEALTHCARE	50 mg/mL
7-AAD staining solution	BD Biosciences	Cat#:559925
Actinomycin D	Sigma Aldrich	Cat#:A9415
AEBSF	Sigma Aldrich	Cat#:SBR00015-1ML
Annexin V-FITC	Miltenyi Biotec	Cat#:130-093-060
β-mercaptoethanol	Sigma Aldrich	Cat#:M3148-100ML
Bovine Serum Albumin (BSA) solution 30%	Sigma Aldrich	Cat#:A9576-50ML
CD14 microbeads, human	Miltenyi Biotec	Cat#:130-050-201
Decitabine (5-aza-2'-deoxycitidine)	Sigma Aldrich	Cat#:A3656-5MG
DMOG	Sigma Aldrich	Cat#:D3695-10MG
DMSO for cell culture	Dutscher	Cat#:702631
DPBS (1X) , no calcium, no magnesium	Life Technologies	Cat#:14190169
EDTA (0.5M), pH 8.0, RNase-free	Life Technologies	Cat#:AM9260G

Fetal Bovine Serum (FBS), qualified, US	Life Technologies	Cat#:26140079
Gimeracil	Sigma Aldrich	Cat#:SML2075-5MG
GSK126	Clinisciences	Cat#:HY-13470-5mg
HEPES (1M)	Life Technologies	Cat#:15630056
Histopaque-1077	Sigma Aldrich	Cat#:10771-6X100ML
Hoescht 33342	Invitrogen	Cat#:H3570
Human serum from male AB plasma (SAB)	Sigma Aldrich	Cat#:H4522-100ML
Leupeptin	Sigma Aldrich	Cat#:L5793-5MG
McCoy's 5A (modified) medium, glutaMAX supplement	Life Technologies	Cat#:36600088
MEM Non-Essential Amino Acids solution (100X)	Life Technologies	Cat#:11140035
Opti-MEM I medium, glutaMAX supplement	Life Technologies	Cat#:51985026
Pepstatin A	Sigma Aldrich	Cat#:P5318-5MG
RPMI 1640 medium, glutaMAX supplement	Life Technologies	Cat#:61870044
TrypLE Express Enzyme (1X), phenol red	Life Technologies	Cat#:12605036
Ultrapure DNase/RNase-free distilled water	Life Technologies	Cat#:10977035
Deposited Data		
Proteomic data	PRIDE	PXD006354
Experimental Models: Cell Lines		
CT26 WT	ATCC	Cat#:CRL-2638
HT-29	ATCC	Cat#:HTB-38
RAW 264.7	ATCC	Cat#:TIB-71
RKO	ATCC	Cat#:CRL-2577
Experimental Models: Organisms/Strains		
Female Mice BALB/c	Charles River	
Oligonucleotides		
Human B2M forward (housekeeping gene)	Eurogentec	5' – GTGCTCGCGCTACTCTCTC – 3'
Human B2M reverse (housekeeping gene)	Eurogentec	5' – CGGATGGATGAAACCCAGACA – 3'
Human DPYD forward	Eurogentec	5' - CGCAGGACCAGGGGTTTTAT - 3'
Human DPYD reverse	Eurogentec	5' - TGGCAATGGAGAGTGACAGG - 3'
Human HPRT1 forward (housekeeping gene)	Eurogentec	5' – TGCTTTCCTTGGTCAGGCAG – 3'
Human HPRT1 reverse (housekeeping gene)	Eurogentec	5' – TTCGTGGGGTCCTTTTCACC – 3'
Human NDRG1 forward	Eurogentec	5' – GCAGGCGCCTACATCCTAACT – 3'
Human NDRG1 reverse	Eurogentec	5' – GCTTGGGTCCATCCTGAGATCTT – 3'
Human P4HA1 forward	Eurogentec	5' – ACGTCTCCAGGATACCTACAATTT – 3'
Human P4HA1 reverse	Eurogentec	5' – GTCCTCAGCCGTTAGAAAAGATTTG – 3'
Human RPL6 forward (housekeeping gene)	Eurogentec	5' – GTTGGTGGTGACAAGAACGG – 3'
Human RPL6 reverse (housekeeping gene)	Eurogentec	5' – TTTTTGCCGTGGCTCAACAG – 3'
Human SLC2A1 forward	Eurogentec	5' – TGGCCGTGGGAGGAGCAGTG – 3'
Human SLC2A1 reverse	Eurogentec	5' – GCGGTGGACCCATGTCTGGTTG – 3'
Human TBP forward (housekeeping gene)	Eurogentec	5' – GAGAGTTCTGGGATTGTACCG – 3'
Human TBP reverse (housekeeping gene)	Eurogentec	5' – ATCCTCATGATTACCGCAGC – 3'
Human VEGFA forward	Eurogentec	5' – CTTCCTACAGCACAACAAAT – 3'
Human VEGFA reverse	Eurogentec	5' – GTCTTGCTCTATCTTTCTTTG – 3'
Human WASF2 forward (housekeeping gene)	Eurogentec	5' – AAGAAAAGCTGGGGACTTCTG – 3'
Human WASF2 reverse (housekeeping gene)	Eurogentec	5' – GCTACTTGCATCCACGTTTTC – 3'
Mouse b2m forward (housekeeping gene)	Eurogentec	5' – TGGTCTTTCTGGTGCTTGTC – 3'
Mouse b2m reverse (housekeeping gene)	Eurogentec	5' – GTTCAGTATGTTCGGCTTCCC – 3'

Mouse dpyd forward	Eurogentec	5' – TCGCGTGTTCATCGTCTTCA – 3'
Mouse dpyd reverse	Eurogentec	5' – ATAACCTTCCGTGGCGAGAG – 3'
Mouse gusb forward (housekeeping gene)	Eurogentec	5' – GGGACAAAAATCACCCTGCG – 3'
Mouse gusb reverse (housekeeping gene)	Eurogentec	5' – GCGTTGCTCACAAAGGTCAC – 3'
Mouse hprt1 forward (housekeeping gene)	Eurogentec	5' – AGCCCCAAAATGGTTAAGGTTG – 3'
Mouse hprt1 reverse (housekeeping gene)	Eurogentec	5' – ATCCAACAAAGTCTGGCCTGT – 3'
siCTL (Non-targeting pool)	Horizon Discovery LTD	Cat#:D-001810-10-05
siRNA human DPYD	Horizon Discovery LTD	Cat#:L-008376-00-0005
siRNA human EIF4E	Horizon Discovery LTD	Cat#:L-003884-00-0005
siRNA human EIF4E2	Horizon Discovery LTD	Cat#:L-019870-01-0005
siRNA human EPAS1 (HIF2a)	Horizon Discovery LTD	Cat#:L-004814-00-0005
siRNA human HIF1a	Horizon Discovery LTD	Cat#:L-004018-00-0005
Recombinant DNA		
pLenti-C-DPYD-mGFP-P2A-Puro plasmid	OriGene	Cat#:RC216374L4V
pLenti-C-DPYD-mGFP-P2A-Puro plasmid	OriGene	Cat#:PS100093V
Softwares		
Graph Pad Prism 7	GraphPad Software Inc	
JMP 14	SAS	
Other		
iScript Ready-to-use cDNA supermix	Biorad	Cat#:1708841
iTaq universal SYBR green supermix	Biorad	Cat#:1725124
HypoxyLab Station	Oxford Optronix	
MicroBCA kit	Life Technologies	Cat#:23235
MycoAlert kit	Lonza	Cat#:LT07-118
NucleoSpin RNA (50)	Macherey Nagel	Cat#:740955.50
Accuri C6 (flow cytometer)	BD Biosciences	
Eclipse TS2 microscope	Nikon	
Transwell Costar	Corning	Cat#:3460

REVIEW ARTICLE

médecine/sciences 2022 ; 38 : 243-54

Les macrophages associés à la tumeur

De nouvelles cibles pour contrecarrer la chimiorésistance au 5-fluorouracile dans les cancers colorectaux ?

Marie Malier[1,2], Khaldoun Gharzeddine[1,2], Marie-Hélène Laverriere[1-3], Thomas Decaens[1,4], Gael Roth[1,2,4], Arnaud Millet[1,2,4]

[1]Université Grenoble Alpes, Inserm U1209, CNRS UMR 5309, Institut pour l'avancée des biosciences, Boulevard de la Chantourne, 38700 La Tronche, France
[2]Équipe de mécanobiologie, immunité et cancer, Institut pour l'avancée des biosciences
[3]Département d'analyse cytologique et pathologique, CHU Grenoble Alpes, Grenoble, France.
[4]Service d'hépato-gastro-entérologie, CHU Grenoble Alpes, Grenoble, France.
arnaud.millet@inserm.fr

› Le fluorouracile (5-FU) est un analogue de base pyrimidique utilisé dans de nombreuses combinaisons de chimiothérapie, notamment contre les cancers colorectaux. Malgré les progrès dans le traitement de ces cancers, le pronostic des formes avancées reste sombre, notamment en raison de la forte prévalence de la chimiorésistance au 5-FU. Les mécanismes impliqués dans cette chimiorésistance sont multiples : modulation du transport du 5-FU dans la cellule (ainsi que son exportation), métabolisme de la molécule, modification de sa cible, modification de l'équilibre entre facteurs apoptotiques et anti-apoptotiques, adaptation au microenvironnement tumoral, et transition épithélio-mésenchymateuse [1]. La plupart des études portant sur la chimiorésistance se sont focalisées sur la cellule cancéreuse elle-même, et l'importance du microenvironnement tumoral a été longtemps minimisée. Des travaux récents, dont ceux de notre laboratoire, montrent cependant que le microenvironnement joue en réalité un rôle beaucoup plus important dans la chimiorésistance des tumeurs.

Rôle des macrophages dans la résistance aux chimiothérapies

Dans de nombreuses tumeurs solides, les macrophages forment une composante essentielle de la réponse immunitaire associée à la tumeur, et leur abondance est habituellement corrélée à un pronostic défavorable. Ces macrophages associés à la tumeur ont été impliqués dans la croissance tumorale, l'échappement immunitaire, la néoangiogenèse, ou encore la résistance aux traitements. En effet, de nombreuses études ont montré que la déplétion des macrophages associés aux tumeurs (en utilisant par exemple des liposomes de clodronate) accroît la sensibilité aux chimiothérapies [2]. Parallèlement, les études de co-culture *in vitro* ont mis en évidence le rôle des macrophages dans l'induction d'une chimiorésistance des cellules tumorales contre le paclitaxel, la doxorubicine, l'étoposide ou la gemcitabine [3, 4]. Les mécanismes impliqués dans ces résistances induites par les macrophages à différentes chimiothérapies reposent le plus souvent sur la sécrétion, par les macrophages, de facteurs modifiant la réponse des cellules cancéreuses. Un exemple d'un tel mécanisme est la sécrétion de désoxycytidine, qui inhibe l'induction d'apoptose par la gemcitabine dans les adénocarcinomes pancréatiques [5].

Dans les cancers colorectaux, l'implication des macrophages dans la chimiorésistance au 5-FU a été suggérée par des études *in vitro* et *in vivo*. Les mécanismes proposés sont divers, mais ils reposent, eux aussi, sur des facteurs sécrétés par les macrophages. La sécrétion d'interleukine 6 (IL-6) par les macrophages a été proposée comme responsable de l'activation, dans les cellules cancéreuses, de STAT3 (*signal transducer and activator of transcription 3*), induisant l'inhibition de la voie de signalisation RAB22A/BCL2 *via* l'expression du microARN miR-204-5p, ce qui favorise la résistance au 5-FU [6]. De manière similaire, la sécrétion de putrescine, un membre de la famille des polyamines, inhibe la voie JNK/caspase 3 dans les cellules cancéreuses, favorisant également leur résistance au 5-FU [7]. Ces mécanismes n'ont toutefois pas été validés dans l'espèce humaine, et leurs effets semblaient quantitativement faibles *in vivo*. Partant du constat que les macrophages associés à la tumeur sont très souvent situés dans les zones hypoxiques, où ils favorisent la néoangiogenèse, nous avons voulu savoir dans quelle mesure l'hypoxie, dont nous avions montré précédemment l'importance pour la modulation de différentes fonctions immunologiques des macrophages [8], pouvait également moduler l'implication de ces cellules dans la chimiorésistance au 5-FU.

Chimiorésistance au 5-FU induite par les macrophages hypoxiques

Nous avons observé que les macrophages hypoxiques, contrairement à leurs homologues normoxiques,

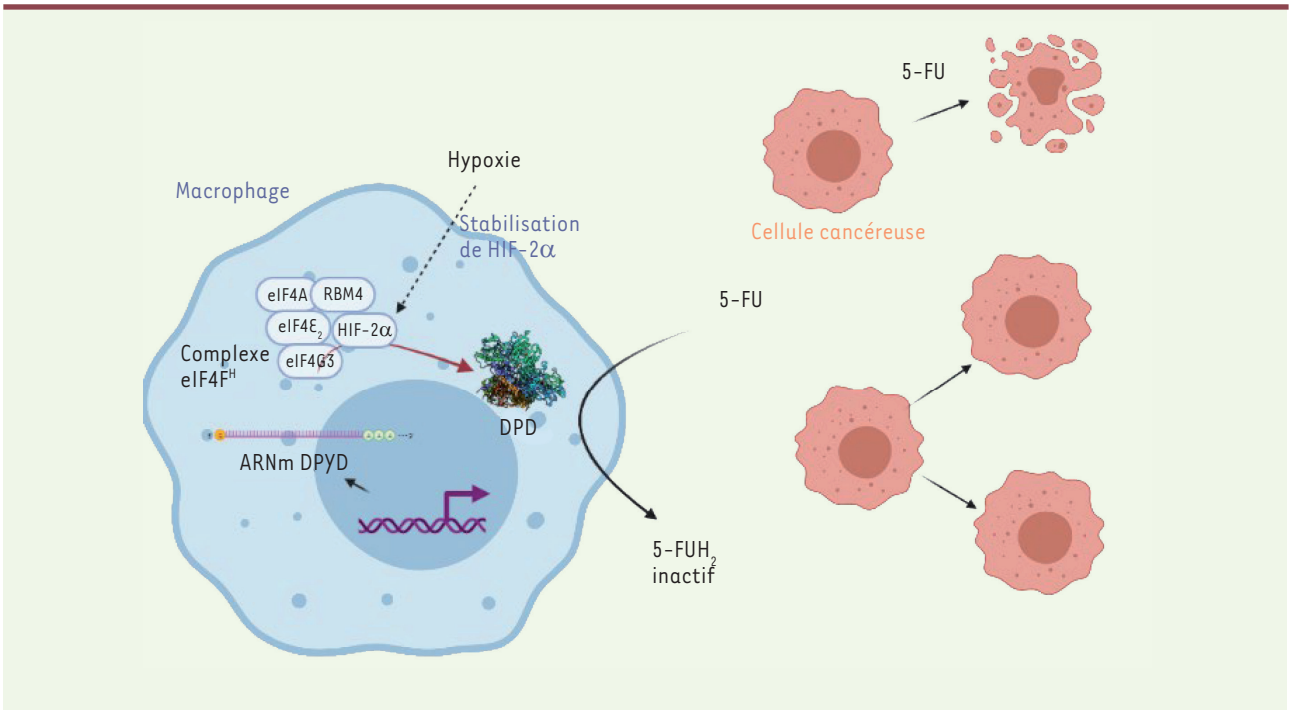

Figure 1. ***Schéma du mécanisme de chimiorésistance au 5-FU impliquant les macrophages en hypoxie.*** Le contrôle traductionnel de l'expression du gène codant la dihydropyrimidine déshydrogénase (DPD) par les macrophages associés à la tumeur est sous la dépendance d'un complexe d'initiation de la traduction comprenant HIF-2α, une protéine stabilisée en condition d'hypoxie. La DPD dégrade le 5-fluorouracile (5-FU) en dihydrofluorouracile (5-FUH_2), qui est une molécule inactive. Ce mécanisme illustre l'importance du microenvironnement tissulaire dans les processus de résistance aux traitements anti-cancéreux.

induisent une résistance complète des cellules tumorales au 5-FU dans des conditions expérimentales reproduisant le rapport macrophages/quantité de 5-FU existant dans les tissus tumoraux *in vivo*. Cette chimiorésistance semble être due à une action directe des macrophages et ne pas impliquer la sécrétion d'un facteur soluble induisant une résistance des cellules cancéreuses au 5-FU. L'étude comparative du protéome des macrophages normoxiques et hypoxiques a mis en évidence l'expression différentielle d'une protéine à l'origine de cette chimiorésistance : la dihydropyrimidine déshydrogénase (DPD). Cette enzyme de la voie du catabolisme des bases pyrimidiques catalyse la réduction du 5-FU en dihydrofluorouracile (5-FUH_2), une molécule inactive. L'implication de la DPD dans la chimiorésistance au 5-FU a été confirmée par des études fonctionnelles, révélant ainsi un rôle clé des macrophages hypoxiques [9]. Pour confirmer l'intérêt médical de ce résultat, nous avons étudié l'expression de la DPD dans des tumeurs primitives et des métastases hépatiques issues de patients porteurs d'un adénocarcinome colorectal. Nous avons alors constaté que cette enzyme est peu ou pas exprimée dans les cellules cancéreuses (expliquant la sensibilité habituelle de ces cancers au 5-FU), tandis qu'elle l'est fortement par les macrophages, qui représentent la principale source d'expression de la DPD dans le microenvironnement de la tumeur primitive comme dans celui des métastases hépatiques [9].

Un mécanisme spécifiquement humain

Ce rôle de la DPD synthétisée par les macrophages hypoxiques comme source principale de chimiorésistance de la tumeur au 5-FU n'avait pas été mis en évidence dans les nombreuses études *in vitro* et *in vivo* publiées jusqu'à présent, vraisemblablement en raison, d'une part, des modèles de macrophages étudiés, et, d'autre part, des conditions de culture utilisées. En effet, nous avons découvert que, contrairement aux hépatocytes murins, qui, comme les hépatocytes humains, expriment le gène de la DPD, les macrophages murins ne l'expriment pas, à cause d'un contrôle inhibiteur épigénétique par méthylation de son promoteur [9]. Nous avons également montré que la concentration en oxygène joue un rôle prépondérant dans l'expression de ce gène par les macrophages humains. Or la majorité des expériences réalisées *in vitro* utilisent des conditions riches en oxygène, qui inhibent fortement l'expression du gène dans les macrophages issus de monocytes, et ne permettent donc pas d'apprécier l'importance de cette enzyme dans le processus de chimiorésistance au 5-FU.

Mécanisme de contrôle de l'expression du gène codant la DPD par l'oxygène

De plus, nous avons montré que le contrôle de l'expression du gène codant la DPD dans les macrophages humains hypoxiques n'est pas transcriptionnel mais traductionnel, sous la dépendance de HIF-2α (*hypoxia-induced factor2α*), alors que HIF-1α ne semble jouer aucun rôle dans l'expression de ce gène par les macrophages [9]. La protéine HIF-2α est stabilisée en condition d'hypoxie modérée (25 mmHg), et intervient dans le contrôle traductionnel, indépendamment de son activité connue comme facteur de transcription. Un des mécanismes envisagés repose sur la participation de HIF-2α à un complexe initiateur de la traduction ($eIF4F^{Hypoxique}$) faisant notamment intervenir $eIF4E_2$, un complexe identifié dans la réponse adaptative à l'hypoxie dans les cellules de mammifères, en remplacement du complexe eiF4F (comprenant eIF4E), actif seulement lorsque l'oxygène est présent en abondance [10].

Nos travaux ont donc mis en évidence le fait que la chimiorésistance d'une tumeur cancéreuse au 5-FU, chez l'homme, est étroitement liée au microenvironnement tumoral, et plus particulièrement au rôle inattendu d'une enzyme catalysant la dégradation du 5-FU, la dihydropyrimidine déshydrogénase, dont la présence dans les macrophages associés à la tumeur est finement contrôlée par la teneur en oxygène *(Figure 1)*. Ce résultat désigne les macrophages présents dans le microenvironnement tumoral comme cibles privilégiées pour contrecarrer la chimiorésistance des cancers colorectaux au 5-FU. ◊

Tumor-associated macrophages: New targets to thwart 5-FU chemoresistance in colorectal cancers?

LIENS D'INTÉRÊT

Les auteurs déclarent n'avoir aucun lien d'intérêt concernant les données publiées dans cet article.

RÉFÉRENCES

1. Marin JJG, de Medina FS, Castaño B, *et al.* Chemoprevention, chemotherapy, and chemoresistance in colorectal cancer. *Drug Metab Rev* 2012 ; 44 : 148-72.
2. Ruffell B, Coussens LM. Macrophages and therapeutic resistance in cancer. *Cancer Cell* 2015 ; 27 : 462-72.
3. Mitchem JB, Brennan DJ, Knolhoff BL, *et al.* Targeting tumor-infiltrating macrophages decreases tumor-initiating cells, relieves immunosuppression, and improves chemotherapeutic responses. *Cancer Res* 2013 ; 73 : 1128-41.
4. Shree T, Olson OC, Elie BT, *et al.* Macrophages and cathepsin proteases blunt chemotherapeutic response in breast cancer. *Genes Dev* 2011 ; 25 : 2465-79.
5. Halbrook CJ, Pontious C, Kovalenko I, *et al.* Macrophage-released pyrimidines inhibit gemcitabine therapy in pancreatic cancer. *Cell Metab* 2019 ; 29 : 1390-9.e6.
6. Yin Y, Yao S, Hu Y, *et al.* The immune-microenvironment confers chemoresistance of colorectal cancer through macrophage-derived IL6. *Clin Cancer Res* 2017 ; 23 : 7375-87.
7. Zhang X, Chen Y, Hao L, *et al.* Macrophages induce resistance to 5-fluorouracil chemotherapy in colorectal cancer through the release of putrescine. *Cancer Lett* 2016 ; 381 : 305-13.
8. Court M, Petre G, Atifi ME, *et al.* Proteomic signature reveals modulation of human macrophage polarization and functions under differinge environmental oxygen conditions. *Mol Cell Proteomics* 2017 ; 16 : 2153-68.
9. Malier M, Gharzeddine K, Laverriere M-H, *et al.* Hypoxia drives dihydropyrimidine dehydrogenase expression in macrophages and confers chemoresistance in colon cancer. *Cancer Res* 2021 ; doi: 10.1158/0008-5472.CAN-21-1572.
10. Uniacke J, Holterman CE, Lachance G, *et al.* An oxygen-regulated switch in the protein synthesis machinery. *Nature* 2012 ; 486 : 126-9.

Chapter Two - Part Four

Supplementary Results

Ex-vivo Tissue Culture

We showed that one of the mechanisms through which CRC patients develop chemoresistance against 5-FU is due to the presence of tumor associated macrophages in the tumor vicinity. These TAMs in the hypoxic tumor microenvironment upregulate the expression of DPD, which in turn catabolize 5-FU into its inactive form conferring this chemoresistance. Thus, we aimed to target TAMs in the tumoral tissues as a mean to improve the 5-FU response in CRC patients.

For that, we developed a protocol for an ex-vivo tissue culture system in a serum-free media, adapted from (Dame et al., 2010), of normal and tumoral tissues sectioned from CRC patients. This allows us to extrapolate the consequences of targeting macrophages in a real tumor microenvironment with real tumor associated macrophages. Following the ex-vivo culture system protocol that is elaborated in the materials and methods section, we first cultured the tissues for 24 and 48 hours after which Hematoxylin and Eosin staining was performed on cultured tissues compared to directly fixed tissues, time zero (t0). Moreover, in order to deplete macrophages, we first followed the widely used approach of depleting macrophages by using 5% of clodronate liposome (LIPOSOMA) for 48 hours. We evaluated the efficiency of macrophage depletion by performing immunohistochemistry staining of CD68, a common macrophage marker. Results unexpectedly revealed that clodronate liposome in our ex-vivo culture system did not deplete macrophages Figure S 1 A. Because our *in vitro* test of 5% clodronate liposome for 48 hours did not lead to the depletion of macrophages, we next used antagonists against the M-CSF R, Edicotinib and BLZ945, which are one of the antagonists used in clinics to target this pathway in macrophages. Thus, the cultured tissues were subjected to Edicotinib and BLZ945 both at 10 µM in order to target macrophages for 24 and 48 hours after which CD68 immunohistochemistry was carried out. Unfortunately, we discovered that the cultured tissues were not morphologically good as directly fixed tissues. Moreover, comparing the vehicle treated tissues, we found that these antagonists are not depleting macrophages in our tissue culture systems Figure S 1 B. We then optimized the protocol by culturing the tissues for shorter period of time, 18 hours, after which the tissues were fixed for histological analysis. Fortunately, H&E stainings of these tissues revealed that the new culture system and the shorter incubation time were optimal to maintain the

morphology of the tissues Figure S 1 C. However, this was not sufficient to obtain a depletion of macrophages. Then, we studied the efficacy of these antagonists *in vitro*.

Figure S 1 Ex-vivo Culture of Normal and Tumoral Tissues from CRC Patients (A)and(B):CD68 Immunohistochemical staining of tumoral tissues ex-vivo cultured for 48 hours with PBS liposome, clodronate liposome and DMSO vehicle, BLZ945 and Edicotinib at 10µM. (B): Hematoxylin and Eosin staining of tumoral and normal tissues directly fixed at t0 or ex-vivo cultured for 18 hours.

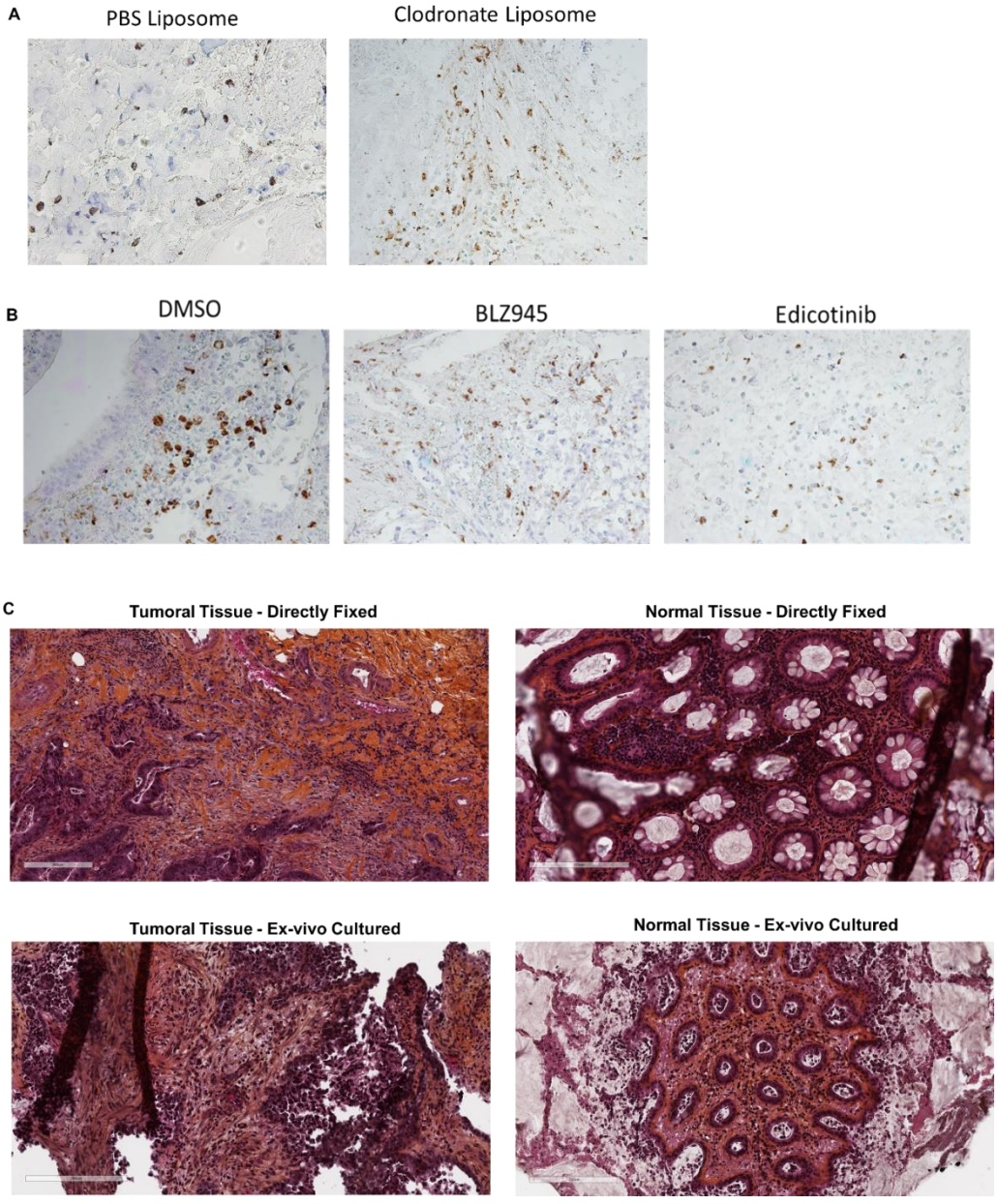

Chapter III

Macrophage Colony Stimulatory Factor Receptor (M-CSF R), a Promising Therapeutic Target

Chapter Three - Part One

Introduction

I. M-CSF R Expression, Structure and Activation

I-1. Receptor Tyrosine Kinase (RTK)

Receptor tyrosine kinases (RTKs) are transmembrane proteins which play major cellular functions through signaling pathway initiation upon the activation of their attached tyrosine kinase moieties (Hubbard & Miller, 2007). There are up to 58 RTKs within the genome of humans. These include fibroblast growth factor receptor (FGFR), epidermal growth factor receptor (EGFR), platelet-derived growth factor receptor (PDGFR), vascular endothelial growth factor receptor (VEGFR) among others. RTKs are known to contribute to the initiation, development and progression of several diseases including various types of cancers (Choura & Rebaï, 2011).

Colony Stimulatory Factor Receptor (CSF-1R), which is also known as and will be addressed throughout this manuscript as macrophage colony stimulatory factor receptor (M-CSF R), is one of the most important receptors amongst class III RTKs (Lemmon & Schlessinger, 2010). This receptor has gained great interest in the past years and is recognized and exploited as a drug target for promising treatment for cancer and inflammatory diseases associated to macrophages.

I-2. Expression and Regulation of M-CSF R

M-CSFR is a cell surface protein belonging to the family of PDGF and is encoded in humans by the CSF-1R proto-oncogene, also known as c-FMS (JA et al., 2009). It is expressed at a low level on hematopoietic stem cells (HSCs) (Mossadegh-Keller et al., 2013; Sarrazin et al., 2009) and more majorly on mononuclear phagocytes such as monocytes, macrophages, dendritic cells and it can be also found on other cell types including osteoclasts, neuronal cells, renal proximal tubule epithelial cells as well as colon epithelial cells. (Byrne et al., 1981; Guilbert & Stanley, 1980; MacDonald et al., 2005; Nandi et al., 2012).

The gene coding M-CSF R in humans is located at chromosome 5(5q32) (Bonifer & Hume, 2008). It constitutes of 21 introns and 22 exons (Sherr, 1990). Transcription of this gene takes place upstream of exon 2 in human macrophages (Roberts et al., 1992). The expression of M-CSF R in macrophages is mainly dependent on the presence of a highly conserved sequence enhancer element know as Fms-intronic regulatory element (FIRE) which encodes an anti-sense M-CSF R transcript that contributes to its ability to overcome repression by intron 2 (Himes et al., 2001; Sauter et al., 2013). The expression of M-CSF R is relatively low on hematopoietic stem cells (HSCs) and is increased by 10 folds on macrophages progenitors which is gradually increased as the differentiation process into macrophages proceeds (Sarrazin et al., 2009; Tushinski et al., 1982).

During the differentiation into macrophages, the upregulation of the expression of M-CSF R occurs in two steps by which the transcription factors assembly consisting of PU.1, Runx1 and C/EBP binding as well as the remodeling of the chromatin at the promoter of macrophages make up the first step (Krysinska et al., 2007, p.; Walsh et al., 2002). The second step is marked by the factor assembly and chromatin remodeling at FIRE. These two steps ensure that M-CSF R is only highly expressed in the more differentiated cells which respond to M-CSF alone.

I-3. Structure of M-CSF R

As other PDGF members, this receptor possesses a highly glycosylated extracellular domain, a transmembrane domain and an intracellular domain (Coussens et al., 1986; Hampe et al., 1989). The extracellular region is comprised of five immunoglobulin domains (D1 – D5) of 498 amino acids while the transmembrane domain consists of 21 amino acids (Hubbard & Till, 2000) as shown in

Figure 10. The intracellular domain is comprised of a juxtamembrane domain (JMD) of 36 amino acids as well as an intracellular tyrosine kinase domain of 398 amino acids, which is interrupted by a kinase insert domain of 73 amino acids.

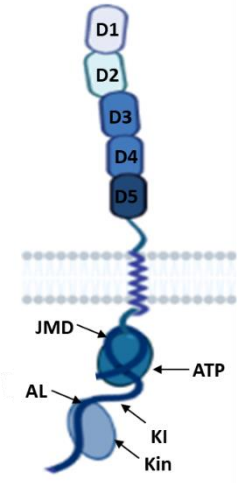

Figure 10 The structure of M-CSF R

The M-CSF R consists of 5 extracellular domains D1 to D5, a transmembrane domain and intracellular domains consisting of JMD, kinase N lobe (ATP), kinase insert (KI), kinase C lobe (Kin, activation loop (AL) and carboxy-terminal amino acid tail. Abbreviations: D1-D5: Domains 1 – 5; JMD: Juxtamembrane domain; AL: Activation Loop; ATP: Adenosine Triphosphate: Kinase C lobe (cyan oval); KI: Kinase Insert; Kin :Kinase C lobe (light blue oval).

I-4. Ligands of M-CSF R

M-CSFR is the only RTK that can be activated by two ligands Interleukin-34 (IL-34) and CSF-1 which is also known as Macrophage colony stimulatory factor (M-CSF) (H. Lin et al., 2008). M-CSF was the first colony stimulatory factors purified. As its name implies, M-CSF stimulates the formation of macrophage colonies. It is produced by a variety of cells including endothelial cells, fibroblasts, bone marrow stromal cells as well as tumoral cells by which its levels increase during inflammation and tumoral growth (Pixley & Stanley, 2010; Stanley et al., 1997). M-CSF is a growth factor which is expressed in three isoforms: a secreted glycoprotein, a secreted chondroitin sulfate proteoglycan and a cell surface membrane spanning glycoprotein (Pixley & Stanley, 2004). These three isoforms are dimeric and possess the same amino-terminal required for biological activity, but have distinct activities that is determined by the carboxy-terminal sequence. They act locally as well as in circulatory mode as they act in an autocrine and paracrine fashion (Dai et al., 2004; Nandi et al., 2006; Van Nguyen & Pollard, 2002).

However, IL-34 is synthesized as a secreted glycoprotein containing one biologically active isoform, which acts locally. Despite the fact that both have low sequence similarity, IL-34 and CSF-1 possess similar four helical bundle folds at their biologically active regions where both are head-to-head dimers (H. Liu et al., 2012; Ma et al., 2012). Although IL-34 and M-CSF have more or less same biological properties (Wei et al., 2010), they differ in their signaling patterns and in their spatiotemporal expression levels (Chihara et al., 2010; Nandi et al., 2012; Wei et al., 2010).

I-5. Activation of M-CSF R

An inactive M-CSF R displays a two-lobed kinase domain, the N lobe and the C lobe (Schubert et al., 2007; Walter et al., 2007). The N-lobe consists of five-stranded anti parallel beta sheets with a single alpha helix contrary to the C-lobe which has two beta strands and seven alpha helices. The N-lobe binds to C-lobe by the kinase insert domain and the hinge region. ATP binding takes place in the cleft between the two lobes where the N lobe and the hinge regions are involved. The C-lobe mediates the binding of the substrate.

The kinase domain activation loop (AL) in the receptor is usually folded onto the ATP-binding cleft when the receptor is inactive. In this scenario, Tyrosine residue 809 of the M-CSF R acts as a pseudo-substrate which blocks the binding of the receptor. Additionally, Asparagine 796 of the invariant DFG (Asp-Phe-Gly) motif, necessary for ATP coordination, is in a ‘’DFG-out’’ conformation allowing its displacement from the active site. Its flipping from ‘’DFG-out’’ to a ‘’DFG-in’’ confirmation as well as the reorganization of AL mediate the activation of the receptor. Also, the JMD acts in an inhibitory way by blocking the alpha helix preventing the activation of AL. This inhibition is reverted due to the phosphorylation of Tyrosine at 561 which is the first

residue to be phosphorylated and activated upon substrate binding and acts as the receptor's switch (Rohde et al., 2004; Xiong et al., 2011; Yu et al., 2012).

The binding of M-CSF to its receptor takes place exclusively via the D2 and D3 domains in the extracellular region (Chen et al., 2008; Elegheert et al., 2011), Figure 11. Moreover, IL-34-M-CSF R complex is similar to that of M-CSF – M-CSF R complex (Felix et al., 2013). The D4 domain mediates the homotypic interactions as this domain is involved in the oligomerization of the two monomers which is induced by ligand binding. Regarding D1 and D5 domains, they point away from the complex. Following, intracellular tyrosine residues will be phosphorylated contributing to several signaling pathways, which will be further detailed in the next section.

The activation of the receptor, that is the binding of the ligand followed by the non-covalent dimerization of the receptor and the phosphorylation of its tyrosine residues, is a rapid mechanism that takes place in presence of the ligand (Yeung & Stanley, 2003). This is followed by an extracellular disulfide linkage between the monomers within the dimer forming a covalent dimerization which initiates a second wave of tyrosine phosphorylation, elevating serine phosphorylation of the receptor as well as the internalization of the ligand-receptor complex, Figure 11 (P. S. Lee et al., 1999; W. Li & Stanley, 1991; Y. Wang et al., 1999). As soon as this complex is internalized, both the ligand CSF-1 and the receptor CSF-1R are degraded lysosomally Figure 11. Moreover, It is worth to mention that all these processes starting from the ligand binding to the activation of the receptor until its internalization take place within the very first minutes prior to the binding of the ligand (Yeung & Stanley, 2003).

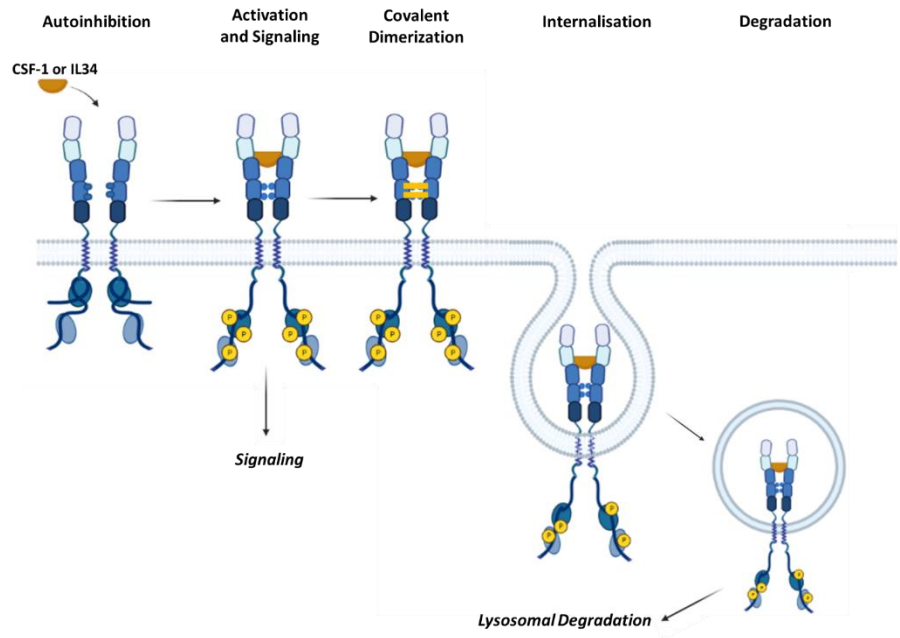

Figure 11 Activation and Internalisation of M-CSF R in Presence of its Ligand(s)

M-CSF R is activated by two ligands: CSF-1 and IL-34. These ligands bind to the D2 and D3 domains of the extracellular region of the initially auto-inhibited receptor. Following, homotypic interactions take place via the D4 domain which subsequently lead to auto-phosphorylation of the kinase domain at the intracellular region which defines an activated receptor. Following activation and phosphorylation of the tyrosine kinases of the receptor, a covalent di-sulfide bond is formed between the monomers of the receptor. This initiates a second wave of phosphorylation and mediates ubiquitination as well as the internalization of the ligand-receptor complex. Finally, lysosomal degradation of this complex take place.

II. M-CSF R Signaling in Macrophages

II-1. Phosphorylation of the Intracellular Tyrosine Residues

M-CSF R comprises several intracellular tyrosine domains that are phosphorylated endorsing important and central functions in macrophages (Stanley & Chitu, 2014a). The functions of tyrosine residues that are known to be phosphorylated in the activated receptor were studied in mice.

Results have demonstrated that the first tyrosine residue to be phosphorylated in response to ligand binding is Tyr-559 (Tyr-561 in humans) which is localized in JMD (Yu et al., 2012). This tyrosine residue acts as a switch by which it keeps the receptor's kinase activity off in absence of ligand (Xiong et al., 2011). Upon ligand binding followed by the phosphorylation of Tyr-559, the auto-inhibitory effect is relieved. Additionally, Tyr-559 recruits SFK that in turn associates with c-Cbl. As a result, ubiquitination of the receptor is mediated following its conformational change and the internalization of the ligand-receptor complex.

Phosphorylation of Tyr-544 (Tyr-546 in humans) is required for the full activation of the kinase activity of the receptor. Moreover, Tyr-807 (Tyr-809 in humans) in the activation loop was shown to confer the activation of the receptor-mediated phosphorylation (Yu et al., 2012). The functions of the former three tyrosine residues were deciphered by adding them back to a receptor backbone where the add-back of these three tyrosines restored full activation of the receptor kinase in vitro as well as the cellular protein tyrosine phosphorylation and proliferation response.

Nonetheless, Tyr-807 is crucial for the differentiation of macrophage which is augmented by Tyr-697 (Tyr-699 in humans), Tyr-706 (Tyr-708 in humans) and Tyr-721 (Tyr-723 in humans) (Rohrschneider et al., 1997).

Phosphorylation of these tyrosine residues allow them to function as docking sites for several signaling molecules and proteins such as members of Src family, Mona, Grb2, phospholipases, phosphatidylinositol 3-kinase (PI3K) as well as suppressor of cytokine signaling-1 (SOCS1) (Shurtleff et al., 1990). Following these distinct downstream signal transduction pathways, several mechanisms are activated in macrophages including survival, proliferation, differentiation as well as motility (Stanley & Chitu, 2014b).

II-2. M-CSF R Signaling Transduction

The central pathway that guarantees the survival of macrophages, illustrated in Figure 12 A, is the PI3K/Akt pathway (Chang et al., 2009). Akt is activated through M-CSF R via the phosphorylation of Tyr-721 that in turn activates PI3K pathway (Sampaio et al., 2011). As a result, Bcl-x is activated and it mediates the survival of macrophages as well as inhibits apoptosis. In addition, PKC activation downstream M-CSF R promotes the translocation of Fms interacting protein (FIMP) from the nucleus, where it acts as M-CSF R signaling inhibitor, to the cytosol and thus mediating the survival of macrophages (Mancini et al., 2004).

Notwithstanding, M-CSF R pathway is implicated in the proliferation of macrophages (Tushinski & Stanley, 1985), which is exemplified in Figure 12 B. One way where it ensures and contributes to that central function is by the phosphorylation of Tyr-807 that activates MEK and PI3K pathways (Munugalavadla et al., 2005). It was also shown that alternatively, Tyr-559, via SFK activation, also mediates macrophage's proliferation (Takeshita et al., 2007). M-CSF stimulates the production of ceramide-1 phosphate (C1P) that activates PI3K/Akt and Erk1/2 thereby leading to proliferation (Gangoiti et al., 2008). Bearing that ERKs are master regulators of cellular proliferation, multiple ERKs are involved in macrophages. For instance, ERK5 is activated by SFK-dependent M-CSF R and is necessary for the proliferation of macrophages (Rovida et al., 2008, p. 5). Also, Erk1/2, which are downstream to MEK, mediate the proliferation of macrophages (Rovida et al., 2002). In spite of that, M-CSF R can also inhibit the phosphorylation of Erk1/2 through PKC which upregulates the expression of dual specificity phosphatase – 1 (DUSP-1) (Valledor et al., 1999). Likewise, proline serine threonine phosphatase interacting protein 2 (PSTPIP2) is an adaptor protein that interacts with PEST-family tyrosine phosphatases 12 (PTPN12), which are both able to inhibit Erk1/2 (Figure 12 B) (Chitu et al., 2012; Yang & Reinherz, 2006). Besides, the transmembrane adaptor protein DAP12 mediates the proliferation through M-CSF R independently from ERK and Akt (Otero et al., 2009). This is mediated by the immunoreceptor tyrosine-based activation motifs (ITAMs) which are displayed in the cytoplasmic domain of DAP12 and are phosphorylated upon activation of M-CSF R. As a result, Syk is activated followed by the activation of Pyk2 tyrosine kinase that phosphorylate B-catenin facilitating several target genes implicated in the cell cycle.

The activation of M-CSF R upregulates the myeloid transcription factor PU.1 in HSCs directing them towards monocytic lineage (Mossadegh-Keller et al., 2013). The signaling downstream M-CSF R mediates the differentiation of multipotent precursor cells into promonocytes, monocytes towards macrophages which is highly dependent on Erk1/2 (Bourgin et al., 2000; Gobert Gosse et al., 2005; Wilson et al., 2005). In primary human monocytes, demonstrated in Figure 12 C, M-CSF triggers activation of PI3K and Erk1/2 pathways which are associated with M-CSF R Tyr-723 (721 in mice) phosphorylation cycles. Via PI3K/Akt pathway, caspase 8 is activated followed by the

activation of caspase 3 which in turn mediates the cleavage of nucleophosmin (NPM) enhancing differentiation (Jacquel et al., 2009).

Nonetheless, M-CSF triggers the ruffling of membrane as well recognition of actin cytoskeleton and focal adhesion to mediate motility of macrophages (Chitu et al., 2005; Webb et al., 1996). The Rho family of small GTPases, Rho, Rac and cdc42 stimulate and regulate actin polymerization, actomyosin contractility as well as adhesion formation (Allen et al., 1997). This first wave of actin polymerization, which mediates mobility of macrophages, is initiated and conducted by M-CSF R pTyr-721 – dependent PI3K pathway (Sampaio et al., 2011).

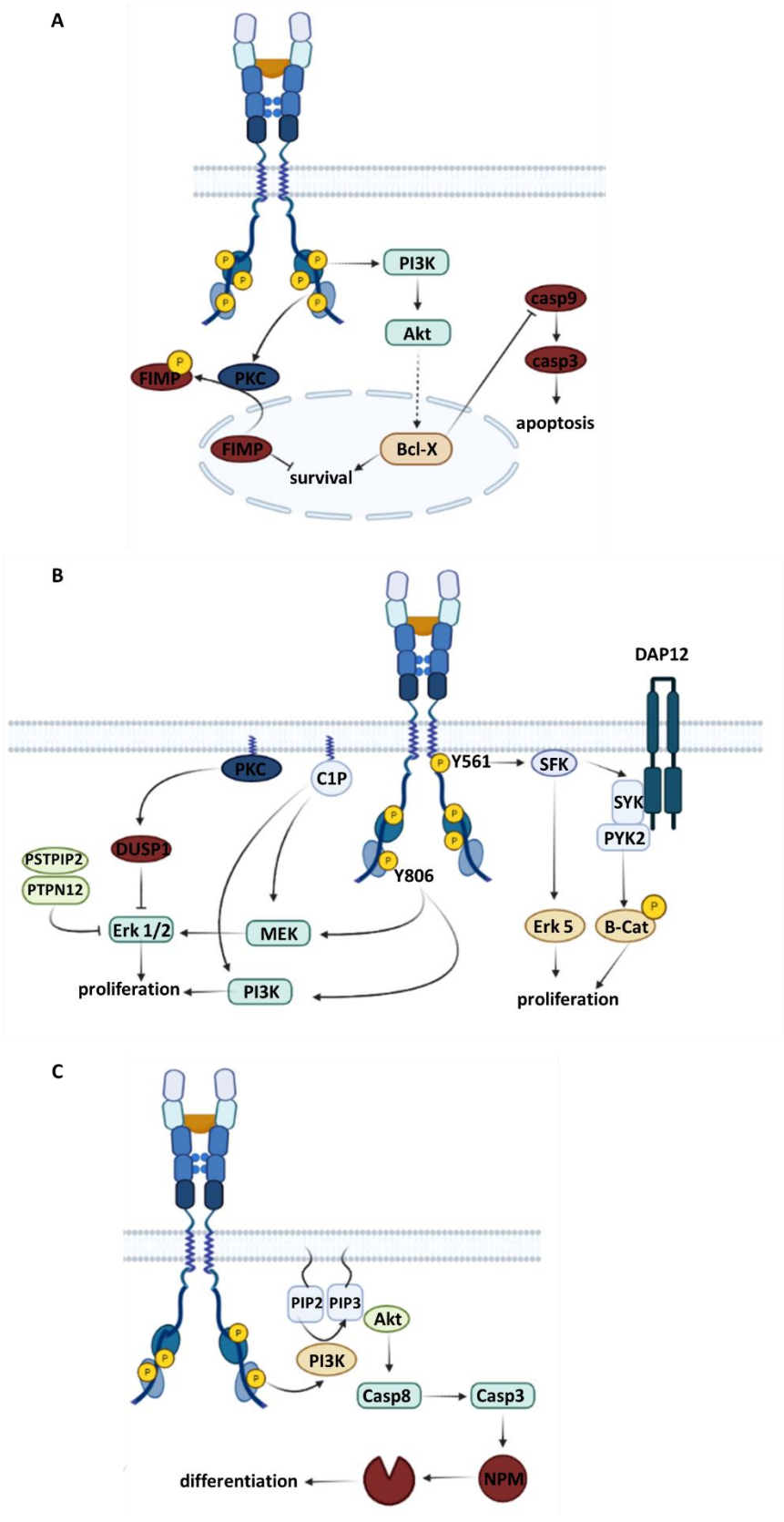

Figure 12 M-CSF R Signaling Transduction

(A) Survival of macrophages is mediated by the PI3K/Akt pathway which activate Bcl-x inhibiting caspase-mediated apoptosis and promoting survival. Moreover, PKC is activated as a result on intracellular phosphorylation of the receptor and subsequently, FMP which inhibits the survival in the nucleus is translocated to the cytosol where it is phosphorylated.
(B) Proliferation of macrophages is also one of the central transduction pathways of M-CSF R. As a result of phosphorylation of tyrosine site 806, PI3K and MEK then subsequently Erk 1/2 are activated enhancing the proliferation of macrophages. This can be also triggered by C1P. In addition, PKC upregulates the expression of DUSP1 which inhibit Erk 1/2. Erk 1/2 can be also inhibited by PSTPIP2 and PTPN12 to control the proliferation. Proliferation of macrophages can be also achieved by phosphorylation at tyrosine 561 through SFK that activated Erk5. Finally, DAP12 through M-CSF R mediates proliferation through β-catenin.
(C) M-CSF R plays a role in the differentiation of macrophages through PIP3K/Akt. As a result of this pathway, caspases 8 and 3 are activated which lead to the cleavage of NPM conferring differentiation of macrophages.
Adapted from (Stanley & Chitu, 2014b)

Abbreviations: FIMP: Fms interacting protein; PKC: protein-kinase C; PI3K: phosphoinositide-3-kinase; Bcl-X: B-cell lymphoma-extra; Casp: caspase; C1P: ceramide-1 phosphate; DUSP1: dual specificity phosphatase – 1; PSTPIP2: proline serine threonine phosphatase interacting protein 2; PTPN12: PEST-family tyrosine phosphatases

12; MEK: mitogen-activated protein kinase (MAP) kinase kinase; ERK: Extracellular signal-regulated kinase; SFK: Src family kinase; SYK: spleen associated tyrosine kinase; PYK2: protein tyrosine kinase 2-beta; β-cat: β-catenin; PIP2: phosphatidylinositol 4,5-bisphosphate; PIP3: phosphatidylinositol 3,4,5-triphosphate; NPM: nucleophosmin.

III. M-CSF R Targeting

High levels of CSF-1 was detected in solid tumors accompanied by increased TAMs localization in the TME which were associated with poor prognosis is various solid tumors (McDermott et al., 2002; Richardsen et al., 2008; Scholl, Bascou, et al., 1994; Scholl, Pallud, et al., 1994; Webster et al., 2010). Genetic manipulation of CSF1 expression in mice tumoral models demonstrated that the depletion of CSF1 resulted in decrease and delay in the progression of the tumor (Zhou et al., 2020). Besides, the immunosuppressive functions that TAMs display are reverted using CSF-1 R inhibitors (Zhu et al., 2014). Studies have demonstrated that inhibition of CSF-1 R enhances immune checkpoint inhibitor-mediated anti-tumor immune response (Przystal et al., 2021). Based on that, several CSF-1 R inhibitors were used and evaluated in combination with immune checkpoint inhibitors (Cannarile et al., 2017).

There are several clinically validated approaches that have been used to inhibit the signaling of CSF-1 R starting from small molecule inhibitors which target the activity of intracellular kinase activity of the receptor (Ordentlich, 2021) to antibodies targeting either CSF1 or its receptor, summarized in Figure 13. These include Pexidartinib (PLX3397), Edicotinib (JNJ-40346527), Sotuletinib (BLZ945) and ARRY382 among others such as PLX5622, GW2580 and Ki20227. Other approaches include the usage of antibodies, which either target the binding domain of the CSF-1R thus disrupting ligand binding such as AMB-05X (AMG820) and others, or inhibit the dimerization of the receptor such as Emactuzumab (RG7155). There are also antibodies, such as Lacnotuzumab (MC5110), which are used to target the ligand CSF-1. Evaluation of CSF-1 R inhibitors in clinics was associated with a well-tolerated response in most cases with some side effects such as increase in serum liver enzyme levels as well as edema. Below, I will mention some of these inhibitors, which are widely studied or used in pre-clinical or clinical studies.

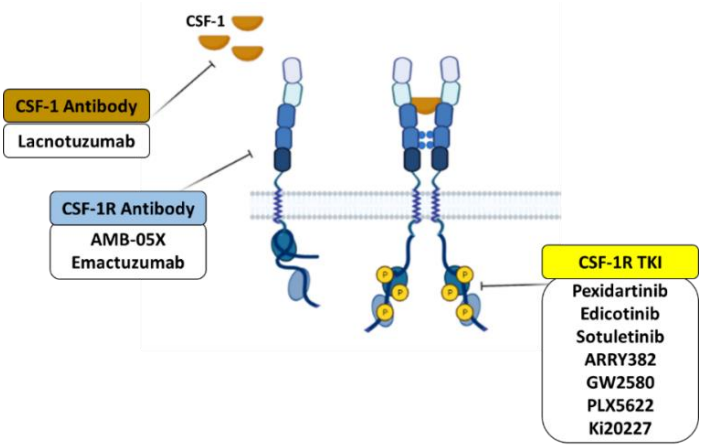

Figure 13 Targeting M-CSF R/CSF-1R

M-CSF R signaling can be targeted by inhibiting the phosphorylation of intracellular tyrosine kinases (CSF-1R TKI) using small molecule inhibitors or using antibodies directed against the ligand CSF-1 or the receptor.

III-1. Small Molecule Inhibitors

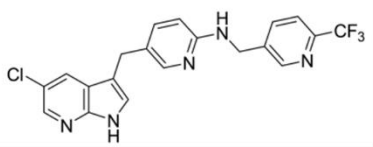

Pexidartinib

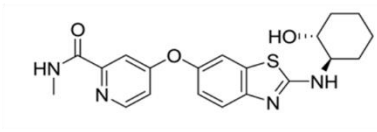

Sotuletinib

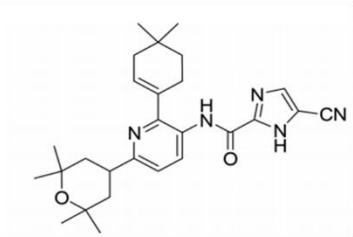

Edicotinib

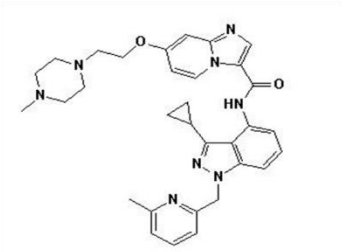

ARRY382

Figure 14 Molecular Structure of Small Molecules Inhibitors of M-CSF R

Molecule Structures of Pexidartinib, Sotuletinib (BLZ945), Edicotinib and ARRY382 which are small molecules inhibitors that target and inhibit the tyrosine kinases of the intracellular domains of M-CSF R.

Pexidartinib (PLX3397)

Pexidartinib is an oral, small molecular inhibitor of receptor tyrosine kinase inhibiting CSF-1 R, c-kit and FLT3 (Benner et al., 2020). It became the first CSF-1R inhibitor to be marketed as a treatment strategy and paved the way to other studies on different receptor tyrosine kinases in the context cancer.

Pexidartinib was evaluated in a multicenter phase I trial (NCT01004861) in a dose-escalation study, which evaluated the safety and pharmacokinetics of the drug, followed by an extension study, that assessed its safety and efficacy in patients having advanced Tensynovial Giant Cell

Tumor (TGCT) (Tap et al., 2015). The efficacy of Pexidartinib was assessed by imaging at baseline and followed every 2 months by which images were evaluated using the tumor volume score that calculates the volume of the tumor as a percentage of the entire synovium. The chosen dose for the extension study, where 23 patients with advanced TGCT were enrolled, was 1000 mg daily. Of these patients, 12 had a partial response representing an overall response rate of 52% while 7 patients had a stable disease. Evaluating the efficacy of Pexidartinib on the tumor burden, 14 patients underwent MRI where a mean of 61% decrease in the tumor volume score was observed in 11 patients compared to 3 patients who showed a stable disease.

To further evaluate the efficacy of Pexidartinib in TGCT, a phase 3 ENLIVEN study (NCT02371369) was carried out in two parts, first a double-blinded placebo-controlled and the second part was open-label extension (Tap et al., 2019). 120 patients were recruited of which 61 patients received pexidartinib, at a dose of 1000 mg for 2 weeks followed by 800 mg daily for 22 weeks, and 59 patients received Placebo. At week 25 following treatment, results by tumor volume score showed that the overall response rate in pexidartinib group is 56% compared to 0% in placebo group. Regarding the safety of the treatment, adverse effects of any grade including fatigue, nausea and elevation of liver enzymes occurred in 98% of patients in pexidartinib group and 93% of patients in the placebo group.

Furthermore, based on preclinical models which showed that inhibition of CSF-1R in glioblastoma resulted in a reduction in tumor burden, a phase II trial of pexidartinib was carried out in patients with recurrent glioblastoma (Butowski et al., 2014). Results revealed an elevation of plasma CSF-1 as well as reduction of monocytes, however no efficacy was showed.

Finally, pexidartinib was also used in combination with the mammalian target of rapamycin (mTOR) inhibitor sirolimus (NCT02584647) in patients suffering from different types of sarcoma where 3 of them were TGCT patients, 5 had leiomyosarcoma, 8 had malignant peripheral nerve sheath tumor and the remaining had other sarcoma subtypes. Results showed a clinical benefit in 12 out of the 18 recorded patients (67%) characterized by a partial response in the three TGCT patients evaluated by more than a 30% decrease of the tumor growth and a stable disease in 9 patients (Manji et al., 2021; Patwardhan et al., 2014).

In addition, Pexidartinib was shown to reprogram TAMs in the TME by reducing the M2-like TAM phenotype as well as enhance the infiltration of CD8+ T cells towards the TME (T. Fujiwara et al., 2021)

Edicotinib (JNJ-40346527)

Edicotinib is a CSF-1R kinase inhibitor belonging to the family of cyanoimidazolecarboxamides. It is an oral kinase inhibitor of IC50 of 3.2 nM for CSF-1R and it inhibits KIT and FLT3 as well. It exhibits a 6 folds higher selectivity to CSF-1R than kit and about 60 folds more versus FLT3

(C.-C. Lin, 2021; Ordentlich, 2021). Edicotinib has been studied and explored in patients suffering from Hodgkin's Lymphoma (HL), rheumatoid arthritis (RA) as well as Crohn's disease.

Knowing that CSF-1/CSF-1R axis in macrophages and its precursor cells contribute to the pathogenesis of RA, a phase II clinical study (NCT01597739) on patients with active RA was carried out following phase I study that demonstrated the high efficacy of Edicotinib on inhibiting CSF-1R activity (Genovese et al., 2015). The randomized, placebo-controlled double-blind phase II study did not show significant difference in efficacy between the two groups: Edicotinib-treated and placebo-treated. Results have revealed higher levels of CSF-1 and decreased CD16+ monocytes indicating that Edicotinib acts by binding to the CSF-1R and inhibits macrophage's response to CSF-1 at a concentration less than 10 nM. However, Edicotinib was not effective in treating RA patients. Adverse effects of Edicotinib were related to an increase in the levels of liver enzymes such as AST, ALT as well as LDH, but periorbital edema was not reported.

Therewithal, Edicotinib was found to inhibit macrophages in animal models affecting the proliferation of HL. Phase I study (NCT01572519) in HL was designed with dose escalation manner followed by phase II study (von Tresckow et al., 2015). According to a single-dose phase I study of doses ranging from 10 mg daily to 450 mg twice daily, absorption of Edicotinib was fast ranging from 1 to 3 hours. A multiple dose study of doses ranging from 50 mg daily to 300 mg twice daily for up to 14 days consecutively, showed a proportional increase between the dose and the maximal concentration. The plasma concentration of CSF-1R 4 hours post dose administration were inhibited by a minimum of 80% confirming the binding of Edicotinib to the receptor. 24 hours post-dose administration analysis showed a decrease in inhibition of plasma CSF-1R daily dose while 150 mg of administration twice daily showed a strong inhibition rendering it as the suitable dose for phase II study. Furthermore, in vivo pharmacological studies demonstrated an inhibition of the receptor's phosphorylation by at least 95% following a dose of 450 mg in the single dose study as well as a dose of 150 mg daily in multiple dose study. Because Edicotinib displays a limited efficacy as monotherapy, the phase II study did not report any noticeable efficiency in patient with advanced HL.

Finally, in multiple lung cancer cell lines, inhibiting the CSF-1R tyrosine kinases by Edicotinib resulted in reduced levels of genes associated with epithelial-to-mesenchymal transition (EMT), stem cells as well as chemoresistance (Pass et al., 2016). This sheds light on the role that CSF-1R plays in chemoresistance in tumors.

Sotuletinib (BLZ945)

BLZ945 is an oral, small molecular which exhibits more than 1000 folds selectivity for CSF-1R, with an IC50 of 1 nM, compared to other tyrosine kinases (Wiesmann et al., 2010). It belongs to the family of pyridine inhibitors, which impacts macrophages and its precursors aiding in preventing the diseases associated with these cells.

BLZ945 has been evaluated in a phase 1 study (NCT02829723) as monotherapy or in combination with spartolizumab for treating advanced solid tumors (C.-C. Lin et al., 2020). Moreover, inhibition of CSF-1R by BLZ945 resulted in a reduction of the turnover rate of TAMs and increased the number of cytotoxic T cells in breast cancer and cervical cancer. A study on Keratin 14-expressing human papilloma virus type 16 (K14-HPV-16) cells revealed that BLZ945 prevented the development of the tumor.

In vitro studies demonstrated that blocking the CSF-1R pathway by BLZ945 in combination with anti-PDL1 effectively retarded the growth of mesothelioma than each monotherapy by itself (Magkouta et al., 2021). Moreover, BLZ945 limited the immunosuppressive functions of TAMs and promoted the cytotoxic effect of CD8+ T cells. Additionally, in a 3D-culture system of NSCLC, the phenotype of macrophages was modulated upon treatment with BLZ945 resulting in decrease in the M2-like TAM phenotype (Rebelo et al., 2018). In a mouse ovarian cancer model, the effect of BLZ945 in combination with docetaxel was evaluated and showed that the combination therapy inhibited the tumor growth and reduced TAMs population show an increased in CD8+ T cells infiltration (X. Lu & Meng, 2019).

ARRY382

ARRY382 is a CSF-1R kinase inhibitor which was developed as an oral small molecule inhibitor by ARRAY Biopharma (Bendell et al., 2013). It is a potent and selective inhibitor of CSF-1R with an IC50 of 9 nM and displays inhibitory effects on the differentiation of osteoclasts as well as bone resorption.

This molecule was tested in 26 patients with advanced or metastatic tumor with different doses ranging from 25 to 500 mg where no major side effects were reported. It was evaluated either as single agent or in combination with pembrolizumab. The phase I study (NCT01316822) as monotherapy showed dose-dependent increase in circulating CSF-1 levels accompanied by a reduction in the levels of circulating monocytes which was obvious starting from a dose of 200 mg and peaked with a 96% decrease at 400 mg (Bendell et al., 2013). This was followed with some side effects including increased fatigue, nausea, vomiting as well as decreased appetite. In addition, a phase Ib/II study of ARRY382 was carried out in combination with pembrolizumab in patients with advanced solid tumors (NCT02880371) (Harb et al., 2017). The combination therapy was well tolerated, however, a limited clinical benefit was observed from this clinical trial.

III-2. Monoclonal Antibodies

AMB-05X (AMG820)

AMB-05X is a human IgG2 monoclonal antibody that efficiently blocks the binding of CSF-1R ligands, CSF-1 and IL-34, to CSF-1R (Razak et al., 2020). Two clinical trials have been reported which evaluated the efficacy of this monoclonal antibody as monotherapy of in combination with pembrolizumab in solid tumors.

The phase I study of AMB-05X as monotherapy (NCT0144404) did not demonstrate any tumoral response despite its functionality against the CSF-1R (Papadopoulos et al., 2017). The levels of CSF-1 were elevated in a dose-dependent manner, which were consistent with the blockade of CSF-1 binding to its receptor. This was followed by reduction in macrophages (CD68+, CD163+ and CD206+). The most common side effects observed with this monotherapy were fatigue, increased levels of AST as well as edema.

AMB-05X was combined with pembrolizumab in a phase Ib/II study (NCT02713529) in patients with relapsed solid tumors such as pancreatic cancer, CRC and NSCLC showing resistance against anti-PD-1 therapy (Razak et al., 2020). In this study 116 patients were recruited. The primary end points were dose-limiting toxicity and adverse effects as well as immune-related partial response and the secondary endpoints were overall survival, progression-free survival, pharmacokinetics as well the immune population of CD4+, CD8+ and CD68+ cells. Results showed that all patients had some of the common adverse effects including fatigue, increase in aspartate aminotransferase and face edema. Immune-related partial response, based on the decrease from the baseline in the sum of the longest diameters of lesions, was observed in 3 of patients of which 2 had CRC and 1 had NSCLC and immune-related stable diseases was recorded in 39 patients who had pancreatic cancer, CRC or NSCLC. For all patients, the median of progression free survival and overall survival were 2.1 months and 5.3 months, respectively. This demonstrated that the efficiency was not met as the anti-tumor activity was insufficient.

Emactuzumab (RG7155)

Emactuzumab is a recombinant humanized IgG1 monoclonal antibody which binds to the dimerization interface of the CSF-1R blocking the ligand binding and its activation (C. A. Gomez-Roca et al., 2015). It significantly decreases the presence of TAMs by inhibiting the CSF-1R with an IC50 of 0.3 nM. It has been studied in several phase I clinical studies as a single agent therapy as well as in combination with either paclitaxel or atezolizumab.

An open-label phase Ia/b study was carried out to assess the safety, clinical activity pharmacokinetics and pharmacodynamics of emactuzumab as monotherapy and in combination

with chemotherapy paclitaxel. A total of 99 patients with solid tumors: ovarian, breast or pancreatic were enrolled of which 29 patients got the treatment of emactuzumab alone as a dose-escalation part of the study and the remaining 70 patients were enrolled into the expansion study. Because of the disease progression, adverse effects or death, 88 patients were withdrawn. Additionally, a total of 54 patients were enrolled to the combination treatment where 42 patients discontinued the study due to the same reasons discussed above. Regarding the clinical activity, no patient receiving the monotherapy showed an objective response while 13 patients showed a stable disease. From the combination therapy, 4 patients showed partial response. Although no relevant clinical antitumor activity was observed, a reduction of immunosuppressive TAMs was showed in both treatment strategies.

Recently, a phase Ib study (NCT02323191) was carried out to evaluate the safety, anti-tumor activity as well as the pharmacokinetics and pharmacodynamics of emactuzumab in combination with the programmed cell death-1 ligand (PD-L1) blocking monoclonal antibody, atezolizumab in 221 patients with various solid tumors either naïve or experienced for the immune checkpoint blockers (ICBs) (C. Gomez-Roca et al., 2022). Dose escalation of emactuzumab was conducted to assess the optimal biological dose, which was determined to be 1000 mg of emactuzumab in combination with 1200 mg of atezolizumab. Pharmacodynamics and clinical activity were evaluated in metastatic urothelial bladder cancer, melanoma and NSCLC. Results showed that the combination strategy displayed a manageable safety profile with a considerable objective response rate of 9.8%, 12.5%, 8.3% and 5.6% for ICB-naïve urothelial bladder cancer, ICB-experienced NSCLC, ICB-experience urothelial bladder cancer and ICB-experienced melanoma. Notwithstanding, resistance to CSF-1R blocking antibody was investigated and results have shown that IL-4 has the potential to rescue the viability of macrophages treated with emactuzumab in vitro (Pradel et al., 2016) where resistant macrophages displayed an increase in the expression of the mannose receptor, CD206.

Lacnotuzumab (MC5110)

Lacnotuzumab is a humanized IgG1 monoclonal antibody that is directed against CSF1. It has been evaluated as monotherapy in patients with TGCT as well as in combination with spartalizumab which is an anti-PD-1 antibody in patients with advanced tumors (Calvo et al., 2018; Pognan et al., 2019). Results from phase I study of lacnotuzumab as monotherapy (NCT01643850) in patients with advanced TGCT demonstrated that the average tumor size in patients who received 5 mg/kg and 10 mg/kg of lacnotuzumab with no difference compared to the placebo for the dose of 3 mg/kg. Following, a phase Ib/II (NCT02807844) was carried out for lacnotuzumab in combination with spartalizumab in patients with anti-PD-1 naïve pancreatic cancer or anti-PD-1 resistance advanced melanoma where the most common dose-dependent adverse effects were edema, elevated blood CPK as well as elevated AST. Efficacy results showed that 1 out of 30 patients with pancreatic cancer achieved partial response.

Chapter Three - Part Two

Aim and Hypothesis

As explained in this chapter, one way to target TAMs as a monotherapy or in combination in solid tumors relies on CSF-1R inhibition. However, no true clinical outcome has been reported as the efficiency of these treatments were not met as expected. Thus, we aimed to deeply explore the effect of using CSF-1R antagonists on the state and functions of human macrophages. We hypothesized that blocking the CSF-1R receptor could reprogram TAMs by modifying its tumor-promoting functions and interfere in the macrophage-induced chemoresistance but would depend on the type of molecule used. We design the current project to study the specificity of various CSF1-R inhibitors to reshape macrophage's metabolic state.

Chapter Three - Part Three

Results

RESEARCH

ARTICLE

2

Metabolic reprogramming of tumor-associated macrophages through CSF1-R targeting

Khaldoun Gharzeddine[1], Marie Malier[1], Clara Hennot[1], Yoshiki Yamaryo-Botté[2], Arnaud Millet[1]

1. Univ.Grenoble Alpes, Inserm U1209, CNRS UMR5309, Institute for Advanced Biosciences, Team Mechanobiology, Immunity and Cancer, 38000 Grenoble, France

2. Univ.Grenoble Alpes, Inserm U1209, CNRS UMR5309, Institute for Advanced Biosciences, Gemeli metabolomic platform, 38000 Grenoble, France

Running title: Metabolic reprogramming of macrophages through CSF1R targeting

Keywords: Metabolic reprogramming, CSF1R antagonists, Hypoxia, tumor-associated macrophages, Cholesterol efflux, dihydropyrimidine dehydrogenase, chemoresistance, STAT6, ERK1/2.

Corresponding author:

Arnaud Millet MD PhD,

e-mail: arnaud.millet@inserm.fr

Team Mechanobiology, Immunity and Cancer, Institute for Advanced Biosciences

Building Albert Bonniot

Boulevard de la Chantourne

38700 La Tronche

France

The authors declare no conflicts of interest.

Abstract

Tumour associated macrophages participate to the complex sustainability network that favours tumour growth. Among the various strategies that have been developed to target these cells, CSF1R blockade is one of the most promising one. Despite its promises, clinical efficiency is deceiving without any clear explanation. Here, we have characterized the resulting state of human macrophages exposed to CSF1R kinase inhibitors. We show that inhibition of the initial activation of the kinase activity of CSF1R does not predict the resulting phenotypic modifications in macrophages, which depends on the type of inhibitor used. We found that edicotinib, a cyanoimidazolecarboxamide, is able to profoundly impair cholesterol synthesis, fatty acid metabolism and hypoxia-driven expression of dihydropyrimidine dehydrogenase, an enzyme responsible for the 5-FU macrophage-mediated chemoresistance contrary to other CSF1R antagonists. Alongside to this, edicotinib demonstrates the ability to avoid the STAT6-dependent IL-4 reprogramming in tumour educated macrophages. These results open the opportunity to reshape macrophage commitment toward an anti-tumoral phenotype by CSF1R targeting.

Introduction

A large body of work has been reported providing compelling evidence that tumour-associated macrophages (TAMs) participate to tumour growth, treatment resistance and metastasis (DeNardo and Ruffell, 2019; Engblom et al., 2016). Indeed, TAMs are associated with bad prognosis in a vast majority of solid tumours (Cortese et al., 2020). Consequently, a huge effort has been done to target TAMs in order to modulate the immune response against the tumour (Mantovani et al., 2022).

CSF1-R is a receptor, possessing an intrinsic tyrosine kinase activity, which recognizes CSF1 (M-CSF, macrophage colony stimulating factor) and IL-34. CSF1-R signalling pathway is involved in the survival, proliferation, differentiation and chemotaxis of macrophages (Stanley and Chitu, 2014). This pivotal role opened the way to use CSF1-R targeting in order to deplete macrophages in various pathological contexts and especially in cancer (Cannarile et al., 2017). CSF1-R targeting has been used in various tumour mice models reaching promising results but only mild beneficial effects in humans (Mantovani et al., 2022). The reasons for this lack of efficiency is unclear. Moreover, the recognition that the type of tumour model used (O'Brien et al., 2021) and the modification of the cellular environment as hypoxia (Pradel et al., 2016) impact the efficiency of the CSF1-R targeting leads to the need to a better understanding of the CSF1-R functional consequences on human macrophages.

Recently, the importance of CSF1-R blockade beyond apoptosis induction has been recognized (Pyonteck et al., 2013). The possibility to reprogram macrophages in order to re-establish an anti-tumoral phenotype brings potential hope to obtain an immunomodulatory

strategy. Nevertheless, the mechanisms involved in macrophage's reprogramming through CSF1-R targeting are unclear.

Here, we have characterized the transcriptional consequences of CSF1R inhibitors on human macrophages. We show that inhibitors of CSF1R present a very different resulting pattern of metabolic reprogramming. This differing pattern is associated with an ability to inhibit the IL-4 mediated reprogramming of macrophages by tumour cells and is also associated with the downregulation of dihydropyrimidine dehydrogenase expression, which is responsible for a hypoxia driven macrophage-mediated chemoresistance in colorectal cancers (Malier et al., 2021).

Results

Differential effect of Edicotinib and Sotuletinib (BLZ945) on human macrophage transcriptomic program is independent of inhibition of CSF1R phosphorylation

To understand the consequences of CSF1-R targeting on human macrophages, we exposed human monocyte derived macrophages to CSF1-R inhibitors after 6 days of differentiation under CSF1 (M-CSF) stimulation (Figure 1A). There exists a large variety of CSF1-R inhibitors with differing ability to inhibit the kinase activity of CSF1-R (El-Gamal et al., 2018), as it is assessed by their IC50 determined *in vitro* (Supplemental Figure 1A). We verified and quantified their ability to inhibit the phosphorylation of the CSF1-R induced by M-CSF on human macrophages (Supplemental Figure 1B). For this study, we subsequently choose two potent inhibitors in this list: sotuletinib (BLZ945) and edicotinib (Figure 1B). We found that during the initial phase of activation of CSF1-R by M-CSF the phosphorylation of the CSF1-R is similarly inhibited by BLZ945 and edicotinib (Figure 1C). To evaluate the impact of CSF1-R inhibitors on human macrophage phenotype, we performed global gene expression analysis using RNA sequencing (RNAseq) on bulk macrophages 48h after exposition to vehicle, Edicotinib and BLZ945. To extract differentially expressed genes between treated and naïve macrophages, we used a moderated t-test with an adjusted p-value (Benjamini-Hochberg procedure) and a threshold of a 2-fold change (FC). We found that BLZ945 is associated with 15 downregulated and 2 upregulated genes (Figure 1D). By contrast, Edicotinib reveals a more profound modification of the transcriptional program of human macrophages associated with 740 downregulated and 481 upregulated genes (Figure 1E). Both inhibitors share the ability to down regulate the 15 genes found for BLZ (*F13A1, GFRA2, P2RY6, IGF1, CD163L1, VCAN, STAB1, FGL2, CD93, CLEC5A, FCN1, CCDC170, SIGLEC1, GPR82*) highlighting a common mechanism (Figure 1F). As the ability of these two inhibitors to prevent the phosphorylation of the CSF1-R when exposed to CSF1 is similar (Figure 1C), this result advocates for a differing mechanism not directly related to the ability of these inhibitors to inhibit the phosphorylation of the CSF1-R itself.

Edicotinib reprograms human macrophages by inhibiting phosphorylation of MAPK1/2 and the cholesterol metabolism through a SREBP2 dependant pathway

We then used a Gene Ontology (GO) enrichment analysis to identify pathways affected by edicotinib. The GO terms of biological processes associated with downregulated genes by edicotinib point toward the inhibition of the ERK1/2 pathway and the cholesterol metabolic pathway (Figure 2A). This pattern is specific to edicotinib as the GO-term analysis for downregulated genes by BLZ945 (with extended criteria using a FC at 1.4) does not reveal a similar metabolic signature (Supplementary Figure 2A). We confirmed the regulation of the ERK1/2 pathway by studying the phosphorylation state of ERK1/2 under edicotinib exposure in human macrophages by immunoblot and found a profound downregulation of its phosphorylation state (Figure 2B). Apart from its signalling function, ERK1/2 has also been implicated to enhance glycolysis and modulate metabolism through pyruvate kinase (PKM2) activation (Supplementary Figure 2B) (Yang et al., 2012). We found that edicotinib is associated with the inhibition of PKM2 and hexokinase 3 (HK3) expressions in macrophages (Supplementary Figure 2C) advocating for the inhibition of the glycolytic activity in macrophages.

Moreover, edicotinib interfere with cholesterol metabolism (Figure 2A). We have explored the expression of genes involved in the metabolic pathway involved in cholesterol synthesis and found that 13 of the 15 enzymes involved in key steps of the synthesis are downregulated in macrophages exposed to edicotinib contrary to controls and BLZ945 (Figure 2C). The cholesterol synthesis pathway is under the control of the transcription factor SREBP2 (*SREBF2*), which controls the expression of various enzymes of the synthesis pathway (*HMGCS1, HMGCR, IDI1, FDPS, FDFT1, MSMO1, SC5D*) (Figure 2D). We found that *SREBF2* is downregulated in macrophages exposed to edicotinib under a transcriptional control (Figure 2E). The cholesterol content of cells is also under the control of LDL uptake by the LDLR, which is also under the control of SREBP2, and its expression was found collapsed under edicotinib exposure (Figure 2F). These results advocate for a profound disruption of cholesterol metabolism in macrophages induced by edicotinib. Cholesterol participates to the organisation of cell membrane and increase its rigidity (Chakraborty et al., 2020). The disruption of cholesterol homeostasis induced by edicotinib leads us to explore the consequences on cell membrane rigidity, which participates to cell stiffness. Using atomic force microscopy, we determined the elastic modulus (Young's modulus) of macrophages and confirmed a decrease of cell rigidity as it is expected with the lowering of cell membrane content of cholesterol (Figure 2I).

Edicotinib interferes with the metabolic response of macrophages in hypoxia inhibiting fatty acid synthesis mediated by SREBP1

Analysis of differentially expressed genes under exposure to edicotinib reveals the upregulation of EPAS1, which encodes the HIF-2α protein (Figure 3A). HIF-2α is a transcription factor involved in the cell response to hypoxia (Lee et al., 2020). Oxygen deprivation avoids

the degradation of HIFs leading to their stabilization (Kaelin and Ratcliffe, 2008). HIF dependent adaptation to hypoxia is associated with a HIF transition when exposition to low oxygen is prolonged leading to a decreased HIF mRNA stability (Bartoszewski et al., 2019). We have confirmed that this mechanism is taking place in human macrophages 48h after a transition to hypoxia (Figure 3B). The increased mRNA level of HIF-2α under the exposition to edicotinib leads us to study the effect of edicotinib on the macrophage's response to hypoxia. We compared mRNA level expression between macrophages in normoxia and macrophages exposed to low level of oxygen (PO_2=25 mmHg ~ 3%) using an RNAseq methodology. Selecting gene differentially expressed between normoxia and hypoxia (p-adjusted <0.05 and log_2 FC <-1 or >1), we studied the impact of CSF1R antagonists (Figure 3C). Some genes are up-regulated by edicotinib in normoxia and maintained their upregulation in hypoxia when compared to vehicle and BLZ (Figure 3C, cluster2), *EPAS1* is one of them. Interestingly, many genes upregulated by exposure to low oxygen levels see their expression inhibited by edicotinib. This inhibition of the hypoxic response (cluster 4 in Figure 3C) is associated with a metabolic signature linked to lipids metabolism, as the GO-term analysis of biological processes of these genes revealed (Figure 3D). To further analyse the consequences of this modulation of lipid metabolism in hypoxia, we measured the cell content of fatty acids in macrophages in hypoxia compared to normoxia as well as hypoxic macrophages exposed to edicotinib. We observed that hypoxia induces the increase of the amount of various fatty acids (mainly C16:0, C18:0, C18:1 cis and C18:2 cis) and that this increase is prevented by edicotinib (Figure 3E). We did not observed any variation of fatty acid content of human macrophages in normoxia under CSF1R antagonist targeting (Supplementary Figure 3). To explain this inhibition of fatty acids synthesis, we analysed the expression of SREBF1, a transcription factor controlling fatty acid synthesis and the fatty acid synthase (FASN) and found that both are downregulated specifically by edicotinib compared to vehicle and BLZ in hypoxia (Figure 3F).

The hypoxic environment modulates the response of human macrophages to the CSF1R antagonist edicotinib

To explore the consequences of CSF1R targeting in hypoxia, we studied the impact of hypoxia on differentially expressed genes under edicotinib in normoxia and hypoxia and we removed oxygen responsive genes. This approach allowed us to study the effect of oxygen on the macrophage's response to hypoxia. We found that upregulated genes by edicotinib could be classified in three groups (Figure 4A): oxygen insensitive (cluster 1), hypoxic sensitive (cluster 2) and normoxic sensitive (cluster 3). Cluster 1 genes display a very specific profile toward cell response to metal ions as it is illustrated by the GO-term analysis of biological processes associated with these genes (Figure 4B). This specific response is mainly supported by the upregulation by edicotinib of the following metallothioneins (Supplemental Figure 4): *MT1E*, *MT1F*, *MT1G*, *MT1H*, *MT1M*, *MT1X*, *MT2A*. Cluster 2 is composed of genes, which are upregulated by edicotinib but only in hypoxia. One illustrative gene of this pattern is the superoxide dismutase 2 *SOD2* (Figure 4C), a master gene controlling ROS production in cells

(Wang et al., 2018). Cluster 3 represents genes upregulated by edicotinib only in normoxia. Illustrative of this cluster is *GADD45A* (Figure 4D), which is involved in the regulation of the p38MAPK pathway (Salerno et al., 2012). Downregulated genes by edicotinib did not display any modulation by oxygen (Figure 4A) and represent mainly the genes involved in the ERK1/2 pathway as revealed by the GSEA analysis (Figure 4E). We confirmed that the inhibition of the phosphorylation of ERK by edicotinib is similar in normoxia and hypoxia (Figure 4F). The GO-term analysis of biological processes associated with genes downregulated by edicotinib in hypoxia confirmed the downregulation of the metabolism of cholesterol (Figure 4G) similarly to what was found in normoxia (Figure 2A).

Edicotinib interferes with tumour educated macrophage reprogramming

Tumour associated macrophages represent a population of immune cells that participate actively to tumour growth and treatment resistance. A large number of studies have explored the signals used by tumours to drive the pro-tumoral function of these cells. It has been reported that IL-4 is one of the key cytokine leading to the tumour educated macrophage phenotype. Indeed, CD4 T cells associated with the tumour secrete IL-4 capable to induce a M2-like phenotype favouring pulmonary metastasis in a MMTV-PyMT mice model of breast cancer (DeNardo et al., 2009). We observed that macrophages targeted by a CSF1R antagonist downregulate some M2 associated genes, more specifically we found that edicotinib is able to down regulate the expression of CD206, CD276 and CD163 (Figure 5A). To explore the possibility to use edicotinib to prevent the IL4-induced education of macrophages in tumours, we studied the effect of edicotinib on M2 specific genes that we identified in human macrophages (Court et al., 2019). We observed that a group of M2 genes is downregulated irrespective of the oxygen level (Supplementary Figure 5). We notably found TGM2 (transglutaminase 2) as a downregulated gene. TGM2 has been described as a specific IL-4 M2 marker in human macrophages (Martinez et al., 2013). Indeed, we observed that edicotinib is able to dampen the increase expression of TGM2 induced by IL-4 (Figure 5B). To characterize the impact of edictotinib on specific IL-4 responsive genes we also studied the expression of ALOX15. ALOX15 is a lipo-oxygenase that we have previously demonstrated to be specifically upregulated in hypoxic IL-4 induced M2 human macrophages (Court et al., 2017). We confirmed the inhibition of ALOX15 expression in IL-4 stimulated hypoxic macrophages under edicotinib exposure (Figure 5B). ALOX15 expression under IL-4 stimulation is driven by the transcription factor STAT6, which mediates through its phosphorylation a large part of the IL-4 response (Sica and Mantovani, 2012). To explore the action of edicotinib of the IL-4 response in human macrophages, we studied the phosphorylation state of STAT6 and found that edicotinib is able to prevent the phosphorylation of STAT6, which is needed for its transcriptional activity in the nucleus (Figure 5C). This inhibition of the IL-4 response was specific to edicotinib and was not observed by using another CSF1R antagonist like BLZ945 (Figure 5B & 5C). It has been proposed that IL-4-induced STAT6 phosphorylation is regulated by ERK1/2 in lymphoid cells (So et al, Mol Immunol 2007). The ability of edicotinib to inhibit ERK1/2 phosphorylation

(Figure 2B, 4E & 4F), leads us to explore the role of ERK1/2 in the IL-4 response in human macrophages. Contrary to this hypothesis, we found that the inhibition of the phosphorylation of ERK by U0126 is not able to inhibit the phosphorylation of STAT6 under IL-4 stimulation in human macrophages in hypoxia (Figure 5D). We also found that Edicotinib starts to impair the phosphorylation of STAT6 during the first stage of IL-4 stimulation (at 6h) (Figure 5D) leading to a nearly complete inhibition at 48h (Figure 5B). Finally, we confirmed the inhibition of M2 polarization by edicotinib on hypoxic TEM (Tumor Educated Macrophages) demonstrating the relevance of this strategy in the tumour environment (Figure 5E).

Edicotinib inhibits DPD expression in hypoxia and reverts macrophage-mediated 5-FU chemoresistance

Macrophages not only participate to tumour growth mediated by their specific phenotype driven by cancer cells, they also participate to treatment resistance (Ruffell and Coussens, 2015). The underappreciated impact of hypoxia on macrophage biology (Court et al., 2017) and the increasingly recognized role of hypoxia in resistance to anticancer treatments and cancer relapse (Henze and Mazzone, 2016), lead us to reassess the role of hypoxic macrophages in chemoresistance. Recently, we demonstrated that hypoxic macrophages convey the chemoresistance to 5-FU, a first line chemotherapy, in colorectal cancer. We showed that the mechanism involved rely on the hypoxic-driven expression of dihydropyrimidine dehydrogenase (DPD), the limiting rate pyrimidine bases catabolic enzyme (Malier et al., 2021). In the present study, we observed that *DPYD*, the gene coding DPD, is differentially expressed in normoxic macrophages exposed to edicotinib but not in hypoxic ones. Interestingly, we observed that the hypoxia-driven expression of DPD in human macrophages is completely antagonized by edicotinib contrary to other CSF1R antagonists (Figure 6A and Supplementary Figure 6A). Alongside to the inhibition of its expression, the metabolic activity of DPD is also antagonized as it is demonstrated by the collapse of the ratio between dihydrouracil and uracil under edicotinib exposure (Figure 6B). We had previously demonstrated that DPD expression in hypoxic macrophages is controlled at the translational level in a HIF-2α dependent mechanism irrespective of its transcriptional activity (Malier et al., 2021). We observed that edicotinib is able to block the expression of DPD during the transition from normoxia to hypoxia (Figure 6C) without interfering with the mRNA level of DPYD during the initial stage of the transition (Figure 6D). Furthermore, we found that edicotinib is able to inhibit HIF-2α expression in hypoxic macrophages (Figure 6E). As IL-4 and GM-CSF have been shown to protect macrophages against CSF1R targeting by emactuzumab leading to macrophage depletion (Pradel et al., 2016), we verified the absence of protection against edicotinib-induced DPD depletion (Supplementary Figure 6B). We also studied the DPD expression during hypoxic transition in THP1 derived macrophages and confirmed the inhibition provided by edicotinib (Supplemental Figure 6C). We then explored the consequences of this HIF-2α mediated inhibition of DPD expression by edicotinib on the chemoresistance to 5-FU. We studied then the growth inhibition of colon cancer cells by 5-FU

conditioned by hypoxic macrophages exposed to CSF1R antagonists compared to 5-FU added to conditioned medium (preventing the direct interaction between 5-FU and macrophages). We observed, as we previously demonstrated, the complete protection against 5-FU that hypoxic macrophages provide and we demonstrated the efficiency of edicotinib to re-establish 5-FU inhibitory activity against cancer cells preventing the macrophage-driven protection against this chemotherapy (Figure 6F).

Discussion

Tumour associated macrophages represent an essential component of the tumour immune microenvironment in a vast majority of cancers. Their implication in angiogenesis, extracellular matrix remodelling, cancer cell proliferation, metastasis spreading and resistance to treatment leads to the development of macrophage-centred therapeutic strategies (Mantovani et al., 2022). The importance of the CSF1/CSF1R axis in macrophage survival, differentiation and activation makes CSF1R targeting a favoured approach to reshape TAMs. Two strategies have been pursued to attain this goal: block the interaction between the ligand (CSF1, IL-34) with its receptor using specific anti-CSF1R antibodies or inhibiting the tyrosine kinase activity of CSF1R resulting from its binding to its ligand using specific inhibitors. Various inhibitors have been developed through the years despite high specificity against CSF1R, these molecules were unable to demonstrate a strong clinical effect when used as monotherapy (El-Gamal et al., 2018; Mantovani et al., 2022). The reasons for this inefficiency are not clear and raise the question of the universality of the activity of these molecules on human macrophages. To decipher the possible differing effect of various CSF1R antagonist, we designed the present study to explore the transcriptional consequences of CSF1R blocking in human macrophages by various antagonists. We selected two of them (edicotinib and BLZ945) for a throughout analysis based on their efficiency to inhibit CSF1R phosphorylation under CSF1 stimulation (Figure 1C, Supplementary Figure 1B) and their known specificity (Supplementary Figure 1A) (El-Gamal et al., 2018). Unexpectedly, we observed that edicotinib affects far more profoundly than BLZ945 the transcriptomic program of human macrophages unchallenged by external CSF1 (Figure 1D & 1E). The GO-term analysis of biological processes associated with downregulated genes with edicotinib revealed the specific modulation of the cholesterol metabolism through the control of SREBP2 expression (Figure 2C-F) and the inhibition of the ERK1/2 signalling pathway (Figure 2B). The downregulation of cholesterol metabolism is of particular interest in the tumour microenvironment. Indeed, cancer cells secreted hyaluronic acid favours cholesterol efflux from macrophages that increase STAT6 dependent IL-4 response of TAM driving tumour progression (Goossens et al., 2019). Our results indicate that edicotinib is able to downregulate the synthesis of cholesterol and also to prevent STAT6-dependent IL-4 macrophage reprogramming by inhibiting STAT6 phosphorylation (Figure 5C).

As cholesterol is synthesized through the metabolic synthesis starting from acetyl-coA, which is produced by the fatty acid β-oxidation pathway, we explored the fatty acid synthesis in macrophages. We found that edicotinib is able to prevent the increase of fatty acid

accumulation driven by hypoxia in human macrophages (Figure 3E) and that cholesterol metabolism downregulation is maintained in hypoxia through the inhibition of *SREBF2* expression (Supplementary Figure 4B).

Alongside with the ability of this CSF1R antagonist to interfere with IL-4-induced reprogramming, we found that edicotinib is also able to interfere with DPD expression in hypoxia. This enzyme is responsible for a potent macrophage-mediated chemoresistance toward 5-FU, a first line chemotherapy in various cancers (Malier et al., 2021). We have demonstrated that the CSF1R antagonist interfere with HIF-2α stabilization in hypoxia (Figure 6E) and prevent the DPD synthesis controlled at the translational level by HIF-2α (Malier et al., 2021). This inhibition leads to the reestablishment of 5-FU sensitivity of cancer cell in the tumour microenvironment (Figure 6F).

In this study, we have provided compelling evidences showing that CSF1R blocking is an effective strategy to prevent TAM commitment driven by cancer cells and to prevent macrophage-induced resistance to chemotherapy. We have also demonstrated the specificity of one CSF1R kinase activity inhibitor to attain this goal through metabolic reprogramming of tumour associated macrophages.

Material and Methods

Resources

Reagent or Resource	Source	Reference
Antibodies		
B-Actin	Sigma	A2228
ALOX15	Abcam	ab119774
Calnexin	Cell Signaling	2679
CD206	Santa Cruz	Sc-376232
CSF-1R	Cell Signaling	3152
p-CSF-1R Y723	Cell Signaling	3155
DPD	Santa Cruz	Sc-271308
Erk1/2	Cell Signaling	4695
p-ERK1/2, Thr202/Tyr204	Cell Signaling	4370
HIF-2a	Santa Cruz	Sc-46691
STAT6	Santa Cruz	Sc-271213
p-STAT6 Tyr641	Santa Cruz	Sc-136019
TGM2	Life Technologies	MA512739
CD206 – PE	Miltenyi	130-095-220
Isotype IgG1 K - PE	BD Biosciences	559320
RNA Extraction and RT-qPCR Kits		
iScript Ready-to-use cDNA supermix	Biorad	1708841
iTaq universal SYBR green supermix	Biorad	1725124
NucleoSpin RNA (250)	Macherey Nagel	740955.250

Media and reagents		
5-Fluorouracil (5-FU)	Roche	
β-mercaptoethanol	Sigma	M3148-100ML
Bovine Serum Albumin (BSA) solution 30%	Sigma	A9576-50ML
BLZ945	MedChemExpress	HY-12768
CD14 microbeads, human	Miltenyi Biotec	130-050-201
Chloroform	Sigma	34854
DMSO for cell culture	Dutscher	702631
DPBS (1X) , no calcium, no magnesium	Life Technologies	14190169
Edicotinib	MedChemExpress	HY-109086
EDTA (0.5M), pH 8.0, RNase-free	Life Technologies	AM9260G
Fetal Bovine Serum (FBS), qualified, US	Life Technologies	26140079
GW2580	MedChemExpress	HY-10917
HEPES (1M)	Life Technologies	15630056
Histopaque-1077	Sigma	10771-6X100ML
Human serum from male AB plasma (SAB)	Sigma	H4522-100ML
Ki20227	MedChemExpress	HY-10408
Methanol	Sigma	34860
Pexidartinib	MedChemExpress	HY-16749
PLX5622	MedChemExpress	HY-114153
RPMI 1640 medium, glutaMAX supplement	Life Technologies	61870044
Scyllo Inositol	Sigma	I8132
TrypLE Express Enzyme (1X), phenol red	Life Technologies	12605036
Tridecanoic Acid	Sigma	91988
U0126	Sigma	662005
Oligonucleotides		
B2M forward	Eurogentec	5’ – GTGCTCGCGCTACTCTCTC – 3’
B2M reverse	Eurogentec	5’ – CGGATGGATGAAACCCAGACA – 3’
DPYD forward	Eurogentec	5’ - CGCAGGACCAGGGGTTTTAT - 3’
DPYD reverse	Eurogentec	5’ - TGGCAATGGAGAGTGACAGG - 3’
RPL6 forward	Eurogentec	5’ – GTTGGTGGTGACAAGAACGG – 3’
RPL6 reverse	Eurogentec	5’ – TTTTTGCCGTGGCTCAACAG – 3’
Others		
7-AAD staining solution	BD Biosciences	559925
Annexin V-FITC	Miltenyi	130-093-060
Software		
Prism v7	GraphPad	
JMP v14	SAS	
Galileo	Integragen	

Human samples

Human blood samples from healthy de-identified donors were obtained from EFS (French national blood service) as part of an authorized protocol (CODECOH DC-2018–3114). Donors gave signed consent for use of their blood in this study.

Cell culture

THP1, RKO and HT-29, were purchased from ATCC. THP1, TH-29 and RKO were maintained in RPMI (Gibco) supplemented with 10% FBS (Gibco) at 37°C. All cells were routinely tested for mycoplasma contamination using MycoAlert detection kit (Lonza). All cells have been used in the following year of their reception.

Human macrophage differentiation from monocytes

Monocytes were isolated from leukoreduction system chambers of healthy EFS donors using differential centrifugation (Histopaque 1077, Sigma) to obtain PBMCs. $CD14^+$ microbeads (Miltenyi Biotec) were used to select monocytes according to the manufacturer's instructions. Monocytes were plated in RPMI (Life Technologies) supplemented with 10% SAB (Sigma), 10 mM HEPES (Life Technologies), MEM Non-essential amino acids (Life Technologies) and 25 ng/mL M-CSF (Miltenyi Biotec). Differentiation was obtained after 6 days of culture. Hypoxic cultures were performed in a hypoxic chamber authorizing an oxygen partial pressure control (HypoxyLab, Oxford Optronix, UK).

Macrophage Conditioned Medium (MCM)

THP1 macrophages were plated and differentiated at 500,000 cells with 50nM of PMA for 24 hours. THP1 macrophages were cultured at 3% oxygen and treated with Edicotinib or BLZ945 at 3µM or DMSO acting as a vehicle for 48 hours. Then, RPMI with 10% SVF with 3µM of Edicotinib, 3µM BLZ945 or DMSO with 1µg/mL of 5-FU was used to generate the 5FU Edicotinib MCM, 5FU BLZ945 MCM or 5FU Vehicle MCM. Additionally, Non-conditioned media (NCM) with Edicotinib 3µM (Edicotinib NCM), BLZ945 3µM (BLZ945 NCM), DMSO (Vehicle NCM), 5-FU 1µg/mL (5FU NCM), Edicotinib 3µM and 5FU 1µg/mL (5FU Edicotinib NCM) or BLZ945 3µM and 5FU 1µg/mL (5FU BLZ945 NCM) were incubated under the same hypoxic conditions for the same time intervals. The produced MCM or NCM were added for 48 hours to two distinct colon cancer cell lines, RKO and HT-29 cells, which were plated previously at 100,000 cells per well for 24 hours. Then cancerous cells were collected and counted and the percentage of growth inhibition was assessed for each condition.

RNAseq

RNA extraction was performed using the NucleoSpin RNA kit components (Macherey Nagel) according to the manufacturer's instructions. RNA sequencing was performed using an Illumina HiSeq 4000 sequencer (Integragen). Gene expression quantification was performed using the STAR software. STAR obtains the number of reads associated to each gene in the Gencode v31 annotation (restricted to protein-coding genes, antisense and lincRNAs). Raw

counts for each sample were imported into R statistical software. Extracted count matrix was normalized for library size and coding length of genes to compute FPKM expression levels. The Bioconductor edgeR package was used to import raw counts into R statistical software. Differential expression analysis was performed using the Bioconductor limma package and the voom transformation. Gene ontology analysis was performed using the GONet software (https://tools.dice-database.org/GOnet/). Gene list from the differential analysis was ordered by decreasing log2 fold change. Gene set enrichment analysis (GSEA) was performed by clusterProfiler::GSEA function using the fgsea algorithm.

Metabolomics

Human macrophages were metabolically quenched in dry ice – ethanol for one minute then washed three times in cold PBS. Total lipids were extracted in chloroform/methanol/water (1/3/1 v/v/V) with standards added Scyllo Inositol (0.5 mM in water) and tridecanoic acid (1 mM in methanol). Butylated hydroxytoluene (BHT) is added as an antioxidant. Tubes are agitated and sonicated. After 2 hours on ice, chloroform is added and tubes are centrifugated (2400 g, 4°C). Aqueous phase is removed and the organic phase was dried for further analysis. All FAs (Fatty acids) were identified by comparison of retention time and mass spectra from GC-MS with authentic chemical standards. The concentration of FAs was quantified after initial normalization to different internal standards and finally to macrophage number.

AFM measurments

AFM measurements were done using the JPK Nanowizard (Bruker) with MLCT-BIO-D cantilever (Bruker) which is a triangular pyramidal tip of 0.03 N/m spring constant. Force spectroscopy measurements were done on 15 to 20 macrophages for each sample where 1 nN force was applied with a piezo amplitude of 5 µm and cantilever speed of 5 µm/s. Force curves were analyzed using JPKSPM Data Processing. Curves were fitted based on Hertz-fit model. Data were collected and then Young's Modulus from the forward curve was obtained, thanks to Jupyter Notebook from Anaconda, which is a Python distribution that is used for data sciences collection and analysis.

Immunoblotting

Cells were lyzed in RIPA buffer supplemented with antiprotease inhibitors (AEBSF 4 mM, Pepstatine A 1 mM and Leupeptine 0.4 mM; Sigma Aldrich) and HIF-hydroxylase inhibitor (DMOG 1 mM, Sigma Aldrich). Proteins were quantified by BCA assay (ThermoFischer) and 15 µg of total protein were run on SDS-PAGE gels. Proteins were transferred from SDS-PAGE gels to PVDF membrane (Biorad), blocked with TBS-Tween supplemented with 5% milk, primary antibodies were incubated at 1 µg/mL overnight 4°C. After washing with TBS, the membrane was incubated with a horseradish peroxidase-conjugated secondary antibody (Jackson Immunoresearch). Signal was detected by chemoluminescence (Chemi-Doc Imaging System, Bio-Rad) after exposition to West Pico ECL (ThermoFischer).

Flow cytometry

Flow cytometry data was acquired on an Accuri C6 (BD) flow cytometer. The reagents used were: AnnexinV-FITC, mouse anti-F4/80-PE clone REA126 and mouse anti-human CD11b-FITC from Miltenyi Biotech and 7-AAD staining solution from BD Pharmingen. Doublet cells were gated out by comparing forward scatter signal height (FSC-H) and area (FSC-A). At least 10,000 events were collected in the analysis gate. Median fluorescence intensity (MFI) was determined using Accuri C6 software (BD).

DPD activity measurements

These analyses were performed in the Pharmacology Laboratory of Institut Claudius-Regaud (France) using an HPLC system composed of Alliance 2695 and diode array detector 2996 (Waters). Uracil (U), Dihydrouracil (UH2), Ammonium sulfate 99%, Acetonitrile (ACN) gradient chromasolv for HPLC and 2-propanol were purchased from Sigma. Ethyl acetate Scharlau was of HPLC grade and purchased from ICS (Lapeyrouse-Fossat, France). Water from Milli-Q Advantage A10 and MultiScreen-HV 96-well Plates were used (Merck Millipore). Calibration ranges were 3.125 – 200 ng/mL for U and 25 - 500 ng/mL for UH2 and 5-FU (5µg/mL) was used as an internal standard.

Statistical analysis

Statistics were performed using Graph Pad Prism 7 (Graph Pad Software Inc). When two groups were compared, we used a two-tailed student's t test for a normal distribution and a Mann-Whitney non parametric test otherwise. When more than two groups were compared, we used a one-way ANOVA analysis with a Tukey post hoc test. All group numbers and values of the likelihood of data according to a null-hypothesis (p-value) are presented within the Figures.

Acknowledgments

KG is supported by the ITN (International Training Network) Phys2Biomed project, which is funded from the European Union's Horizon 2020 research and innovation programme under the Marie Skłodowska-Curie grant agreement No 812772. MM is supported by the APMC Fondation (Agir pour les Maladies Chroniques). This work is supported by the ERiCAN program of Fondation MSD-Avenir (Reference DS-2018-0015). We thank Kajangi Gnanachandran and Malgorzata Lekka for their help in AFM measurements. We thank Dr Lemoigne, Dr Federspiel and Dr Plasse from the University Hospital of Grenoble-Alpes for kindly providing clinical grade 5-Fluorouracil.

References

Bartoszewski, R., Moszyńska, A., Serocki, M., Cabaj, A., Polten, A., Ochocka, R., Dell'Italia, L., Bartoszewska, S., Króliczewski, J., Dąbrowski, M., et al. (2019). Primary endothelial cell–specific regulation of hypoxia-inducible factor (HIF)-1 and HIF-2 and their target gene expression profiles during hypoxia. FASEB J. *33*, 7929–7941. https://doi.org/https://doi.org/10.1096/fj.201802650RR.

Cannarile, M.A., Weisser, M., Jacob, W., Jegg, A.-M., Ries, C.H., and Rüttinger, D. (2017). Colony-stimulating factor 1 receptor (CSF1R) inhibitors in cancer therapy. J. Immunother. Cancer *5*, 53. https://doi.org/10.1186/s40425-017-0257-y.

Chakraborty, S., Doktorova, M., Molugu, T.R., Heberle, F.A., Scott, H.L., Dzikovski, B., Nagao, M., Stingaciu, L.-R., Standaert, R.F., Barrera, F.N., et al. (2020). How cholesterol stiffens unsaturated lipid membranes. Proc. Natl. Acad. Sci. *117*, 21896–21905. https://doi.org/10.1073/pnas.2004807117.

Cortese, N., Carriero, R., Laghi, L., Mantovani, A., and Marchesi, F. (2020). Prognostic significance of tumor-associated macrophages: past, present and future. Semin. Immunol. *48*, 101408. https://doi.org/10.1016/j.smim.2020.101408.

Court, M., Petre, G., Atifi, M.E., and Millet, A. (2017). Proteomic Signature Reveals Modulation of Human Macrophage Polarization and Functions Under Differing Environmental Oxygen Conditions. Mol. Cell. Proteomics MCP *16*, 2153–2168. https://doi.org/10.1074/mcp.RA117.000082.

Court, M., Malier, M., and Millet, A. (2019). 3D type I collagen environment leads up to a reassessment of the classification of human macrophage polarizations. Biomaterials *208*, 98–109. https://doi.org/10.1016/j.biomaterials.2019.04.018.

DeNardo, D.G., and Ruffell, B. (2019). Macrophages as regulators of tumour immunity and immunotherapy. Nat. Rev. Immunol. *19*, 369–382. https://doi.org/10.1038/s41577-019-0127-6.

DeNardo, D.G., Barreto, J.B., Andreu, P., Vasquez, L., Tawfik, D., Kolhatkar, N., and Coussens, L.M. (2009). CD4+ T Cells Regulate Pulmonary Metastasis of Mammary Carcinomas by Enhancing Protumor Properties of Macrophages. Cancer Cell *16*, 91–102. https://doi.org/10.1016/j.ccr.2009.06.018.

El-Gamal, M.I., Al-Ameen, S.K., Al-Koumi, D.M., Hamad, M.G., Jalal, N.A., and Oh, C.-H. (2018). Recent Advances of Colony-Stimulating Factor-1 Receptor (CSF-1R) Kinase and Its Inhibitors. J. Med. Chem. *61*, 5450–5466. https://doi.org/10.1021/acs.jmedchem.7b00873.

Engblom, C., Pfirschke, C., and Pittet, M.J. (2016). The role of myeloid cells in cancer therapies. Nat. Rev. Cancer *16*, 447–462. https://doi.org/10.1038/nrc.2016.54.

Goossens, P., Rodriguez-Vita, J., Etzerodt, A., Masse, M., Rastoin, O., Gouirand, V., Ulas, T., Papantonopoulou, O., Van Eck, M., Auphan-Anezin, N., et al. (2019). Membrane Cholesterol Efflux Drives Tumor-Associated Macrophage Reprogramming and Tumor Progression. Cell Metab. *29*, 1376–1389.e4. https://doi.org/10.1016/j.cmet.2019.02.016.

Henze, A.-T., and Mazzone, M. (2016). The impact of hypoxia on tumor-associated macrophages. J. Clin. Invest. *126*, 3672–3679. https://doi.org/10.1172/JCI84427.

Kaelin, W.G., and Ratcliffe, P.J. (2008). Oxygen Sensing by Metazoans: The Central Role of the HIF Hydroxylase Pathway. Mol. Cell *30*, 393–402. https://doi.org/10.1016/j.molcel.2008.04.009.

Lee, P., Chandel, N.S., and Simon, M.C. (2020). Cellular adaptation to hypoxia through hypoxia inducible factors and beyond. Nat. Rev. Mol. Cell Biol. *21*, 268–283. https://doi.org/10.1038/s41580-020-0227-y.

Malier, M., Gharzeddine, K., Laverriere, M.-H., Marsili, S., Thomas, F., Decaens, T., Roth, G., and Millet, A. (2021). Hypoxia Drives Dihydropyrimidine Dehydrogenase Expression in Macrophages and Confers Chemoresistance in Colorectal Cancer. Cancer Res. *81*, 5963–5976. https://doi.org/https://doi.org/10.1158/0008-5472.CAN-21-1572.

Mantovani, A., Allavena, P., Marchesi, F., and Garlanda, C. (2022). Macrophages as tools and targets in cancer therapy. Nat. Rev. Drug Discov. 1–22. https://doi.org/10.1038/s41573-022-00520-5.

Martinez, F.O., Helming, L., Milde, R., Varin, A., Melgert, B.N., Draijer, C., Thomas, B., Fabbri, M., Crawshaw, A., Ho, L.P., et al. (2013). Genetic programs expressed in resting and IL-4 alternatively activated mouse and human macrophages: similarities and differences. Blood *121*, e57-69. https://doi.org/10.1182/blood-2012-06-436212.

O'Brien, S.A., Orf, J., Skrzypczynska, K.M., Tan, H., Kim, J., DeVoss, J., Belmontes, B., and Egen, J.G. (2021). Activity of tumor-associated macrophage depletion by CSF1R blockade is highly dependent on the tumor model and timing of treatment. Cancer Immunol. Immunother. *70*, 2401–2410. https://doi.org/10.1007/s00262-021-02861-3.

Pradel, L.P., Ooi, C.-H., Romagnoli, S., Cannarile, M.A., Sade, H., Rüttinger, D., and Ries, C.H. (2016). Macrophage Susceptibility to Emactuzumab (RG7155) Treatment. Mol. Cancer Ther. *15*, 3077–3086. https://doi.org/10.1158/1535-7163.MCT-16-0157.

Pyonteck, S.M., Akkari, L., Schuhmacher, A.J., Bowman, R.L., Sevenich, L., Quail, D.F., Olson, O.C., Quick, M.L., Huse, J.T., Teijeiro, V., et al. (2013). CSF-1R inhibition alters macrophage polarization and blocks glioma progression. Nat. Med. *19*, 1264–1272. https://doi.org/10.1038/nm.3337.

Ruffell, B., and Coussens, L.M. (2015). Macrophages and therapeutic resistance in cancer. Cancer Cell *27*, 462–472. https://doi.org/10.1016/j.ccell.2015.02.015.

Salerno, D.M., Tront, J.S., Hoffman, B., and Liebermann, D.A. (2012). Gadd45a and Gadd45b modulate innate immune functions of granulocytes and macrophages by differential

regulation of p38 and JNK signaling. J. Cell. Physiol. *227*, 3613–3620. https://doi.org/https://doi.org/10.1002/jcp.24067.

Sica, A., and Mantovani, A. (2012). Macrophage plasticity and polarization: in vivo veritas. J. Clin. Invest. *122*, 787–795. https://doi.org/10.1172/JCI59643.

Stanley, E.R., and Chitu, V. (2014). CSF-1 Receptor Signaling in Myeloid Cells. Cold Spring Harb. Perspect. Biol. *6*, a021857. https://doi.org/10.1101/cshperspect.a021857.

Wang, Y., Branicky, R., Noë, A., and Hekimi, S. (2018). Superoxide dismutases: Dual roles in controlling ROS damage and regulating ROS signaling. J. Cell Biol. *217*, 1915–1928. https://doi.org/10.1083/jcb.201708007.

Yang, W., Zheng, Y., Xia, Y., Ji, H., Chen, X., Guo, F., Lyssiotis, C.A., Aldape, K., Cantley, L.C., and Lu, Z. (2012). ERK1/2-dependent phosphorylation and nuclear translocation of PKM2 promotes the Warburg effect. Nat. Cell Biol. *14*, 1295–1304. https://doi.org/10.1038/ncb2629.

Figure Legend

Figure 1 Differential effect of Edicotinib and Sotuletinib on human macrophages

(A) Schematic representation of the experimental procedure used in this study

(B) Chemical structures of Sotuletinib and Edicotinib

(C) Immunoblot analysis of the phosphorylation state at Tyr699 and Tyr723 sites of the CSF1R the activation of MCSF and the combined exposition to vehicle, Sotuletinib and Edicotinib. Representative result of three independent experiments.

(D) Volcano-plot representation of the differential expression of genes of macrophages exposed to Sotuletinib (n=4 human donors).

(E) Volcano-plot representation of the differential expression of genes of macrophages exposed to Edicotinib (n=4 human donors).

(F) Heat map of the 15 differentially under-regulated genes from the Sotuletenib volcano-plot. (n=4 human donors).

Figure 2 Edicotinib reprograms human macrophages by inhibiting phosphorylation of MAPK1/2 and the cholesterol metabolism

(A) GO-term of biological processes analysis of down-regulated genes under Edicotinib. Number of genes in Go terms for biological processes are indicated in circles. The FDR < 0.05 is represented by a vertical line.

(B) Immunoblot analysis of phosphorylation of ERK1/2 at site Thr202/Tyr204 for ERK1 and Thr184/Tyr187 for ERK2. Representative result of three independent experiments.

(C) Cholesterol synthesis pathway. Genes down-regulated by edicotinib are highlighted in red.

(D) SREBP2 transcription factor control of a large number of genes involved in the cholesterol synthesis pathway.

(E) mRNA level expression of *SREBF2* in macrophages exposed to vehicle, Edicotinib and Sotulitinib (n=4 human donors).

(F) mRNA level expression of *LDLR* in macrophages exposed to vehicle, Edicotinib and Sotulitinib (n=4 human donors).

(G) Cell mechanics measured by atomic force microscopy.

Figure 3 Edicotinib interferes with the metabolic response of macrophages in hypoxia

(A) mRNA level expression of *EPAS1* in macrophages exposed to vehicle, Edicotinib and Sotulitinib (n=4 human donors).

(B) Immunoblot analysis (upper panel) of HIF-2α expression in human macrophages in normoxia nad hypoxia (representative results from 5 independent experiments). mRNA level

expression (lower panel) of *EPAS1* in macrophages in normoxia and hypoxia (n=4 human donors).

(C) Heat-map of the hierarchical clustering of differentially expressed genes between normoxia and hypoxia.

(D) GO-term analysis for biological processes associated with genes of cluster 4

(E) Quantification of fatty acid content of macrophages determined by GC-MS analysis in normoxia, hypoxia and hypoxia with edicotinib (n=4 human donors).

(F) mRNA level expression of *SREBF1 and FASN* in macrophages exposed to vehicle, Edicotinib and Sotulitinib in hypoxia (n=4 human donors).

Figure 4 The hypoxic environment modulates the response of human macrophages to the CSF1R antagonist edicotinib

(A) Heat-map of the hierarchical clustering of differentially expressed genes under edicotinib exposure in normoxia and hypoxia with the exclusion of oxygen sensitive genes.

(B) Go-term analysis of biological processes of genes in cluster 1

(C) mRNA level expression of *SOD2* in macrophages exposed to vehicle and Edicotinib in normoxia and hypoxia (n=4 human donors).

(D) mRNA level expression of *GADD45A* in macrophages exposed to vehicle and Edicotinib in normoxia and hypoxia (n=4 human donors).

(E) GSEA analysis of genes down regulated by edicotinib irrespective of the oxygen levels

(F) Immunblot analysis of the phosphorylation state of ERK1/2 in normoxia and hypoxia when exposed to vehicle, edicotinib and sotulitinib. Representative result of three independent experiments.

(G) GO-term of biological processes analysis of down-regulated genes under Edicotinib in hypoxia. Number of genes in Go terms for biological processes are indicated in circles. The FDR < 0.05 is represented by a vertical line.

Figure 5 Edicotinib interferes with tumour educated macrophage reprogramming

(A) mRNA level expression of *CD206 (MRC1), CD276* and *CD163* in macrophages exposed to vehicle, edicotinib and BLZ945 in normoxia and hypoxia (n=4 human donors).

(B) Immunoblot analysis of TGM2 and ALOX15 expression under IL-4 stimulation in hypoxic macrophages exposed to vehicle, edicotinib and BLZ945. Representative result of three indepdendent experiments.

(C) Immunoblot analysis of the phosphorylation state of STAT6 at Tyr641 expression under IL-4 stimulation in hypoxic macrophages exposed to vehicle, edicotinib and BLZ945. Representative result of three independent experiments.

(D) Immunoblot analysis of the phosphorylation state of STAT6 at Tyr641 expression under IL-4 stimulation in hypoxic macrophages exposed to vehicle, U0126. Representative result of three independent experiments.

(E) Flow cytometry analysis of CD206 expression at the surface of TEM (macrophages educated by the conditioned medium of RKO cancer cells + IL-4) exposed to vehicle and edicotinib.

Figure 6 Edicotinib inhibits DPD expression in hypoxia

(A) Immunoblot analysis of DPD expression in normoxic and hypoxic macrophages exposed to vehicle, edicotinib and BLZ945. Representative result of seven independent experiments.

(B) Quantification of the ratio between dihydrouracil (UH_2) and uracil (U) secreted by normoxic and hypoxic macrophages exposed to vehicle, edicotinib and BLZ945 (n=4 human donors).

(C) Immunoblot analysis of DPD expression after 6, 24 and 48h of hypoxia in macrophages exposed to vehicle, edicotinib and BLZ945. Representative result of three independent experiments.

(D) Quantification of the relative expression level of DPYD mRNA obtained by qPCR after 6, 24 and 48h of hypoxia in macrophages exposed to vehicle and edicotinib (n=3 human donors).

(E) Immunoblot analysis of HIF-2α expression after 6h of hypoxia in macrophages exposed to vehicle, edicotinib and BLZ945. Representative result of three independent experiments.

(F) Quantification of the growth inhibition induced by THP1 macrophage condition medium (MCM) exposed to vehicle, edicotinib and BLZ945 on colon cancer cells (RKO in the left panel and HT-29 in the right panel). 5-FU (1 µg/mL) was added secondarily to MCM (MCM +5FU) prior to cancer cell exposition or directly conditioned by macrophages MCM (5-FU) and then added to cancer cells. N=3 independent experiments.

Supplemental Figure Legend

Supplemental Figure 1

(A) Table representing the inhibitors used in this study and their respective IC50 for the CSF1R

(B) Immunoblot analysis of the phosphorylation state at at Tyr699 and Tyr723 sites of the CSF1R under the activation of MCSF and the combined exposition to vehicle and CSF1R inhibitors. Representative result of three independent experiments.

Supplemental Figure 2

(A) GO-term of biological processes analysis of down-regulated genes under Sotuletinib. Number of genes in Go terms for biological processes are indicated in circles. The FDR < 0.05 is represented by a vertical line.

(B) Glycolytic pathway and its connection with phosphorylated ERK ½

(C) mRNA level expression of *HK3* and *PKM1/2* in macrophages exposed to vehicle, Edicotinib and Sotulitinib (n=4 human donors).

Supplemental Figure 3

Quantification of fatty acid content of macrophages determined by GC-MS analysis in normoxia for macrophages exposed to vehicle, edicotinib and sotuletinib (n=4 human donors).

Supplemental Figure 4

(A) mRNA level expression of *MT1E*, *MT1F*, *MT1G*, *MT1H*, *MT1M*, *MT1X*, *MT2A* in macrophages exposed to vehicle and Edicotinib in normoxia and hypoxia (n=4 human donors).

(B) mRNA level expression of SREBF2 in hypoxic macrophages exposed to vehicle, edicotinib and BLZ945 (n=4 human donors).

Supplemental Figure 5

Heat-map of the hierarchical clustering of M2 specific genes under edicotinib exposure in normoxia and hypoxia.

Supplemental Figure 6

(A) Immunoblot analysis of DPD expression in macrophages exposed to vehicle, Pexidartinib, PLX5622, Ki 20227 and GW2550 in normoxia and hypoxia. Representative result of three independent experiments.

(B) Immunoblot analysis of DPD expression in macrophages exposed to vehicle, edicotinib and BLZ945 in hypoxia stimulated by IL-4 and GM-CSF. Representative result of three independent experiments.

(C) Immunoblot analysis of DPD expression in THP1 macrophages exposed to vehicle, edicotinib and BLZ945 in normoxia and hypoxia. Representative of five independent experiments.

Figure 1

A

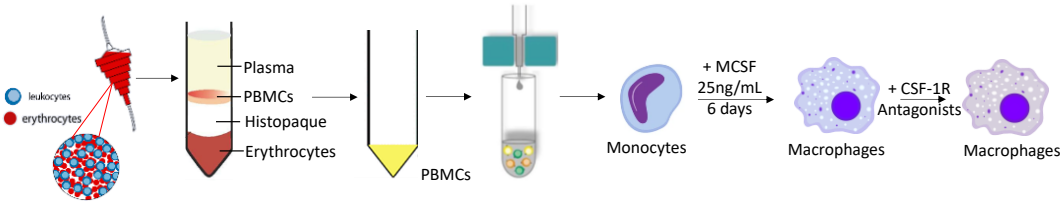

B

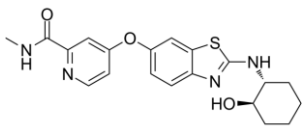

Sotuletinib (BLZ945)

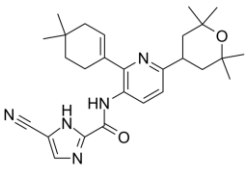

Edicotinib

C

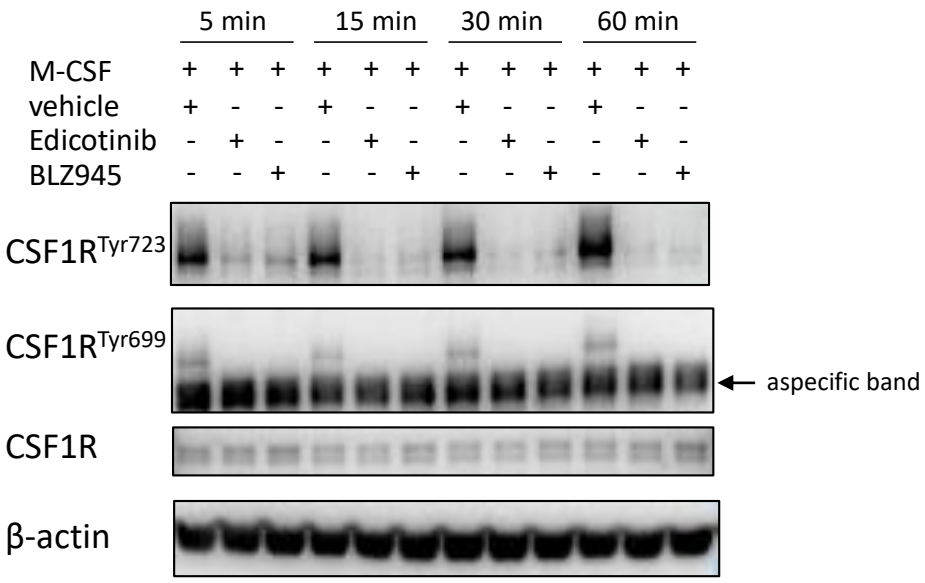

D

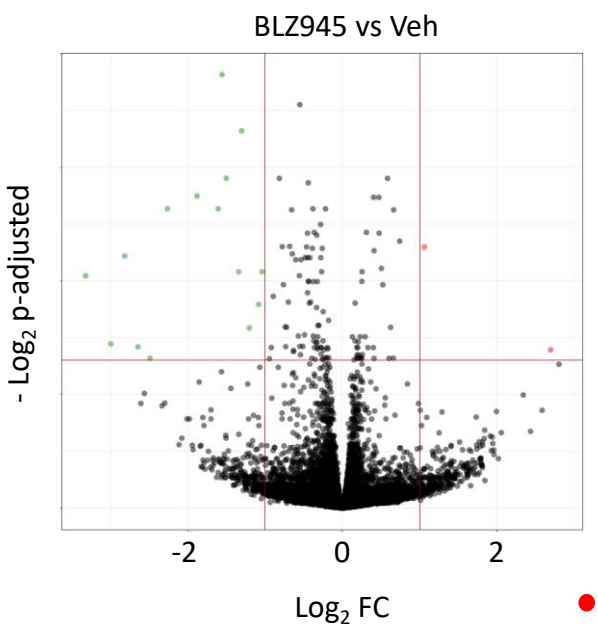

E

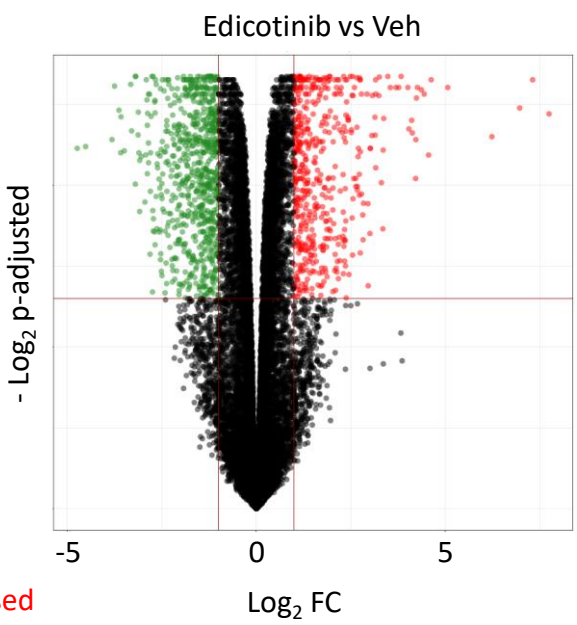

overexpressed
underexpressed

F

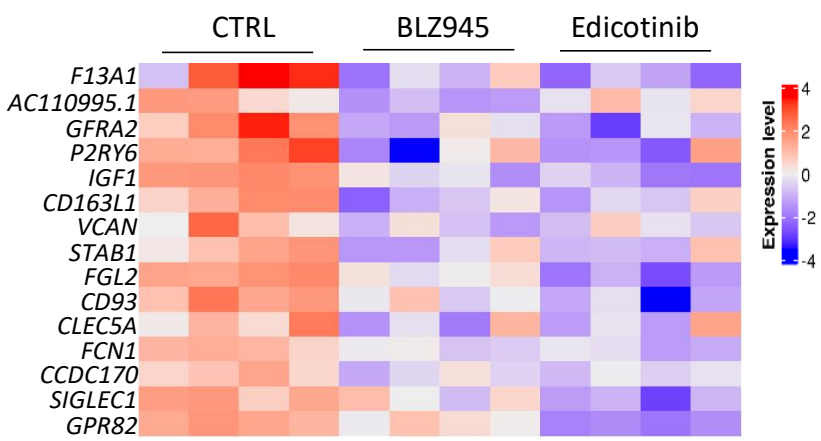

Figure 2

A

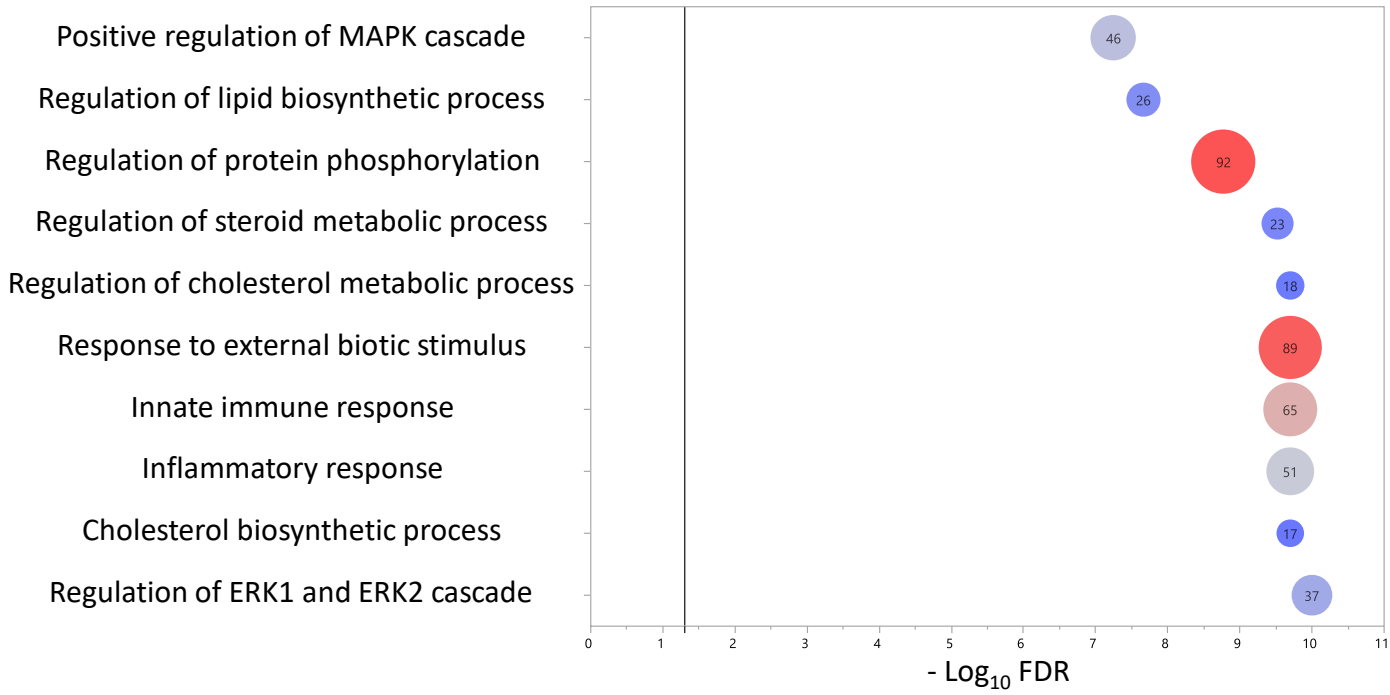

B

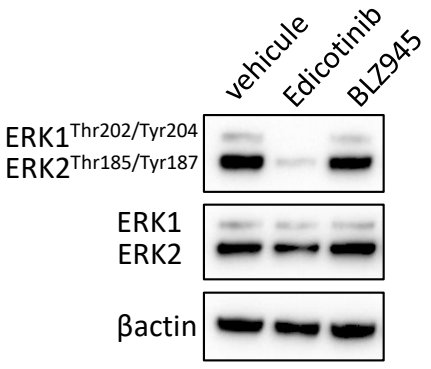

C

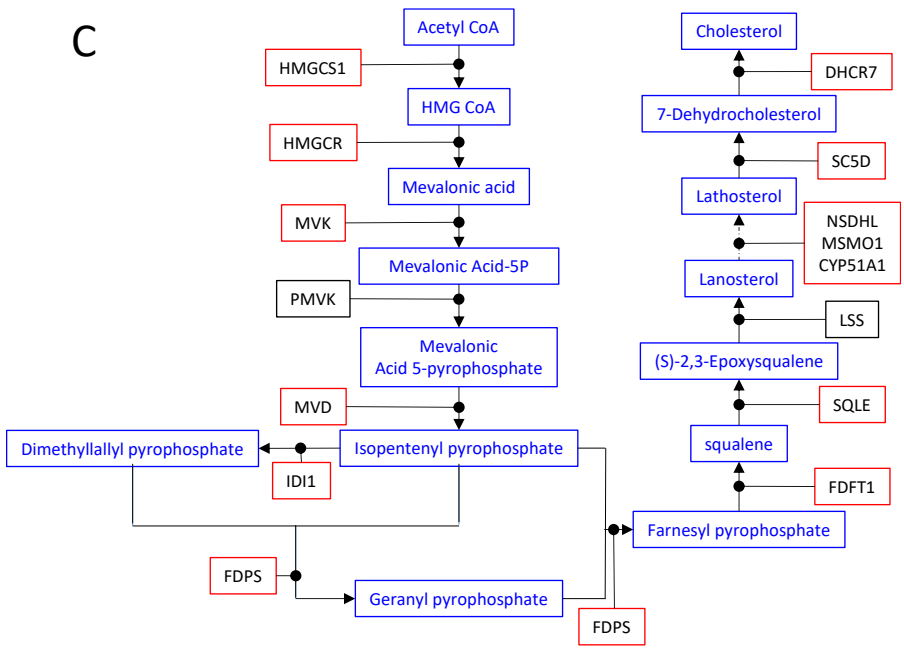

D

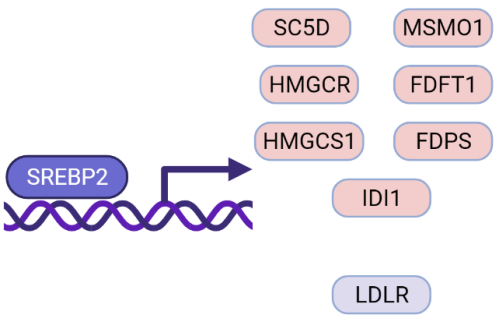

E

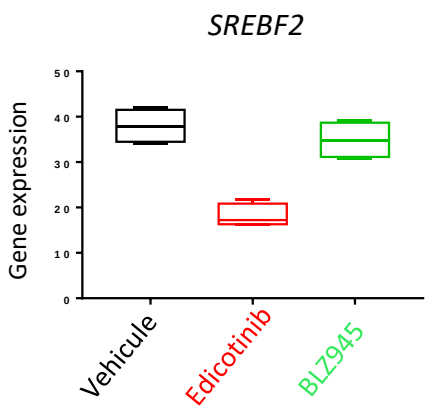

F

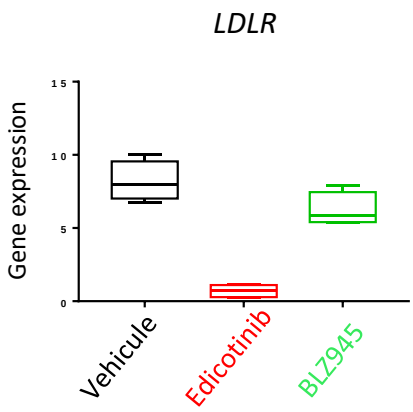

G

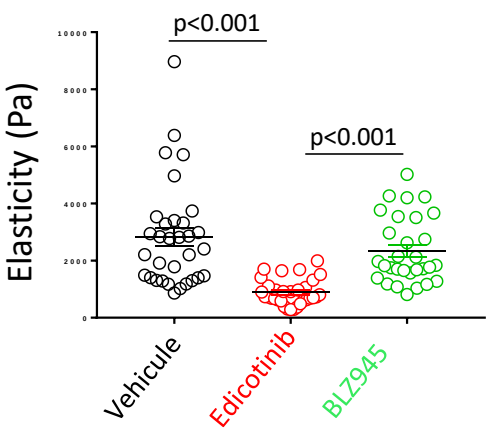

Figure 3

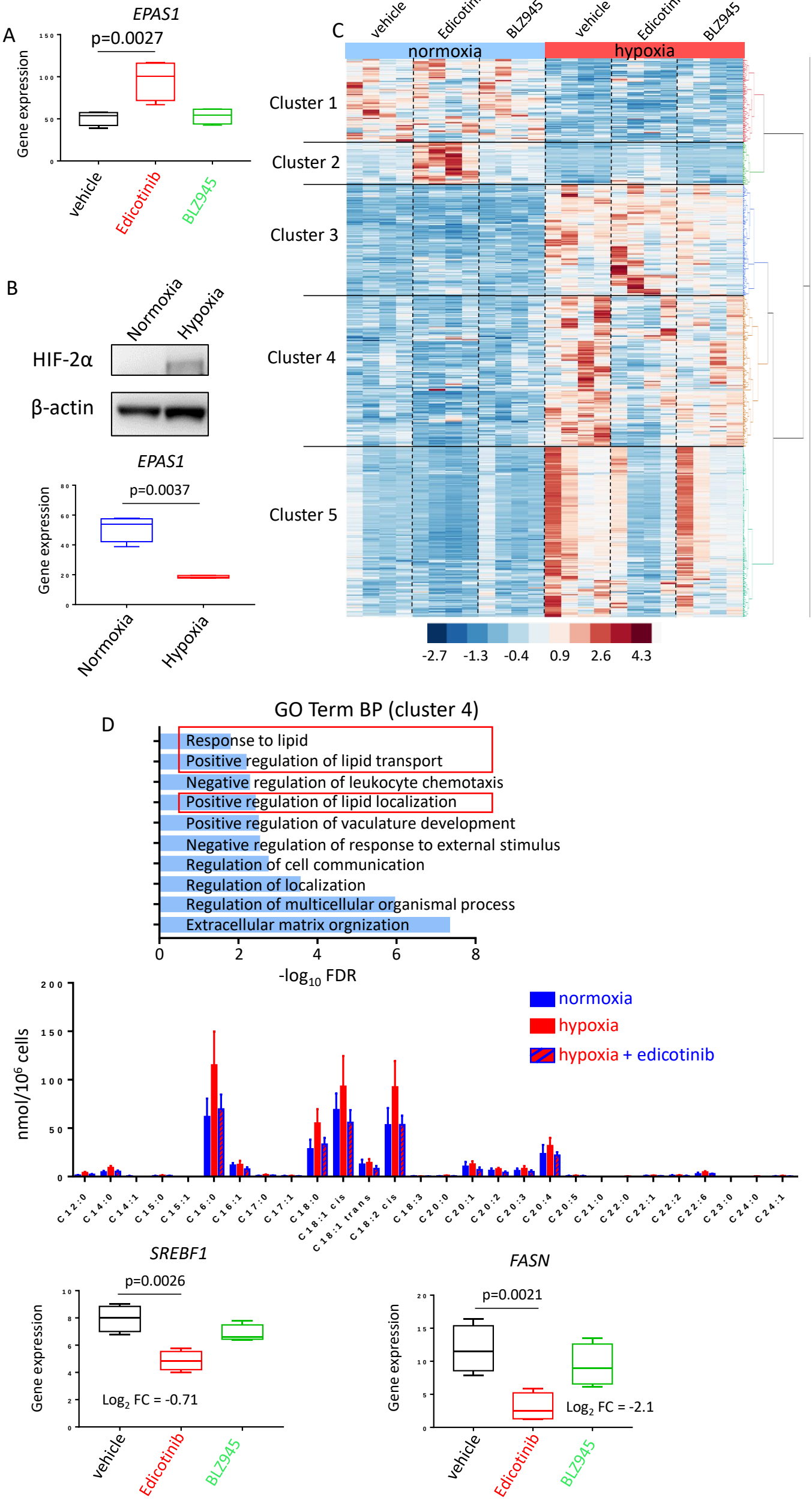
A
EPAS1
p=0.0027
Gene expression
vehicle
Edicotinib
BLZ945
B
Normoxia
Hypoxia
HIF-2α
β-actin
EPAS1
p=0.0037
Gene expression
Normoxia
Hypoxia
C
vehicle
Edicotinib
BLZ945
vehicle
Edicotinib
BLZ945
normoxia
hypoxia
Cluster 1
Cluster 2
Cluster 3
Cluster 4
Cluster 5
-2.7
-1.3
-0.4
0.9
2.6
4.3
D
GO Term BP (cluster 4)
Response to lipid
Positive regulation of lipid transport
Negative regulation of leukocyte chemotaxis
Positive regulation of lipid localization
Positive regulation of vaculature development
Negative regulation of response to external stimulus
Regulation of cell communication
Regulation of localization
Regulation of multicellular organismal process
Extracellular matrix orgnization
-log10 FDR
E
nmol/10^6 cells
normoxia
hypoxia
hypoxia + edicotinib
F
SREBF1
p=0.0026
Gene expression
Log2 FC = -0.71
vehicle
Edicotinib
BLZ945
FASN
p=0.0021
Gene expression
Log2 FC = -2.1
vehicle
Edicotinib
BLZ945

Figure 4

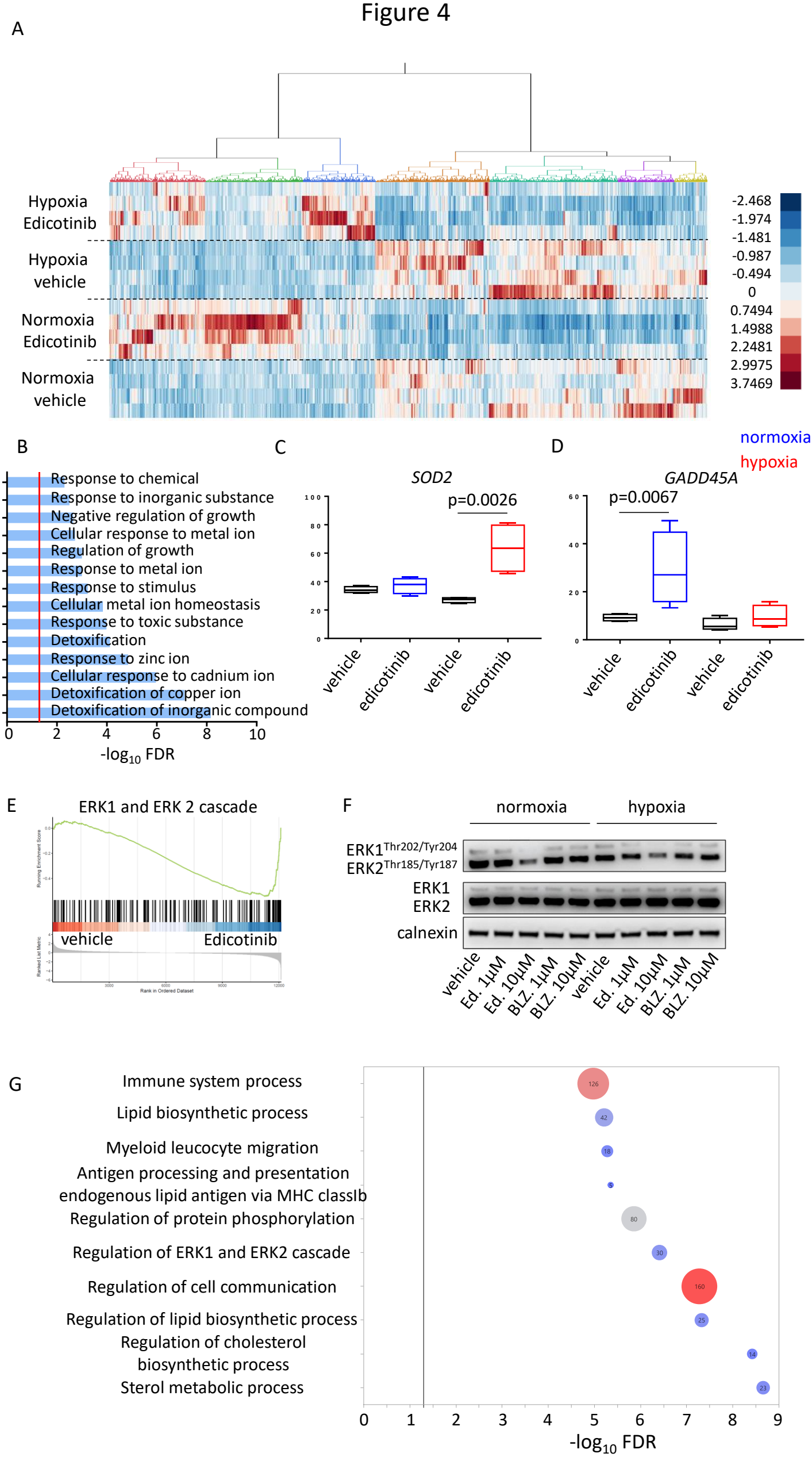
A
Hypoxia Edicotinib
Hypoxia vehicle
Normoxia Edicotinib
Normoxia vehicle
-2.468
-1.974
-1.481
-0.987
-0.494
0
0.7494
1.4988
2.2481
2.9975
3.7469
B
Response to chemical
Response to inorganic substance
Negative regulation of growth
Cellular response to metal ion
Regulation of growth
Response to metal ion
Response to stimulus
Cellular metal ion homeostasis
Response to toxic substance
Detoxification
Response to zinc ion
Cellular response to cadnium ion
Detoxification of copper ion
Detoxification of inorganic compound
0 2 4 6 8 10
-log10 FDR
C
SOD2
p=0.0026
vehicle
edicotinib
vehicle
edicotinib
D
normoxia
hypoxia
GADD45A
p=0.0067
vehicle
edicotinib
vehicle
edicotinib
E
ERK1 and ERK 2 cascade
vehicle
Edicotinib
Rank in Ordered Dataset
F
normoxia
hypoxia
ERK1Thr202/Tyr204
ERK2Thr185/Tyr187
ERK1
ERK2
calnexin
vehicle
Ed. 1μM
Ed. 10μM
BLZ. 1μM
BLZ. 10μM
vehicle
Ed. 1μM
Ed. 10μM
BLZ. 1μM
BLZ. 10μM
G
Immune system process
Lipid biosynthetic process
Myeloid leucocyte migration
Antigen processing and presentation
endogenous lipid antigen via MHC classIb
Regulation of protein phosphorylation
Regulation of ERK1 and ERK2 cascade
Regulation of cell communication
Regulation of lipid biosynthetic process
Regulation of cholesterol
biosynthetic process
Sterol metabolic process
126
42
18
5
80
30
160
25
14
23
0 1 2 3 4 5 6 7 8 9
-log10 FDR

Figure 5

A

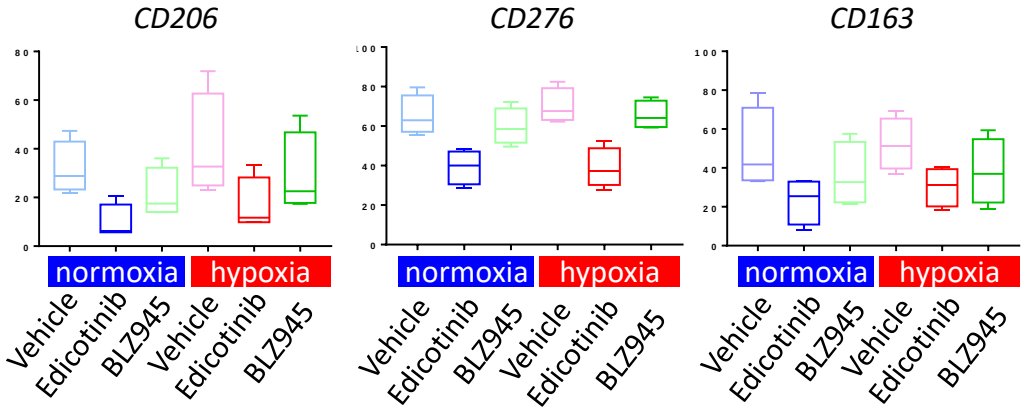

B

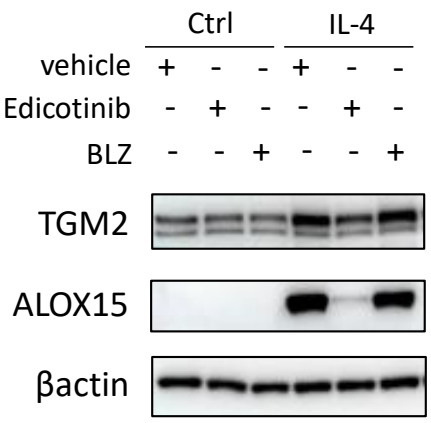

C

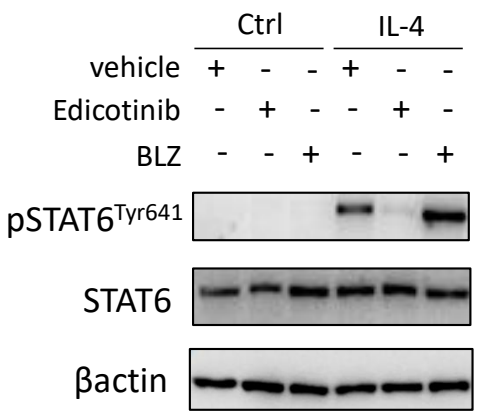

D

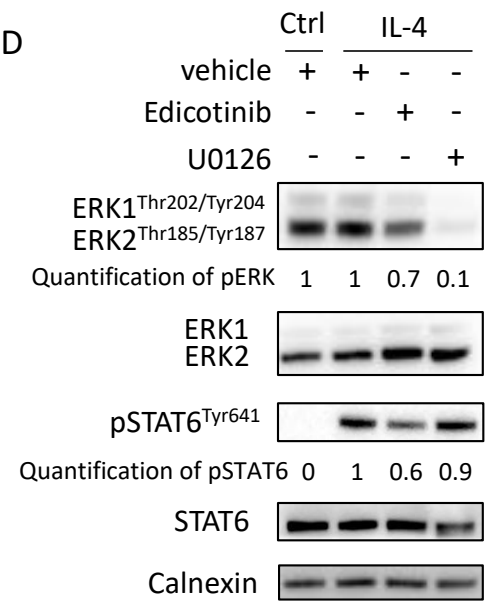

E

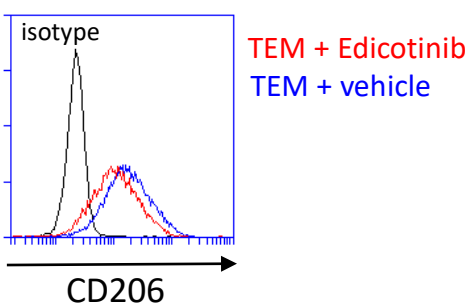

Figure 6

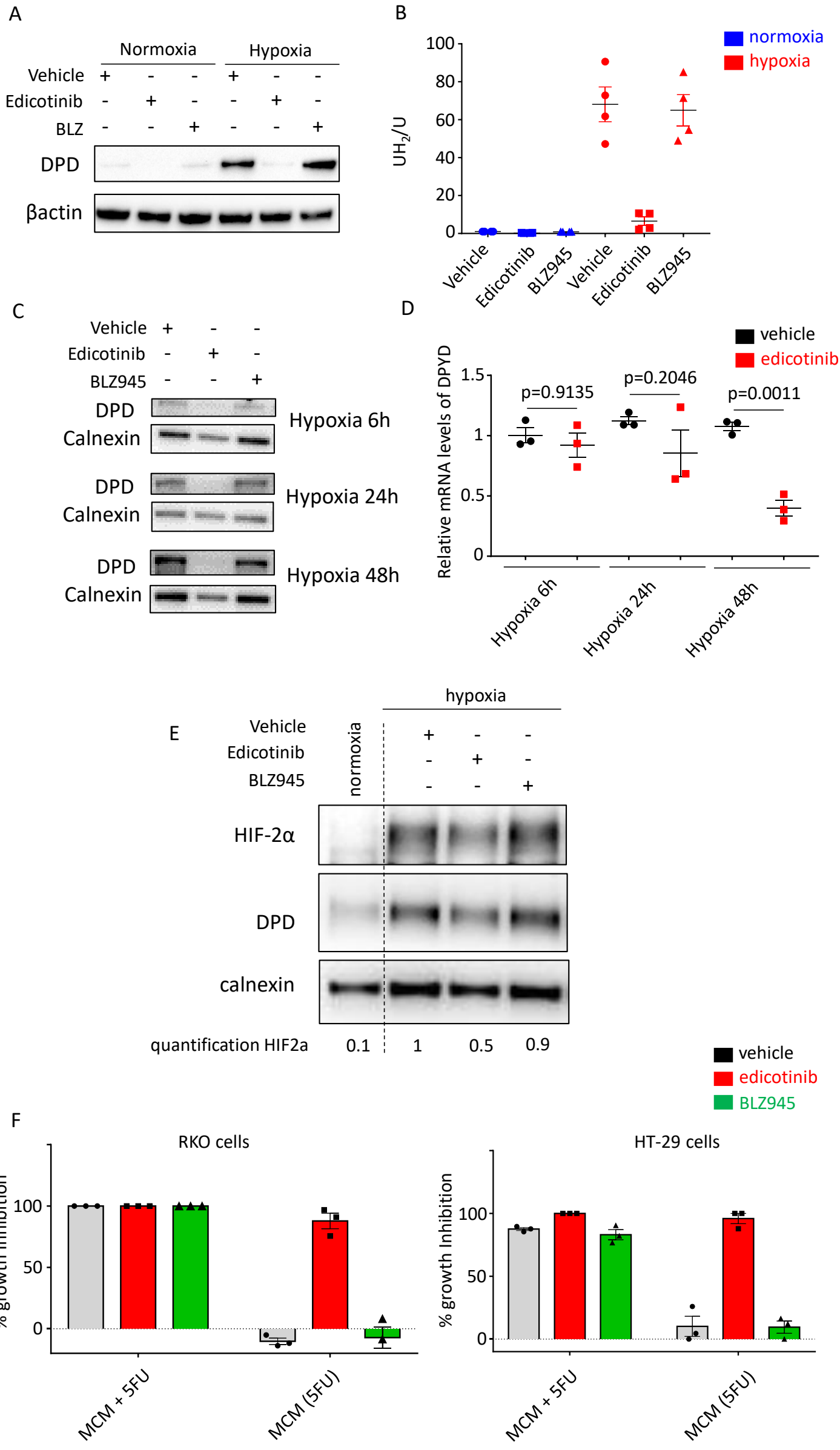
A
Normoxia
Hypoxia
Vehicle
Edicotinib
BLZ
DPD
βactin
B
normoxia
hypoxia
UH2/U
Vehicle
Edicotinib
BLZ945
C
DPD
Calnexin
Hypoxia 6h
Hypoxia 24h
Hypoxia 48h
D
vehicle
edicotinib
Relative mRNA levels of DPYD
p=0.9135
p=0.2046
p=0.0011
E
hypoxia
normoxia
HIF-2α
DPD
calnexin
quantification HIF2a
0.1
1
0.5
0.9
F
RKO cells
HT-29 cells
% growth Inhibition
MCM + 5FU
MCM (5FU)

Supplementary Figure 1

A

Name	IC50 for CSF1R (nM)
Sotuletinib (BLZ945)	1
Edicotinib (JNJ-40346527)	3.2
Pexidartinib	20
PLX5622	5.9
Ki20227	2
GW2580	60

B

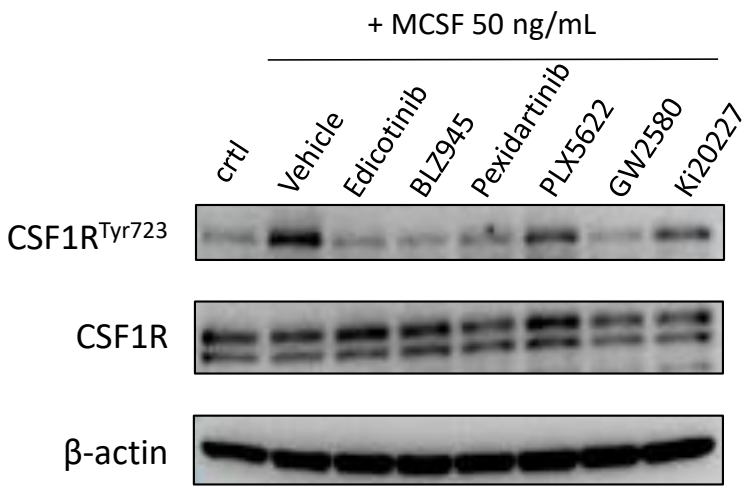

Quantification CSF1R^{Tyr723} Normalized to Ctrl	1	4.2	0.9	0.8	1.7	2.9	0.8	2.4

Supplementary Figure 2

A

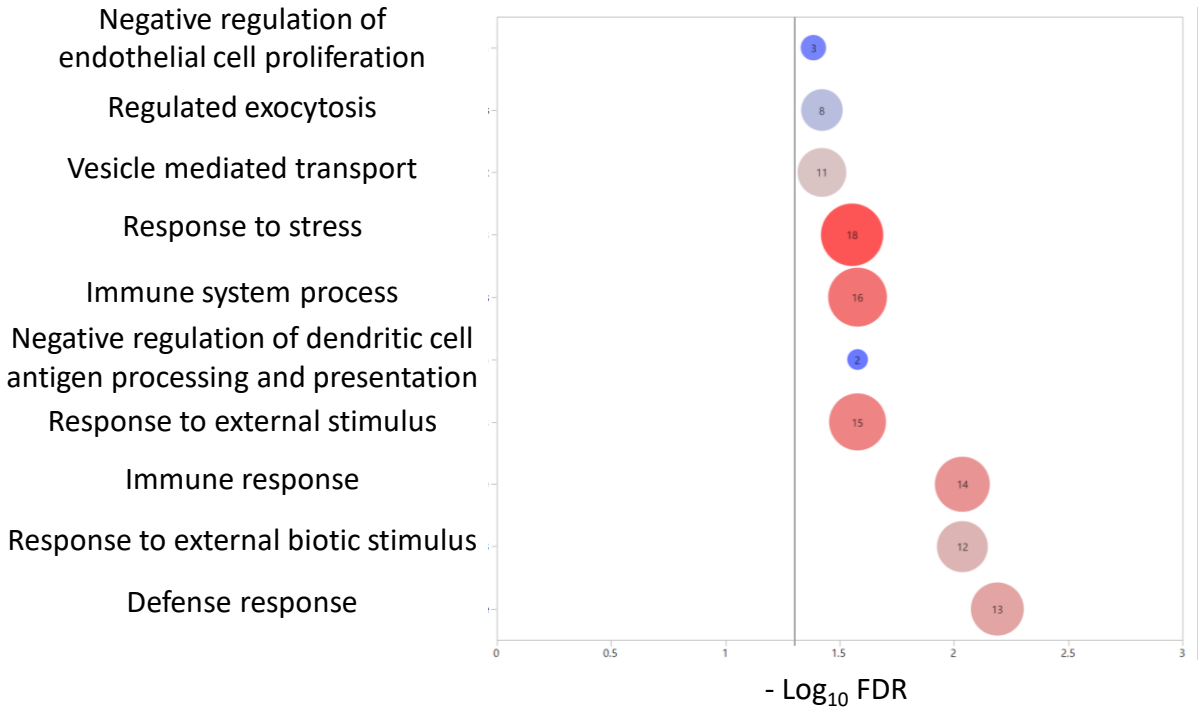

B

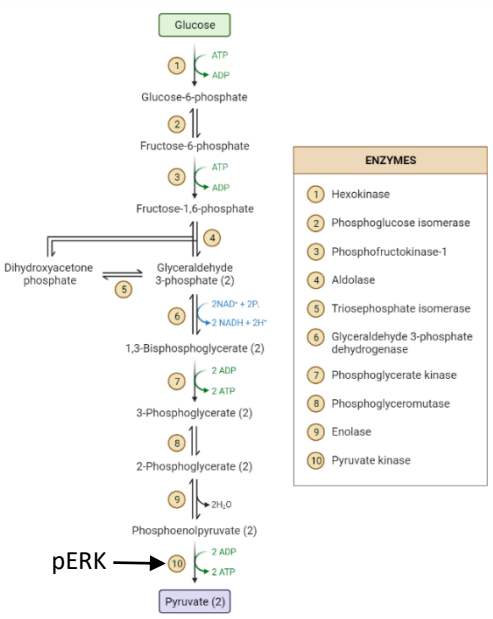

c

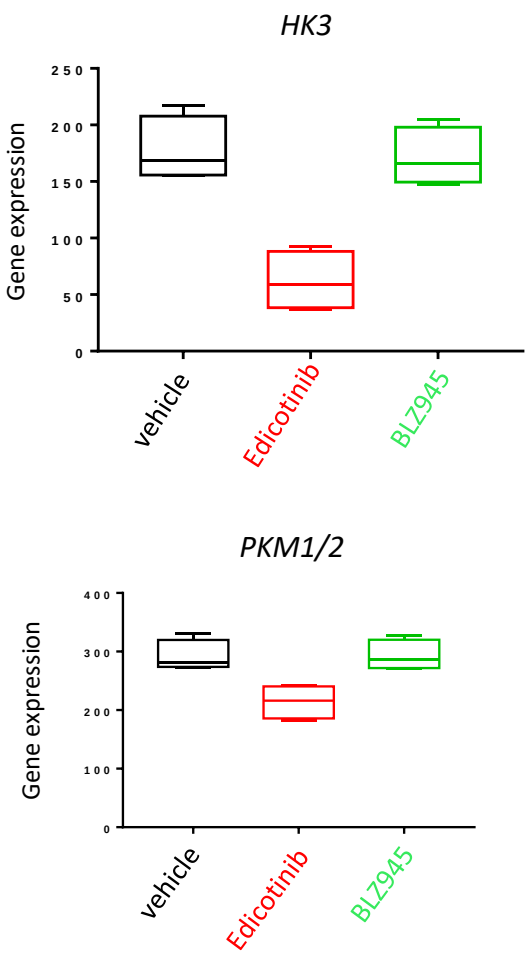

Supplementary Figure 3

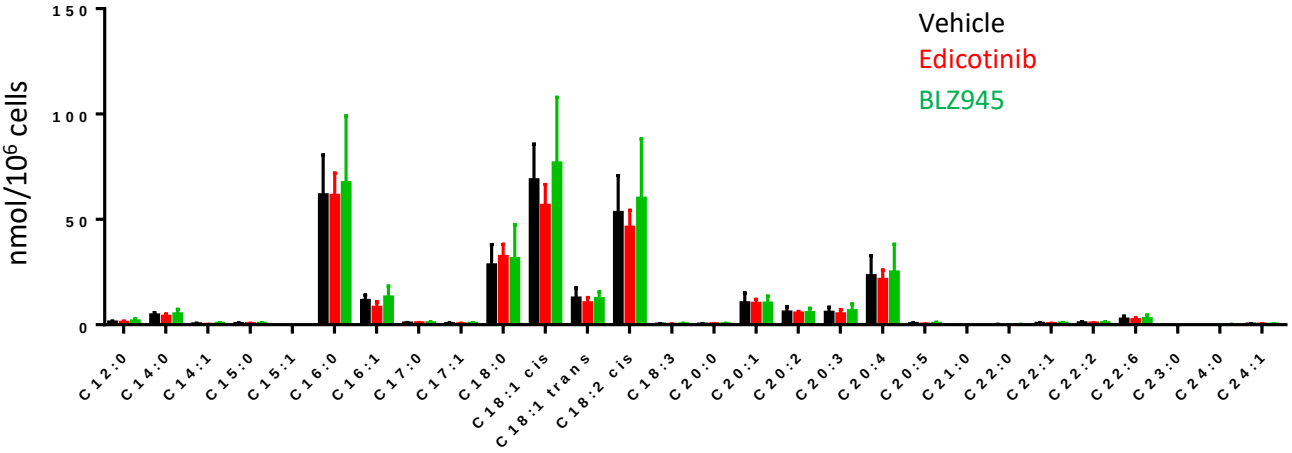

Supplementary Figure 4

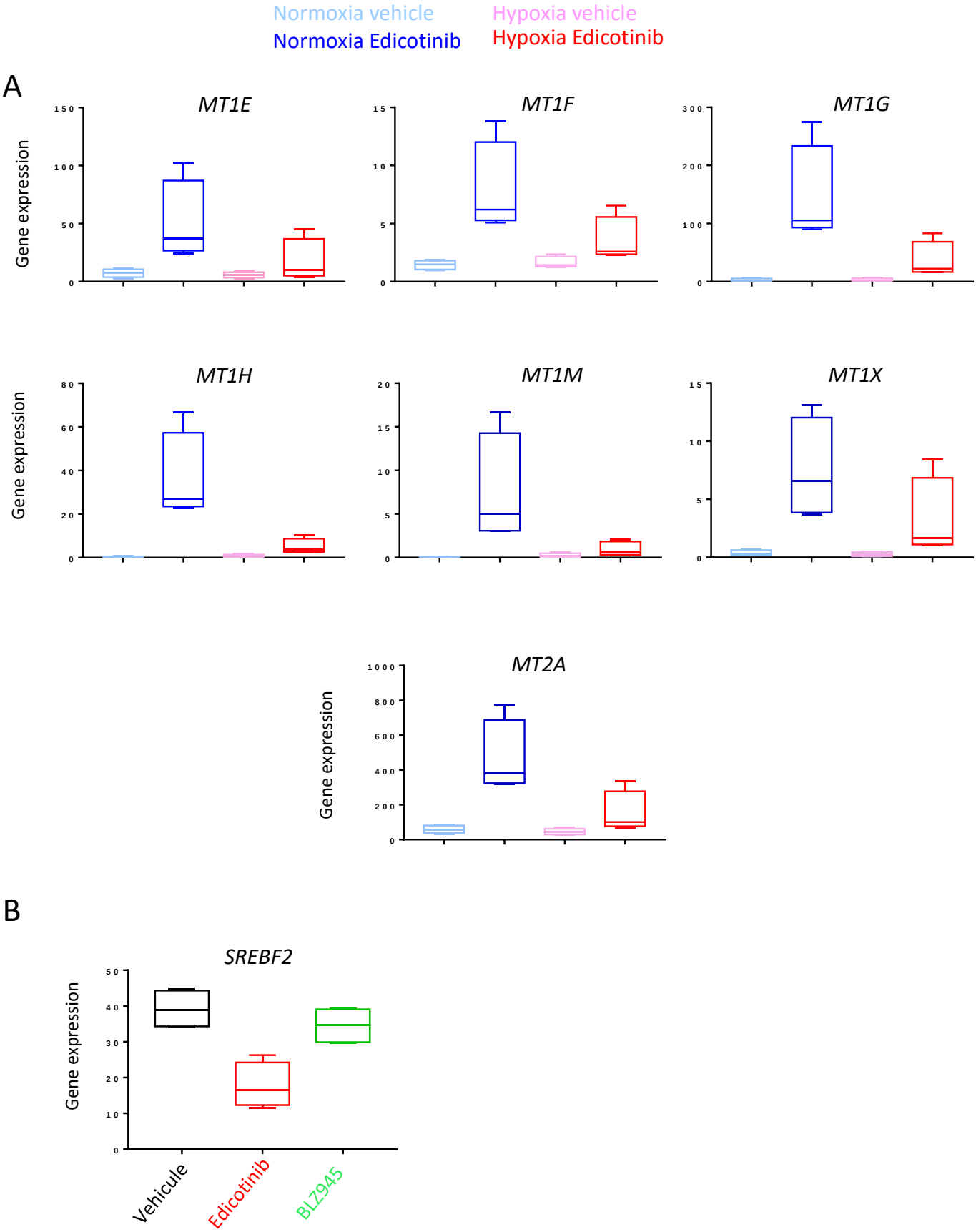

Supplementary Figure 5

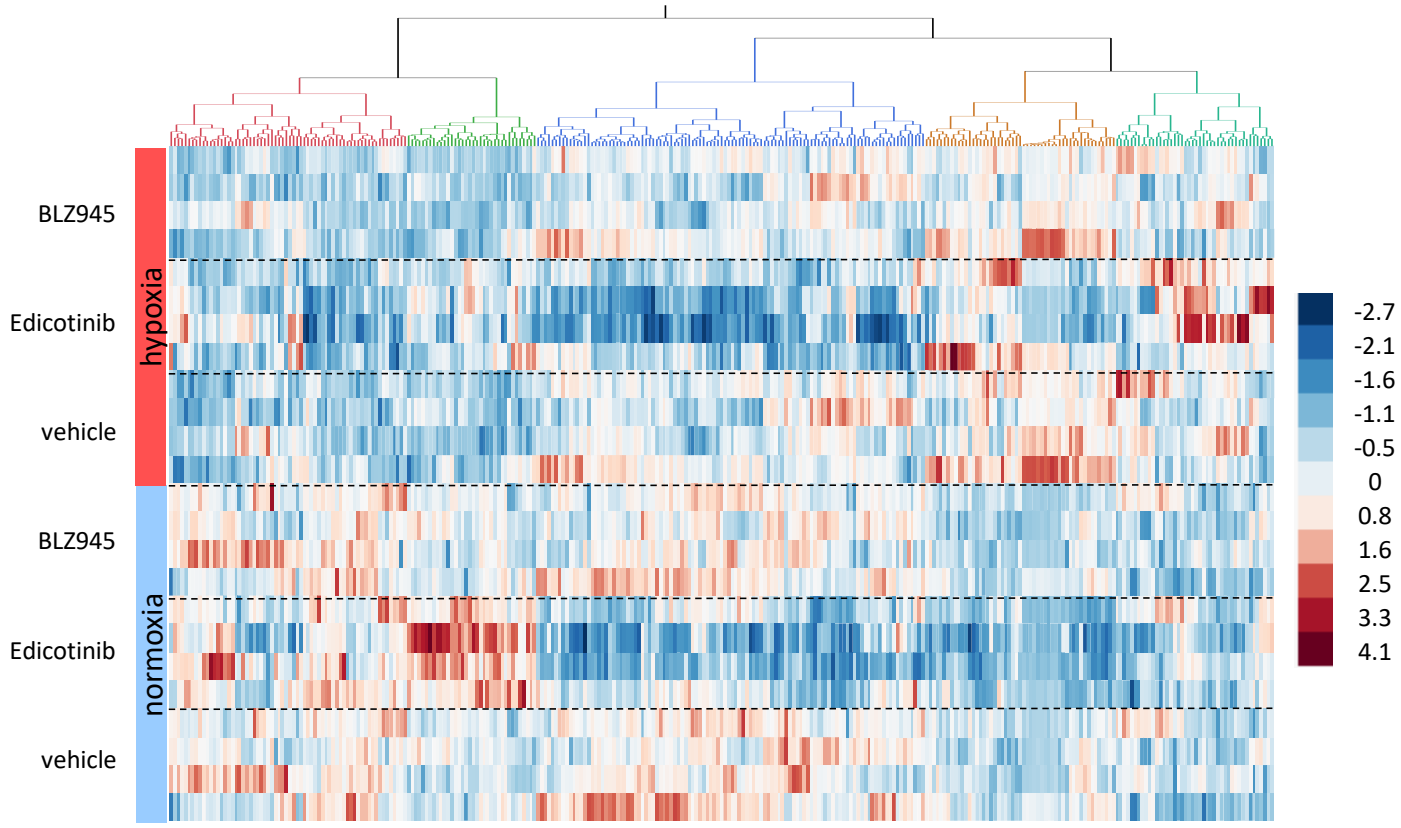

Supplementary Figure 6

A

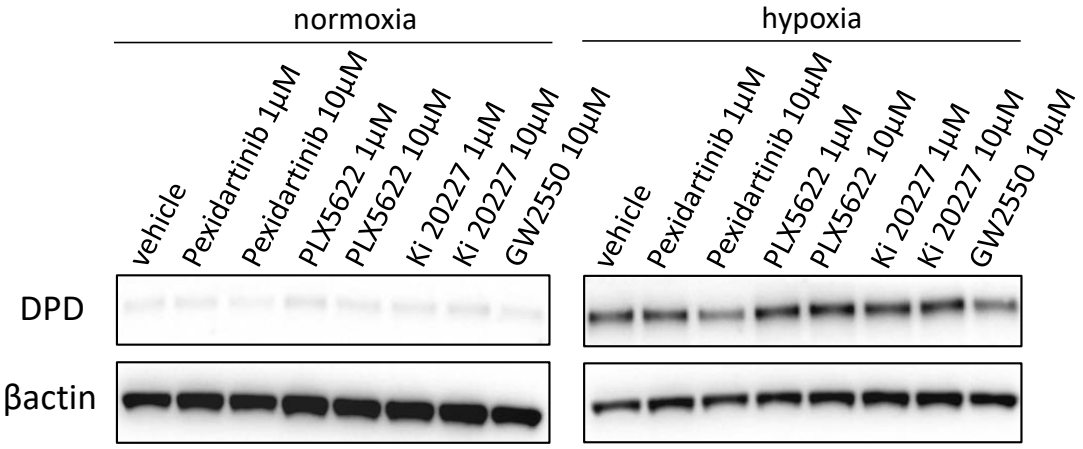

B

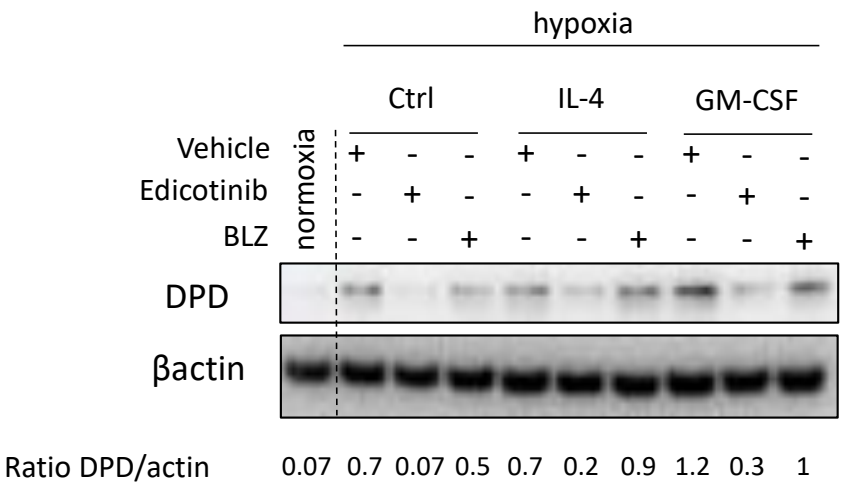

C

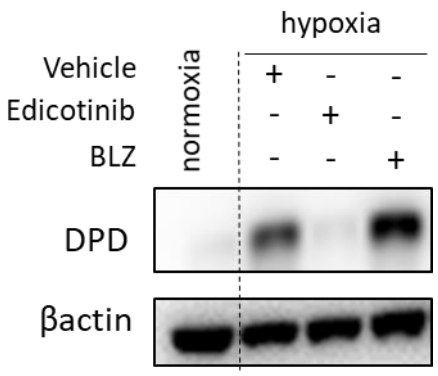

Chapter Three - Part Four

Supplementary Results

I Effect of M-CSF R antagonists on the DPD protein expression in THP1 Macrophages

THP1, a human monocytic cell line, is a well-used human macrophage model profiting from their ability to be differentiated into macrophage by PMA. Moreover, similarly to human primary macrophages, THP1 macrophages express DPD and this expression is increased under hypoxia. Thus, we wanted to confirm the previous results that showed that Edicotinib downregulates the expression of DPD using this model. As a consequence, THP1 cells were differentiated with 20 nM of PMA for 48 hours for their full differentiation into macrophages. Following, THP1 macrophages were transitioned to hypoxia of 25mmHg oxygen level and then treated with Edicotinib or BLZ945 at 3µM for 48 hours after which proteins were extracted in RIPA lysis buffer with anti-phosphatases and anti-proteases. The protein expression of DPD was assessed through immunodetection where results showed that Edicotinib at 3µM downregulates the expression of DPD contrary to BLZ945 confirming the results of primary macrophages Figure S 2 A and B. However, as compared to primary macrophages, Edicotinib and BLZ945 at 10µM exerted a toxic effect on THP1 macrophages giving insights that THP1 macrophages are more sensitive to these antagonists than primary macrophages.

We then sought to study the kinetics of the effect of Edicotinib and BLZ945 on THP1 macrophages at the protein level. Thus, following their differentiation, THP1 macrophages were transitioned to hypoxic conditions and treated with Edicotinib or BLZ945 at 3µM for 6 hours, 24 hours and 48 hours. Following each time point, proteins were extracted. The protein expression of DPD was then assessed by immunoblotting. Immunoblots have showed that Edicotnib, exclusively, downregulates the protein expression of DPD at 6 hours, 24 hours and 48 hours mimicking its effect on primary macrophages Figure S 2 C. This confirms that THP1 macrophages

are a good model to study the effect of Edicotinib on DPD, and for this reason we have used THP1 macrophages in some of our studies.

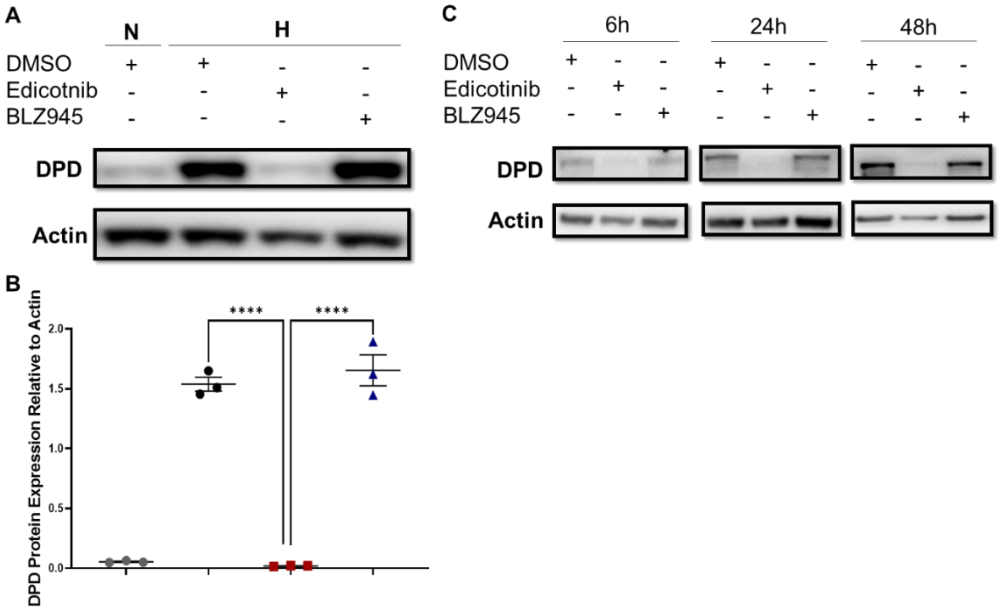

Figure S 2 DPD protein expression in THP1 macrophages treated with Edicotinib and BLZ945

(A): Immunoblot of DPD and actin of TP1 macrophages treated in normoxia (N) or hypoxia (H) with DMSO vehicle, Edicotinib 3µM or BLZ945 3µM for 48 hours. (B): Relative expression of DPD normalized to Actin. (C): Immunoblot of DPD and Actin of THP1 macrophages cultured in H for 6 hours, 24 hours or 48 hours in hypoxia with DMSO vehicle, Edicotinib 3µM or BLZ945 3µM. Experiments were performed three times. One-way ANOVA statistical test was run. ****: $p<0.0001$.

II Effect of M-CSF R antagonists on the protein expression of M-CSF R in human primary macrophages

Having validated the inhibitory effect of Edicotinib and BLZ945 on the phosphorylation of the M-CSF R, we thereafter assessed the surface expression of the receptor. RNASeq data demonstrated that Edicotinib downregulates the mRNA expression of the receptor 48 hours after the exposure Figure S 3 A. Knowing that M-CSF R following its activation, it is internalized and recycled. Thus, we wanted to demonstrate whether Edicotinib is modulating the recycling of the receptor. For this desired reason, primary macrophages were treated with Edicotinib and BLZ945 at 10µM for 24 hours, 48 hours or 72 hours under normoxic conditions. Following each time point, macrophages were taken and stained with aCSF1R – FITC by Flow cytometer Figure S 3 B. Results did not show any significant modulation in the expression of the receptor during these time points with the antagonists Figure S 3 C. This was also demonstrated by immunoblots detecting the total expression

of M-CSF R from macrophages treated with either of the antagonists for 48 hours, results not shown.

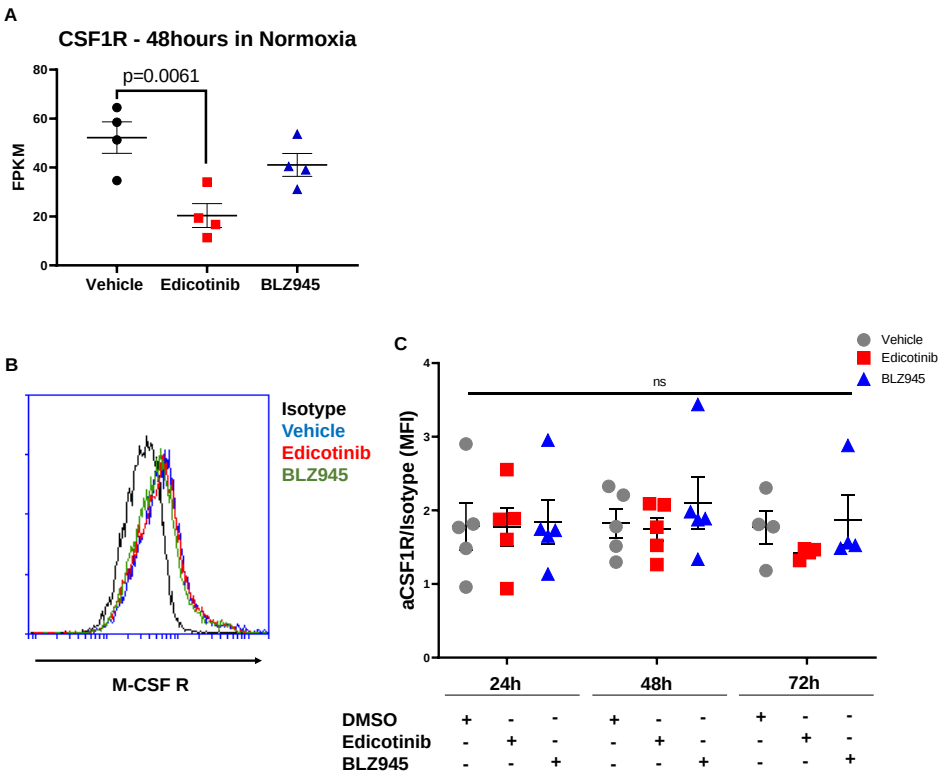

Figure S 3 Cell-surface expression of M-CSF R in primary macrophages treated with Edicotinib or BLZ945 for 24 hours, 48 hours or 72 hours in normoxia.

(A): M-CSF R mRNA expression in macrophages treated with vehicle, Edicotinib or BLZ945 for 48 hours. (B): M-CSF R staining in vehicle, Edicotinib or BLZ945 treated macrophages for 48 hours compared to isotype staining. (C): M-CSF R expression in macrophages treated in normoxia for 24 hours, 48 hours or 72 hours with vehicle, Edicotinib or BLZ945. Results are represented as Median Fluorescence Intensity (MFI) of aCSF1R normalized to that of the istotype. Experiments were carried out four or five times. One-way ANOVA test was carried out. ns: not significant.

III Effect of M-CSF R Antagonist on the protein expression of M-CSF R in THP1 Macrophages.

We next wanted to check whether this is also alike in THP1 macrophages. Thus, THP1 macrophages were treated with Edicotinib or BLZ945 at 3 µM for 48 hours either in hypoxia or normoxia. The expression of the surface and the total M-CSF R was assessed by FACS and western blot, respectively. The total expression of the receptor by western blots showed a significant decrease of the receptor in cells treated with Edicotinib compared to controls and BLZ945, Figure S 4 A and B. Results from FACS staining with aCSF 1R conveyed that the expression of the M-CSF R at the surface of THP1 macrophages, contrary to primary macrophages, is significantly downregulated upon treatment with Edicotinib but not BLZ945 Figure S 4 C and D. These results

further prove that THP1 macrophages are more sensitive to Edicotinib than primary macrophages and these two macrophages models are distinct, at least in regards to the M-CSF R.

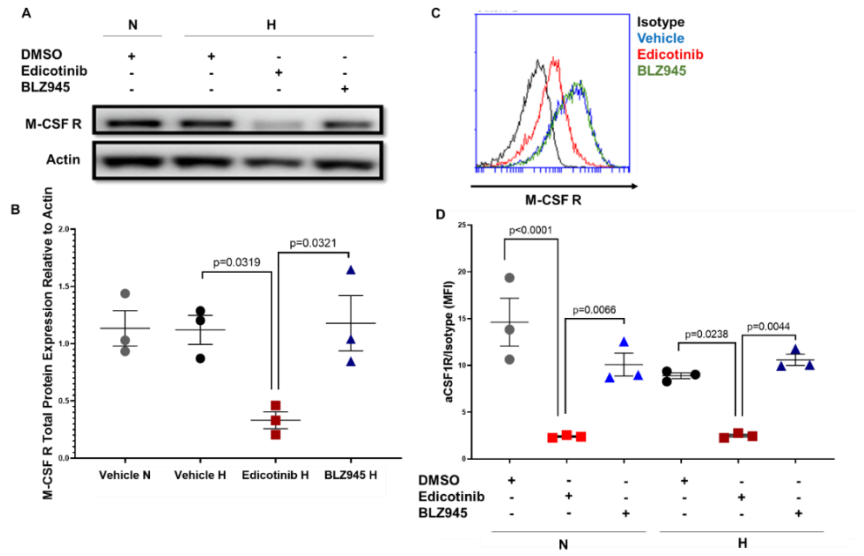

Figure S 4 M-CSF R Expression in THP1 Macrophages Treated with M-CSF R Antagonists

(A): Immunoblot of M-CSF R and Actin of THP1 macrophages treated with 3µM of Edicotinib, BLZ945 or vehicle in hypoxia and vehicle in normoxia. (B): Quantification of the M-CSF R total protein expression. (C): M-CSFR staining in THP1 macrophages treated or not in hypoxia with Edicotinib or BLZ945 for 48 hours. (D): Mean Fluorescence Intensity (MFI) of M-CSF R stained to that of the isotype of THP1 macrophages treated or not with Edicotinib or BLZ945 in normoxia (N) or hypoxia (H). Experiments were performed three times. One-way ANOVA test was performed with Tukey's comparisons.

IV Effect of M-CSF R Antagonists on the Cytotoxicity of Macrophages

We have previously demonstrated that Edicotinib downregulates the expression of DPD and reprograms macrophages metabolically. Accordingly, as our aim is not to deplete macrophages but rather to reprogram them, we wanted to verify that these drugs are not toxic to macrophages and that this downregulation of DPD by Edicotinib is not due to macrophage depletion. Hence, Annexin V/7AAD staining was conducted on macrophages treated with either of these drugs at 1µM, 10µM or 50µM for 48 hours either in normoxia or hypoxia to assess whether these macrophages are engaging apoptosis and/or late apoptosis/necrosis. Comparing Edicotinib at 1µM and 10µM to their vehicle, results did not show any toxic effect, opposing to Edicotinib 50 µM where approximately 50% of macrophages were undergoing apoptosis as represented in Figure S5 A and B.

Moreover, an MTT assay was carried out to further establish the toxic effect of our antagonists. Results validated what was observed for the AV/7AAD staining that these drugs at 10 µM are not toxic to macrophages, Figure S5 C.

These salient results confirm that Edicotinib is targeting M-CSF R pathway as well as the expression and activity of DPD in macrophages without engaging their apoptosis.These results

confirm that Edicotinib at 10µM is insufficient to induce apoptosis or strong toxic effect in human macrophages but is able to reprogram macrophages metabolically.

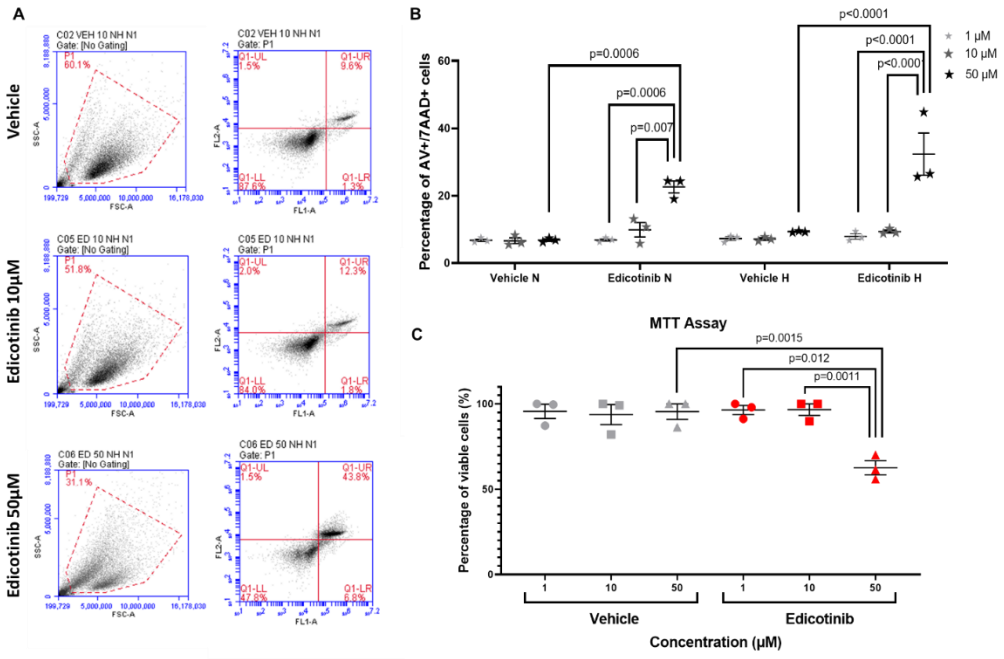

Figure S 5 Effect of M-CSF R Antagonists on the cytotoxicity of Macrophages

(A): Annexin-V and 7AAD staining of macrophages cultured in N or H for 48 hours with Edicotinib or BLZ945 at 10µM. Annexin V staining was assessed on channel FL2-A whilst 7AAD staining was evaluated on channel FL3-A. (B): Percentage of Annexin V/7AAD double positive cells was assessed. (C): Percentage of viable cells of primary macrophages was assessed in macrophages treated for 48 hours in normoxia with 1, 10 and 50 µM of Edicotinib or BLZ945 by MTT assay. Experiments were carried out three times. One-way ANOVA test was done with Tukey's multiple comparisons.

V Effect of M-CSF R Antagonists on the Inflammatory Response of Macrophages

Next, we sought to check whether the function of macrophages is maintained during and after the treatment with Edicotinib, aiming to check whether macrophages will respond normally to LPS stimulations. Thus, fully differentiated macrophages were subjected to either DMSO, Edicotinib at 10 µM or BLZ945 at 10 µM for 24 hours under either hypoxic or normoxic conditions.

Following 24 hours, the media was replaced with fresh new macrophage media and macrophages were stimulated with LPS at 1 ng/mL for 4 hours and the supernatants were taken. In order to check whether macrophages will respond in the same manner to LPS stimulations, the concentrations of secreted TNF-α were assessed from the supernatants by ELISA,Figure S 6. Results confirm that upon removing Edicotinib and BLZ945 from macrophages, macrophages are able to respond normally to LPS by secreting TNF-α.

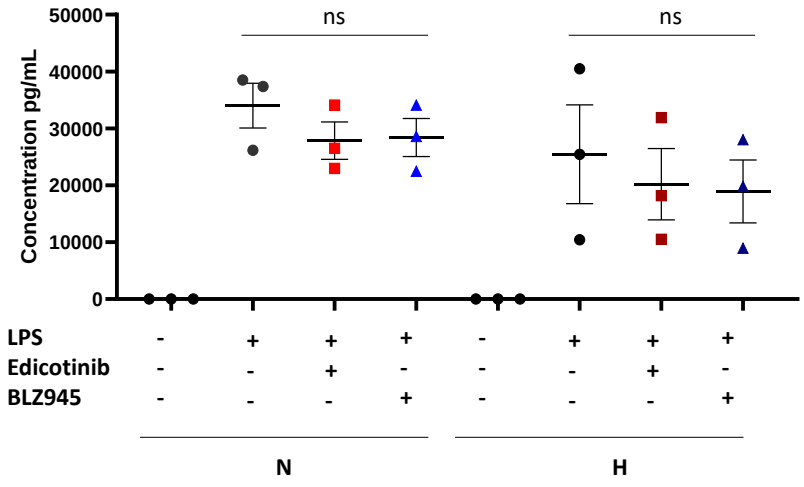

Figure S 6 Effect of Edicotinib and BLZ945 on the Inflammatory Response of Macrophages Macrophages were treated with Edicotinib or BLZ945 at 10µM or vehicle for 24 hours in normoxia (N) or hypoxia (H). Following, media was changed then macrophages were stimulated with LPS 1ng/ml for 4 hours after which supernatants were taken and the concentration of TNF-α was measured by ELISA.Experiments were carried out three times. One-way ANOVA test was performed. ns: not significant**.**

Hypothesis – DPYD Regulation in Human Macrophages

In an attempt to target the oxygen controlled chemoresistance that is mediated by the upregulation in the expression of DPD in hypoxic macrophages, we aimed to target its upstream pathway which is controlling its expression. It was shown in cancerous cells that *DPYD* is controlled by the transcription factor SP1 (X. Zhang et al., 2006). So, we postulated that this stands still in macrophages. Moreover, it was proven in monocytes that SP1 is activated and translocated to the nucleus through the activation of the ERK pathway (Curry et al., 2008), and bearing that ERK pathway is one of the downstream pathways activated by M-CSF R, we aimed to target the M-CSF R. Thus, our hypothesis states that *DPYD* is transcribed by SP1, which is activated by the phosphorylation of ERK that in turn is mediated by M-CSF R signaling pathway.

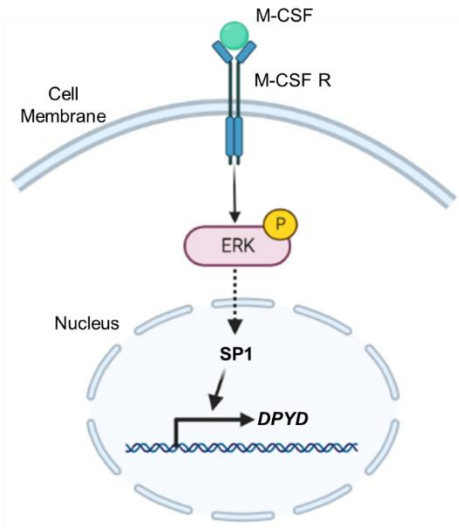

Figure S 7 Hypothesis of DPYD regulation by M-CSF R / ERK1/2 / SP1 pathway in human macrophages

VI Implication of ERK signaling in DPYD expression downstream M-CSF R in primary human macrophages

Having proved the effect of Edicotinib to target the expression and activity of DPD in human macrophages, we then wanted to validate our hypothesis which states that through M-CSF R pathway, p-ERK is activated and this activates SP1 mediating its translocation to the nucleus facilitating the transcription of *DPYD*. So, we first assessed the protein expression of DPD, p-ERK and ERK in human primary macrophages treated with Edicotinib and BLZ945 at two different concentrations: 1µM and 10 µM for 48 hours either under normoxic or hypoxic conditions. Concerning DPD expression, immunoblots demonstrated what we already proved that Edicotinib significantly downregulated the expression of DPD at 10 µM contrary to 1 µM and to BLZ945. Moreover, the immunoblots showed that Edicotinib at 10 µM, where DPD is downregulated, has significantly inhibited the phosphorylation of ERK maintaining a stable expression of ERK between the conditions Figure S 8 A. These results were also confirmed at the transcriptional level, as RNA sequencing was performed on primary macrophages treated with Edicotinib or BLZ945 at 10 µM for 48 hours after which mRNA was extracted. Gene Set Enrichment Analysis (GSEA) from the RNASeq data showed that there is a significant downregulation of the ERK signaling in Edicotinib treated conditions, results shown in article 2.

At the first glance, these results supported our hypothesis that Edicotinib is inhibiting the expression of DPD through inhibiting p-ERK signaling pathway. Next, we wanted to validate this hypothesis by treating the primary macrophages for 48 hours under hypoxic or normoxic conditions with an inhibitor of MEK, which is upstream ERK1/2. Proteins were extracted and immunoblots were performed. We first confirmed the inhibitory effect at the level of p-ERK by

immunoblots then we assessed the protein expression of DPD. Results showed an expected significant and strong inhibition of p-ERK in macrophages treated with U0126 but surprisingly showed that the protein expression of DPD is not modulated in U0126-treated macrophages Figure S 8 B. These results prove that Edicotinib has an inhibitory effect on ERK signaling as well as the expression of DPD, but these two inhibitory activities are independent on each other.

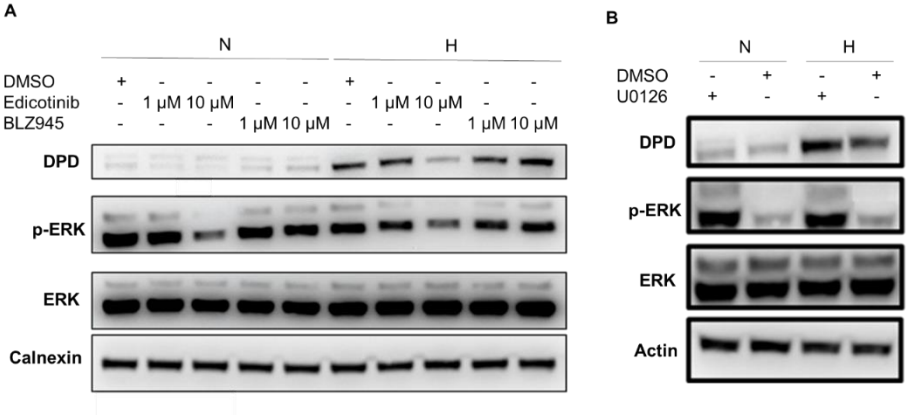

Figure S 8 Implication of ERK pathway in the DPYD expression downstream M-CSF R

(A): Immunoblot of DPD, p-ERK, ERK and Calnexin of human primary macrophages cultured in N or H for 48 hours with 1µM or 10µM of Edicotinib and BLZ945. (B): Immunoblot of DPD, p-ERK, ERK and Actin of primary macrophages cultured for 24 hours in hypoxia (H) or normoxia (N) with MEK inhibitor, U0126 at 10µM.

VII SP1 as a Potential Transcription Factor for DPYD

It was already shown that SP1 is a transcription factor that mediates the transcription of *DPYD* in cancerous cells. Thus, we wanted to explore if this is also the same for human macrophages. To do so, we depleted macrophages from SP1 through siRNA transfection with lipofectamine. Six days following their differentiation, macrophages were subjected to 50 nM of SiSP1 for 6 hours following media change. 48 hours after their incubation in normoxia, macrophages were lysed and protein were extracted. The SiSP1 transfection was monitored and confirmed through SP1 immunoblots as results demonstrated the depletion of SP1. To study whether SP1 is the transcription factor for *DPYD*, DPD was assessed through immunodetection as well. Results showed that the protein expression of DPD is not highly modulated in SiSP1 transfected macrophages as there was no significant decrease in the expression of DPD in macrophages whose expression of SP1 was knocked out. This shows that the mechanism by which DPD is regulated and expressed is far more complicated than we hypothesized.

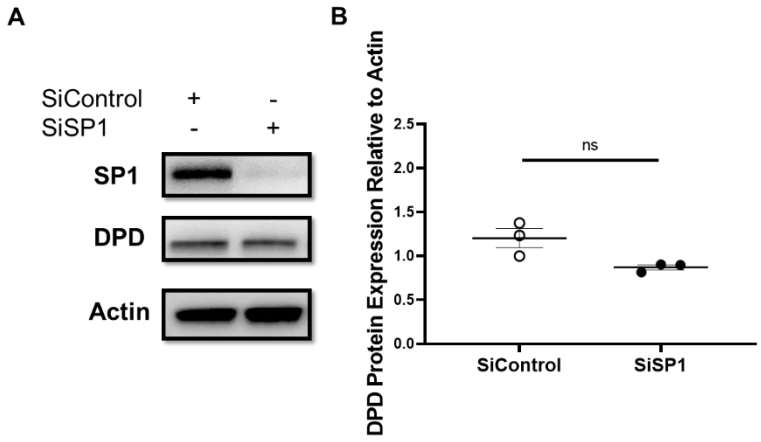

Figure S 9 Effect of siSP1 Transfection on DPD in Human Primary Macrophage

(A): Immunoblot of SP1, DPD and Actin in human primary macrophages where SP1 was knocked out. (B): Quantification of results of DPD expression normalized to Actin in three independent experiments. Mann-Whitney t test was performed. ns: not significant.

Materials and Methods

Cell Culture

THP1, a human monocyte lineage from an acute monocytic leukemia patient, was purchased from ATCC and used as a macrophage model in some of the experiments. Human colon cancer cell lines, RKO and HT-29, were purchased from ATCC. Mice macrophage cell line, RAW.267 and mice colon cancer cell line, CT-26 were purchased from ATCC. These cell lines were maintained and cultured in RPMI medium with Glutamax 1X (Gibco) supplemented with 10% of fetal bovine serum (FBS) (Gibco). The cell lines were passaged and seeded based on the ATCC instructions. All cell lines were tested routinely for the contamination of Mycoplasma using the MycoAlert detection kit (Lonza). The cell lines used are tabulated in ***Table M 1***.

Table M 1 List of cell lines

Cell line	Type	Origin	Source
THP1	Monocyte	Human	ATCC
RAW.267	Macrophage	Mice	ATCC
CT-26	Colon cancer	Mice	ATCC
RKO	Colon cancer	Human	ATCC
HT-29	Colon cancer	Human	ATCC

Table M 2 Cell Culture Inhibitors

Inhibitor	**Target**	**Reference**
Edicotinib	CSF-1R	HY-109086, MedChemExpress
Sotuletinib (BLZ945)	CSF-1R	HY-12768, MedChemExpress
Pexidartinib	CSF-1R	HY-16749, MedChemExpress
PLX5622	CSF-1R	HY-114153, MedChemExpress
GW2580	CSF-1R	HY-10917, MedChemExpress
Ki20227	CSF-1R	HY-10408, MedChemExpress
U0126	MEK	662005, Sigma

Human Samples

Human blood samples from healthy donors were obtained from the French national blood service (EFS). Donors gave their conscious and signed consent for the use of their blood for research purposes as part of an authorized protocol.

Tumor samples were obtained from the department of pathology of the university hospital of Grenoble as part of a declared sample collection. Tissue samples were taken from primary colorectal tumor or liver metastasis. All patient gave their signed consent for the study.

Human Monocyte Isolation and Macrophage Differentiation

Monocytes were isolated from leukoreduction system chambers of healthy EFS donors which was supplying us with blood. Blood was diluted with PBS 1X (Invitrogen) and separation of the blood constituents was performed using differential centrifugation by Histopaque 1077 (Sigma) of density 1.077 g/mL by which diluted blood was pipetted on top of the histopaque, ***Figure M 1***. Following centrifugation at 700 xg for 25 minutes, a ring of peripheral blood mononuclear cells (PBMCs) is formed and taken. PBMCs were then washed and resuspended in macrophage medium after which they were counted using the Mallasez chamber.

Following, PBMCs were taken and resuspended in macrophage sorting buffer consisiting of PBS 1X with 0.5 % BSA (Sigma) and 2 mM EDTA (Invitrogen). Resuspended PBMCs were incubated for 15 minutes at 4 °C with CD14 microbeads (130-050-201, Miltenyi Biotec). Monocytes which are CD14 + cells, were isolated from the negative selected cells by magnetic separation using LS columns (130-042-401, Miltenyi Biotec). Monocytes were plated in a treated 12-wells plate (CytoOne) at a concentration of 750,000 cells in 1 mL of macrophage complete medium composed of RPMI with Glutamax supplemented with MEM Non-essential amino acids (NEAA), 10 mM HEPES (Life technologies) as well as 10% of human male serum (SAB) (Sigma) with 25 ng/mL of human macrophage colony stimulatory factor (M-CSF) (130-096-489, Miltenyi Biotec). Differentiation of macrophages was achieved after 6 days of culture.

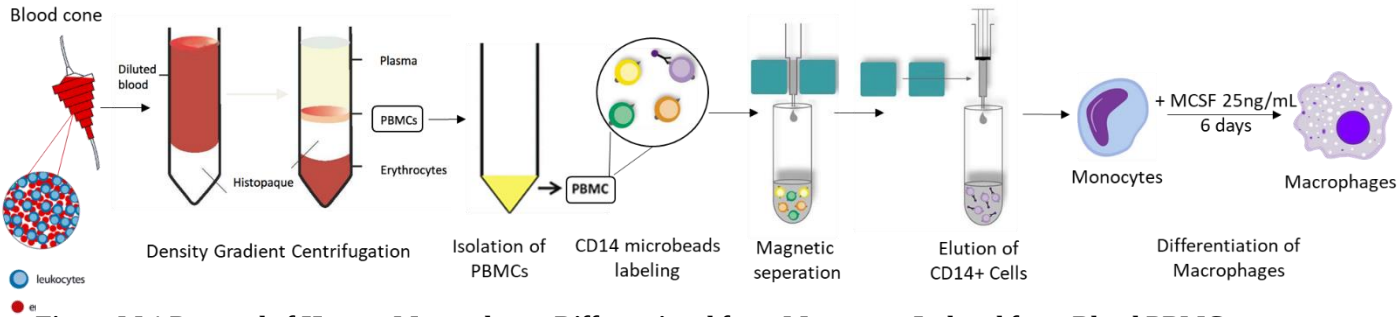

Figure M 1 Protocol of Human Macrophages Differentiated from Monocytes Isolated from Blood PBMCs

THP1 Macrophage Differentiation

THP1 cells were used as a macrophage model in some experiments, when stated. THP1 cells were plated in a treated 12-wells plate (CytoOne) at a concentration of 500,000 cells in 1 mL in RPMI medium supplemented with 10% FBS. Their differentiation was achieved using 20 nM or 50 nM of Phorbol 12-myristate 13-acetate (PMA) (P1585, Sigma) for 48 hours or 24 hours, respectively.

Targeting M-CSF R in Macrophages

Fully differentiated human monocyte-derived macrophages at the 6th day of plating (D6) were treated with either Edicotinib at 10µM or BLZ945 at 10µM as illustrated in **Figure M 2**. The vehicle that was used was DMSO corresponding to 10µM. Depending on the protocol, macrophages were incubated with the antagonists or vehicle for 48 hours either in the normal incubator of 18.6% oxygen, here known as normoxia (N), or in the hypoxic chamber of 3% oxygen, here known as hypoxia (H).

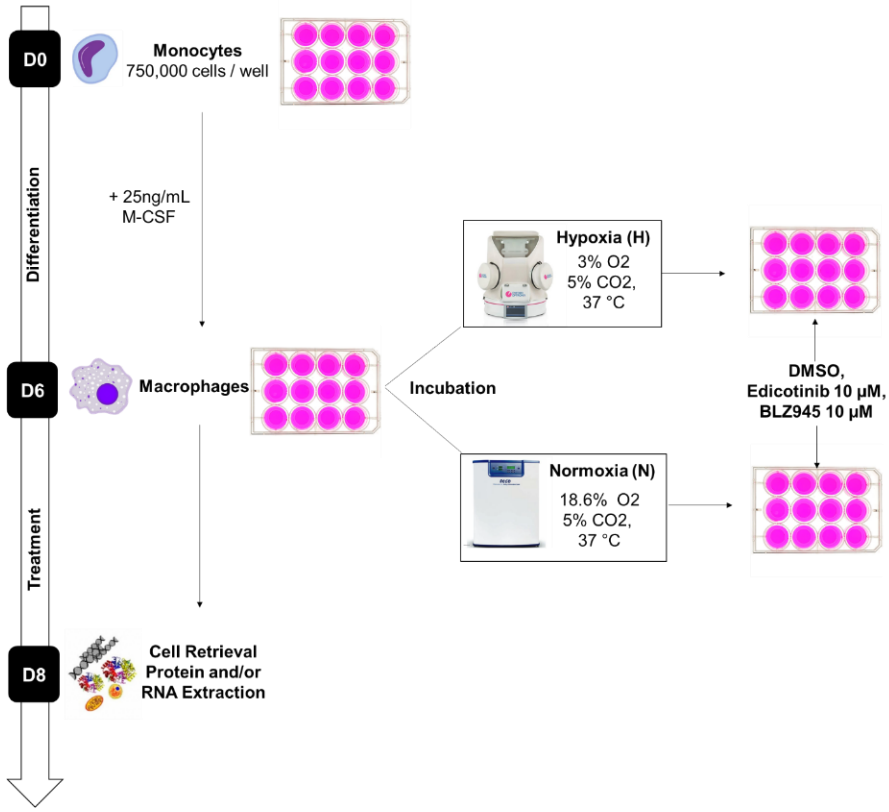

Figure M 2 Protocol of targeting M-CSF R in monocyte-derived macrophages

Targeting M-CSF R in THP1 Macrophages

THP1 monocytes were plated at 500,000 cells per well in a 12-wells treated plate (CytoOne) and differentiated with 20 nM of PMA for 48 hours in the normal CO2 incubator. Following that, THP1 macrophages were transited under the hypoxic chamber of 25 mmHg after which their media was changed and replaced with RPMI + 10%FBS preincubated for 24 hours in hypoxic conditions, ***Figure M 3***. Then, THP1 macrophages were treated with 3 µM of either Edicotinib or BLZ945 or the vehicle DMSO for 48 hours in hypoxia after which cells were directly lysed by Laemmli 2X with 10% B-mercaptoethanol.

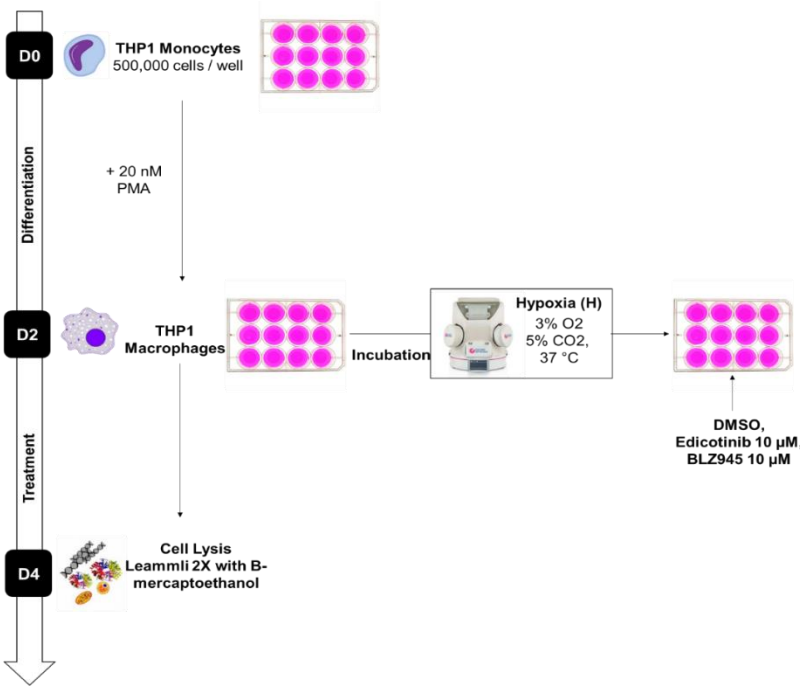

Figure M 3 Protocol of targeting M-CSF R in THP1 differentiated macrophages

Inhibiting the Phosphorylation of M-CSF R

To study the effect of M-CSF R antagonists on the phosphorylation of the receptor, fully differentiated human monocyte-derived macrophages at the 6th day of plating (D6) were starved from the serum for 18 hours. Following, media was changed and replaced with cold macrophage media by which the cells were stimulated with 50 ng/mL of MCSF at 4°C for 5, 15, 30 and 60 minutes in presence or absence of M-CSF R antagonists which are Edicotinib, BLZ945, Pexidartinib, PLX5622, GW2580 and Ki202227 at 10µM.

Inhibiting the Phosphorylation of ERK

In order to check whether the ERK pathway is implicated in the regulation of DPD expression, phosphorylation of ERK was inhibited using U0126 which is an inhibitor of MEK, that is upstream of ERK1/2. Fully differentiated macrophages were transited under the hypoxic chamber after which their media was changed and replaced with macrophage complete media which was already preincubated under hypoxic conditions for at least 24 hours. 10 µM of U0126 was added on the cells where DMSO was used as the vehicle. Following 48 hours of treatment, cells were lysed and proteins were extracted for further explorations.

siSP1 Transfection

In order to explore whether SP1 is a potential transcription factor regulating the expression of *dpyd* in human primary macrophages, SP1 was knocked down by siRNA transfection (-Target Plus Human SP1 siRNA Smart Pool, L-026959-00-0005, Horizon Discovery LTD). Fully differentiated macrophages at day 6 were transfected by siSP1 at a final concentration of 50 nM in lipofectamine (13778-075, Life Technologies) in Opti-MEM media (51985026, Life technologies). 6 hours later, the media was changed and replaced with fresh new macrophage complete media. Cells were incubated under the normal CO2 incubator for 48 hours after which they were lysed and proteins were extracted to check the protein expression of SP1 and DPD through immunoblots.

Assessing the Effect of M-CSF R Antagonists on M-CSF R Expression

In order to explore whether M-CSF R antagonists, Edicotinib and BLZ945, modulate the expression of M-CSF R in macrophages, monocyte-derived macrophages were treated with Edicotinib or BLZ945, both at 10 µM or vehicle for 24 hours, 48 hours and 72 hours in normoxia. Afterwards, cells were detached and stained with aCSF1R-PE (565368, BD Biosciences) or isotype IgG1 K – PE (553925, BD Biosciences) for 20 minutes at 4°C in dark. Following, cells were washed and analyzed using accuri C6 flow cytometer. Median fluorescence intensity was assessed and the ratio of stained to that of the isotype was calculated.

In addition, the effect of Edicotinib and BLZ945 was also explored in THP1 macrophages using flow cytometer and immunoblots. THP1 differentiated macrophages were treated with Edicotinib, BLZ945 or vehicle for 48 hours in normoxia or hypoxia. Following, proteins were either extracted to assess the total expression of M-CSF R by immunoblots, or cells were detached and stained

with aCSF1R to assess the expression of the receptor at the surface. Same protocol staining and analyses were followed as that for macrophages.

Polarization of Macrophages and M-CSF R Targeting

To study the effect of Edicotinib and BLZ945 on the polarization states of macrophages, fully differentiated macrophages at day 6 were transited under the hypoxic chamber where they were either unpolarized (M0), or polarized towards M1 or M2 states by stimulating them with 20 ng/mL of LPS or 20 ng/mL of IL-4 and 20 ng/mL of IL-10, respectively. The protocol is illustrated in ***Figure M 4***. Moreover, M0, M1 and M2 macrophages were subjected to DMSO, Edicotinib at 10 µM or BLZ945 at 10 µM. 48 hours succeeding the polarization and the treatment, macrophages were lysed and proteins were extracted by RIPA buffer with anti-phosphatases and anti-proteases.

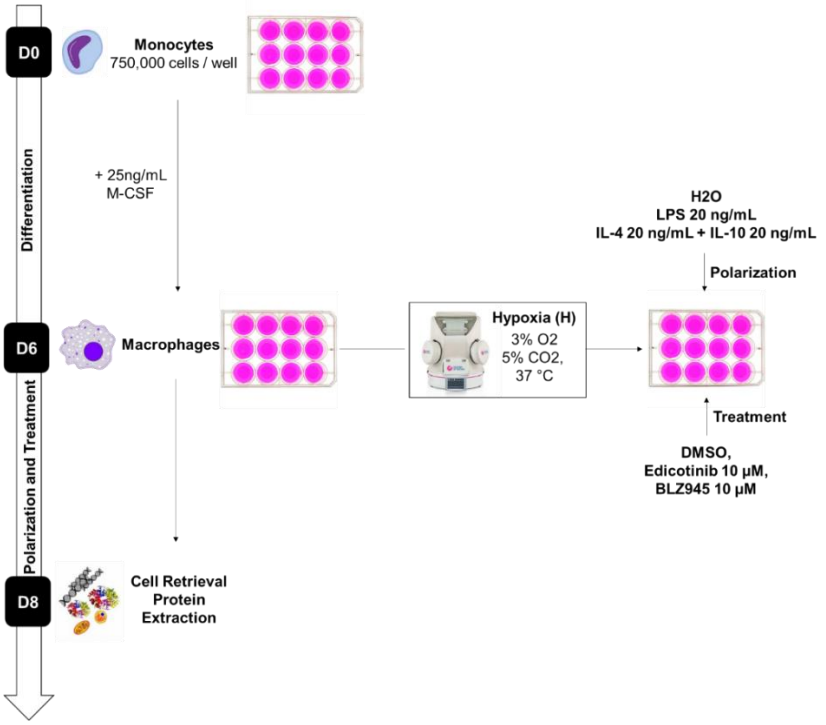

Figure M 4 Protocol of polarizing monocyte-derived macrophages towards M1 and M2 phenotype

Annexin V / 7AAD Staining

Macrophages were stained for Annexin V and 7 AAD to assess whether they are engaging early apoptosis or late apoptosis/necrosis, respectively, upon their treatment with Edicotinib or BLZ945. Fully differentiated human monocyte-derived macrophages at day 6 were treated with Edicotinib or BLZ945 at 1 µM, 10 µM or 50 µM for 48 hours under normoxic or hypoxic conditions. Following, cells were detached by TrypLE and then stained with Annexin V – FITC (Miltenyi Biotec) accompanied by 7AAD staining. Live and dead cells were gated by which the Annexin V positive cells and 7AAD positive cells were counted through FL1-A and FL2-A channels,

respectively. The percentage of the single positive and double positive cells was shown in the figures.

MTT Assay

MTT Assay was carried out in a 96-wells plate. 100,000 monocytes were cultured and differentiated into macrophages for 6 days. Ensuing, fully differentiated macrophages were cultured with Edicotinib or BLZ945 at 1 µM, 10 µM or 50 µM for 48 hours under normoxic conditions. The assay was then carried out using Cell Titer 96 Non-radioactive Cell Proliferation Assay (G4000, Promega) according to the manufacturer's instructions. Following the end of the treatment, media was replaced with 200 µl of fresh new media where 15µl of MTT dye solution was added for 4 hours at 37°C. Afterwards, 200 µl of solubilization/stop solution was added for 1 hour. Finally, the absorbance was measure using the CLARIOSTAR at 570nm. The percentage of viable cells was calculated by the ratio of the optical densities measured for the sample to that of the control sample of cells without any treatment multiplied by 100.

Assessing the Functionality of Macrophages

In order to assess whether the macrophages are still functional and have the same response to stimulations during or after the treatment with the antagonists, fully differentiated macrophages at day 6 were subjected to either DMSO, Edicotinib at 10 µM or BLZ945 at 10 µM under hypoxic or normoxic conditions for 24 hours. Next, media was changed thenceforward macrophages were stimulated with 1 ng/mL of LPS for 4 hours whereafter their supernatants were taken and stored at – 80 °C, ***Figure M 5***.

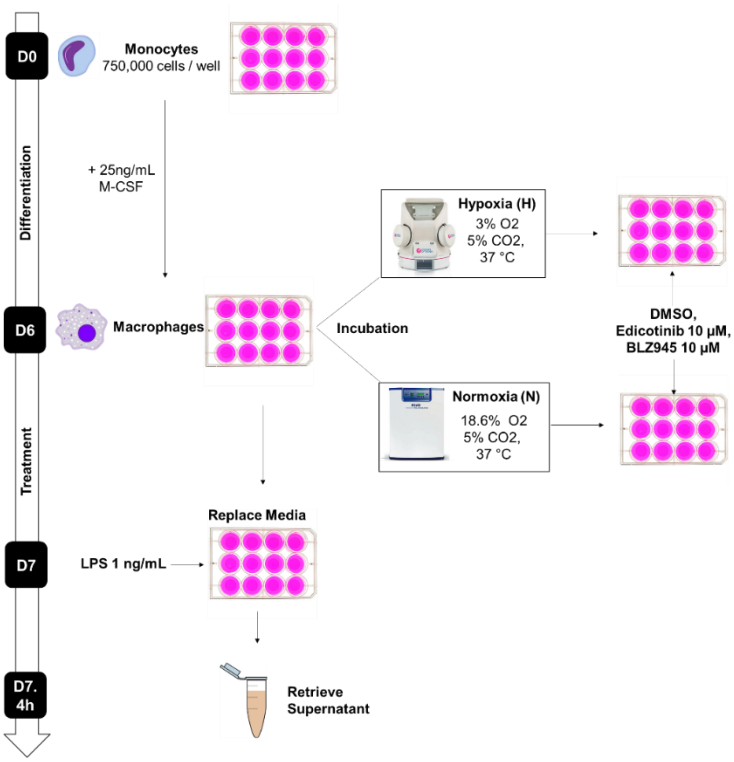

Figure M 5 Protocol of Assessing the functionality of macrophages following M-CSF R targeting

Assessing the Concentrations of TNFα by ELISA

In order to study whether macrophages responded in the same way to LPS stimulations for the assessment of their functions, the concentrations of TNF-α were assessed from the supernatants of these macrophages by ELISA. Human uncoated TNF-α ELISA kit (**88-7346-77**, ThermoFisher) was used and the protocol was followed as instructed. In a 96-wells plate, wells were coated with TNF-α capture antibody overnight at 4°C. In the next day, wells were washed and blocked with ELISA/ELISPOT diluent 1X. Supernatants were diluted 1/60 in ELISA/ELISPOT diluent 1X and then added to the wells for 2 hours along with a serial dilution of standards. Following, samples were incubated with detection antibody for 1 hour after which Streptavidin-HRP was added for 30 minutes. 5 minutes after addition of substrate TMB, reaction was stopped by HCL 1N. Finally, the absorbance was measured at 450 nm using TECAN reader.

DPD Measurements

To assess the effect of M-CSF R antagonists on the activity of DPD, monocyte-derived macrophages were treated with Edicotinib, BLZ945, both at 10 µM or vehicle for 48 hours in normoxia or hypoxia. Following, supernatants from each condition was retrieved and stored at -80°C. Then, analyses were performed in the Pharmacology Laboratory of Institute Claudius-

Regaud (France) using an HPLC system composed of Alliance 2695 and diode array detector 2996 (Waters). Uracil (U), Dihydrouracil (UH2), Ammonium sulfate 99%, Acetonitrile (ACN) gradient chromasolv for HPLC and 2-propanol were purchased from Sigma. Ethyl acetate Scharlau was of HPLC grade and purchased from ICS (Lapeyrouse-Fossat, France). Water from Milli-Q Advantage A10 and MultiScreen-HV 96-well Plates were used (Merck Millipore). Calibration ranges were 3.125 – 200 ng/mL for U and 25 - 500 ng/mL for UH2 and 5-FU (5µg/mL) was used as an internal standard.

Assessing the Stabilization of HIF-2α

To check whether Edicotinib destabilizes HIF-2a, fully differentiated macrophages were transited to the hypoxic chamber by which media was changed and replaced with a hypoxic-preincubated macrophage complete media. Edicotinib or BLZ945 at 10µM each were added to these macrophages. Following 6 hours and 24 hours, macrophages were detached with TrypLE and directly lysed with Laemmli 2X.

Macrophage Conditioned Media (MCM)

THP1 macrophages were plated and differentiated at 500,000 cells with 50nM of PMA for 24 hours. Following, THP1 macrophages were transited under the hypoxic chamber of 3% oxygen and treated with Edicotinib or BLZ945 at 3µM or DMSO acting as a vehicle for 48 hours, ***Figure M 6***. Thereupon, the media was changed and replaced with RPMI with 10% SVF with 3µM of Edicotinib, 3µM BLZ945 or DMSO with 1µg/mL of 5-FU to generate the 5FU Edicotinib MCM, 5FU BLZ945 MCM or 5FU Vehicle MCM. Besides, control MCM with the antagonists: Edicotinib MCM, BLZ945 MCM or Vehicle MCM were generated by treating THP1 macrophages with Edicotinib 3µM, BLZ945 3µM or DMSO for 72 hours, respectively by which media was changed and replaced with new media with antagonists after 48 hours. Succeeding, the supernatant was taken and centrifuged to remove any floating cell and then froze at -80°C for further use. Additionally, Non-conditioned media (NCM) with Edicotinib 3µM (Edicotinib NCM), BLZ945 3µM (BLZ945 NCM), DMSO (Vehicle NCM), 5-FU 1µg/mL (5FU NCM), Edicotinib 3µM and 5FU 1µg/mL (5FU Edicotinib NCM) or BLZ945 3µM and 5FU 1µg/mL (5FU BLZ945 NCM) were incubated under the same hypoxic conditions for the same time intervals. The produced MCM or NCM were added for 48 hours to two distinct colon cancer cell lines, RKO and HT-29 cells, which were plated previously at 100,000 cells per well for 24 hours. Then cancerous cells were collected and counted and the percentage of growth inhibition was assessed for each condition.

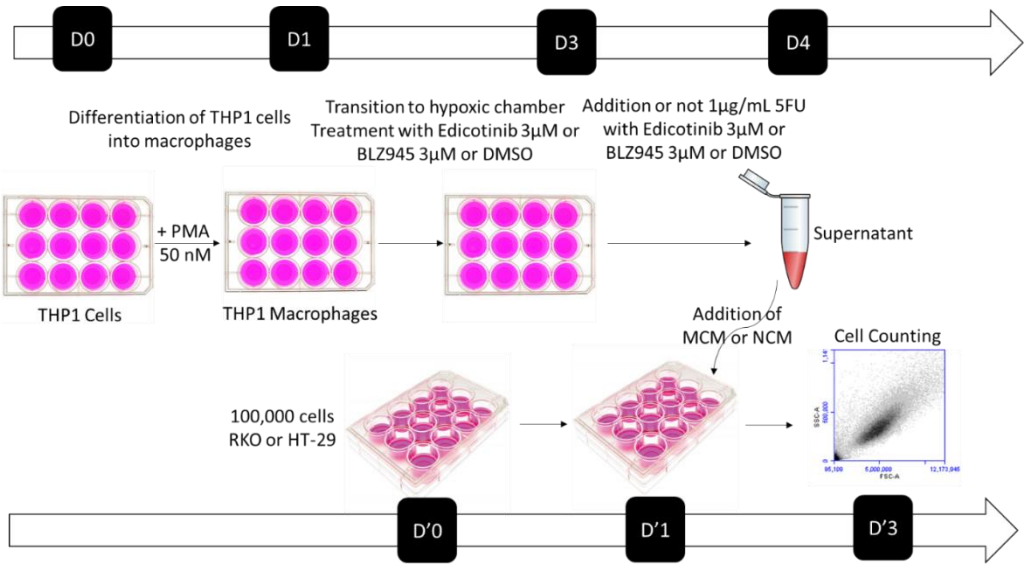

Figure M 6 Protocol of Assessing the Functional Assay of Edicotinib on DPD

Generation of Tumor Educated Macrophages (TEMs)

Monocytes isolated from human blood PBMCs as explained earlier were fully differentiated into macrophages in presence of 25 ng/ml of M-CSF in Macrophage complete medium with 10% SAB for 6 days in the normal CO_2 incubator. At day 6, macrophages were incubated under the hypoxic chamber and the media was changed and replaced with TEMs media consisting of 50% of Macrophage complete media with 10% SAB and 50% of RKO conditioned-media (CM) with 10% SAB with 20 ng/ml of IL-4. To study whether Edicotinib reprograms TEMs, 10 µM of Edicotinib was added to TEMs. Following 24 hours, TEMs were detached and taken for FACS analysis and Western Blot.

Flow Cytometry

For Flow cytometry staining, macrophages were detached by TrypLE for 15 minutes. Following, the cell pellet was resuspended with PBS/BSA/EDTA and stained with antibodies CD206-PE (130-095-220, Miltenyi Biotec), aCSF-1R-PE (565368, BD Biosciences) or isotype IgG1 K-PE (559320, BD Biosciences) for 20 minutes at 4°C. Afterwards, cells were washed and analyzed using Accuri C6 flowcytometer by which live cells were gated and the percentage of stained cells was observed at FL2A channel. The expressions of CD206 and M-CSF R were assessed by calculating the ratio of median fluorescence intensity of stained to that of the isotype.

Metabolomics

In order to assess the metabolic reprogramming of macrophages by Edicotinib and BLZ945, monocyte-derived macrophages were treated with Edicotinib, BLZ945 at 10µM or vehicle for 48 hours either in normoxia or hypoxia. Metabolic assessement was performed using 4:3:3

Chloroform/Methanol/Water biphasic separation. 48 hours following the treatment, cells were lysed with TrypLE then metabolically quenched with ethanol bath. Afterwards, cells were centrifuged at 4°C, pelleted and washed with cold PBS twice. Next, cells were resuspended with a solvent mixture of 1:3:3 of chloroform/methanol/water with internal standards of scyllo inositol (I8132, Sigma) and tridecanoic acid (91988, Sigma). Following, sonication was performed and cells were kept in ice for 2 hours. Afterwards, water was added followed by the addition of chloroform to reach a ratio of 4:3:3 of chloroform/methanol/water. Next, biphasic separation was achieved by centrifugation for 5 minutes at 0 °C where 2 layers are resulted, an upper layer of organic phase and a lower layer of aqueous phase. Organic phase was taken and stored at – 80 °C for analyses. Following, the organic is dried at 60 °C for 10 minutes. After drying it, methylating reagent TMSH (701520.101, Machery-Nagel) in chloroform/methanol is added after which samples were run on GC-MS with 1µL injection Methanolysis 2 program. Finally, samples are analysed by GC-MS 1µL injection Polar standard program. All FAs (Fatty acids) were identified by comparison of retention time and mass spectra from GC-MS with authentic chemical standards. The concentration of FAs was quantified after initial normalization to different internal standards and finally to macrophage number.

RNA Extraction and Dosage

RNA extraction was performed using the NucleoSpin RNA kit compnents and protocol from Machery Nagel (740955.250, Macher Nagel). Cells were directly lysed using RA1 buffer composed of guanidine thiocynate supplemented with 10% B-mercaptoethanol after which the viscosity was reduced and the lysate was cleared by filtration through NucleoSpin filters. Following, 70% ethanol was added to the homogenized lysate at a ratio of 1:1 followed by homogenization. Subsequently, lysate was pipetted onto NucleoSpin RNA column where nucleic acid will bind following the centrifugation. Afterwards, the silica membrane is desalted using Membrane Desalting Buffer and the membrane is dried by centrifugation. Next, samples are treated with rDNases for 15 minutes followed by washing steps. Finally, RNA is eluted using RNase-free water in a two-step elution for better yield. RNA samples were stored at -20 °C and dosed using the Nanodrop.

RT-qPCR

Reverse transcription was performed using the iScript Ready-to-use cDNA supermix components (1708841, Biorad) in 8-wells strips (TLS0801, Biorad) by which 500 ng of starting RNA was used. Thermal cycler (CFX96, Biorad) was used by which priming was performed at 25 °C for 5 minutes, followed by the reverse transcription at 46 °C for 20 minutes finalizing in the inactivation of reverse transcription for 1 minute at 95 °C. Following the reverse transcription, cDNA were diluted in RNase-free water (Invitrogen) and qPCR was then performed with the iTaq universal SYBR green supermix components (172-5124, Biorad) by which 25 ng of cDNA and 400 nM of

forward and reverse primers were used. CFX96 (Biorad) was used to run the qPCR starting by polymerase activation and DNA denaturation at 95 °C for 30 seconds, followed by amplification which is performed first by denaturation at 95 °C for 2-5 seconds and second by the annealing and plate reading at 60 °C for 30 seconds for 40 cycles. Finally, melting curve analysis was performed. Hprt-1, B2M, Gusb and Rpl6 were used as reference genes. Quantification was performed using the ΔΔCt method.

Agilent Nano Bioanalyzer

The quality of the RNA and the RNA integrity number (RIN) were checked and determined using the Agilent RNA 6000 Nano Bioanalyser according to the manufacturer's instructions.

RNA Sequencing

RNA extraction was performed using the NucleoSpin RNA kit components (Macherey Nagel) as detailed above. RNA sequencing was performed using a sequencer (Integragen). Gene expression quantification was performed using the STAR software. STAR obtains the number of reads associated to each gene in the Gencode v31 annotation (restricted to protein-coding genes, antisense and lincRNAs). Raw counts for each sample were imported into R statistical software. Extracted count matrix was normalized for library size and coding length of genes to compute FPKM expression levels. The Bioconductor edgeR package was used to import raw counts into R statistical software. Differential expression analysis was performed using the Bioconductor limma package and the voom transformation. Gene ontology analysis was performed using the GONet software (https://tools.dice-database.org/GOnet/). Gene list from the differential analysis was ordered by decreasing log2 fold change. Gene set enrichment analysis (GSEA) was performed by clusterProfiler::GSEA function using the fgsea algorithm.

Protein Extraction and Dosage

Lysis of cells was achieved by RIPA buffer supplemented with anti-protease inhibitors and anti-phosphatase inhibitors. Cell media was changed and cells were washed with PBS 1X. Following; 200 µl of RIPA was directly added to each well followed by homogenization and vortexing. Samples were kept at – 20 °C for at least 2 hours. Then, samples were sonicated for 30 seconds followed by centrifugation at 12000 xg for 10 minutes at 4 °C. Finally, the supernatant containing protein lysate was taken after which proteins were denatured by Laemmli 2X with 10 % B-mercaptoethanol at 95 °C for 5 minutes. Protein concentrations were determined by BCA dosage assay (23235, Thermofisher Scientific).

Immunoblots

10 or 15 µg of total proteins were loaded and run on SDS-PAGE gels. Proteins were transferred from the gels to PVDF membranes followed by blocking with 5% milk or 5% BSA in TBST for normal or phosphorylated proteins, respectively. Membranes were incubated with antibodies overnight at 4°C according to the table below, ***Table M 3***, followed by an incubation with anti-mouse or anti-rabbit horseradish peroxidase conjugated secondary antibody. Detection of signals was achieved by West Pico ECL (ThermoFisher) using the camera Vilber.

Table M 3 List of Antibodies used for Western Blots

Antibody	Reference	Origin	Molecular Weight (kDa)	Concentration	Diluent
Actin	A2228, Sigma	Mouse	42	0.5 µg/ml	5% milk
ALOX15	ab119774, Abcam	Mouse	78	1 µg/ml	5% milk
Calnexin	2679, Cell Signaling	Rabbit	90	1 µg/ml	5% milk
CD206	Sc-376232, Santa Cruz	Mouse	160-170	1 µg/ml	5% milk
CSF1R/ MCSFR	3152, Cell Signaling	Rabbit	175	1 µg/ml	5% milk
p-CSF1R/ p-MCSF R (Tyr 723)	3155, Cell Signaling	Rabbit	175	1 µg/ml	3% BSA
p-CSF1R/ p-MCSF R (Tyr 546)	3083, Cell Signaling	Rabbit	175	1 µg/ml	3% BSA
p-CSF1R/ p-MCSF R (Tyr 699)	3399, Cell Signaling	Rabbit	175	1 µg/ml	3% BSA
p-CSF1R/ p-MCSF R (Tyr 809)	3154, Cell Signaling	Rabbit	175	1 µg/ml	3% BSA
DPD	Sc-271308 Santa Cruz	Mouse	110	0.6 µg/ml	5% milk
ERK1/2 (p44/42 MAPK)	4695, Cell Signaling	Rabbit	42, 44	0.5 µg/ml	5% milk
p-ERK1/2 (Thr202/ Tyr204)	4370, Cell Signaling	Rabbit	42, 44	1 µg/ml	3% BSA
HIF2a	Sc-46691, Santa Cruz	Mouse	115	1 µg/ml	5% milk
SP1	9389, Cell Signaling	Rabbit	90	1 µg/ml	5% milk

STAT6	Sc-271213, Santa Cruz	Mouse	120	1 µg/ml	5% milk
p-STAT6 (Tyr641)	Sc-136019, Santa Cruz	Mouse	105	1 µg/ml	3% BSA
TGM2	MA512739, Life Technologies	Mouse	78	1 µg/ml	5% milk

Human Tissue Handling

Primary tumoral tissues were sectioned from colons of CRC patients. Normal tissues were sectioned from same colons few centimeters away from the tumoral area. Tissues were kept and transported in ice in CMRL + Hams F12 media supplemented with glucose as well as antibiotics including penicillin-streptomycin and gentamicin and antifungal amphotericin B.

Ex-Vivo Tissue Culture

Tumoral and Normal tissues from CRC patients were cut into tiny pieces. Onto each well from the untreated 6-wells plate, 1 mL of Ex-vivo serum-free medium was added. Following, an insert of 0.4 µm diameter was put in each well, **Error! Reference source not found.**. Pieces of tissues was added on the insert and tissues were either incubated for 18 hours in the normal incubator or subjected to Edicotinib, BLZ945 at 10 µM to deplete TAMs and then incubated for 24 or 48 hours after which tissues were fixed for histological analysis. The composition of the ex-vivo culture media, adapted from Dame et al., 2016 is listed in the table below, ***Table M 4***.

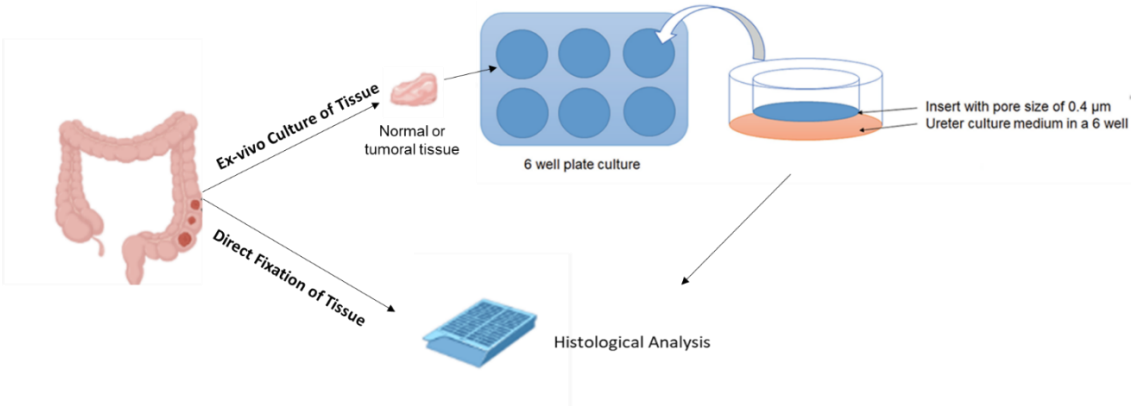

Figure M 7 Protocol of CRC Tumor Tissue Fixation and Ex-vivo Culture

Table M 4 List of Ex-Vivo Tissue Culture Components

Component	Reference	Percentage / Concentration
CMRL Media	21530027, Life Technologies	80 %
Hams' F12 Nutrient Mix	31765068, Life Technologies	20 %
Glutamax	35050061, Life Technologies	18 mM
Glucose	G7021, Sigma	25 mM
Insulin from bovine pancreas	I6634, Sigma	10 µg/mL
Glucagon	G2044, Sigma	50 ng/mL
Sodium Selenite	S5261, Sigma	0.1 µM
Zinc sulfate	Z0251, Sigma	3 µM
Menandione sodium bisulfate	M2518, Sigma	145 nM
a-tocepherol acetate	T1157, Sigma	45 nM
3,3',5-Triiodo-L-thyronine sodium salt	T5516, Sigma	0.5 ng/mL
Hydrocortisone	H0888, Sigma	3 µg/mL
Bovine Serum Albumin	A9576, Sigma	1 mg/mL
Bovine pituitary extract	P1476, Sigma	50 µg/mL
Gentamicin	10977035, Life Technologies	50 µg/mL

Tissue Fixation and Paraffin Embedding

Tissues directly sectioned from CRC patients or ex-vivo cultured were fixed in 4% formaldehyde for 24 hours. Following, tissues were put in tissue cassettes and sent to the histology and pathology department for paraffin embedding and tissue cutting.

Immunohistochemistry

A total of 3-mm-thick consecutive tissue sections were prepared from formalin-fixed and paraffin-embedded tissues. Deparaffinization, rehydration, antigen retrieval, and peroxidase blocking were performed on a fully automated system BENCHMARK ULTRA (Roche) according to manufacturer recommendations. The sections were incubated with the following primary antibodies: anti-CD68 clone Kp1 (Dako) and anti-DPD (Thermo Fisher Scientific). Revelation was performed using the Ultraview DAB revelation kit (Roche). Nuclei were counterstained with hematoxylin solution (Dako). Images were captured using an APERIO ATS scanner (Leica).

Immunfluorescence

Formalin-fixed and paraffin-embedded human tissue samples from either primary colon tumors or metastases liver were sectioned at 3 mm thickness. Samples were deparaffinized by xylene and hydrated by baths of decreasing concentrations of ethanol. Antigen retrieval was achieved using IHC-TekTM Epitope Retrieval Steamer Set (IW-1102, IHCworld) in IHC-TekTM Epitope Retrieval buffer (IW-1100, IHCworld) for 40 minutes. Nonspecific binding sites were blocked by 1% BSA in PBS. Samples were incubated with the primary antibodies: Monoclonal Mouse anti-Human CD68 clone PG-M1 at 0.4 mg/mL, Mouse anti-Human CD163 clone EDHu-1 at 10 mg/mL, anti-Human HIF2a at 4 mg/mL and DPD polyclonal antibody at 3 mg/mL for 1 hour at room temperature followed by an incubation of secondary antibodies: Alexa Fluor 488 goat anti-mouse IgG (H+L) and Alexa Fluor 546 goat anti-rabbit IgG (H+L) both at 4 mg/mL for 30 minutes at room temperature. Nuclei were stained by Hoechst 33342 at 5 mg/mL for 5 minutes at room temperature. Images were captured under 20 magnification using ApoTome microscope (Carl Zeiss) equipped with a camera AxioCam MRm, collected by AxioVision software and analyzed using ImageJ software.

Atomic Force Microscopy

Principle of the technique

Atomic Force Microscopy (AFM) is a noteworthy technique that studies live cells' properties including their ability to deform. It provides insights about the elasticity of cells as well as tissues. The main functional parts of the AFM are the cantilever containing a probed tip, a detection system and a system that ensures the scanning and positioning. The basic idea of AFM is that the attractive or repulsive forces that occur between the tip and the sample, cells or tissues, are depicted in the deflection that the cantilever does. This deflection is converted into a signal which is detected by a laser beam. As the cantilever deflects, the angle of the reflected laser beam changes and a spot is detected and the signal is then calculated. In other words, initially the laser beam is focused at the cantilever tip. Then, as the cantilever is approaching the sample, interaction forces promotes the deflection of the cantilever moving the spot position of the deflected laser beam on the photodiode. The position of this spot delivers the displacement of the cantilever. This displacement is then converted into a force using Hooke's law reflected by the formula: $\boldsymbol{F = k \times z}$, where F is the force (N), k is the spring constant of the cantilever (N/m) and z is the displacement (m).

Cell Preparation and Treatment

200,000 THP1 cells were differentiated into macrophages with 20 nM of PMA for 48 hours on a treated petri dish. Following, media was changed and fully differentiated macrophages were treated with Edicotinib or BLZ945 at 3µM for 48 hours. Afterwards and before AFM measurement, media was changed, cells were washed with warm PBS 1X and then 2 mL of warm RPMI with 10% FBS media was added on the cells.

AFM Measurements

AFM measurements were done using the JPK Nanowizard (Bruker) with MLCT-BIO-D cantilever (Bruker) which is a triangular pyramidal tip of 0.03 N/m spring constant. Force spectroscopy measurements were done on 15 to 20 cells for each sample where 9 force curves, corresponding to function of force versus tip-sample distance, were generated from each cell. 1 nN force was applied with a Z length of 5 µm and Z speed of 5 µm/s.

Data Analysis

Force curves were analyzed using JPKSPM Data Processing. Curves were fitted based on Hertz-fit model. Data were collected and then Young's Modulus, modulus of elasticity in tension or compression which reflects the stiffness of the cells, was obtained, thanks to Jupyter Notebook from Anaconda which is a Python distribution that is used for data sciences collection and analysis.

Statistical Analyses

Statistics were performed using Graph Pad Prism 7 (Graph Pad Software Inc). When two groups were compared, we used a two-tailed student's t test for a normal distribution and a Mann-Whitney non parametric test otherwise. When more than two groups were compared, we used a one-way ANOVA analysis with a Tukey post hoc test. All group numbers and values of the likelihood of data according to a null-hypothesis (p-value) are presented within the Figures.

Discussion and Perspectives

Cancerous cells are not the only components that make up solid tumors (Hui & Chen, 2015). However, solid tumors comprise a complex, dynamic and heterogeneous network of cells, secretions and extracellular matrix, which make up the tumor microenvironment (TME). The components of the TME collectively influence the development, progression, metastasis of tumors as well as their resistance to therapies. Recent advances in tumor biology have demonstrated the cross-talk between the components of the TME which provides a suitable environment in the favor of the tumor (Petrova et al., 2018). Immune cells are one of the major important parameters within TME that have been studied. Of these cells, tumor associated macrophages constitute the largest population.

Macrophages play important functions including phagocytosis, efferocytosis, antigen presentation, tissue remodeling and wound healing (Okabe & Medzhitov, 2016). In the context of cancer, macrophages play distinct roles in tumor development, neoangiogenesis, chemoresistance or inhibiting the growth of the tumor. These different and opposing functions that macrophages display is due to their plastic phenotype and their ability to respond to any stimuli (Murray, 2017). Recently, macrophages have been found to interfere in the resistance of tumors against chemotherapies. By depleting macrophages from the tumor in mice models, chemosensitivity of the tumor is reestablished (Ruffell & Coussens, 2015). For instance, it was demonstrated that macrophages (RAW264.7 implanted in mice) promote chemoresistance in CRC through a IL6/STAT3 dependent mechanism (Yin et al., 2017). Moreover, within the TME, tissue oxygenation is an important parameter which affects the state of the tumor (Foster et al., 2014). Although several studies have reported that hypoxia plays a role in chemoresistance, it remains an underappreciated parameter in tumor biology studies. It has been previously demonstrated in our lab that hypoxia modulates and modifies the biology of macrophages as well their functions. In this context, we proved that hypoxia modulates the ability of macrophages to eliminate apoptotic cells.

Thus, taking the complexity of the TME into account as well knowing that colon tumors are exposed to a hypoxic environment, we studied and explored impact of hypoxia on driving the role of macrophages in chemoresistance mechanisms in CRC (Keeley & Mann, 2019). When coculturing macrophages with colon cancer cell lines in normoxia and hypoxia, we showed a chemoresistance profile mediated by macrophages in hypoxic conditions. We then proved that this mechanism is directly linked to hypoxic macrophages. Exploring the mechanism by which hypoxic macrophages confers chemoresistance, we studied the whole proteome of hypoxic and normoxic macrophages. We interestingly found that the expression of dihydropyrimidine dehydrogenase (DPD) is strongly and significantly upregulated in hypoxic macrophages compared to normoxic cells. DPD is a rate limiting enzyme in the catabolism of fluorouracils (Diasio, 1998). Although, it has been shown previously that this enzyme, which is highly expressed in the liver, is responsible for 5-fluorouracil (5-FU) availability in the blood, no studies have showed the implication of DPD in human macrophages in TME. Being the first to explore and prove that hypoxia upregulates the expression of DPD in macrophages conferring chemoresistance against 5-FU, we demonstrated

that this upregulation is controlled at the translational level only. We showed that this upregulation of DPD expression is mediated by the hypoxic translation complex eIF4E2, which was previously demonstrated to be an important complex implicated in the translation of several hypoxic proteins, and the stabilization of HIF-2α (P. Lee et al., 2020). Moreover, we further proved this by coimmunostaining of DPD and HIF-2α in tumoral tissues from primary CRC and liver metastases patients.

Moreover, the expression of DPD in cancerous cells is considered as a marker that predicts chemoresistance. However, we showed that the expression of DPD in colon cancer cells is relatively low compared to the strong expression in macrophages. We further confirmed the sole expression of DPD by macrophages in tumoral tissues from primary CRC and liver metastases patients as almost all DPD positive cells were CD68+ cells, which are macrophages. This emphasizes on the important role that hypoxic macrophages display in the chemoresistance in CRC.

It is common and known that several mice *invivo* models have been developed for studying tumor development and progression as well as for the exploration of chemoresistance (Rottenberg & Borst, 2012). Although, these models gave promising results, they remained questionable when translating them to humans. In our study, we have interestingly showed that the expression of DPD in macrophages is exclusively related to humans, as our studies have shown that rodent's macrophages including mice and rats do not express DPD. To understand the reason behind this null expression of DPD in mice macrophages, we demonstrated that an epigenetic mechanism by the hypermethylation of *dpyd* promoter could be in part responsible for the absence of DPD in mice macrophages. These findings let us reassess and further explore several previous mice models in this context.

To further validate the chemoresistance mechanism that is induced by hypoxic macrophages, we developed an *in vivo* mice model humanized to DPD. In our model, mice macrophages were transduced by human DPD. This model validated the 5-FU chemoresistance as the assessment of the tumor volume and size in mice expressing human DPD demonstrated a development profile even though 5-FU was administered. However, this developed chemoresistance was reverted when using a specific DPD inhibitor, Gimeracil.

These studies showed new and important findings, which shed lights on the importance of the components of the TME including TAMs and hypoxia. Further studies should be carried out to confirm the relevance of our observations in clinics. Importantly, these studies pave the way to develop a way to assess and predict the response to 5-FU in CRC, as the expression of DPD in macrophages could be used as a predictive marker.

Having proved the importance of macrophages in the mechanism of chemoresistance in CRC, we next sought to target these cells in real tumoral tissues from CRC patients. Thus, we aimed to develop a relevant model mimicking a real tumor. Several mechanisms have been developed and

tested to target macrophages. These include the usage of clodronate liposome or antagonists against CSF-1R. For that purpose, an *ex-vivo* tissue culture protocol was developed using a serum-free culture media adapted from (Dame et al., 2010). Tissue samples sectioned from CRC patients were cultured in this system for 48 hours and then the morphology of these tissues was assessed by Hematoxylin and Eosin staining comparing them with directly fixed tissues. In addition, macrophages were targeted using clodronate liposome and M-CSF R antagonists, Edicotinib and BLZ945. Unfortunately, the morphology of the *ex-vivo* cultured tissues was very difficult to maintain as expected and the depletion assessed by a CD68 staining was not successful. We then optimized the *ex-vivo* culture protocol by decreasing the culture duration from 48 to 18 hours authorizing the maintenance of the tissue morphology . However, incubation for a shorter period of time did not result in successful targeting of macrophages as a large population of macrophages was still present in the treated ex-vivo cultured tissues. This had led us to explore the efficiency of these antagonists on primary human macrophages *in vitro*.

Assessing the effect of targeting M-CSF R in human monocyte-derived macrophages, we proved that one peculiar antagonist, Edicotinib, significantly and strongly downregulates the protein expression of DPD after 48 hours treatment in hypoxia, despite not succeeding to deplete the macrophages. This downregulation was not observed in any other used M-CSF R such as BLZ945, Pexidartinib, PLX5622, GW2580 or Ki20227. Moreover, we validated this inhibitory effect on THP1 macrophage model. THP1 cells are widely used as a macrophage model due to their ability to mimic macrophages by being differentiated by PMA. Our results confirm that Edicotinib specifically and significantly downregulates the protein expression of DPD. Due to similar action of Edicotinib, we used THP1 macrophage model in some of our experiments.

Next, we assessed whether all of these antagonists exert the same function on the M-CSF R pathway. Thus, we checked the expression of phosphorylation of M-CSF R during the very first minutes prior to stimulation with MCSF with the antagonists after starving the macrophages overnight. These experiments were carried out at 4°C, as it was previously reported that the phosphorylation of the receptor is maintained at 4°C due to the reduced activity of protein tyrosine phosphatases (Yeung & Stanley, 2003). We proved the action of MCSF in driving the phosphorylation of Tyrosine 723 of the receptor upon its addition. However, the phosphorylation of the receptor was found inhibited in macrophages treated with M-CSF R antagonists. These results show that all of these antagonists are functioning at the level of M-CSF R, but only Edicotinib is able to downregulate the activity of DPD. This difference in the actions of these antagonists could explain the reason behind the absence of a strong clinical efficiency and benefit of using these antagonists as monotherapies (Cannarile et al., 2017). Having proved this and based on their half maximal inhibitory concentration (IC50), we chose two of the most potent CSF-1R antagonists, Edicotinib and BLZ945, for our further studies.

It is noteworthy to mention that in addition to its ability to target M-CSF R, Edicotinib as well as the other mentioned M-CSF R antagonists are able to target Flt3 and c-kit (Cannarile et al., 2017).

However, our previous data demonstrate that human macrophages do not express Flt3 and c-kit. This shows so far that these antagonists are acting at the M-CSF R level in macrophages.

Because DPD is a rate limiting enzyme in the catabolism of 5-FU, its activity is directly related to its ability to catabolize 5-FU into dihyroflourouracil (5-FUH2). Thus, we assessed the activity of DPD by measuring the ratio of dihydrouracil (UH2) to that of uracil (U) (UH2/U) in the supernatants from macrophages treated with Edicotinib, BLZ945 or vehicle for 48 hours. Results have further confirmed and demonstrated that Edicotinib selectively inhibits the protein expression and the activity of DPD.

These interesting and crucial findings demonstrate a promising way to overcome the chemoresistance to 5-FU in CRC which is driven by hypoxic macrophages. To confirm the functionality and relevance of our findings, we explored whether Edicotinib treatment reverts the chemoresistance to 5-FU in two distinct colon cancer cell lines: RKO and HT-29. Culturing colon cancer cell lines with macrophage conditioned medium with 5-FU (5-FU MCM) with Edicotinib, BLZ945 or vehicle demonstrated that Edicotinib 5-FU MCM significantly restored the chemosensitivity of RKO and HT29 cells towards 5-FU. This proves the efficiency of Edicotinib to block the oxygen-controlled chemoresistance driven by macrophages in CRC. These promising findings open the way in clinics not only to use the expression of DPD in macrophages as a predictive marker to chemoresistance, but also to reestablish the chemosensitivity to 5-FU by targeting DPD in macrophages using Edicotinib.

Moreover, we want to further validate the effect of Edicotinib on the expression of DPD in real tumor associated macrophages (TAMs) extracted from tumoral tissues from CRC patients. We have already developed a protocol to isolate CD163+ TAMs from tumoral tissues. In addition to this, we are currently developing an *in vivo* mice model where human macrophages and human cancer cells are implanted. We want to test the relevance of Edicotinib as a promising therapeutic treatment along with 5-FU in this model to further validate the effect of Edicotinib in restoring the sensitivity of cancerous cells towards 5-FU.

In addition, because these antagonists are widely used in clinics to target and deplete macrophages, we wanted to assess the effect of these antagonists on the cytotoxicity of macrophages. Several approaches were carried out. We performed Annexin V/7AAD staining as well as MTT assay where both approaches showed that the concentration of Edicotinib and BLZ945 that we have used to target DPD in macrophages do not engage their apoptosis and are not toxic to macrophages. These results are quite important to prove that Edicotinib is able to reprogram macrophages metabolically without leading to its death. Furthermore, we challenged the macrophages, which were previously treated with Edicotinib with LPS stimulation to check whether these cells are able to maintain their functions and respond normally to any stimuli. It is known that macrophages stimulated with LPS secrete high levels of TNF-α. Thus, we assessed the concentrations of secreted TNF-α from the supernatants of macrophages treated or not with Edicotinib and BLZ945. We demonstrated that macrophages, after their treatment, still maintain their functions. These findings

were important to evidence that Edicotinib is not toxic to macrophages and can be used to reprogram macrophages metabolically.

Next, we sought to understand the mechanism underlying the modification of the expression of DPD by Edicotinib. It was demonstrated previously in cancerous cells that SP1 is a transcription factor driving the transcription of *DPYD* (X. Zhang et al., 2006). Moreover, it has been demonstrated that in THP1, which is a human monocytic cell line, SP1 is activated and translocated to the nucleus by the activation of ERK signaling (Curry et al., 2008). Because ERK pathway is one of the most important pathways activated downstream M-CSF R and because Edicotinib is known to inhibit the phosphorylation of ERK, we hypothesized that the expression of DPD in human macrophages is controlled by M-CSF R / ERK / SP1. Having validated the inhibitory effect of Edicotinib on DPD, we next assessed whether Edicotinib interferes in ERK pathway. In human macrophages, we demonstrated that Edicotinib, but not BLZ945, significantly blocks the phosphorylation of ERK after 48 hours which was in parallel with its inhibition of DPD. This result led us to directly evaluate the implication of ERK1/2 in DPD expression by assessing the protein expression of DPD upon inhibiting MEK, which is upstream of ERK1/2, by U0126. Unexpectedly, results showed that U0126 did not modulate the expression of DPD. These findings postulate that Edicotinib exerts its inhibitory effect on DPD independently from ERK1/2.

Then, we assessed whether SP1 is a transcription factor implicated in the expression of DPD. We knocked out the expression of SP1 by siRNA against SP1 and assessed the protein expression of DPD following 48 hours in hypoxia and normoxia. Results did not reveal any significant modulation in the expression of DPD. Moreover, SP1 and SP3 have been shown in cancerous cells to drive the transcription of *DPYD*. Based on that, we assessed the expression of DPD in macrophages whose SP1, SP3 or SP1 and SP3 were knocked out. Results did not show any modification in DPD expression. These results clearly demonstrate that SP1 is not the transcription factor driving the expression of DPD in human macrophages. PU.1 was reported to be implicated in the transcription of *DPYD*, as it was shown that in cancerous cells histone H3K27me3 blocks the binding of PU.1 on *DPYD* promoter inhibiting its transcription (Wu et al., 2016). Trying to explore the implication of PU.1 in the expression of DPD in macrophages, PU.1 was knocked out by siPU.1 transfection. As an important transcription factor in macrophage's survival, knocking out PU.1 engaged the death of macrophages. Finally, the implication of PU.1 as a transcription factor for *DPYD* in human macrophages should be deeply explored. The expression of PU.1 and its localization within macrophages should be assessed upon Edicotinib treatment of macrophages.

Nevertheless, we wanted to explore whether Edicotinib regulates the expression of DPD at the transcriptional or translational level. We found that the protein expression of DPD is downregulated in hypoxia gradually at 6 hours, 24 hours and 48 hours. This observation was not shown at the mRNA level as mRNA level of DPD was revealed to be significantly downregulated only after 48 hours exposure to Edicotinib. This led us to hypothesize that Edicotinib downreglates DPD at the translational level rather than at the transcriptional level, at least during the first exposure time points. We already showed that in hypoxia, the protein expression of HIF2-α is

upregulated. This is in contradiction with its mRNA expression as the mRNA levels is downregulated. These data suggest the presence of control mechanism by HIF-2α, which was not known yet. Interestingly, we discovered that Edicotinib downregulates the protein expression of HIF-2α during the transition from normoxia to hypoxia. Moreover, our data from RNA sequencing show that the mRNA expression of *EPAS1* (HIF-2α gene) is significantly upregulated in macrophages treated with Edicotinib. These results interestingly suggest that the upregulation of mRNA expression of *EPAS1* by Edicotinib is due to the destabilization of the HIF-2α protein.

In addition, results have demonstrated that Edicotinib significantly downregulates the mRNA expression of several genes such as CD206, TGM2 and CD163 which are known to be M2 macrophages-related genes (Court et al., 2019). This led us to reassess this at the protein level by polarizing macrophages towards an M2-like phenotype induced by IL-4 in presence or absence of Edicotinib and BLZ945.

Previous studies have shown the usage of CSF-1R antagonists in the reprogramming of macrophages towards an anti-tumoral phenotype. For instance, in a mouse model of pancreatic and ductal cancer, blockage of CSF-1R enhances the antigen presentation ability of macrophages and facilitates the T-cell antitumor response (Zhu et al., 2014). Additionally, in a mice sarcoma mode, Pexidartinib was reported to exert an anti-tumor effect as the *in vitro* blockade of CSF-1R in TAMs resulted in a decreased viability and chemotaxis of macrophages as well as its reprogramming toward a M1-like phenotype (T. Fujiwara et al., 2021). In this regard, our RNA sequencing data demonstrated that Edicotinib significantly downregulates the protein expression of IL4-induced-M2 macrophages such as CD206, TGM2 and ALOX15. This was not observed in macrophages treated with BLZ945, although it was reported in some studies, including that of mice glioma model that BLZ945 reduces the M2 polarization (Pyonteck et al., 2013). Moreover, no studies to date have explored or reported the consequences of Edicotinib on macrophage's reprogramming in this regard. Our results clearly show differences in the actions of these antagonists and importantly shed lights on the biological difference between mice and human macrophages which we already demonstrated in regards to DPD expression. These findings encourage us to reassess several mice models used for clinical studies and insist on the differences between the actions of the present M-CSF R antagonists.

Nevertheless, it is noteworthy to mention that our lab previously demonstrated that ALOX15 is upregulated in M2 macrophages under hypoxic environment (Court et al., 2017). Moreover, it is reported that the expression of ALOX15 along with other IL4-induced M2 macrophages-related proteins are regulated by the transcription factor STAT6 (Sica & Mantovani, 2012). In that concern, we demonstrated that the phosphorylation of STAT6 is blocked by Edicotinib explaining the significant and strong inhibition of CD206, TGM2 and ALOX15 in IL4-induced M2 macrophages exposed to Edicotinib. Finally, we demonstrated the relevance of this effect using tumor educated macrophages, which are macrophages exposed to the environment of RKO colon cancer cells. These results evidently demonstrate that Edicotinib reprograms macrophages by inhibiting its M2-like phenotype and thus prove that this antagonist not only it reverts the

chemoresistance against 5-FU but also reprograms macrophages. Insightful of the studies that demonstrate that M2 TAMs are associated with poor prognosis and that their reprogramming towards an M1-like phenotype improves the antitumoral effect (Yahaya et al., 2019), our findings manifestly point out that Edicotinib, by reprogramming macrophages, could be a promising therapeutic strategy.

Further to this, our experiments that aimed to study the effect of M-CSF R antagonists on reprograming of macrophages were carried out without any external M-CSF. Yet, Edicotinib was able to modulate the biology of macrophages. However, it is known that macrophages secrete M-CSF in an autocrine manner (Achkova & Maher, 2016) so this could be explained by the presence of an autocrine secretion of M-CSF. Moreover, in the context of cancer, cancerous cells secrete M-CSF recruiting macrophages and promote their pro-tumoral functions (DeNardo et al., 2011). We demonstrated that Edicotinib reprograms TEMs which are macrophages educated to the RKO colon cancer cell supernatants. In this concern, assessing the levels of M-CSF secreted from cancerous cells as well those expected to be autocrine secreted from macrophages should be evaluated.

Knowing that Edicotinib inhibits the phosphorylation of ERK1/2 and owing to the findings that reported that IL4-induced STAT6 phosphorylated is regulated by ERK1/2 in lymphoid cells, we explored whether inhibiting MEK interferes with the phosphorylation of STAT6 after 6 hours of inhibition of phosphorylation of ERK. Our results demonstrated that the inhibition of the phosphorylation of STAT6 is independent from ERK1/2 in human macrophages, at least for the time point that we studied. This finding requires further investigation for longer incubation time with MEK inhibitor, as we discovered that the inhibition of phosphorylation of STAT6 by Edicotinib at 6 hours is not achieved as compared to 24 and 48 hours. These findings suggest the probability of activation of phosphatases by Edicotinib, which will be assessed in order to better understand the main mechanism behind this inhibition.

In addition to this, RNA sequencing results showed that Edicotinib modulates various genes in macrophages compared to BLZ945. From these downregulated genes by Edicotinib, GO term analysis further confirmed the inhibitory effect that Edicotinib display on ERK1/2 signaling. Interestingly, the cholesterol metabolism was also shown to be modulated by Edicotinib. Cholesterol metabolism is important within the TME. Cancerous cells favor the efflux of cholesterol from macrophages in the favor of the tumor (Vats et al., 2006). Indeed, it is known that the metabolism of fatty acids shape TAMs whereby M2-like TAMs exhibit elevated consumption of fatty acids. This is due to IL-4 – driven activation of signal transducer and activator of transcription 6 (STAT6) accompanied by increased fatty acid oxidation. We found that most of the enzymes implicated in cholesterol metabolism were downregulated by Edicotinib compared to vehicle and BLZ945. Nevertheless, SREBP2 is a transcription factor that controls most enzymes in the cholesterol pathway (Madison, 2016). We demonstrated that the modulation of cholesterol metabolism by Edicotinib is dependent on the expression of SREBP2 as its mRNA was significantly downregulated. This result has to be confirmed at the protein level. Thus, in our

current study, we demonstrated that Edicotinib prevents the efflux of cholesterol from macrophages in addition to the inhibitory role that it plays on IL-4 induced STAT6 pathway. These findings demonstrate that Edicotinib reprograms the metabolism of macrophages away from the tumor-promoting role. In addition, as cholesterol is related to the β-oxidation of fatty acids, we investigated the fatty acid synthesis in macrophages treated or not with Edicotinib or BLZ945. We found that Edicotinib ceases the accumulation of fatty acids in macrophages, which is driven by hypoxia. Moreover, our studies will next focus on deeply assessing the impact of Edicotinib on the metabolism of cholesterol by evaluating its efflux of and measuring its levels in macrophages.

Moreover, it is known that cholesterol plays an important function in maintain the rigidity of cell membranes (Chakraborty et al., 2020). We then assessed the effect of Edicotinib and BLZ945 on the stiffness of macrophages Using atomic force microscopy, we showed that Edicotinib renders macrophages softer than those treated with vehicle or BLZ945. This softening of cells, or decrease in their membrane rigidity, is explained by the decrease of the cholesterol content due to Edicotinib. These results further confirm the metabolic reprogramming that Edicotinib acts on macrophages by inhibiting cholesterol synthesis.

These paramount findings shed lights on the importance of the tumor microenvironment generally, and macrophage specifically in the development and progression of the tumor. We have clearly demonstrated that a hypoxic tumor microenvironment upregulates the protein expression of DPD in macrophages conferring chemoresistance in CRC. This finding paves the way to consider DPD and assess its expression in macrophages in patients with CRC to better understand the chemotherapy outcome. We further discovered a way to target this chemoresistance by metabolically reprogramming macrophages using a special M-CSF R antagonist, Edicotinib (Figure 15). This finding is crucial and provides a promising strategy in colorectal cancer treatment.

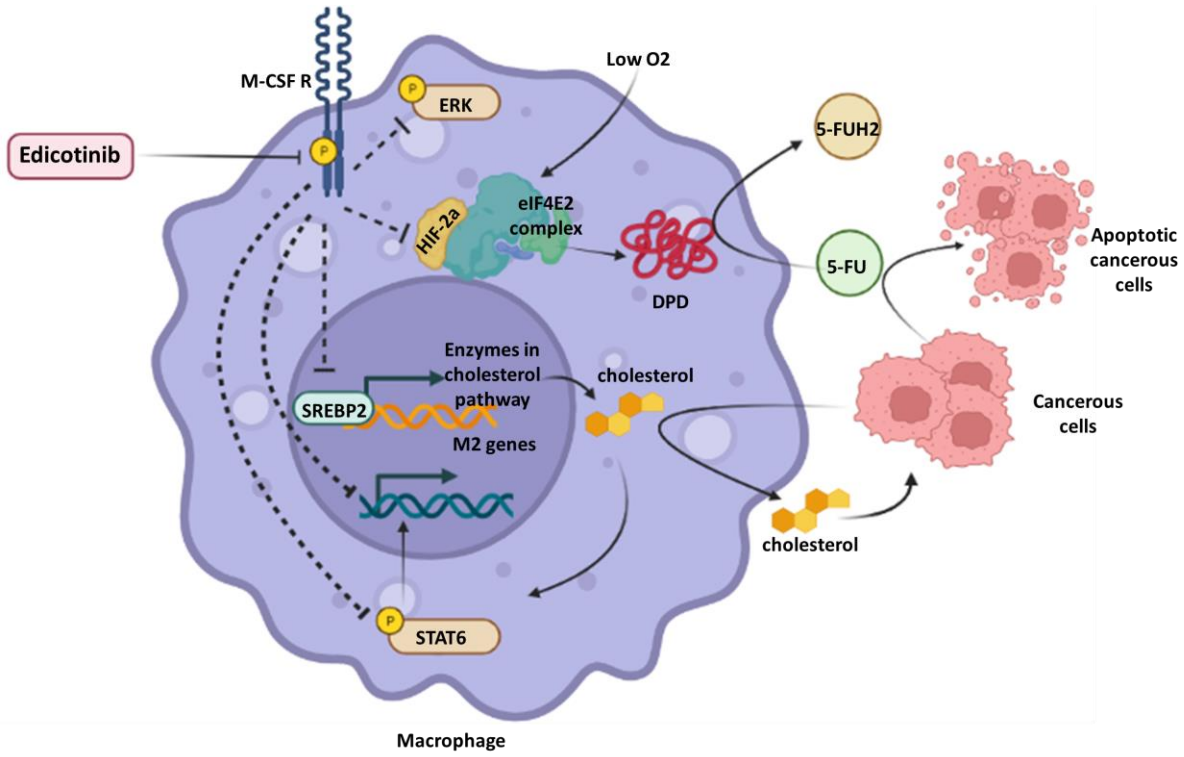

Figure 15 Metabolic Reprogramming of Macrophages by Edicotinib

Dotted inhibiting arrow: Putative indirect effect of Edicotinib through M-CSF R

Plane arrow: Direct effect

Bibliography

Achkova, D., & Maher, J. (2016). Role of the colony-stimulating factor (CSF)/CSF-1 receptor axis in cancer. *Biochemical Society Transactions*, *44*(2), 333–341. https://doi.org/10.1042/BST20150245

Adams, S., Kozhaya, L., Martiniuk, F., Meng, T.-C., Chiriboga, L., Liebes, L., Hochman, T., Shuman, N., Axelrod, D., Speyer, J., Novik, Y., Tiersten, A., Goldberg, J. D., Formenti, S. C., Bhardwaj, N., Unutmaz, D., & Demaria, S. (2012). Topical TLR7 agonist imiquimod can induce immune-mediated rejection of skin metastases in patients with breast cancer. *Clinical Cancer Research: An Official Journal of the American Association for Cancer Research*, *18*(24), 6748–6757. https://doi.org/10.1158/1078-0432.CCR-12-1149

Allavena, P., Sica, A., Solinas, G., Porta, C., & Mantovani, A. (2008). The inflammatory micro-environment in tumor progression: The role of tumor-associated macrophages. *Critical Reviews in Oncology/Hematology*, *66*(1), 1–9. https://doi.org/10.1016/j.critrevonc.2007.07.004

Allen, W. E., Jones, G. E., Pollard, J. W., & Ridley, A. J. (1997). Rho, Rac and Cdc42 regulate actin organization and cell adhesion in macrophages. *Journal of Cell Science*, *110 (Pt 6)*, 707–720. https://doi.org/10.1242/jcs.110.6.707

Alleva, D. G., Burger, C. J., & Elgert, K. D. (1993). Tumor growth increases Ia- macrophage synthesis of tumor necrosis factor-alpha and prostaglandin E2: Changes in macrophage suppressor activity. *Journal of Leukocyte Biology*, *53*(5), 550–558. https://doi.org/10.1002/jlb.53.5.550

Baenke, F., Peck, B., Miess, H., & Schulze, A. (2013). Hooked on fat: The role of lipid synthesis in cancer metabolism and tumour development. *Disease Models & Mechanisms*, *6*(6), 1353–1363. https://doi.org/10.1242/dmm.011338

Balkwill, F., & Mantovani, A. (2001). Inflammation and cancer: Back to Virchow? *The Lancet*, *357*(9255), 539–545. https://doi.org/10.1016/S0140-6736(00)04046-0

Balkwill, F. R., Capasso, M., & Hagemann, T. (2012). The tumor microenvironment at a glance. *Journal of Cell Science*, *125*(23), 5591–5596. https://doi.org/10.1242/jcs.116392

Bashir, S., Sharma, Y., Elahi, A., & Khan, F. (2016). Macrophage polarization: The link between inflammation and related diseases. *Inflammation Research: Official Journal of the European Histamine Research Society ... [et Al.]*, *65*(1), 1–11. https://doi.org/10.1007/s00011-015-0874-1

Bendell, J. C., Tolcher, A. W., Jones, S. F., Beeram, M., Infante, J. R., Larsen, P., Rasor, K., Garrus, J. E., Li, J., Cable, P. L., Eberhardt, C., Schreiber, J., Rush, S., Wood, K. W., Barrett, E., & Patnaik, A. (2013). Abstract A252: A phase 1 study of ARRY-382, an oral inhibitor of colony-stimulating factor-1 receptor (CSF1R), in patients with advanced or metastatic cancers. *Molecular Cancer Therapeutics*, *12*(11_Supplement), A252. https://doi.org/10.1158/1535-7163.TARG-13-A252

Benner, B., Good, L., Quiroga, D., Schultz, T. E., Kassem, M., Carson, W. E., Cherian, M. A., Sardesai, S., & Wesolowski, R. (2020). Pexidartinib, a Novel Small Molecule CSF-1R Inhibitor in Use for Tenosynovial Giant Cell Tumor: A Systematic Review of Pre-Clinical and Clinical Development . *Drug Design, Development and Therapy*, *14*, 1693–1704. https://doi.org/10.2147/DDDT.S253232

Bernsmeier, C., van der Merwe, S., & Périanin, A. (2020). Innate immune cells in cirrhosis. *Journal of Hepatology*, *73*(1), 186–201. https://doi.org/10.1016/j.jhep.2020.03.027

Blondy, S., David, V., Verdier, M., Mathonnet, M., Perraud, A., & Christou, N. (2020). 5-Fluorouracil resistance mechanisms in colorectal cancer: From classical pathways to promising processes. *Cancer Science*, *111*(9), 3142–3154. https://doi.org/10.1111/cas.14532

Bocci, G., Barbara, C., Vannozzi, F., Di Paolo, A., Melosi, A., Barsanti, G., Allegrini, G., Falcone, A., Del Tacca, M., & Danesi, R. (2006). A pharmacokinetic-based test to prevent severe 5-fluorouracil toxicity. *Clinical Pharmacology and Therapeutics*, *80*(4), 384–395. https://doi.org/10.1016/j.clpt.2006.06.007

Bonifer, C., & Hume, D. A. (2008). The transcriptional regulation of the Colony-Stimulating Factor 1 Receptor (csf1r) gene during hematopoiesis. *Frontiers in Bioscience: A Journal and Virtual Library*, *13*, 549–560. https://doi.org/10.2741/2700

Bosco, M. C., Reffo, G., Puppo, M., & Varesio, L. (2004). Hypoxia inhibits the expression of the CCR5 chemokine receptor in macrophages. *Cellular Immunology*, *228*(1), 1–7. https://doi.org/10.1016/j.cellimm.2004.03.006

Bourgin, C., Bourette, R., Mouchiroud, G., & Arnaud, S. (2000). Expression of Mona (monocytic adapter) in myeloid progenitor cells results in increased and prolonged MAP kinase activation upon macrophage colony-stimulating factor stimulation. *FEBS Letters*, *480*(2–3), 113–117. https://doi.org/10.1016/s0014-5793(00)01906-2

Boutilier, A. J., & Elsawa, S. F. (2021). Macrophage Polarization States in the Tumor Microenvironment. *International Journal of Molecular Sciences*, *22*(13), Article 13. https://doi.org/10.3390/ijms22136995

Bowman, R. L., Klemm, F., Akkari, L., Pyonteck, S. M., Sevenich, L., Quail, D. F., Dhara, S., Simpson, K., Gardner, E. E., Iacobuzio-Donahue, C. A., Brennan, C. W., Tabar, V., Gutin, P. H., & Joyce, J. A. (2016). Macrophage Ontogeny Underlies Differences in Tumor-Specific Education in Brain Malignancies. *Cell Reports*, *17*(9), 2445–2459. https://doi.org/10.1016/j.celrep.2016.10.052

Bray, F., Ferlay, J., Soerjomataram, I., Siegel, R. L., Torre, L. A., & Jemal, A. (2018). Global cancer statistics 2018: GLOBOCAN estimates of incidence and mortality worldwide for 36 cancers in 185 countries. *CA: A Cancer Journal for Clinicians*, *68*(6), 394–424. https://doi.org/10.3322/caac.21492

Bronte, V., Brandau, S., Chen, S.-H., Colombo, M. P., Frey, A. B., Greten, T. F., Mandruzzato, S., Murray, P. J., Ochoa, A., Ostrand-Rosenberg, S., Rodriguez, P. C., Sica, A., Umansky, V., Vonderheide, R. H., & Gabrilovich, D. I. (2016). Recommendations for myeloid-derived suppressor cell nomenclature and characterization standards. *Nature Communications*, *7*, 12150. https://doi.org/10.1038/ncomms12150

Bruns, H., Büttner, M., Fabri, M., Mougiakakos, D., Bittenbring, J. T., Hoffmann, M. H., Beier, F., Pasemann, S., Jitschin, R., Hofmann, A. D., Neumann, F., Daniel, C., Maurberger, A., Kempkes, B., Amann, K., Mackensen, A., & Gerbitz, A. (2015). Vitamin D-dependent induction of cathelicidin in human macrophages results in cytotoxicity against high-grade B cell lymphoma. *Science Translational Medicine*, *7*(282), 282ra47. https://doi.org/10.1126/scitranslmed.aaa3230

Burke, B., Giannoudis, A., Corke, K. P., Gill, D., Wells, M., Ziegler-Heitbrock, L., & Lewis, C. E. (2003). Hypoxia-induced gene expression in human macrophages: Implications for ischemic tissues and hypoxia-regulated gene therapy. *The American Journal of Pathology*, *163*(4), 1233–1243. https://doi.org/10.1016/S0002-9440(10)63483-9

Butowski, N. A., Colman, H., De Groot, J. F., Omuro, A. M. P., Nayak, L., Cloughesy, T. F., Marimuthu, A., Perry, A., Phillips, J. J., West, B., Prados, M., Nolop, K. B., Hsu, H. H., & Ligon, K. L. (2014). A phase 2 study of orally administered PLX3397 in patients with recurrent glioblastoma. *Journal of Clinical Oncology*, *32*(15_suppl), 2023–2023. https://doi.org/10.1200/jco.2014.32.15_suppl.2023

Byrne, P. V., Guilbert, L. J., & Stanley, E. R. (1981). Distribution of cells bearing receptors for a colony-stimulating factor (CSF-1) in murine tissues. *The Journal of Cell Biology*, *91*(3 Pt 1), 848–853. https://doi.org/10.1083/jcb.91.3.848

Calvo, A., Joensuu, H., Sebastian, M., Naing, A., Bang, Y.-J., Martin, M., Roda, D., Hodi, F. S., Veloso, A., Mataraza, J., Baneyx, G., Guerreiro, N., Liao, S., Rabault, B., Fjaellskog, M.-L., & Cervantes, A. (2018). Phase Ib/II study of lacnotuzumab (MCS110) combined with spartalizumab (PDR001) in patients (pts) with advanced tumors. *Journal of Clinical Oncology*, *36*(15_suppl), 3014–3014. https://doi.org/10.1200/JCO.2018.36.15_suppl.3014

Cannarile, M. A., Weisser, M., Jacob, W., Jegg, A.-M., Ries, C. H., & Rüttinger, D. (2017). Colony-stimulating factor 1 receptor (CSF1R) inhibitors in cancer therapy. *Journal for ImmunoTherapy of Cancer*, *5*(1), 53. https://doi.org/10.1186/s40425-017-0257-y

Carmona-Fontaine, C., Deforet, M., Akkari, L., Thompson, C. B., Joyce, J. A., & Xavier, J. B. (2017). Metabolic origins of spatial organization in the tumor microenvironment. *Proceedings of the National Academy of Sciences*, *114*(11), 2934–2939. https://doi.org/10.1073/pnas.1700600114

Casazza, A., Laoui, D., Wenes, M., Rizzolio, S., Bassani, N., Mambretti, M., Deschoemaeker, S., Van Ginderachter, J. A., Tamagnone, L., & Mazzone, M. (2013). Impeding macrophage entry into hypoxic tumor areas by Sema3A/Nrp1 signaling blockade inhibits angiogenesis and restores antitumor immunity. *Cancer Cell*, *24*(6), 695–709. https://doi.org/10.1016/j.ccr.2013.11.007

Cassetta, L., Cassol, E., & Poli, G. (2011). Macrophage polarization in health and disease. *TheScientificWorldJournal*, *11*, 2391–2402. https://doi.org/10.1100/2011/213962

Chakraborty, S., Doktorova, M., Molugu, T. R., Heberle, F. A., Scott, H. L., Dzikovski, B., Nagao, M., Stingaciu, L.-R., Standaert, R. F., Barrera, F. N., Katsaras, J., Khelashvili, G., Brown, M. F., & Ashkar, R. (2020). How cholesterol stiffens unsaturated lipid membranes. *Proceedings of the National Academy of Sciences of the United States of America*, *117*(36), 21896–21905. https://doi.org/10.1073/pnas.2004807117

Chang, M., Hamilton, J. A., Scholz, G. M., Masendycz, P., Macaulay, S. L., & Elsegood, C. L. (2009). Phosphatidylinostitol-3 kinase and phospholipase C enhance CSF-1-dependent macrophage survival by controlling glucose uptake. *Cellular Signalling*, *21*(9), 1361–1369. https://doi.org/10.1016/j.cellsig.2009.04.003

Chen, X., Liu, H., Focia, P. J., Shim, A. H.-R., & He, X. (2008). Structure of macrophage colony stimulating factor bound to FMS: Diverse signaling assemblies of class III receptor tyrosine kinases. *Proceedings of the National Academy of Sciences of the United States of America*, *105*(47), 18267–18272. https://doi.org/10.1073/pnas.0807762105

Chihara, T., Suzu, S., Hassan, R., Chutiwitoonchai, N., Hiyoshi, M., Motoyoshi, K., Kimura, F., & Okada, S. (2010). IL-34 and M-CSF share the receptor Fms but are not identical in biological activity and signal activation. *Cell Death & Differentiation*, *17*(12), Article 12. https://doi.org/10.1038/cdd.2010.60

Chionh, F., Lau, D., Yeung, Y., Price, T., & Tebbutt, N. (2017). Oral versus intravenous fluoropyrimidines for colorectal cancer. *The Cochrane Database of Systematic Reviews*, *7*, CD008398. https://doi.org/10.1002/14651858.CD008398.pub2

Chitu, V., Nacu, V., Charles, J. F., Henne, W. M., McMahon, H. T., Nandi, S., Ketchum, H., Harris, R., Nakamura, M. C., & Stanley, E. R. (2012). PSTPIP2 deficiency in mice causes osteopenia and increased differentiation of multipotent myeloid precursors into osteoclasts. *Blood*, *120*(15), 3126–3135. https://doi.org/10.1182/blood-2012-04-425595

Chitu, V., Pixley, F. J., Macaluso, F., Larson, D. R., Condeelis, J., Yeung, Y.-G., & Stanley, E. R. (2005). The PCH family member MAYP/PSTPIP2 directly regulates F-actin bundling and enhances filopodia formation and motility in macrophages. *Molecular Biology of the Cell*, *16*(6), 2947–2959. https://doi.org/10.1091/mbc.e04-10-0914

Choi, J., Stradmann-Bellinghausen, B., Yakubov, E., Savaskan, N. E., & Régnier-Vigouroux, A. (2015). Glioblastoma cells induce differential glutamatergic gene expressions in human tumor-associated microglia/macrophages and monocyte-derived macrophages. *Cancer Biology & Therapy*, *16*(8), 1205–1213. https://doi.org/10.1080/15384047.2015.1056406

Choura, M., & Rebaï, A. (2011). Receptor tyrosine kinases: From biology to pathology. *Journal of Receptor and Signal Transduction Research*, *31*(6), 387–394. https://doi.org/10.3109/10799893.2011.625425

Ciaparrone, M., Quirino, M., Schinzari, G., Zannoni, G., Corsi, D. C., Vecchio, F. M., Cassano, A., La Torre, G., & Barone, C. (2006). Predictive role of thymidylate synthase, dihydropyrimidine dehydrogenase and thymidine phosphorylase expression in colorectal cancer patients receiving adjuvant 5-fluorouracil. *Oncology*, *70*(5), 366–377. https://doi.org/10.1159/000098110

Ciccolini, J., Mercier, C., Evrard, A., Dahan, L., Boyer, J.-C., Duffaud, F., Richard, K., Blanquicett, C., Milano, G., Blesius, A., Durand, A., Seitz, J.-F., Favre, R., & Lacarelle, B. (2006). A rapid and inexpensive method for anticipating severe toxicity to fluorouracil and fluorouracil-based chemotherapy. *Therapeutic Drug Monitoring*, *28*(5), 678–685. https://doi.org/10.1097/01.ftd.0000245771.82720.c7

Colegio, O. R., Chu, N.-Q., Szabo, A. L., Chu, T., Rhebergen, A. M., Jairam, V., Cyrus, N., Brokowski, C. E., Eisenbarth, S. C., Phillips, G. M., Cline, G. W., Phillips, A. J., & Medzhitov, R. (2014). Functional polarization of tumour-associated macrophages by tumour-derived lactic acid. *Nature*, *513*(7519), Article 7519. https://doi.org/10.1038/nature13490

Court, M., Malier, M., & Millet, A. (2019). 3D type I collagen environment leads up to a reassessment of the classification of human macrophage polarizations. *Biomaterials*, *208*, 98–109. https://doi.org/10.1016/j.biomaterials.2019.04.018

Court, M., Petre, G., Atifi, M. E., & Millet, A. (2017). Proteomic Signature Reveals Modulation of Human Macrophage Polarization and Functions Under Differing Environmental Oxygen Conditions. *Molecular & Cellular Proteomics: MCP*, *16*(12), 2153–2168. https://doi.org/10.1074/mcp.RA117.000082

Coussens, L., Van Beveren, C., Smith, D., Chen, E., Mitchell, R. L., Isacke, C. M., Verma, I. M., & Ullrich, A. (1986). Structural alteration of viral homologue of receptor proto-oncogene fms at carboxyl terminus. *Nature*, *320*(6059), 277–280. https://doi.org/10.1038/320277a0

Curry, J. M., Eubank, T. D., Roberts, R. D., Wang, Y., Pore, N., Maity, A., & Marsh, C. B. (2008). M-CSF signals through the MAPK/ERK pathway via Sp1 to induce VEGF production and induces angiogenesis in vivo. *PloS One*, *3*(10), e3405. https://doi.org/10.1371/journal.pone.0003405

Dabral, S., Muecke, C., Valasarajan, C., Schmoranzer, M., Wietelmann, A., Semenza, G. L., Meister, M., Muley, T., Seeger-Nukpezah, T., Samakovlis, C., Weissmann, N., Grimminger, F., Seeger, W., Savai, R., & Pullamsetti, S. S. (2019). A RASSF1A-HIF1α loop drives Warburg effect in cancer and pulmonary hypertension. *Nature Communications*, *10*, 2130. https://doi.org/10.1038/s41467-019-10044-z

Daher, G. C., Harris, B. E., & Diasio, R. B. (1990). Metabolism of pyrimidine analogues and their nucleosides. *Pharmacology & Therapeutics*, *48*(2), 189–222. https://doi.org/10.1016/0163-7258(90)90080-L

Dai, X.-M., Zong, X.-H., Sylvestre, V., & Stanley, E. R. (2004). Incomplete restoration of colony-stimulating factor 1 (CSF-1) function in CSF-1-deficient Csf1op/Csf1op mice by transgenic expression of cell surface CSF-1. *Blood*, *103*(3), 1114–1123. https://doi.org/10.1182/blood-2003-08-2739

Dame, M. K., Bhagavathula, N., Mankey, C., DaSilva, M., Paruchuri, T., Aslam, M. N., & Varani, J. (2010). Human colon tissue in organ culture: Preservation of normal and neoplastic characteristics. *In Vitro Cellular & Developmental Biology. Animal*, *46*(2), 114–122. https://doi.org/10.1007/s11626-009-9247-9

Daurkin, I., Eruslanov, E., Stoffs, T., Perrin, G. Q., Algood, C., Gilbert, S. M., Rosser, C. J., Su, L.-M., Vieweg, J., & Kusmartsev, S. (2011). Tumor-associated macrophages mediate immunosuppression in the renal cancer microenvironment by activating the 15-lipoxygenase-2 pathway. *Cancer Research*, *71*(20), 6400–6409. https://doi.org/10.1158/0008-5472.CAN-11-1261

Dekker, E., Tanis, P. J., Vleugels, J. L. A., Kasi, P. M., & Wallace, M. B. (2019). Colorectal cancer. *The Lancet*, *394*(10207), 1467–1480. https://doi.org/10.1016/S0140-6736(19)32319-0

DeNardo, D. G., Brennan, D. J., Rexhepaj, E., Ruffell, B., Shiao, S. L., Madden, S. F., Gallagher, W. M., Wadhwani, N., Keil, S. D., Junaid, S. A., Rugo, H. S., Hwang, E. S., Jirström, K., West, B. L., & Coussens, L. M. (2011). Leukocyte complexity predicts breast cancer survival and functionally regulates response to chemotherapy. *Cancer Discovery*, *1*(1), 54–67. https://doi.org/10.1158/2159-8274.CD-10-0028

De Palma, M., & Lewis, C. E. (2013). Macrophage Regulation of Tumor Responses to Anticancer Therapies. *Cancer Cell*, *23*(3), 277–286. https://doi.org/10.1016/j.ccr.2013.02.013

Diasio, R. B. (1998). The role of dihydropyrimidine dehydrogenase (DPD) modulation in 5-FU pharmacology. *Oncology (Williston Park, N.Y.)*, *12*(10 Suppl 7), 23–27.

Diasio, R. B., Beavers, T. L., & Carpenter, J. T. (1988). Familial deficiency of dihydropyrimidine dehydrogenase. Biochemical basis for familial pyrimidinemia and severe 5-fluorouracil-induced toxicity. *The Journal of Clinical Investigation*, *81*(1), 47–51. https://doi.org/10.1172/JCI113308

Dudek, A. Z., Yunis, C., Harrison, L. I., Kumar, S., Hawkinson, R., Cooley, S., Vasilakos, J. P., Gorski, K. S., & Miller, J. S. (2007). First in human phase I trial of 852A, a novel systemic toll-like receptor 7 agonist, to activate innate immune responses in patients with advanced cancer. *Clinical Cancer Research: An Official Journal of the American Association for Cancer Research*, *13*(23), 7119–7125. https://doi.org/10.1158/1078-0432.CCR-07-1443

Elegheert, J., Desfosses, A., Shkumatov, A. V., Wu, X., Bracke, N., Verstraete, K., Van Craenenbroeck, K., Brooks, B. R., Svergun, D. I., Vergauwen, B., Gutsche, I., & Savvides, S. N. (2011). Extracellular complexes of the hematopoietic human and mouse CSF-1 receptor are driven by common assembly principles. *Structure (London, England: 1993)*, *19*(12), 1762–1772. https://doi.org/10.1016/j.str.2011.10.012

Etienne, M. C., Lagrange, J. L., Dassonville, O., Fleming, R., Thyss, A., Renée, N., Schneider, M., Demard, F., & Milano, G. (1994). Population study of dihydropyrimidine dehydrogenase in cancer patients. *Journal of Clinical Oncology: Official Journal of the American Society of Clinical Oncology*, *12*(11), 2248–2253. https://doi.org/10.1200/JCO.1994.12.11.2248

Ezzeldin, H. H., Lee, A. M., Mattison, L. K., & Diasio, R. B. (2005). Methylation of the DPYD promoter: An alternative mechanism for dihydropyrimidine dehydrogenase deficiency in cancer patients. *Clinical Cancer Research: An Official Journal of the American Association for Cancer Research*, *11*(24 Pt 1), 8699–8705. https://doi.org/10.1158/1078-0432.CCR-05-1520

Felix, J., Elegheert, J., Gutsche, I., Shkumatov, A. V., Wen, Y., Bracke, N., Pannecoucke, E., Vandenberghe, I., Devreese, B., Svergun, D. I., Pauwels, E., Vergauwen, B., & Savvides, S. N. (2013). Human IL-34 and CSF-1 establish structurally similar extracellular assemblies with their common hematopoietic receptor. *Structure (London, England: 1993)*, *21*(4), 528–539. https://doi.org/10.1016/j.str.2013.01.018

Forsythe, J. A., Jiang, B. H., Iyer, N. V., Agani, F., Leung, S. W., Koos, R. D., & Semenza, G. L. (1996). Activation of vascular endothelial growth factor gene transcription by hypoxia-inducible factor 1. *Molecular and Cellular Biology*, *16*(9), 4604–4613. https://doi.org/10.1128/MCB.16.9.4604

Foster, J. G., Wong, S. C. K., & Sharp, T. V. (2014). The hypoxic tumor microenvironment: Driving the tumorigenesis of non-small-cell lung cancer. *Future Oncology (London, England)*, *10*(16), 2659–2674. https://doi.org/10.2217/fon.14.201

Franklin, R. A., Liao, W., Sarkar, A., Kim, M. V., Bivona, M. R., Liu, K., Pamer, E. G., & Li, M. O. (2014). The cellular and molecular origin of tumor-associated macrophages. *Science (New York, N.Y.)*, *344*(6186), 921–925. https://doi.org/10.1126/science.1252510

Franovic, A., Holterman, C. E., Payette, J., & Lee, S. (2009). Human cancers converge at the HIF-2alpha oncogenic axis. *Proceedings of the National Academy of Sciences of the United States of America*, *106*(50), 21306–21311. https://doi.org/10.1073/pnas.0906432106

Fujiwara, N., & Kobayashi, K. (2005). Macrophages in inflammation. *Current Drug Targets. Inflammation and Allergy*, *4*(3), 281–286. https://doi.org/10.2174/1568010054022024

Fujiwara, T., Yakoub, M. A., Chandler, A., Christ, A. B., Yang, G., Ouerfelli, O., Rajasekhar, V. K., Yoshida, A., Kondo, H., Hata, T., Tazawa, H., Dogan, Y., Moore, M. A. S., Fujiwara, T., Ozaki, T., Purdue, E., & Healey, J. H. (2021). CSF1/CSF1R Signaling Inhibitor Pexidartinib (PLX3397) Reprograms Tumor-Associated Macrophages and Stimulates T-cell Infiltration in the Sarcoma Microenvironment. *Molecular Cancer Therapeutics*, *20*(8), 1388–1399. https://doi.org/10.1158/1535-7163.MCT-20-0591

Gangoiti, P., Granado, M. H., Wang, S. W., Kong, J. Y., Steinbrecher, U. P., & Gómez-Muñoz, A. (2008). Ceramide 1-phosphate stimulates macrophage proliferation through activation of the PI3-kinase/PKB, JNK and ERK1/2 pathways. *Cellular Signalling*, *20*(4), 726–736. https://doi.org/10.1016/j.cellsig.2007.12.008

Gatenby, R. A., Gillies, R. J., & Brown, J. S. (2010). The evolutionary dynamics of cancer prevention. *Nature Reviews Cancer*, *10*(8), Article 8. https://doi.org/10.1038/nrc2892

Gautier, E. L., Shay, T., Miller, J., Greter, M., Jakubzick, C., Ivanov, S., Helft, J., Chow, A., Elpek, K. G., Gordonov, S., Mazloom, A. R., Ma'ayan, A., Chua, W.-J., Hansen, T. H., Turley, S. J., Merad, M., Randolph, G. J., & Immunological Genome Consortium. (2012). Gene-expression profiles and transcriptional regulatory pathways that underlie the identity and diversity of mouse tissue macrophages. *Nature Immunology*, *13*(11), 1118–1128. https://doi.org/10.1038/ni.2419

Genovese, M. C., Hsia, E., Belkowski, S. M., Chien, C., Masterson, T., Thurmond, R. L., Manthey, C. L., Yan, X. D., Ge, T., Franks, C., & Greenspan, A. (2015). Results from a Phase IIA Parallel Group Study of JNJ-40346527, an Oral CSF-1R Inhibitor, in Patients with Active Rheumatoid Arthritis despite Disease-modifying Antirheumatic Drug Therapy. *The Journal of Rheumatology*, *42*(10), 1752–1760. https://doi.org/10.3899/jrheum.141580

Gentek, R., Molawi, K., & Sieweke, M. H. (2014). Tissue macrophage identity and self-renewal. *Immunological Reviews*, *262*(1), 56–73. https://doi.org/10.1111/imr.12224

Gerlinger, M., Rowan, A. J., Horswell, S., Larkin, J., Endesfelder, D., Gronroos, E., Martinez, P., Matthews, N., Stewart, A., Tarpey, P., Varela, I., Phillimore, B., Begum, S., McDonald, N. Q., Butler, A., Jones, D., Raine, K., Latimer, C., Santos, C. R., … Swanton, C. (2012). Intratumor Heterogeneity and Branched Evolution Revealed by Multiregion Sequencing. *New England Journal of Medicine*, *366*(10), 883–892. https://doi.org/10.1056/NEJMoa1113205

Giacchetti, S., Perpoint, B., Zidani, R., Le Bail, N., Faggiuolo, R., Focan, C., Chollet, P., Llory, J. F., Letourneau, Y., Coudert, B., Bertheaut-Cvitkovic, F., Larregain-Fournier, D., Le Rol, A., Walter, S., Adam, R., Misset, J. L., & Lévi, F. (2000). Phase III multicenter randomized trial of oxaliplatin added to chronomodulated fluorouracil-leucovorin as first-line treatment of metastatic colorectal cancer. *Journal of Clinical Oncology: Official Journal of the American Society of Clinical Oncology*, *18*(1), 136–147. https://doi.org/10.1200/JCO.2000.18.1.136

Ginhoux, F., Greter, M., Leboeuf, M., Nandi, S., See, P., Gokhan, S., Mehler, M. F., Conway, S. J., Ng, L. G., Stanley, E. R., Samokhvalov, I. M., & Merad, M. (2010). Fate mapping analysis reveals that adult microglia derive from primitive macrophages. *Science (New York, N.Y.)*, *330*(6005), 841–845. https://doi.org/10.1126/science.1194637

Gobert Gosse, S., Bourgin, C., Liu, W. Q., Garbay, C., & Mouchiroud, G. (2005). M-CSF stimulated differentiation requires persistent MEK activity and MAPK phosphorylation independent of Grb2-Sos association and phosphatidylinositol 3-kinase activity. *Cellular Signalling*, *17*(11), 1352–1362. https://doi.org/10.1016/j.cellsig.2005.02.002

Gomez-Roca, C. A., Cassier, P. A., Italiano, A., Cannarile, M., Ries, C., Brillouet, A., Mueller, C., Jegg, A.-M., Meneses-Lorente, G., Baehner, M., Abiraj, K., Loirat, D., Toulmonde, M., D'Angelo, S. P., Weber, K., Campone, M., Ruettinger, D., Blay, J.-Y., Delord, J.-P., & Le Tourneau, C. (2015). Phase I study of RG7155, a novel anti-CSF1R antibody, in patients with advanced/metastatic solid tumors. *Journal of Clinical Oncology*, *33*(15_suppl), 3005–3005. https://doi.org/10.1200/jco.2015.33.15_suppl.3005

Gomez-Roca, C., Cassier, P., Zamarin, D., Machiels, J.-P., Luis Perez Gracia, J., Stephen Hodi, F., Taus, A., Martinez Garcia, M., Boni, V., Eder, J. P., Hafez, N., Sullivan, R., Mcdermott, D., Champiat, S., Aspeslagh, S., Terret, C., Jegg, A.-M., Jacob, W., Cannarile, M. A., … Marabelle, A. (2022). Anti-CSF-1R emactuzumab in combination with anti-PD-L1 atezolizumab in advanced solid tumor patients naïve or experienced for immune checkpoint blockade. *Journal for Immunotherapy of Cancer*, *10*(5), e004076. https://doi.org/10.1136/jitc-2021-004076

Gordon, S. (2016). Elie Metchnikoff, the Man and the Myth. *Journal of Innate Immunity*, *8*(3), 223–227. https://doi.org/10.1159/000443331

Gordon, S. R., Maute, R. L., Dulken, B. W., Hutter, G., George, B. M., McCracken, M. N., Gupta, R., Tsai, J. M., Sinha, R., Corey, D., Ring, A. M., Connolly, A. J., & Weissman, I. L. (2017). PD-1 expression by tumour-associated macrophages inhibits phagocytosis and tumour immunity. *Nature*, *545*(7655), Article 7655. https://doi.org/10.1038/nature22396

Gordon, S., & Taylor, P. R. (2005). Monocyte and macrophage heterogeneity. *Nature Reviews. Immunology*, *5*(12), 953–964. https://doi.org/10.1038/nri1733

Gordy, C., Pua, H., Sempowski, G. D., & He, Y.-W. (2011). Regulation of steady-state neutrophil homeostasis by macrophages. *Blood*, *117*(2), 618–629. https://doi.org/10.1182/blood-2010-01-265959

Goren, I., Allmann, N., Yogev, N., Schürmann, C., Linke, A., Holdener, M., Waisman, A., Pfeilschifter, J., & Frank, S. (2009). A transgenic mouse model of inducible macrophage depletion: Effects of diphtheria toxin-driven lysozyme M-specific cell lineage ablation on wound inflammatory, angiogenic, and contractive processes. *The American Journal of Pathology*, *175*(1), 132–147. https://doi.org/10.2353/ajpath.2009.081002

Grimshaw, M. J., Hagemann, T., Ayhan, A., Gillett, C. E., Binder, C., & Balkwill, F. R. (2004). A role for endothelin-2 and its receptors in breast tumor cell invasion. *Cancer Research*, *64*(7), 2461–2468. https://doi.org/10.1158/0008-5472.can-03-1069

Guilbert, L. J., & Stanley, E. R. (1980). Specific interaction of murine colony-stimulating factor with mononuclear phagocytic cells. *The Journal of Cell Biology*, *85*(1), 153–159. https://doi.org/10.1083/jcb.85.1.153

Gustavsson, B., Carlsson, G., Machover, D., Petrelli, N., Roth, A., Schmoll, H.-J., Tveit, K.-M., & Gibson, F. (2015). A review of the evolution of systemic chemotherapy in the management of colorectal cancer. *Clinical Colorectal Cancer*, *14*(1), 1–10. https://doi.org/10.1016/j.clcc.2014.11.002

Hammond, W. A., Swaika, A., & Mody, K. (2016). Pharmacologic resistance in colorectal cancer: A review. *Therapeutic Advances in Medical Oncology*, *8*(1), 57–84. https://doi.org/10.1177/1758834015614530

Hampe, A., Shamoon, B. M., Gobet, M., Sherr, C. J., & Galibert, F. (1989). Nucleotide sequence and structural organization of the human FMS proto-oncogene. *Oncogene Research*, *4*(1), 9–17.

Hanahan, D., & Weinberg, R. A. (2011). Hallmarks of cancer: The next generation. *Cell*, *144*(5), 646–674. https://doi.org/10.1016/j.cell.2011.02.013

Harb, W. A., Johnson, M. L., Goldman, J. W., Weise, A. M., Call, J. A., Dudek, A. Z., Gonzalez, R., Cowey, C. L., Eves, P. T., Gollerkeri, A., & Gainor, J. F. (2017). A phase 1b/2 study of ARRY-382, an oral inhibitor of colony stimulating factor 1 receptor (CSF1R), in combination with pembrolizumab (Pembro) for the treatment of patients (Pts) with advanced solid tumors. *Journal of Clinical Oncology*, *35*(15_suppl), TPS3110–TPS3110. https://doi.org/10.1200/JCO.2017.35.15_suppl.TPS3110

Hasegawa, T., Kim, H.-S., Fukushima, M., & Wataya, Y. (2005). Sequence analysis of the 5'-flanking regions of human dihydropyrimidine dehydrogenase gene: Identification of a new polymorphism related with effects of 5-fluorouracil. *Nucleosides, Nucleotides & Nucleic Acids*, *24*(4), 233–242. https://doi.org/10.1081/NCN-59679

Hedbrant, A., Erlandsson, A., Delbro, D., & Wijkander, J. (2015). Conditioned media from human macrophages of M1 phenotype attenuate the cytotoxic effect of 5-fluorouracil on the HT-29 colon cancer cell line. *International Journal of Oncology*, *46*(1), 37–46. https://doi.org/10.3892/ijo.2014.2696

Heidelberger, C., Chaudhuri, N. K., Danneberg, P., Mooren, D., Griesbach, L., Duschinsky, R., Schnitzer, R. J., Pleven, E., & Scheiner, J. (1957). Fluorinated Pyrimidines, A New Class of Tumour-Inhibitory Compounds. *Nature*, *179*(4561), Article 4561. https://doi.org/10.1038/179663a0

Himes, S. R., Tagoh, H., Goonetilleke, N., Sasmono, T., Oceandy, D., Clark, R., Bonifer, C., & Hume, D. A. (2001). A highly conserved c-fms gene intronic element controls macrophage-specific and regulated expression. *Journal of Leukocyte Biology*, *70*(5), 812–820.

Horowitz, J., & Chargaff, E. (1959). Massive Incorporation of 5-Fluorouracil into a Bacterial Ribonucleic Acid. *Nature*, *184*(4694), Article 4694. https://doi.org/10.1038/1841213a0

Hossain, F., Al-Khami, A. A., Wyczechowska, D., Hernandez, C., Zheng, L., Reiss, K., Valle, L. D., Trillo-Tinoco, J., Maj, T., Zou, W., Rodriguez, P. C., & Ochoa, A. C. (2015). Inhibition of Fatty Acid Oxidation Modulates Immunosuppressive Functions of Myeloid-Derived Suppressor Cells and Enhances Cancer Therapies. *Cancer Immunology Research*, *3*(11), 1236–1247. https://doi.org/10.1158/2326-6066.CIR-15-0036

Hoves, S., Ooi, C.-H., Wolter, C., Sade, H., Bissinger, S., Schmittnaegel, M., Ast, O., Giusti, A. M., Wartha, K., Runza, V., Xu, W., Kienast, Y., Cannarile, M. A., Levitsky, H., Romagnoli, S., De Palma, M., Rüttinger, D., & Ries, C. H. (2018). Rapid activation of tumor-associated macrophages boosts preexisting tumor immunity. *The Journal of Experimental Medicine*, *215*(3), 859–876. https://doi.org/10.1084/jem.20171440

Hubbard, S. R., & Miller, W. T. (2007). Receptor tyrosine kinases: Mechanisms of activation and signaling. *Current Opinion in Cell Biology*, *19*(2), 117–123. https://doi.org/10.1016/j.ceb.2007.02.010

Hubbard, S. R., & Till, J. H. (2000). Protein tyrosine kinase structure and function. *Annual Review of Biochemistry*, *69*, 373–398. https://doi.org/10.1146/annurev.biochem.69.1.373

Hui, L., & Chen, Y. (2015). Tumor microenvironment: Sanctuary of the devil. *Cancer Letters*, *368*(1), 7–13. https://doi.org/10.1016/j.canlet.2015.07.039

Italiani, P., & Boraschi, D. (2014). From Monocytes to M1/M2 Macrophages: Phenotypical vs. Functional Differentiation. *Frontiers in Immunology*, *5*. https://www.frontiersin.org/articles/10.3389/fimmu.2014.00514

JA, F., Rossetti, S., & Sacchi, N. (2009). CSF1R (colony stimulating factor 1 receptor, formerly McDonough feline sarcoma viral (v-fms) oncogene homolog). *Atlas Genet Cytogenet Oncol Haematol.*, *13*, 120–125. https://doi.org/10.4267/2042/44403

Jaakkola, P., Mole, D. R., Tian, Y. M., Wilson, M. I., Gielbert, J., Gaskell, S. J., von Kriegsheim, A., Hebestreit, H. F., Mukherji, M., Schofield, C. J., Maxwell, P. H., Pugh, C. W., & Ratcliffe, P. J. (2001). Targeting of HIF-alpha to the von Hippel-Lindau ubiquitylation complex by O2-regulated prolyl hydroxylation. *Science (New York, N.Y.)*, *292*(5516), 468–472. https://doi.org/10.1126/science.1059796

Jacquel, A., Benikhlef, N., Paggetti, J., Lalaoui, N., Guery, L., Dufour, E. K., Ciudad, M., Racoeur, C., Micheau, O., Delva, L., Droin, N., & Solary, E. (2009). Colony-stimulating factor-1-induced oscillations in phosphatidylinositol-3 kinase/AKT are required for caspase activation in monocytes undergoing differentiation into macrophages. *Blood*, *114*(17), 3633–3641. https://doi.org/10.1182/blood-2009-03-208843

Jaguin, M., Houlbert, N., Fardel, O., & Lecureur, V. (2013). Polarization profiles of human M-CSF-generated macrophages and comparison of M1-markers in classically activated macrophages from GM-CSF and M-CSF origin. *Cellular Immunology*, *281*(1), 51–61. https://doi.org/10.1016/j.cellimm.2013.01.010

Jensen, S. A., Vainer, B., & Sørensen, J. B. (2007). The prognostic significance of thymidylate synthase and dihydropyrimidine dehydrogenase in colorectal cancer of 303 patients adjuvantly treated with 5-fluorouracil. *International Journal of Cancer*, *120*(3), 694–701. https://doi.org/10.1002/ijc.22318

Jeong, H., Kim, S., Hong, B.-J., Lee, C.-J., Kim, Y.-E., Bok, S., Oh, J.-M., Gwak, S.-H., Yoo, M. Y., Lee, M. S., Chung, S.-J., Defrêne, J., Tessier, P., Pelletier, M., Jeon, H., Roh, T.-Y., Kim, B., Kim, K. H., Ju, J. H., … Ahn, G.-O. (2019). Tumor-Associated Macrophages Enhance Tumor Hypoxia and Aerobic Glycolysis. *Cancer Research*, *79*(4), 795–806. https://doi.org/10.1158/0008-5472.CAN-18-2545

Jetten, N., Verbruggen, S., Gijbels, M. J., Post, M. J., De Winther, M. P. J., & Donners, M. M. P. C. (2014). Anti-inflammatory M2, but not pro-inflammatory M1 macrophages promote angiogenesis in vivo. *Angiogenesis*, *17*(1), 109–118. https://doi.org/10.1007/s10456-013-9381-6

Johnson, M. R., Hageboutros, A., Wang, K., High, L., Smith, J. B., & Diasio, R. B. (1999). Life-threatening toxicity in a dihydropyrimidine dehydrogenase-deficient patient after treatment with topical 5-fluorouracil. *Clinical Cancer Research: An Official Journal of the American Association for Cancer Research*, *5*(8), 2006–2011.

Johnson, M. R., Wang, K., Tillmanns, S., Albin, N., & Diasio, R. B. (1997). Structural organization of the human dihydropyrimidine dehydrogenase gene. *Cancer Research*, *57*(9), 1660–1663.

Joyce, J. A., & Pollard, J. W. (2009). Microenvironmental regulation of metastasis. *Nature Reviews Cancer*, *9*(4), Article 4. https://doi.org/10.1038/nrc2618

Junttila, M. R., & de Sauvage, F. J. (2013). Influence of tumour micro-environment heterogeneity on therapeutic response. *Nature*, *501*(7467), Article 7467. https://doi.org/10.1038/nature12626

Kaczanowska, S., Joseph, A. M., & Davila, E. (2013). TLR agonists: Our best frenemy in cancer immunotherapy. *Journal of Leukocyte Biology*, *93*(6), 847–863. https://doi.org/10.1189/jlb.1012501

Kaelin, W. G., & Ratcliffe, P. J. (2008). Oxygen sensing by metazoans: The central role of the HIF hydroxylase pathway. *Molecular Cell*, *30*(4), 393–402. https://doi.org/10.1016/j.molcel.2008.04.009

Kaneda, M. M., Messer, K. S., Ralainirina, N., Li, H., Leem, C. J., Gorjestani, S., Woo, G., Nguyen, A. V., Figueiredo, C. C., Foubert, P., Schmid, M. C., Pink, M., Winkler, D. G., Rausch, M., Palombella, V. J., Kutok, J., McGovern, K., Frazer, K. A., Wu, X., … Varner, J. A. (2016). PI3Kγ is a molecular switch that controls immune suppression. *Nature*, *539*(7629), 437–442. https://doi.org/10.1038/nature19834

Keeley, T. P., & Mann, G. E. (2019). Defining Physiological Normoxia for Improved Translation of Cell Physiology to Animal Models and Humans. *Physiological Reviews*, *99*(1), 161–234. https://doi.org/10.1152/physrev.00041.2017

Kes, M. M. G., Van den Bossche, J., Griffioen, A. W., & Huijbers, E. J. M. (2020). Oncometabolites lactate and succinate drive pro-angiogenic macrophage response in tumors. *Biochimica Et Biophysica Acta. Reviews on Cancer*, *1874*(2), 188427. https://doi.org/10.1016/j.bbcan.2020.188427

Krysinska, H., Hoogenkamp, M., Ingram, R., Wilson, N., Tagoh, H., Laslo, P., Singh, H., & Bonifer, C. (2007). A two-step, PU.1-dependent mechanism for developmentally regulated chromatin remodeling and transcription of the c-fms gene. *Molecular and Cellular Biology*, *27*(3), 878–887. https://doi.org/10.1128/MCB.01915-06

Kunicka, T., Prochazka, P., Krus, I., Bendova, P., Protivova, M., Susova, S., Hlavac, V., Liska, V., Novak, P., Schneiderova, M., Pitule, P., Bruha, J., Vycital, O., Vodicka, P., & Soucek, P. (2016). Molecular profile of 5-fluorouracil pathway genes in colorectal carcinoma. *BMC Cancer*, *16*(1), 795. https://doi.org/10.1186/s12885-016-2826-8

Lavin, Y., Winter, D., Blecher-Gonen, R., David, E., Keren-Shaul, H., Merad, M., Jung, S., & Amit, I. (2014). Tissue-resident macrophage enhancer landscapes are shaped by the local microenvironment. *Cell*, *159*(6), 1312–1326. https://doi.org/10.1016/j.cell.2014.11.018

Lebrecht, A., Grimm, C., Lantzsch, T., Ludwig, E., Hefler, L., Ulbrich, E., & Koelbl, H. (2004). Monocyte chemoattractant protein-1 serum levels in patients with breast cancer. *Tumour Biology: The Journal of the International Society for Oncodevelopmental Biology and Medicine*, *25*(1–2), 14–17. https://doi.org/10.1159/000077718

Lee, P., Chandel, N. S., & Simon, M. C. (2020). Cellular adaptation to hypoxia through hypoxia inducible factors and beyond. *Nature Reviews. Molecular Cell Biology*, *21*(5), 268–283. https://doi.org/10.1038/s41580-020-0227-y

Lee, P. S., Wang, Y., Dominguez, M. G., Yeung, Y. G., Murphy, M. A., Bowtell, D. D., & Stanley, E. R. (1999). The Cbl protooncoprotein stimulates CSF-1 receptor multiubiquitination and endocytosis, and attenuates macrophage proliferation. *The EMBO Journal*, *18*(13), 3616–3628. https://doi.org/10.1093/emboj/18.13.3616

Lemmon, M. A., & Schlessinger, J. (2010). Cell Signaling by Receptor Tyrosine Kinases. *Cell*, *141*(7), 1117–1134. https://doi.org/10.1016/j.cell.2010.06.011

Li, M., Knight, D. A., A Snyder, L., Smyth, M. J., & Stewart, T. J. (2013). A role for CCL2 in both tumor progression and immunosurveillance. *Oncoimmunology*, *2*(7), e25474. https://doi.org/10.4161/onci.25474

Li, W., & Stanley, E. R. (1991). Role of dimerization and modification of the CSF-1 receptor in its activation and internalization during the CSF-1 response. *The EMBO Journal*, *10*(2), 277–288. https://doi.org/10.1002/j.1460-2075.1991.tb07948.x

Lin, C.-C. (2021). Clinical Development of Colony-Stimulating Factor 1 Receptor (CSF1R) Inhibitors. *Journal of Immunotherapy and Precision Oncology*, *4*(2), 105–114. https://doi.org/10.36401/JIPO-20-32

Lin, C.-C., Gil-Martin, M., Bauer, T. M., Naing, A., Lim, D. W.-T., Sarantopoulos, J., Geva, R., Ando, Y., Fan, L., Choudhury, S., Tu, P.-J., Quadt, C., & Santoro, A. (2020). Abstract CT171: Phase I study of BLZ945 alone and with spartalizumab (PDR001) in patients (pts) with advanced solid tumors. *Cancer Research*, *80*(16_Supplement), CT171. https://doi.org/10.1158/1538-7445.AM2020-CT171

Lin, H., Lee, E., Hestir, K., Leo, C., Huang, M., Bosch, E., Halenbeck, R., Wu, G., Zhou, A., Behrens, D., Hollenbaugh, D., Linnemann, T., Qin, M., Wong, J., Chu, K., Doberstein, S. K., & Williams, L. T. (2008). Discovery of a Cytokine and Its Receptor by Functional Screening of the Extracellular Proteome. *Science*, *320*(5877), 807–811. https://doi.org/10.1126/science.1154370

Lin, S., Sun, L., Lyu, X., Ai, X., Du, D., Su, N., Li, H., Zhang, L., Yu, J., & Yuan, S. (2017). Lactate-activated macrophages induced aerobic glycolysis and epithelial-mesenchymal transition in breast cancer by regulation of CCL5-CCR5 axis: A positive metabolic feedback loop. *Oncotarget*, *8*(66), 110426–110443. https://doi.org/10.18632/oncotarget.22786

Liu, H., Leo, C., Chen, X., Wong, B. R., Williams, L. T., Lin, H., & He, X. (2012). The mechanism of shared but distinct CSF-1R signaling by the non-homologous cytokines IL-34 and CSF-1. *Biochimica Et Biophysica Acta*, *1824*(7), 938–945. https://doi.org/10.1016/j.bbapap.2012.04.012

Liu, N., Luo, J., Kuang, D., Xu, S., Duan, Y., Xia, Y., Wei, Z., Xie, X., Yin, B., Chen, F., Luo, S., Liu, H., Wang, J., Jiang, K., Gong, F., Tang, Z., Cheng, X., Li, H., Li, Z., … Yang, X.-P. (2019). Lactate inhibits ATP6V0d2 expression in tumor-associated macrophages to promote HIF-2**α**–mediated tumor progression. *The Journal of Clinical Investigation*, *129*(2), 631–646. https://doi.org/10.1172/JCI123027

Loberg, R. D., Ying, C., Craig, M., Day, L. L., Sargent, E., Neeley, C., Wojno, K., Snyder, L. A., Yan, L., & Pienta, K. J. (2007). Targeting CCL2 with systemic delivery of neutralizing antibodies induces prostate cancer tumor regression in vivo. *Cancer Research*, *67*(19), 9417–9424. https://doi.org/10.1158/0008-5472.CAN-07-1286

Locati, M., Mantovani, A., & Sica, A. (2013). Macrophage activation and polarization as an adaptive component of innate immunity. *Advances in Immunology*, *120*, 163–184. https://doi.org/10.1016/B978-0-12-417028-5.00006-5

Longley, D. B., Harkin, D. P., & Johnston, P. G. (2003). 5-Fluorouracil: Mechanisms of action and clinical strategies. *Nature Reviews Cancer*, *3*(5), Article 5. https://doi.org/10.1038/nrc1074

Longley, D. B., & Johnston, P. G. (2005). Molecular mechanisms of drug resistance. *The Journal of Pathology*, *205*(2), 275–292. https://doi.org/10.1002/path.1706

Loyher, P.-L., Hamon, P., Laviron, M., Meghraoui-Kheddar, A., Goncalves, E., Deng, Z., Torstensson, S., Bercovici, N., Baudesson de Chanville, C., Combadière, B., Geissmann, F., Savina, A., Combadière, C., & Boissonnas, A. (2018). Macrophages of distinct origins contribute to tumor development in the lung. *The Journal of Experimental Medicine*, *215*(10), 2536–2553. https://doi.org/10.1084/jem.20180534

Lu, P., Weaver, V. M., & Werb, Z. (2012). The extracellular matrix: A dynamic niche in cancer progression. *The Journal of Cell Biology*, *196*(4), 395–406. https://doi.org/10.1083/jcb.201102147

Lu, X., & Meng, T. (2019). Depletion of tumor-associated macrophages enhances the anti-tumor effect of docetaxel in a murine epithelial ovarian cancer. *Immunobiology*, *224*(3), 355–361. https://doi.org/10.1016/j.imbio.2019.03.002

Lyss, A. P., Lilenbaum, R. C., Harris, B. E., & Diasio, R. B. (1993). Severe 5-fluorouracil toxicity in a patient with decreased dihydropyrimidine dehydrogenase activity. *Cancer Investigation*, *11*(2), 239–240. https://doi.org/10.3109/07357909309024846

Ma, X., Lin, W. Y., Chen, Y., Stawicki, S., Mukhyala, K., Wu, Y., Martin, F., Bazan, J. F., & Starovasnik, M. A. (2012). Structural basis for the dual recognition of helical cytokines IL-34 and CSF-1 by CSF-1R. *Structure (London, England: 1993)*, *20*(4), 676–687. https://doi.org/10.1016/j.str.2012.02.010

MacDonald, K. P. A., Rowe, V., Bofinger, H. M., Thomas, R., Sasmono, T., Hume, D. A., & Hill, G. R. (2005). The colony-stimulating factor 1 receptor is expressed on dendritic cells during differentiation and regulates their expansion. *Journal of Immunology (Baltimore, Md.: 1950)*, *175*(3), 1399–1405. https://doi.org/10.4049/jimmunol.175.3.1399

Madison, B. B. (2016). Srebp2: A master regulator of sterol and fatty acid synthesis1. *Journal of Lipid Research*, *57*(3), 333–335. https://doi.org/10.1194/jlr.C066712

Magkouta, S. F., Vaitsi, P. C., Pappas, A. G., Iliopoulou, M., Kosti, C. N., Psarra, K., & Kalomenidis, I. T. (2021). CSF1/CSF1R Axis Blockade Limits Mesothelioma and Enhances Efficiency of Anti-PDL1 Immunotherapy. *Cancers*, *13*(11), 2546. https://doi.org/10.3390/cancers13112546

Majmundar, A. J., Wong, W. J., & Simon, M. C. (2010). Hypoxia-inducible factors and the response to hypoxic stress. *Molecular Cell*, *40*(2), 294–309. https://doi.org/10.1016/j.molcel.2010.09.022

Mancini, A., Koch, A., Whetton, A. D., & Tamura, T. (2004). The M-CSF receptor substrate and interacting protein FMIP is governed in its subcellular localization by protein kinase C-mediated phosphorylation, and thereby potentiates M-CSF-mediated differentiation. *Oncogene*, *23*(39), 6581–6589. https://doi.org/10.1038/sj.onc.1207841

Manji, G. A., Van Tine, B. A., Lee, S. M., Raufi, A. G., Pellicciotta, I., Hirbe, A. C., Pradhan, J., Chen, A., Rabadan, R., & Schwartz, G. K. (2021). A Phase I Study of the Combination of Pexidartinib and Sirolimus to Target Tumor-Associated Macrophages in Unresectable Sarcoma and Malignant Peripheral Nerve Sheath Tumors. *Clinical Cancer Research: An Official Journal of the American Association for Cancer Research*, *27*(20), 5519–5527. https://doi.org/10.1158/1078-0432.CCR-21-1779

Mansoori, B., Mohammadi, A., Davudian, S., Shirjang, S., & Baradaran, B. (2017). The Different Mechanisms of Cancer Drug Resistance: A Brief Review. *Advanced Pharmaceutical Bulletin*, *7*(3), 339–348. https://doi.org/10.15171/apb.2017.041

Mantovani, A., Marchesi, F., Malesci, A., Laghi, L., & Allavena, P. (2017). Tumour-associated macrophages as treatment targets in oncology. *Nature Reviews. Clinical Oncology*, *14*(7), 399–416. https://doi.org/10.1038/nrclinonc.2016.217

Mantovani, A., Sica, A., Sozzani, S., Allavena, P., Vecchi, A., & Locati, M. (2004). The chemokine system in diverse forms of macrophage activation and polarization. *Trends in Immunology*, *25*(12), 677–686. https://doi.org/10.1016/j.it.2004.09.015

Masoud, G. N., & Li, W. (2015). HIF-1α pathway: Role, regulation and intervention for cancer therapy. *Acta Pharmaceutica Sinica. B*, *5*(5), 378–389. https://doi.org/10.1016/j.apsb.2015.05.007

Matlung, H. L., Szilagyi, K., Barclay, N. A., & van den Berg, T. K. (2017). The CD47-SIRPα signaling axis as an innate immune checkpoint in cancer. *Immunological Reviews*, *276*(1), 145–164. https://doi.org/10.1111/imr.12527

Matsuyama, R., Togo, S., Shimizu, D., Momiyama, N., Ishikawa, T., Ichikawa, Y., Endo, I., Kunisaki, C., Suzuki, H., Hayasizaki, Y., & Shimada, H. (2006). Predicting 5-fluorouracil chemosensitivity of liver metastases from colorectal cancer using primary tumor specimens: Three-gene expression model predicts clinical response. *International Journal of Cancer*, *119*(2), 406–413. https://doi.org/10.1002/ijc.21843

Mauro, D. J., De Riel, J. K., Tallarida, R. J., & Sirover, M. A. (1993). Mechanisms of excision of 5-fluorouracil by uracil DNA glycosylase in normal human cells. *Molecular Pharmacology*, *43*(6), 854–857.

Maxwell, P. H., Wiesener, M. S., Chang, G. W., Clifford, S. C., Vaux, E. C., Cockman, M. E., Wykoff, C. C., Pugh, C. W., Maher, E. R., & Ratcliffe, P. J. (1999). The tumour suppressor protein VHL targets hypoxia-inducible factors for oxygen-dependent proteolysis. *Nature*, *399*(6733), 271–275. https://doi.org/10.1038/20459

Mazure, N. M., Chen, E. Y., Yeh, P., Laderoute, K. R., & Giaccia, A. J. (1996). Oncogenic transformation and hypoxia synergistically act to modulate vascular endothelial growth factor expression. *Cancer Research*, *56*(15), 3436–3440.

McDermott, R. S., Deneux, L., Mosseri, V., Védrenne, J., Clough, K., Fourquet, A., Rodriguez, J., Cosset, J.-M., Sastre, X., Beuzeboc, P., Pouillart, P., & Scholl, S. M. (2002). Circulating macrophage colony stimulating factor as a marker of tumour progression. *European Cytokine Network*, *13*(1), 121–127.

Meulendijks, D., Henricks, L. M., Sonke, G. S., Deenen, M. J., Froehlich, T. K., Amstutz, U., Largiadèr, C. R., Jennings, B. A., Marinaki, A. M., Sanderson, J. D., Kleibl, Z., Kleiblova, P., Schwab, M., Zanger, U. M., Palles, C., Tomlinson, I., Gross, E., van Kuilenburg, A. B. P., Punt, C. J. A., … Schellens, J. H. M. (2015). Clinical relevance of DPYD variants c.1679T>G, c.1236G>A/HapB3, and c.1601G>A as predictors of severe fluoropyrimidine-associated toxicity: A systematic review and meta-analysis of individual patient data. *The Lancet. Oncology*, *16*(16), 1639–1650. https://doi.org/10.1016/S1470-2045(15)00286-7

Meyerhardt, J. A., & Mayer, R. J. (2005). Systemic therapy for colorectal cancer. *The New England Journal of Medicine*, *352*(5), 476–487. https://doi.org/10.1056/NEJMra040958

Mezrich, J. D., Fechner, J. H., Zhang, X., Johnson, B. P., Burlingham, W. J., & Bradfield, C. A. (2010). An interaction between kynurenine and the aryl hydrocarbon receptor can generate regulatory T cells. *Journal of Immunology (Baltimore, Md.: 1950)*, *185*(6), 3190–3198. https://doi.org/10.4049/jimmunol.0903670

Milano, G., Etienne, M. C., Cassuto-Viguier, E., Thyss, A., Santini, J., Frenay, M., Renee, N., Schneider, M., & Demard, F. (1992). Influence of sex and age on fluorouracil clearance. *Journal of Clinical Oncology: Official Journal of the American Society of Clinical Oncology*, *10*(7), 1171–1175. https://doi.org/10.1200/JCO.1992.10.7.1171

Milano, G., Etienne, M. C., Pierrefite, V., Barberi-Heyob, M., Deporte-Fety, R., & Renée, N. (1999). Dihydropyrimidine dehydrogenase deficiency and fluorouracil-related toxicity. *British Journal of Cancer*, *79*(3–4), 627–630. https://doi.org/10.1038/sj.bjc.6690098

Milano, G., & McLeod, H. L. (2000). Can dihydropyrimidine dehydrogenase impact 5-fluorouracil-based treatment? *European Journal of Cancer*, *36*(1), 37–42. https://doi.org/10.1016/S0959-8049(99)00211-7

Miller, A., Nagy, C., Knapp, B., Laengle, J., Ponweiser, E., Groeger, M., Starkl, P., Bergmann, M., Wagner, O., & Haschemi, A. (2017). Exploring Metabolic Configurations of Single Cells within Complex Tissue Microenvironments. *Cell Metabolism*, *26*(5), 788-800.e6. https://doi.org/10.1016/j.cmet.2017.08.014

Mitrovski, B., Pressacco, J., Mandelbaum, S., & Erlichman, C. (1994). Biochemical effects of folate-based inhibitors of thymidylate synthase in MGH-U1 cells. *Cancer Chemotherapy and Pharmacology*, *35*(2), 109–114. https://doi.org/10.1007/BF00686631

Miura, K., Kinouchi, M., Ishida, K., Fujibuchi, W., Naitoh, T., Ogawa, H., Ando, T., Yazaki, N., Watanabe, K., Haneda, S., Shibata, C., & Sasaki, I. (2010). 5-FU Metabolism in Cancer and Orally-Administrable 5-FU Drugs. *Cancers*, *2*(3), Article 3. https://doi.org/10.3390/cancers2031717

Mondini, M., Loyher, P.-L., Hamon, P., Gerbé de Thoré, M., Laviron, M., Berthelot, K., Clémenson, C., Salomon, B. L., Combadière, C., Deutsch, E., & Boissonnas, A. (2019). CCR2-Dependent Recruitment of Tregs and Monocytes Following Radiotherapy Is Associated with TNFα-Mediated Resistance. *Cancer Immunology Research*, *7*(3), 376–387. https://doi.org/10.1158/2326-6066.CIR-18-0633

Mossadegh-Keller, N., Sarrazin, S., Kandalla, P. K., Espinosa, L., Stanley, E. R., Nutt, S. L., Moore, J., & Sieweke, M. H. (2013). M-CSF instructs myeloid lineage fate in single haematopoietic stem cells. *Nature*, *497*(7448), 239–243. https://doi.org/10.1038/nature12026

Mu, X., Shi, W., Xu, Y., Xu, C., Zhao, T., Geng, B., Yang, J., Pan, J., Hu, S., Zhang, C., Zhang, J., Wang, C., Shen, J., Che, Y., Liu, Z., Lv, Y., Wen, H., & You, Q. (2018). Tumor-derived lactate induces M2 macrophage polarization via the activation of the ERK/STAT3 signaling pathway in breast cancer. *Cell Cycle (Georgetown, Tex.)*, *17*(4), 428–438. https://doi.org/10.1080/15384101.2018.1444305

Munugalavadla, V., Borneo, J., Ingram, D. A., & Kapur, R. (2005). P85alpha subunit of class IA PI-3 kinase is crucial for macrophage growth and migration. *Blood*, *106*(1), 103–109. https://doi.org/10.1182/blood-2004-10-4041

Murdoch, C., Giannoudis, A., & Lewis, C. E. (2004). Mechanisms regulating the recruitment of macrophages into hypoxic areas of tumors and other ischemic tissues. *Blood*, *104*(8), 2224–2234. https://doi.org/10.1182/blood-2004-03-1109

Murray, P. J. (2017). Macrophage Polarization. *Annual Review of Physiology*, *79*, 541–566. https://doi.org/10.1146/annurev-physiol-022516-034339

Naguib, F. N., el Kouni, M. H., & Cha, S. (1985). Enzymes of uracil catabolism in normal and neoplastic human tissues. *Cancer Research*, *45*(11 Pt 1), 5405–5412.

Nandi, S., Akhter, M. P., Seifert, M. F., Dai, X.-M., & Stanley, E. R. (2006). Developmental and functional significance of the CSF-1 proteoglycan chondroitin sulfate chain. *Blood*, *107*(2), 786–795. https://doi.org/10.1182/blood-2005-05-1822

Nandi, S., Gokhan, S., Dai, X.-M., Wei, S., Enikolopov, G., Lin, H., Mehler, M. F., & Stanley, E. R. (2012). The CSF-1 receptor ligands IL-34 and CSF-1 exhibit distinct developmental brain expression patterns and regulate neural progenitor cell maintenance and maturation. *Developmental Biology*, *367*(2), 100–113. https://doi.org/10.1016/j.ydbio.2012.03.026

Ngambenjawong, C., Gustafson, H. H., & Pun, S. H. (2017). Progress in tumor-associated macrophage (TAM)-targeted therapeutics. *Advanced Drug Delivery Reviews*, *114*, 206–221. https://doi.org/10.1016/j.addr.2017.04.010

Nowak, A. K., Cook, A. M., McDonnell, A. M., Millward, M. J., Creaney, J., Francis, R. J., Hasani, A., Segal, A., Musk, A. W., Turlach, B. A., McCoy, M. J., Robinson, B. W. S., & Lake, R. A. (2015). A phase 1b clinical trial of the CD40-activating antibody CP-870,893 in combination with cisplatin and pemetrexed in malignant pleural mesothelioma. *Annals of Oncology: Official Journal of the European Society for Medical Oncology*, *26*(12), 2483–2490. https://doi.org/10.1093/annonc/mdv387

Nywening, T. M., Wang-Gillam, A., Sanford, D. E., Belt, B. A., Panni, R. Z., Cusworth, B. M., Toriola, A. T., Nieman, R. K., Worley, L. A., Yano, M., Fowler, K. J., Lockhart, A. C., Suresh, R., Tan, B. R., Lim, K.-H., Fields, R. C., Strasberg, S. M., Hawkins, W. G., DeNardo, D. G., … Linehan, D. C. (2016). Targeting tumour-associated macrophages with CCR2 inhibition in combination with FOLFIRINOX in patients with borderline resectable and locally advanced pancreatic cancer: A single-centre, open-label, dose-finding, non-randomised, phase 1b trial. *The Lancet. Oncology*, *17*(5), 651–662. https://doi.org/10.1016/S1470-2045(16)00078-4

Okabe, Y., & Medzhitov, R. (2016). Tissue biology perspective on macrophages. *Nature Immunology*, *17*(1), Article 1. https://doi.org/10.1038/ni.3320

Omura, K. (2003). Clinical implications of dihydropyrimidine dehydrogenase (DPD) activity in 5-FU-based chemotherapy: Mutations in the DPD gene, and DPD inhibitory fluoropyrimidines. *International Journal of Clinical Oncology*, *8*(3), 132–138. https://doi.org/10.1007/s10147-003-0330-z

Ordentlich, P. (2021). Clinical evaluation of colony-stimulating factor 1 receptor inhibitors. *Seminars in Immunology*, *54*, 101514. https://doi.org/10.1016/j.smim.2021.101514

Orkin, S. H., & Zon, L. I. (2008). Hematopoiesis: An evolving paradigm for stem cell biology. *Cell*, *132*(4), 631–644. https://doi.org/10.1016/j.cell.2008.01.025

Otero, K., Turnbull, I. R., Poliani, P. L., Vermi, W., Cerutti, E., Aoshi, T., Tassi, I., Takai, T., Stanley, S. L., Miller, M., Shaw, A. S., & Colonna, M. (2009). Macrophage colony-stimulating factor induces the proliferation and survival of macrophages via a pathway involving DAP12 and beta-catenin. *Nature Immunology*, *10*(7), 734–743. https://doi.org/10.1038/ni.1744

Palmieri, E. M., Menga, A., Martín-Pérez, R., Quinto, A., Riera-Domingo, C., De Tullio, G., Hooper, D. C., Lamers, W. H., Ghesquière, B., McVicar, D. W., Guarini, A., Mazzone, M., & Castegna, A. (2017). Pharmacologic or Genetic Targeting of Glutamine Synthetase Skews Macrophages toward an M1-like Phenotype and Inhibits Tumor Metastasis. *Cell Reports*, *20*(7), 1654–1666. https://doi.org/10.1016/j.celrep.2017.07.054

Panczyk, M. (2014). Pharmacogenetics research on chemotherapy resistance in colorectal cancer over the last 20 years. *World Journal of Gastroenterology*, *20*(29), 9775–9827. https://doi.org/10.3748/wjg.v20.i29.9775

Papadopoulos, K. P., Gluck, L., Martin, L. P., Olszanski, A. J., Tolcher, A. W., Ngarmchamnanrith, G., Rasmussen, E., Amore, B. M., Nagorsen, D., Hill, J. S., & Stephenson, J., Jr. (2017). First-in-Human Study of AMG 820, a Monoclonal Anti-Colony-Stimulating Factor 1 Receptor Antibody, in Patients with Advanced Solid Tumors. *Clinical Cancer Research*, *23*(19), 5703–5710. https://doi.org/10.1158/1078-0432.CCR-16-3261

Park, J., Lee, S. E., Hur, J., Hong, E. B., Choi, J.-I., Yang, J.-M., Kim, J.-Y., Kim, Y.-C., Cho, H.-J., Peters, J. M., Ryoo, S.-B., Kim, Y. T., & Kim, H.-S. (2015). M-CSF from Cancer Cells Induces Fatty Acid Synthase and PPARβ/δ Activation in Tumor Myeloid Cells, Leading to Tumor Progression. *Cell Reports*, *10*(9), 1614–1625. https://doi.org/10.1016/j.celrep.2015.02.024

Pass, H. I., Lavilla, C., Canino, C., Goparaju, C., Preiss, J., Noreen, S., Blandino, G., & Cioce, M. (2016). Inhibition of the colony-stimulating-factor-1 receptor affects the resistance of lung cancer cells to cisplatin. *Oncotarget*, *7*(35), 56408–56421. https://doi.org/10.18632/oncotarget.10895

Patwardhan, P. P., Surriga, O., Beckman, M. J., de Stanchina, E., Dematteo, R. P., Tap, W. D., & Schwartz, G. K. (2014). Sustained Inhibition of Receptor Tyrosine Kinases and Macrophage Depletion by PLX3397 and Rapamycin as a Potential New Approach for the Treatment of MPNSTs. *Clinical Cancer Research*, *20*(12), 3146–3158. https://doi.org/10.1158/1078-0432.CCR-13-2576

Peterson, T. E., Kirkpatrick, N. D., Huang, Y., Farrar, C. T., Marijt, K. A., Kloepper, J., Datta, M., Amoozgar, Z., Seano, G., Jung, K., Kamoun, W. S., Vardam, T., Snuderl, M., Goveia, J., Chatterjee, S., Batista, A., Muzikansky, A., Leow, C. C., Xu, L., … Jain, R. K. (2016). Dual inhibition of Ang-2 and VEGF receptors normalizes tumor vasculature and prolongs survival in glioblastoma by altering macrophages. *Proceedings of the National Academy of Sciences of the United States of America*, *113*(16), 4470–4475. https://doi.org/10.1073/pnas.1525349113

Petrova, V., Annicchiarico-Petruzzelli, M., Melino, G., & Amelio, I. (2018). The hypoxic tumour microenvironment. *Oncogenesis*, *7*(1), 10. https://doi.org/10.1038/s41389-017-0011-9

Pixley, F. J., & Stanley, E. R. (2004). CSF-1 regulation of the wandering macrophage: Complexity in action. *Trends in Cell Biology*, *14*(11), 628–638. https://doi.org/10.1016/j.tcb.2004.09.016

Pixley, F. J., & Stanley, E. R. (2010). Chapter 319—Cytokines and Cytokine Receptors Regulating Cell Survival, Proliferation, and Differentiation in Hematopoiesis. In R. A. Bradshaw & E. A. Dennis (Eds.), *Handbook of Cell Signaling (Second Edition)* (pp. 2733–2742). Academic Press. https://doi.org/10.1016/B978-0-12-374145-5.00319-3

Pognan, F., Couttet, P., Demin, I., Jaitner, B., Pang, Y., Roubenoff, R., Sutter, E., Timsit, Y., Valentin, M. A., Vogel, B., Woerly, G., Wolf, A., & Schramm, U. (2019). Colony-Stimulating Factor-1 Antibody Lacnotuzumab in a Phase 1 Healthy Volunteer Study and Mechanistic Investigation of Safety Outcomes. *Journal of Pharmacology and Experimental Therapeutics*, *369*(3), 428–442. https://doi.org/10.1124/jpet.118.254128

Porta, C., Riboldi, E., Ippolito, A., & Sica, A. (2015). Molecular and epigenetic basis of macrophage polarized activation. *Seminars in Immunology*, *27*(4), 237–248. https://doi.org/10.1016/j.smim.2015.10.003

Pouysségur, J., Dayan, F., & Mazure, N. M. (2006). Hypoxia signalling in cancer and approaches to enforce tumour regression. *Nature*, *441*(7092), Article 7092. https://doi.org/10.1038/nature04871

Pradel, L. P., Ooi, C.-H., Romagnoli, S., Cannarile, M. A., Sade, H., Rüttinger, D., & Ries, C. H. (2016). Macrophage Susceptibility to Emactuzumab (RG7155) Treatment. *Molecular Cancer Therapeutics*, *15*(12), 3077–3086. https://doi.org/10.1158/1535-7163.MCT-16-0157

Przystal, J. M., Becker, H., Canjuga, D., Tsiami, F., Anderle, N., Keller, A.-L., Pohl, A., Ries, C. H., Schmittnaegel, M., Korinetska, N., Koch, M., Schittenhelm, J., Tatagiba, M., Schmees, C., Beck, S. C., & Tabatabai, G. (2021). Targeting CSF1R Alone or in Combination with PD1 in Experimental Glioma. *Cancers*, *13*(10), Article 10. https://doi.org/10.3390/cancers13102400

Pyonteck, S. M., Akkari, L., Schuhmacher, A. J., Bowman, R. L., Sevenich, L., Quail, D. F., Olson, O. C., Quick, M. L., Huse, J. T., Teijeiro, V., Setty, M., Leslie, C. S., Oei, Y., Pedraza, A., Zhang, J., Brennan, C. W., Sutton, J. C., Holland, E. C., Daniel, D., & Joyce, J. A. (2013). CSF-1R inhibition alters macrophage polarization and blocks glioma progression. *Nature Medicine*, *19*(10), 1264–1272. https://doi.org/10.1038/nm.3337

Qian, B.-Z., & Pollard, J. W. (2010). Macrophage diversity enhances tumor progression and metastasis. *Cell*, *141*(1), 39–51. https://doi.org/10.1016/j.cell.2010.03.014

Rabold, K., Netea, M. G., Adema, G. J., & Netea-Maier, R. T. (2017). Cellular metabolism of tumor-associated macrophages—Functional impact and consequences. *FEBS Letters*, *591*(19), 3022–3041. https://doi.org/10.1002/1873-3468.12771

Razak, A. R., Cleary, J. M., Moreno, V., Boyer, M., Aller, E. C., Edenfield, W., Tie, J., Harvey, R. D., Rutten, A., Shah, M. A., Olszanski, A. J., Jäger, D., Lakhani, N., Ryan, D. P., Rasmussen, E., Juan, G., Wong, H., Soman, N., Smit, M.-A. D., … Papadopoulos, K. P. (2020). Safety and efficacy of AMG 820, an anti-colony-stimulating factor 1 receptor antibody, in combination with pembrolizumab in adults with advanced solid tumors. *Journal for ImmunoTherapy of Cancer*, *8*(2), e001006. https://doi.org/10.1136/jitc-2020-001006

Rebelo, S. P., Pinto, C., Martins, T. R., Harrer, N., Estrada, M. F., Loza-Alvarez, P., Cabeçadas, J., Alves, P. M., Gualda, E. J., Sommergruber, W., & Brito, C. (2018). 3D-3-culture: A tool to unveil macrophage plasticity in the tumour microenvironment. *Biomaterials*, *163*, 185–197. https://doi.org/10.1016/j.biomaterials.2018.02.030

Richardsen, E., Uglehus, R. D., Due, J., Busch, C., & Busund, L.-T. R. (2008). The prognostic impact of M-CSF, CSF-1 receptor, CD68 and CD3 in prostatic carcinoma. *Histopathology*, *53*(1), 30–38. https://doi.org/10.1111/j.1365-2559.2008.03058.x

Roberts, W. M., Shapiro, L. H., Ashmun, R. A., & Look, A. T. (1992). Transcription of the human colony-stimulating factor-1 receptor gene is regulated by separate tissue-specific promoters. *Blood*, *79*(3), 586–593.

Rogers, T. L., & Holen, I. (2011). Tumour macrophages as potential targets of bisphosphonates. *Journal of Translational Medicine*, *9*, 177. https://doi.org/10.1186/1479-5876-9-177

Rohde, C. M., Schrum, J., & Lee, A. W.-M. (2004). A juxtamembrane tyrosine in the colony stimulating factor-1 receptor regulates ligand-induced Src association, receptor kinase function, and down-regulation. *The Journal of Biological Chemistry*, *279*(42), 43448–43461. https://doi.org/10.1074/jbc.M314170200

Rohrschneider, L. R., Bourette, R. P., Lioubin, M. N., Algate, P. A., Myles, G. M., & Carlberg, K. (1997). Growth and differentiation signals regulated by the M-CSF receptor. *Molecular Reproduction and Development*, *46*(1), 96–103. https://doi.org/10.1002/(SICI)1098-2795(199701)46:1<96::AID-MRD15>3.0.CO;2-1

Rottenberg, S., & Borst, P. (2012). Drug resistance in the mouse cancer clinic. *Drug Resistance Updates: Reviews and Commentaries in Antimicrobial and Anticancer Chemotherapy*, *15*(1–2), 81–89. https://doi.org/10.1016/j.drup.2012.01.001

Rovida, E., Baccarini, M., Olivotto, M., & Dello Sbarba, P. (2002). Opposite effects of different doses of MCSF on ERK phosphorylation and cell proliferation in macrophages. *Oncogene*, *21*(23), 3670–3676. https://doi.org/10.1038/sj.onc.1205409

Rovida, E., Spinelli, E., Sdelci, S., Barbetti, V., Morandi, A., Giuntoli, S., & Dello Sbarba, P. (2008). ERK5/BMK1 is indispensable for optimal colony-stimulating factor 1 (CSF-1)-induced proliferation in macrophages in a Src-dependent fashion. *Journal of Immunology (Baltimore, Md.: 1950)*, *180*(6), 4166–4172. https://doi.org/10.4049/jimmunol.180.6.4166

Ruffell, B., & Coussens, L. M. (2015). Macrophages and therapeutic resistance in cancer. *Cancer Cell*, *27*(4), 462–472. https://doi.org/10.1016/j.ccell.2015.02.015

Rutkowski, M. R., Stephen, T. L., & Conejo-Garcia, J. R. (2012). Anti-tumor immunity: Myeloid leukocytes control the immune landscape. *Cellular Immunology*, *278*(1–2), 21–26. https://doi.org/10.1016/j.cellimm.2012.06.014

Rutman, R. J., Cantarow, A., & Paschkis, K. E. (1954). THE CATABOLISM OF URACIL IN VIVO AND IN VITRO. *Journal of Biological Chemistry*, *210*(1), 321–329. https://doi.org/10.1016/S0021-9258(18)65456-0

Salonga, D., Danenberg, K. D., Johnson, M., Metzger, R., Groshen, S., Tsao-Wei, D. D., Lenz, H. J., Leichman, C. G., Leichman, L., Diasio, R. B., & Danenberg, P. V. (2000). Colorectal tumors responding to 5-fluorouracil have low gene expression levels of dihydropyrimidine dehydrogenase, thymidylate synthase, and thymidine phosphorylase. *Clinical Cancer Research: An Official Journal of the American Association for Cancer Research*, *6*(4), 1322–1327.

Samokhvalov, I. M., Samokhvalova, N. I., & Nishikawa, S. (2007). Cell tracing shows the contribution of the yolk sac to adult haematopoiesis. *Nature*, *446*(7139), 1056–1061. https://doi.org/10.1038/nature05725

Sampaio, N. G., Yu, W., Cox, D., Wyckoff, J., Condeelis, J., Stanley, E. R., & Pixley, F. J. (2011). Phosphorylation of CSF-1R Y721 mediates its association with PI3K to regulate macrophage motility and enhancement of tumor cell invasion. *Journal of Cell Science*, *124*(Pt 12), 2021–2031. https://doi.org/10.1242/jcs.075309

Sandhu, S. K., Papadopoulos, K., Fong, P. C., Patnaik, A., Messiou, C., Olmos, D., Wang, G., Tromp, B. J., Puchalski, T. A., Balkwill, F., Berns, B., Seetharam, S., de Bono, J. S., & Tolcher, A. W. (2013). A first-in-human, first-in-class, phase I study of carlumab (CNTO 888), a human monoclonal antibody against CC-chemokine ligand 2 in patients with solid tumors. *Cancer Chemotherapy and Pharmacology*, *71*(4), 1041–1050. https://doi.org/10.1007/s00280-013-2099-8

Sargent, D., Sobrero, A., Grothey, A., O'Connell, M. J., Buyse, M., Andre, T., Zheng, Y., Green, E., Labianca, R., O'Callaghan, C., Seitz, J. F., Francini, G., Haller, D., Yothers, G., Goldberg, R., & de Gramont, A. (2009). Evidence for cure by adjuvant therapy in colon cancer: Observations based on individual patient data from 20,898 patients on 18 randomized trials. *Journal of Clinical Oncology: Official Journal of the American Society of Clinical Oncology*, *27*(6), 872–877. https://doi.org/10.1200/JCO.2008.19.5362

Sarrazin, S., Mossadegh-Keller, N., Fukao, T., Aziz, A., Mourcin, F., Vanhille, L., Kelly Modis, L., Kastner, P., Chan, S., Duprez, E., Otto, C., & Sieweke, M. H. (2009). MafB restricts M-CSF-dependent myeloid commitment divisions of hematopoietic stem cells. *Cell*, *138*(2), 300–313. https://doi.org/10.1016/j.cell.2009.04.057

Sauter, K. A., Bouhlel, M. A., O'Neal, J., Sester, D. P., Tagoh, H., Ingram, R. M., Pridans, C., Bonifer, C., & Hume, D. A. (2013). The function of the conserved regulatory element within the second intron of the mammalian Csf1r locus. *PloS One*, *8*(1), e54935. https://doi.org/10.1371/journal.pone.0054935

Schiavoni, G., Gabriele, L., & Mattei, F. (2013). The tumor microenvironment: A pitch for multiple players. *Frontiers in Oncology*, *3*, 90. https://doi.org/10.3389/fonc.2013.00090

Scholl, S. M., Bascou, C. H., Mosseri, V., Olivares, R., Magdelenat, H., Dorval, T., Palangié, T., Validire, P., Pouillart, P., & Stanley, E. R. (1994). Circulating levels of colony-stimulating factor 1 as a prognostic indicator in 82 patients with epithelial ovarian cancer. *British Journal of Cancer*, *69*(2), 342–346. https://doi.org/10.1038/bjc.1994.62

Scholl, S. M., Pallud, C., Beuvon, F., Hacene, K., Stanley, E. R., Rohrschneider, L., Tang, R., Pouillart, P., & Lidereau, R. (1994). Anti-colony-stimulating factor-1 antibody staining in primary breast adenocarcinomas correlates with marked inflammatory cell infiltrates and prognosis. *Journal of the National Cancer Institute*, *86*(2), 120–126. https://doi.org/10.1093/jnci/86.2.120

Schubert, C., Schalk-Hihi, C., Struble, G. T., Ma, H.-C., Petrounia, I. P., Brandt, B., Deckman, I. C., Patch, R. J., Player, M. R., Spurlino, J. C., & Springer, B. A. (2007). Crystal structure of the tyrosine kinase domain of colony-stimulating factor-1 receptor (cFMS) in complex with two inhibitors. *The Journal of Biological Chemistry*, *282*(6), 4094–4101. https://doi.org/10.1074/jbc.M608183200

Schulz, C., Gomez Perdiguero, E., Chorro, L., Szabo-Rogers, H., Cagnard, N., Kierdorf, K., Prinz, M., Wu, B., Jacobsen, S. E. W., Pollard, J. W., Frampton, J., Liu, K. J., & Geissmann, F. (2012). A lineage of myeloid cells independent of Myb and hematopoietic stem cells. *Science (New York, N.Y.)*, *336*(6077), 86–90. https://doi.org/10.1126/science.1219179

Semenza, G. L. (2010). HIF-1: Upstream and downstream of cancer metabolism. *Current Opinion in Genetics & Development*, *20*(1), 51–56. https://doi.org/10.1016/j.gde.2009.10.009

Sharda, D. R., Yu, S., Ray, M., Squadrito, M. L., De Palma, M., Wynn, T. A., Morris, S. M., & Hankey, P. A. (2011). Regulation of macrophage arginase expression and tumor growth by the Ron receptor tyrosine kinase. *Journal of Immunology (Baltimore, Md.: 1950)*, *187*(5), 2181–2192. https://doi.org/10.4049/jimmunol.1003460

Sharma, P., Hu-Lieskovan, S., Wargo, J. A., & Ribas, A. (2017). Primary, Adaptive, and Acquired Resistance to Cancer Immunotherapy. *Cell*, *168*(4), 707–723. https://doi.org/10.1016/j.cell.2017.01.017

Sherr, C. J. (1990). Colony-stimulating factor-1 receptor. *Blood*, *75*(1), 1–12.

Shurtleff, S. A., Downing, J. R., Rock, C. O., Hawkins, S. A., Roussel, M. F., & Sherr, C. J. (1990). Structural features of the colony-stimulating factor 1 receptor that affect its association with phosphatidylinositol 3-kinase. *The EMBO Journal*, *9*(8), 2415–2421. https://doi.org/10.1002/j.1460-2075.1990.tb07417.x

Shweiki, D., Itin, A., Soffer, D., & Keshet, E. (1992). Vascular endothelial growth factor induced by hypoxia may mediate hypoxia-initiated angiogenesis. *Nature*, *359*(6398), 843–845. https://doi.org/10.1038/359843a0

Sica, A., & Mantovani, A. (2012). Macrophage plasticity and polarization: In vivo veritas. *The Journal of Clinical Investigation*, *122*(3), 787–795. https://doi.org/10.1172/JCI59643

Singh, M., Khong, H., Dai, Z., Huang, X.-F., Wargo, J. A., Cooper, Z. A., Vasilakos, J. P., Hwu, P., & Overwijk, W. W. (2014). Effective innate and adaptive antimelanoma immunity through localized TLR7/8 activation. *Journal of Immunology (Baltimore, Md.: 1950)*, *193*(9), 4722–4731. https://doi.org/10.4049/jimmunol.1401160

Smith, D. A., Conkling, P., Richards, D. A., Nemunaitis, J. J., Boyd, T. E., Mita, A. C., de La Bourdonnaye, G., Wages, D., & Bexon, A. S. (2014). Antitumor activity and safety of combination therapy with the Toll-like receptor 9 agonist IMO-2055, erlotinib, and bevacizumab in advanced or metastatic non-small cell lung cancer patients who have progressed following chemotherapy. *Cancer Immunology, Immunotherapy: CII*, *63*(8), 787–796. https://doi.org/10.1007/s00262-014-1547-6

Snodgrass, R. G., & Brüne, B. (2019). Regulation and Functions of 15-Lipoxygenases in Human Macrophages. *Frontiers in Pharmacology*, *10*, 719. https://doi.org/10.3389/fphar.2019.00719

Stanley, E. R., Berg, K. L., Einstein, D. B., Lee, P. S., Pixley, F. J., Wang, Y., & Yeung, Y. G. (1997). Biology and action of colony—Stimulating factor-1. *Molecular Reproduction and Development*, *46*(1), 4–10. https://doi.org/10.1002/(SICI)1098-2795(199701)46:1<4::AID-MRD2>3.0.CO;2-V

Stanley, E. R., & Chitu, V. (2014a). CSF-1 receptor signaling in myeloid cells. *Cold Spring Harbor Perspectives in Biology*, *6*(6), a021857. https://doi.org/10.1101/cshperspect.a021857

Stanley, E. R., & Chitu, V. (2014b). CSF-1 receptor signaling in myeloid cells. *Cold Spring Harbor Perspectives in Biology*, *6*(6), a021857. https://doi.org/10.1101/cshperspect.a021857

Stöger, J. L., Gijbels, M. J. J., van der Velden, S., Manca, M., van der Loos, C. M., Biessen, E. A. L., Daemen, M. J. A. P., Lutgens, E., & de Winther, M. P. J. (2012). Distribution of macrophage polarization markers in human atherosclerosis. *Atherosclerosis*, *225*(2), 461–468. https://doi.org/10.1016/j.atherosclerosis.2012.09.013

Sulzyc-Bielicka, V., Bińczak-Kuleta, A., Pioch, W., Kładny, J., Gziut, K., Bielicki, D., & Ciechanowicz, A. (2008). 5-Fluorouracil toxicity-attributable IVS14 + 1G > A mutation of the dihydropyrimidine dehydrogenase gene in Polish colorectal cancer patients. *Pharmacological Reports: PR*, *60*(2), 238–242.

Takeshita, S., Faccio, R., Chappel, J., Zheng, L., Feng, X., Weber, J. D., Teitelbaum, S. L., & Ross, F. P. (2007). C-Fms tyrosine 559 is a major mediator of M-CSF-induced proliferation of primary macrophages. *The Journal of Biological Chemistry*, *282*(26), 18980–18990. https://doi.org/10.1074/jbc.M610938200

Takiuchi, H., & Ajani, J. A. (1998). Uracil-tegafur in gastric carcinoma: A comprehensive review. *Journal of Clinical Oncology: Official Journal of the American Society of Clinical Oncology*, *16*(8), 2877–2885. https://doi.org/10.1200/JCO.1998.16.8.2877

Tanaka, F., Fukuse, T., Wada, H., & Fukushima, M. (2000). The history, mechanism and clinical use of oral 5-fluorouracil derivative chemotherapeutic agents. *Current Pharmaceutical Biotechnology*, *1*(2), 137–164. https://doi.org/10.2174/1389201003378979

Tap, W. D., Gelderblom, H., Palmerini, E., Desai, J., Bauer, S., Blay, J.-Y., Alcindor, T., Ganjoo, K., Martín-Broto, J., Ryan, C. W., Thomas, D. M., Peterfy, C., Healey, J. H., van de Sande, M., Gelhorn, H. L., Shuster, D. E., Wang, Q., Yver, A., Hsu, H. H., … ENLIVEN investigators. (2019). Pexidartinib versus placebo for advanced tenosynovial giant cell tumour (ENLIVEN): A randomised phase 3 trial. *Lancet (London, England)*, *394*(10197), 478–487. https://doi.org/10.1016/S0140-6736(19)30764-0

Tap, W. D., Wainberg, Z. A., Anthony, S. P., Ibrahim, P. N., Zhang, C., Healey, J. H., Chmielowski, B., Staddon, A. P., Cohn, A. L., Shapiro, G. I., Keedy, V. L., Singh, A. S., Puzanov, I., Kwak, E. L., Wagner, A. J., Von Hoff, D. D., Weiss, G. J., Ramanathan, R. K., Zhang, J., … Bollag, G. (2015). Structure-Guided Blockade of CSF1R Kinase in Tenosynovial Giant-Cell Tumor. *New England Journal of Medicine*, *373*(5), 428–437. https://doi.org/10.1056/NEJMoa1411366

Tóth, J., Varga, B., Kovács, M., Málnási-Csizmadia, A., & Vértessy, B. G. (2007). Kinetic Mechanism of Human dUTPase, an Essential Nucleotide Pyrophosphatase Enzyme*. *Journal of Biological Chemistry*, *282*(46), 33572–33582. https://doi.org/10.1074/jbc.M706230200

Tournigand, C., André, T., Achille, E., Lledo, G., Flesh, M., Mery-Mignard, D., Quinaux, E., Couteau, C., Buyse, M., Ganem, G., Landi, B., Colin, P., Louvet, C., & de Gramont, A. (2004). FOLFIRI followed by FOLFOX6 or the reverse sequence in advanced colorectal cancer: A randomized GERCOR study. *Journal of Clinical Oncology: Official Journal of the American Society of Clinical Oncology*, *22*(2), 229–237. https://doi.org/10.1200/JCO.2004.05.113

Tripathi, C., Tewari, B. N., Kanchan, R. K., Baghel, K. S., Nautiyal, N., Shrivastava, R., Kaur, H., Bhatt, M. L. B., & Bhadauria, S. (2014). Macrophages are recruited to hypoxic tumor areas and acquire a pro-angiogenic M2-polarized phenotype via hypoxic cancer cell derived cytokines Oncostatin M and Eotaxin. *Oncotarget*, *5*(14), 5350–5368. https://doi.org/10.18632/oncotarget.2110

Tushinski, R. J., Oliver, I. T., Guilbert, L. J., Tynan, P. W., Warner, J. R., & Stanley, E. R. (1982). Survival of mononuclear phagocytes depends on a lineage-specific growth factor that the differentiated cells selectively destroy. *Cell*, *28*(1), 71–81. https://doi.org/10.1016/0092-8674(82)90376-2

Tushinski, R. J., & Stanley, E. R. (1985). The regulation of mononuclear phagocyte entry into S phase by the colony stimulating factor CSF-1. *Journal of Cellular Physiology*, *122*(2), 221–228. https://doi.org/10.1002/jcp.1041220210

Vallböhmer, D., Kuramochi, H., Shimizu, D., Danenberg, K. D., Lindebjerg, J., Nielsen, J. N., Jakobsen, A., & Danenberg, P. V. (2006). Molecular factors of 5-fluorouracil metabolism in colorectal cancer: Analysis of primary tumor and lymph node metastasis. *International Journal of Oncology*, *28*(2), 527–533. https://doi.org/10.3892/ijo.28.2.527

Valledor, A. F., Xaus, J., Marquès, L., & Celada, A. (1999). Macrophage colony-stimulating factor induces the expression of mitogen-activated protein kinase phosphatase-1 through a protein kinase C-dependent pathway. *Journal of Immunology (Baltimore, Md.: 1950)*, *163*(5), 2452–2462.

van Furth, R., & Cohn, Z. A. (1968). The origin and kinetics of mononuclear phagocytes. *The Journal of Experimental Medicine*, *128*(3), 415–435. https://doi.org/10.1084/jem.128.3.415

van Kuilenburg, A. B. P. (2004). Dihydropyrimidine dehydrogenase and the efficacy and toxicity of 5-fluorouracil. *European Journal of Cancer (Oxford, England: 1990)*, *40*(7), 939–950. https://doi.org/10.1016/j.ejca.2003.12.004

Van Kuilenburg, A. B., Van Lenthe, H., Wanders, R. J., & Van Gennip, A. H. (1997). Subcellular localization of dihydropyrimidine dehydrogenase. *Biological Chemistry*, *378*(9), 1047–1053. https://doi.org/10.1515/bchm.1997.378.9.1047

Van Nguyen, A., & Pollard, J. W. (2002). Colony stimulating factor-1 is required to recruit macrophages into the mammary gland to facilitate mammary ductal outgrowth. *Developmental Biology*, *247*(1), 11–25. https://doi.org/10.1006/dbio.2002.0669

Van Overmeire, E., Laoui, D., Keirsse, J., Van Ginderachter, J. A., & Sarukhan, A. (2014). Mechanisms Driving Macrophage Diversity and Specialization in Distinct Tumor Microenvironments and Parallelisms with Other Tissues. *Frontiers in Immunology*, *5*, 127. https://doi.org/10.3389/fimmu.2014.00127

Varol, C., Mildner, A., & Jung, S. (2015). Macrophages: Development and tissue specialization. *Annual Review of Immunology*, *33*, 643–675. https://doi.org/10.1146/annurev-immunol-032414-112220

Vats, D., Mukundan, L., Odegaard, J. I., Zhang, L., Smith, K. L., Morel, C. R., Wagner, R. A., Greaves, D. R., Murray, P. J., & Chawla, A. (2006). Oxidative metabolism and PGC-1beta attenuate macrophage-mediated inflammation. *Cell Metabolism*, *4*(1), 13–24. https://doi.org/10.1016/j.cmet.2006.05.011

Vaupel, P., & Harrison, L. (2004). Tumor hypoxia: Causative factors, compensatory mechanisms, and cellular response. *The Oncologist*, *9 Suppl 5*, 4–9. https://doi.org/10.1634/theoncologist.9-90005-4

Vaupel, P., Kallinowski, F., & Okunieff, P. (1989). Blood flow, oxygen and nutrient supply, and metabolic microenvironment of human tumors: A review. *Cancer Research*, *49*(23), 6449–6465.

Veenstra, C. M., & Krauss, J. C. (2018). Emerging Systemic Therapies for Colorectal Cancer. *Clinics in Colon and Rectal Surgery*, *31*(3), 179–191. https://doi.org/10.1055/s-0037-1602238

Verreck, F. A. W., de Boer, T., Langenberg, D. M. L., Hoeve, M. A., Kramer, M., Vaisberg, E., Kastelein, R., Kolk, A., de Waal-Malefyt, R., & Ottenhoff, T. H. M. (2004). Human IL-23-producing type 1 macrophages promote but IL-10-producing type 2 macrophages subvert immunity to (myco)bacteria. *Proceedings of the National Academy of Sciences of the United States of America*, *101*(13), 4560–4565. https://doi.org/10.1073/pnas.0400983101

Vértessy, B. G., & Tóth, J. (2009). Keeping Uracil Out of DNA: Physiological Role, Structure and Catalytic Mechanism of dUTPases. *Accounts of Chemical Research*, *42*(1), 97–106. https://doi.org/10.1021/ar800114w

Vodenkova, S., Buchler, T., Cervena, K., Veskrnova, V., Vodicka, P., & Vymetalkova, V. (2020). 5-fluorouracil and other fluoropyrimidines in colorectal cancer: Past, present and future. *Pharmacology & Therapeutics*, *206*, 107447. https://doi.org/10.1016/j.pharmthera.2019.107447

Volkman, A., Chang, N. C., Strausbauch, P. H., & Morahan, P. S. (1983). Differential effects of chronic monocyte depletion on macrophage populations. *Laboratory Investigation; a Journal of Technical Methods and Pathology*, *49*(3), 291–298.

von Tresckow, B., Morschhauser, F., Ribrag, V., Topp, M. S., Chien, C., Seetharam, S., Aquino, R., Kotoulek, S., de Boer, C. J., & Engert, A. (2015). An Open-Label, Multicenter, Phase I/II Study of JNJ-40346527, a CSF-1R Inhibitor, in Patients with Relapsed or Refractory Hodgkin Lymphoma. *Clinical Cancer Research: An Official Journal of the American Association for Cancer Research*, *21*(8), 1843–1850. https://doi.org/10.1158/1078-0432.CCR-14-1845

Vonderheide, R. H., Flaherty, K. T., Khalil, M., Stumacher, M. S., Bajor, D. L., Hutnick, N. A., Sullivan, P., Mahany, J. J., Gallagher, M., Kramer, A., Green, S. J., O'Dwyer, P. J., Running, K. L., Huhn, R. D., & Antonia, S. J. (2007). Clinical activity and immune modulation in cancer patients treated with CP-870,893, a novel CD40 agonist monoclonal antibody. *Journal of Clinical Oncology: Official Journal of the American Society of Clinical Oncology*, *25*(7), 876–883. https://doi.org/10.1200/JCO.2006.08.3311

Walsh, J. C., DeKoter, R. P., Lee, H. J., Smith, E. D., Lancki, D. W., Gurish, M. F., Friend, D. S., Stevens, R. L., Anastasi, J., & Singh, H. (2002). Cooperative and antagonistic interplay between PU.1 and GATA-2 in the specification of myeloid cell fates. *Immunity*, *17*(5), 665–676. https://doi.org/10.1016/s1074-7613(02)00452-1

Walter, M., Lucet, I. S., Patel, O., Broughton, S. E., Bamert, R., Williams, N. K., Fantino, E., Wilks, A. F., & Rossjohn, J. (2007). The 2.7 A crystal structure of the autoinhibited human c-Fms kinase domain. *Journal of Molecular Biology*, *367*(3), 839–847. https://doi.org/10.1016/j.jmb.2007.01.036

Wang, G. L., Jiang, B. H., Rue, E. A., & Semenza, G. L. (1995). Hypoxia-inducible factor 1 is a basic-helix-loop-helix-PAS heterodimer regulated by cellular O2 tension. *Proceedings of the National Academy of Sciences of the United States of America*, *92*(12), 5510–5514. https://doi.org/10.1073/pnas.92.12.5510

Wang, N., Liang, H., & Zen, K. (2014). Molecular Mechanisms That Influence the Macrophage M1–M2 Polarization Balance. *Frontiers in Immunology*, *5*, 614. https://doi.org/10.3389/fimmu.2014.00614

Wang, Y., Yeung, Y. G., & Stanley, E. R. (1999). CSF-1 stimulated multiubiquitination of the CSF-1 receptor and of Cbl follows their tyrosine phosphorylation and association with other signaling proteins. *Journal of Cellular Biochemistry*, *72*(1), 119–134.

Webb, S. E., Pollard, J. W., & Jones, G. E. (1996). Direct observation and quantification of macrophage chemoattraction to the growth factor CSF-1. *Journal of Cell Science*, *109 (Pt 4)*, 793–803. https://doi.org/10.1242/jcs.109.4.793

Webster, J. A., Beck, A. H., Sharma, M., Espinosa, I., Weigelt, B., Schreuder, M., Montgomery, K. D., Jensen, K. C., van de Rijn, M., & West, R. (2010). Variations in stromal signatures in breast and colorectal cancer metastases. *The Journal of Pathology*, *222*(2), 158–165. https://doi.org/10.1002/path.2738

Wei, S., Nandi, S., Chitu, V., Yeung, Y.-G., Yu, W., Huang, M., Williams, L. T., Lin, H., & Stanley, E. R. (2010). Functional overlap but differential expression of CSF-1 and IL-34 in their CSF-1 receptor-mediated regulation of myeloid cells. *Journal of Leukocyte Biology*, *88*(3), 495–505. https://doi.org/10.1189/jlb.1209822

Wenes, M., Shang, M., Di Matteo, M., Goveia, J., Martín-Pérez, R., Serneels, J., Prenen, H., Ghesquière, B., Carmeliet, P., & Mazzone, M. (2016). Macrophage Metabolism Controls Tumor Blood Vessel Morphogenesis and Metastasis. *Cell Metabolism*, *24*(5), 701–715. https://doi.org/10.1016/j.cmet.2016.09.008

Wiesmann, M., Daniel, D. L., Pryer, N., Sutton, J., Sung, V., Wang, T., Jeffry, U., Oei, Y., Kaufman, S., Lenahan, W., Lee, I., Huh, K., & Sim, J. (2010). Abstract 3629: BLZ945, a selective c-fms (CSF-1R) kinase inhibitor for the suppression of tumor-induced osteolytic lesions in bone. *Cancer Research*, *70*(8_Supplement), 3629. https://doi.org/10.1158/1538-7445.AM10-3629

Wilson, N. J., Cross, M., Nguyen, T., & Hamilton, J. A. (2005). CAMP inhibits CSF-1-stimulated tyrosine phosphorylation but augments CSF-1R-mediated macrophage differentiation and ERK activation. *The FEBS Journal*, *272*(16), 4141–4152. https://doi.org/10.1111/j.1742-4658.2005.04826.x

Wu, R., Nie, Q., Tapper, E. E., Jerde, C. R., Dunlap, G. S., Shrestha, S., Elraiyah, T. A., Offer, S. M., & Diasio, R. B. (2016). Histone H3K27 Trimethylation Modulates 5-Fluorouracil Resistance by Inhibiting PU.1 Binding to the DPYD Promoter. *Cancer Research*, *76*(21), 6362–6373. https://doi.org/10.1158/0008-5472.CAN-16-1306

Wyckoff, J., Wang, W., Lin, E. Y., Wang, Y., Pixley, F., Stanley, E. R., Graf, T., Pollard, J. W., Segall, J., & Condeelis, J. (2004). A paracrine loop between tumor cells and macrophages is required for tumor cell migration in mammary tumors. *Cancer Research*, *64*(19), 7022–7029. https://doi.org/10.1158/0008-5472.CAN-04-1449

Wynn, T. A., Chawla, A., & Pollard, J. W. (2013). Macrophage biology in development, homeostasis and disease. *Nature*, *496*(7446), 445–455. https://doi.org/10.1038/nature12034

Xiong, Y., Song, D., Cai, Y., Yu, W., Yeung, Y.-G., & Stanley, E. R. (2011). A CSF-1 receptor phosphotyrosine 559 signaling pathway regulates receptor ubiquitination and tyrosine phosphorylation. *The Journal of Biological Chemistry*, *286*(2), 952–960. https://doi.org/10.1074/jbc.M110.166702

Yahaya, M. A. F., Lila, M. A. M., Ismail, S., Zainol, M., & Afizan, N. A. R. N. M. (2019). Tumour-Associated Macrophages (TAMs) in Colon Cancer and How to Reeducate Them. *Journal of Immunology Research*, *2019*, 2368249. https://doi.org/10.1155/2019/2368249

Yang, H., & Reinherz, E. L. (2006). CD2BP1 modulates CD2-dependent T cell activation via linkage to protein tyrosine phosphatase (PTP)-PEST. *Journal of Immunology (Baltimore, Md.: 1950)*, *176*(10), 5898–5907. https://doi.org/10.4049/jimmunol.176.10.5898

Ye, H., Zhou, Q., Zheng, S., Li, G., Lin, Q., Wei, L., Fu, Z., Zhang, B., Liu, Y., Li, Z., & Chen, R. (2018). Tumor-associated macrophages promote progression and the Warburg effect via CCL18/NF-kB/VCAM-1 pathway in pancreatic ductal adenocarcinoma. *Cell Death & Disease*, *9*(5), 453. https://doi.org/10.1038/s41419-018-0486-0

Ye, L.-Y., Chen, W., Bai, X.-L., Xu, X.-Y., Zhang, Q., Xia, X.-F., Sun, X., Li, G.-G., Hu, Q.-D., Fu, Q.-H., & Liang, T.-B. (2016). Hypoxia-Induced Epithelial-to-Mesenchymal Transition in Hepatocellular Carcinoma Induces an Immunosuppressive Tumor Microenvironment to Promote Metastasis. *Cancer Research*, *76*(4), 818–830. https://doi.org/10.1158/0008-5472.CAN-15-0977

Yeung, Y.-G., & Stanley, E. R. (2003). Proteomic approaches to the analysis of early events in colony-stimulating factor-1 signal transduction. *Molecular & Cellular Proteomics: MCP*, *2*(11), 1143–1155. https://doi.org/10.1074/mcp.R300009-MCP200

Yin, Y., Yao, S., Hu, Y., Feng, Y., Li, M., Bian, Z., Zhang, J., Qin, Y., Qi, X., Zhou, L., Fei, B., Zou, J., Hua, D., & Huang, Z. (2017). The Immune-microenvironment Confers Chemoresistance of Colorectal Cancer through Macrophage-Derived IL6. *Clinical Cancer Research: An Official Journal of the American Association for Cancer Research*, *23*(23), 7375–7387. https://doi.org/10.1158/1078-0432.CCR-17-1283

Yoshioka, A., Tanaka, S., Hiraoka, O., Koyama, Y., Hirota, Y., Ayusawa, D., Seno, T., Garrett, C., & Wataya, Y. (1987). Deoxyribonucleoside triphosphate imbalance. 5-Fluorodeoxyuridine-induced DNA double strand breaks in mouse FM3A cells and the mechanism of cell death. *Journal of Biological Chemistry*, *262*(17), 8235–8241. https://doi.org/10.1016/S0021-9258(18)47554-0

Yu, W., Chen, J., Xiong, Y., Pixley, F. J., Yeung, Y.-G., & Stanley, E. R. (2012). Macrophage proliferation is regulated through CSF-1 receptor tyrosines 544, 559, and 807. *The Journal of Biological Chemistry*, *287*(17), 13694–13704. https://doi.org/10.1074/jbc.M112.355610

Zhang, J., Yan, Y., Yang, Y., Wang, L., Li, M., Wang, J., Liu, X., Duan, X., & Wang, J. (2016). High Infiltration of Tumor-Associated Macrophages Influences Poor Prognosis in Human Gastric Cancer Patients, Associates With the Phenomenon of EMT. *Medicine*, *95*(6), e2636. https://doi.org/10.1097/MD.0000000000002636

Zhang, L., & Li, S. (2020). Lactic acid promotes macrophage polarization through MCT-HIF1α signaling in gastric cancer. *Experimental Cell Research*, *388*(2), 111846. https://doi.org/10.1016/j.yexcr.2020.111846

Zhang, Q., Liu, L., Gong, C., Shi, H., Zeng, Y., Wang, X., Zhao, Y., & Wei, Y. (2012). Prognostic significance of tumor-associated macrophages in solid tumor: A meta-analysis of the literature. *PloS One*, *7*(12), e50946. https://doi.org/10.1371/journal.pone.0050946

Zhang, X., Chen, W., Fan, J., Wang, S., Xian, Z., Luan, J., Li, Y., Wang, Y., Nan, Y., Luo, M., Li, S., Tian, W., & Ju, D. (2018). Disrupting CD47-SIRPα axis alone or combined with autophagy depletion for the therapy of glioblastoma. *Carcinogenesis*, *39*(5), 689–699. https://doi.org/10.1093/carcin/bgy041

Zhang, X., Chen, Y., Hao, L., Hou, A., Chen, X., Li, Y., Wang, R., Luo, P., Ruan, Z., Ou, J., Shi, C., Miao, H., & Liang, H. (2016). Macrophages induce resistance to 5-fluorouracil chemotherapy in colorectal cancer through the release of putrescine. *Cancer Letters*, *381*(2), 305–313. https://doi.org/10.1016/j.canlet.2016.08.004

Zhang, X., Li, L., Fourie, J., Davie, J. R., Guarcello, V., & Diasio, R. B. (2006). The role of Sp1 and Sp3 in the constitutive DPYD gene expression. *Biochimica Et Biophysica Acta*, *1759*(5), 247–256. https://doi.org/10.1016/j.bbaexp.2006.05.001

Zhao, Q., Kuang, D.-M., Wu, Y., Xiao, X., Li, X.-F., Li, T.-J., & Zheng, L. (2012). Activated CD69+ T cells foster immune privilege by regulating IDO expression in tumor-associated macrophages. *Journal of Immunology (Baltimore, Md.: 1950)*, *188*(3), 1117–1124. https://doi.org/10.4049/jimmunol.1100164

Zheng, X., Mansouri, S., Krager, A., Grimminger, F., Seeger, W., Pullamsetti, S. S., Wheelock, C. E., & Savai, R. (2020). Metabolism in tumour-associated macrophages: A quid pro quo with the tumour microenvironment. *European Respiratory Review: An Official Journal of the European Respiratory Society*, *29*(157), 200134. https://doi.org/10.1183/16000617.0134-2020

Zheng, X., Turkowski, K., Mora, J., Brüne, B., Seeger, W., Weigert, A., & Savai, R. (2017). Redirecting tumor-associated macrophages to become tumoricidal effectors as a novel strategy for cancer therapy. *Oncotarget*, *8*(29), 48436–48452. https://doi.org/10.18632/oncotarget.17061

Zhou, K., Cheng, T., Zhan, J., Peng, X., Zhang, Y., Wen, J., Chen, X., & Ying, M. (2020). Targeting tumor-associated macrophages in the tumor microenvironment (Review). *Oncology Letters*, *20*(5), 1–1. https://doi.org/10.3892/ol.2020.12097

Zhu, Y., Herndon, J. M., Sojka, D. K., Kim, K.-W., Knolhoff, B. L., Zuo, C., Cullinan, D. R., Luo, J., Bearden, A. R., Lavine, K. J., Yokoyama, W. M., Hawkins, W. G., Fields, R. C., Randolph, G. J., & DeNardo, D. G. (2017). Tissue-Resident Macrophages in Pancreatic Ductal Adenocarcinoma Originate from Embryonic Hematopoiesis and Promote Tumor Progression. *Immunity*, *47*(3), 597. https://doi.org/10.1016/j.immuni.2017.08.018

Zhu, Y., Knolhoff, B. L., Meyer, M. A., Nywening, T. M., West, B. L., Luo, J., Wang-Gillam, A., Goedegebuure, S. P., Linehan, D. C., & DeNardo, D. G. (2014). CSF1/CSF1R Blockade Reprograms Tumor-Infiltrating Macrophages and Improves Response to T-cell Checkpoint Immunotherapy in Pancreatic Cancer Models. *Cancer Research*, *74*(18), 5057–5069. https://doi.org/10.1158/0008-5472.CAN-13-3723

Zimna, A., & Kurpisz, M. (2015). Hypoxia-Inducible Factor-1 in Physiological and Pathophysiological Angiogenesis: Applications and Therapies. *BioMed Research International*, *2015*, 549412. https://doi.org/10.1155/2015/549412